Observer-based Fault Detection and Isolation for Nonlinear Systems

Lootsma, T.F.

Publication date:
2001

Document Version
Også kaldet Forlagets PDF

Observer-based Fault Detection and Isolation for Nonlinear Systems

Ph.D. Thesis

Tako F. Lootsma

Department of Control Engineering
Aalborg University
Fredrik Bajers Vej 7 C, DK-9220 Aalborg Ø, Denmark.

ISBN 87-90664-10-8
Doc. no. D-2001-4446
January 2001

This thesis was typeset using LaTeX2$_\varepsilon$ in `report` document class.

Drawings were made in CorelDraw™ from Corel Corporation.
Graphs were generated in MatLab™ and SIMULINK™ from The MathWorks Inc.

Preface and Acknowledgments

This thesis is submitted in partial fulfillment of the requirements for the European Doctor of Philosophy at the Department of Control Engineering, Aalborg University, Denmark. The work has been carried out in the period from November 1997 to January 2001 under the supervision of Professor Mogens Blanke.

The thesis considers the design of fault detection and isolation for nonlinear systems using nonlinear observers and the geometric approach. It can be applied to ordinary industrial processes that are not categorized as high risk applications, but where high availability is desirable. The results presented in the thesis are partially based on the involvement in two projects. The Theme 2 group of the COSY ('control of complex systems') framework under the European Science foundation and the ATOMOS project under the European Union which deals with the 'Advanced Technology to Optimize Maritime Operational Safety'.

Looking back over the last three years I can see several people that deserve credit for their contribution (in one way or the other) to this thesis.

First of all, I am gratefully indebted to my supervisor Professor Mogens Blanke for his guidance throughout the project and also for giving me the opportunity to participate in the above named international projects. Through him I was able to appreciate why the title Ph.D. is so-called, in particular the philosophical aspects.

I would particularly like to mention Professor Henk Nijmeijer who encouraged me to burn the midnight oil, so that I could manage to keep my deadlines. The comprehensive support during my stays at the University of Twente, the meetings at the TU Eindhoven, and the time in-between is highly appreciated.

Furthermore, I would like to thank Dr. Roozbeh Izadi-Zamanabadi very much for being far more than a colleague. Without his support and friendship during my study I would not have the great pleasure of writing this page. I will never forget the discussions we had (and hopefully will have), both technical and philosophical.

I would further like to thank Professor H. Kwakernaak for the possibility to visit the Systems, Signals and Control Department of the Faculty of Mathematical Sciences at the University of Twente; also for the chance to attend the DISC (Dutch Institute for Systems and Control) courses in the spring of 1999 in Utrecht. In that period I learned a lot and met a lot of nice people.

Another important role was played by the staff of the Department of Control Engineering at Aalborg University. I would like to thank them all very much for their support and especially their patience with my Danish. A special thanks goes to Jette D., Ole B., Rafael W., and Thomas B..

During these three years of my Ph.D. study I met a lot of colleagues that in their own and special way gave me the support needed to keep going, hence, I would also like to thank Prof. P.M. Frank, Dr. C.W. Frei, Prof. H.J.C. Huiberts, Prof. S.D. Katebi, Dr. M. Kinnaert, Prof. J. Lunze, J. Schroeder, Dr. D. Shields, and Prof. M. Staroswiecki.

A special thanks goes also to my friends, Bernd and Tracy, and my family, there especially Auke, Douwe, Gryts, Oma & Opa Thieme, Rob, and Sandra, for believing in me and their strong and moral support. A very special thanks goes out to my father for his unending support.

I also want to acknowledge the financial support from the Danish Research Council (STVF and SNF), under contract number 9601719 and 9601542, and the ATOMOS II project, supported by EU-DG VII.

Finally, I would like to commemorate this thesis to my late mother.

January 2001, Aalborg, Denmark
Tako Freerk Lootsma

Summary

With the rise in automation
the increase in fault detection and isolation & reconfiguration is inevitable.

Interest in fault detection and isolation (FDI) for nonlinear systems has grown significantly in recent years. The design of FDI is motivated by the need for knowledge about occurring faults in fault-tolerant control systems (FTC systems). The idea of FTC systems is to detect, isolate, and handle faults in such a way that the systems can still perform in a required manner. One prefers reduced performance after occurrence of a fault to the shut down of (sub-) systems. Hence, the idea of fault-tolerance can be applied to ordinary industrial processes that are not categorized as high risk applications, but where high availability is desirable. The quality of fault-tolerant control is totally dependent on the quality of the underlying algorithms. They detect possible faults, and later reconfigure control software to handle the effects of the particular fault event. In the past mainly linear FDI methods were developed, but as most industrial plants show nonlinear behavior, nonlinear methods for fault diagnosis could probably perform better.

This thesis considers the design of FDI for nonlinear systems. It consists of four different contributions. First, it presents a review of the idea and the theory behind the geometric approach for FDI. Starting from the original solution for linear systems up to the latest results for input-affine systems the theory and solutions are described. Then the geometric approach is applied to a nonlinear ship propulsion system benchmark. The calculations and application results are presented in detail to give an illustrative example. The obtained subsystems are considered for the design of nonlinear observers in order to obtain FDI. Additionally, an adaptive nonlinear observer design is given for comparison. The simulation results are used to discuss different aspects of the geometric approach,

e.g. the possibility to use it as a general approach. The third contribution considers stability analysis of observers used for FDI. It gives proofs of stability for the observers designed for the ship propulsion system. Furthermore, it stresses the importance of the time-variant character of the linearization along a trajectory. It leads to a different stability analysis than for linearization at one operation point. Finally, the preliminary concept of (actuator) fault-output decoupling is described. It is a new idea based on the solution of the input-output decoupling problem. The idea is to include FDI considerations already during the control design.

Sammenfatning

Stigende automationsgrad medfører stigende behov for fejldiagnose og fejltolerant regulering.

Diagnose af fejl i ikke-lineære systemer er vigtigt for en række tekniske anvendelser. Området er generelt genstand for en generelt stigende opmærksomhed på internationalt plan, og speciel interresse knytter sig til anvendelsen af resultatet af en teknisk diagnose til aktiv indgriben i et automatisk styret system.

Når resultat af en fejldiagnose udnyttes til automatisk at foretage en påkrævet ændring i en regulator eller en nødvendig omkobling i den regulerede proces, indgår diagnosen i et koncept, der bredt benævnes fejltolerant styring og regulering. Denne anvendelse af fejldiagnose stiller en række krav til diagnoseresultatets kvalitet, herunder sandsynligheden for forkert detektion og til den tid der hengår fra en fejl indtræder til diagnosens resultat foreligger. Kvaliteten af det samlede fejltolerante koncept bliver helt afhængig af kvaliteten af den foretagne diagnose idet en forkert diagnose kan føre til et fejlagtigt indgreb fra styresystemets side.

Anvendelse af fejldiagnosens resultat til aktiv indgriben gør det muligt at opnå, at en reguleret proces kører videre på trods af fejl, men eventuelt med nedsat reguleringskvalitet eller til kontrolleret nedlukning hvis nødvendigt. Et velfungerende fejltolerant system vil kunne forhindre, at banale fejl fører til driftstop eller at de udvikler sig til ulykker. Anvendelsesområdet for det fejltolerante koncept er den brede klasse af industrielle systemer, hvor stop i regulerede delsystemer indebærer sikkerhedsmæssige eller økonomiske risici. Anvendelsesområdet er ikke høj risiko anvendelser, hvor fuld tilgængelighed og styrekvalitet er krævet uanset enkeltfejl. I den industrielle sammenhæng er uliniariteter en kilde til forkert diagnose, og forbedring af diagnosekvalitet for systemer med væsentlige

ulinearitetер vil kunne forbedre det samlede fejltolerante koncept.

Teorien for ikke-lineære systemer har taget en ny og væsentlig drejning inden for det seneste årti, hvor de såkaldte geometriske metoder fra matematikken er under forandring til at kunne benyttes i teknisk videnskabelig sammenhænge. Der er desuden sket fremskridt indenfor anvendelse af observerteknik til diagnose på ulineære systemer. Det har været formålet med nærværende forskningsarbejde at belyse anvendelsen af nyere metoder til diagnose af tekniske systemer med væsentlige ulinearitetер.

Denne afhandling behandler derfor fejldiagnose for ikke-lineære systemer. Afhandlingen har fire hovedbidrag. Først præsenteres en oversigt over resultater fra den geometriske teori, og anvendelse på diagnoseproblemet introduceres. Med udgangspunkt i den geometriske løsning på det lineære diagnoseproblem behandles nyere teori og metoder, herunder de seneste resultater for input-affine systemer. Den geometriske metode anvendes herefter på styringen af et skibs fremdrivningsmaskineri, et realistisk eksempel som har været anvendt i internationale sammenhænge til studiet af fejldiagnose. Fejldiagnosen for fremdrivningssystemet er gennemgået i nogen detalje for at tjene som et illustrativt eksempel på beregninger og resultater. Omfattende simuleringstest illustrerer relevante aspekter af design og resultater. Hovedvægten er her lagt på ikke-lineære fejldetekterende observere. En adaptiv observer er designet for at kunne sammenligne resultater.

Det tredie bidrag er stabilitetsanalyse af observere anvendt til fejldiagnose. Specielt fremhæves betydningen af korrekt linearisering af et tidsvarierende system langs en trajektorie, hvilket giver et andet resultat end traditionel analyse om et ligevægtspunkt. Den teoretiske gennemgang er igen illustreret med anvendelsen på skibsfremdrivning, og et formelt stabilitetsbevis er udarbejdet for dette system. Som et fjerde bidrag foreslås en ny metode til aktuator fejl-afkobling. Dette er en idé som udspringer af løsning af input-output afkoblings problemet. Kernen i den nye idé er at kunne tage hensyn til fejl-diagnose allerede ved første design af regulatorsløjfer i et automatiseret system.

Contents

List of Figures

List of Tables

Nomenclature

Symbols

In the following all symbols are listed that are used in this thesis. Some of them have several meanings, however, the correct meaning is always obvious from the context.

a_{ij}	Coefficients, matrix elements
A, A_0, $\overline{A}$, $A(\cdot)$	Matrix, map, system matrix
$A_{\Delta n}$, $A_{\Delta\theta}$	Matrix, to implement sensor faults as pseudo-actuator faults
A^e	Matrix, system matrix of cascaded system
$A^{'}$	Dual map of A
$\sigma(A)$	Spectrum (eigenvalues) of A
$A \subseteq \mathcal{S}$	A is a subset or equal of/to $\mathcal{S}$
$A : \mathcal{S}$	Restriction of A to $\mathcal{S}$
$A^{-k}KerC$	$= \{x \,:\, A^k x \in KerC\}$
$\langle A \vert \mathcal{B} \rangle$	Infimal A-invariant subspace containing $\mathcal{B}$, i.e. the reachable subspace of (A, B)
$\langle KerC \vert A \rangle$	Supreme A-invariant subspace contained in $KerC$, i.e. the unobservable subspace of (C, A)
$B, B(\cdot)$	Matrix, map, input matrix
B^e	Matrix, input matrix of cascaded system
B^{-l}	Left inverse of B (i.e. $B^{-l}B = I$)
ImB	Image (range) of B, $ImB = \mathcal{B}$
$\mathcal{B}$	Subspace, image (range) of B, $\mathcal{B} = ImB$
$\mathcal{B}^e$	Subspace, image (range) of B^e,$\mathcal{B}^e = ImB^e$
$C, C(\cdot)$	Matrix, map, output matrix
$C_{\Delta n}, C_{\Delta\theta}$	Matrix, to implement sensor faults as pseudo-actuator faults

C^{-r}	Right inverse of C (i.e. $CC^{-r} = I$)
$KerC$	Kernel of C
ImC	Image (range) of C, $ImC = \mathcal{C}$
$\mathbb{C}$	Complex space
$\mathcal{C}^\infty$	Class of differential functions
$d(\mathcal{X})$	Dimension of $\mathcal{X}$
D, D_0, D_1	Matrix, map, feedthrough matrix, controller feedback matrix
D	Domain
D_x	Differential operator
$\underline{\mathcal{D}}(\mathcal{W})$	Set of all D such that $(A + DC)\mathcal{W} \subseteq \mathcal{W}$
e	Estimation error
e_n	Estimation error $e_n = n - \hat{n}$
e_U	Estimation error $e_U = U - \hat{U}$
E	Matrix
$f(\cdot), f^e, \tilde{f}$	Smooth vector field
f_i	Fault signal
f_r	Function of class $\mathcal{C}^\infty$
F	Matrix
F_x, F_y	Fault signature matrix
$g_i, g_i^e, \tilde{g}_i$	Smooth vector field
g_k	Decision funtion
G	Matrix
$h, h^e, \tilde{h}$	Smooth vector field
h_j	Smooth function
h_r	Function of class $\mathcal{C}^\infty$
$H, \overline{HC}$	Output matrix
H	(Observability) space
H^e	Output matrix of cascaded system
H_0, H_1	Statistical hypotheses
i	Index number
$\inf$	Infimum, the greatest lower bound
I_m	$m \times m$ identity matrix
I_m	Inertia of the ship's shaft system
j	Index number

k	Dimension of ν or number of faults
k_i	Dimension of ν_i, in general $k_i = 1$
$\mathbf{k}$	Finite set $\{1, \ldots, k\}$
k_r	Governor gain
k_t	Gain
k_y	Diesel engine gain
K	Matrix
K	Anti-windup gain
K^e	Feedthrough matrix of cascaded system
$K^{\hat{n}}_{\Delta k_y}$,$K^{\hat{U}}_{\Delta k_y}$	Observer gain
$K^{\hat{\theta}}_{\Delta\theta}$	Observer gain
l	Dimension of y or number of outputs
$\mathbf{l}$	Finite set $\{1, \ldots, l\}$
$l(x)$,$l_i(x)$	Smooth vector field, fault signature
$l^e(x^e)$	Smooth vector field, fault signature
l^{new}	New/changed vector field
L	Adaptive observer gain
$L_{\Delta n}$, $L_{\Delta\theta}$	Matrix, to implement sensor faults as pseudo-actuator faults
L_i	Fault signature of the i^{th} fault
L^e	Fault signature in the cascaded system
$L_X h$	Lie derivative of h along X
$\overline{L}_{11}$	Fault signature in the transformed system
$\mathcal{L}$	Subspace, range of L
$\mathcal{L}^e$	Subspace, range of L^e
L^∞_{loc}	Space of locally bounded measurable functions
m_k	Time-variant threshold
M, M^*	Matrix
M^u_{dec}	Decoupling matrix with respect to u
M^ν_{dec}	Decoupling matrix with respect to ν
$\mathcal{M}_i$	Vector space for fault ν_i, $d(\mathcal{M}_i) = k_i$
m	Dimension of u or number of inputs
$\mathbf{m}$	Finite set $\{1, \ldots, m\}$
m	(Mass) weight of the ship
n	Dimension of x or number of states

$\mathbf{n}$	Finite set $\{1, \ldots, n\}$
n	Shaft speed
n_m	Measured shaft speed
n_{max}	Maximal shaft speed
n_{ref}	Shaft speed reference
$\hat{n}$	Shaft speed estimate
N, N^*	Matrix
$\mathcal{N}$	Neighborhood of the origin in $\mathbb{R}^n$
$\mathcal{N}^e$	Neighborhood of $x^e = (x, z) = (0, 0)$
$\mathcal{O}, \mathcal{O}^e$	Observation space, observability subspace
$d\mathcal{O}, d\mathcal{O}^e$	Observability subspace
p	Dimension of r or number of residuals
$\mathbf{p}$	Finite set $\{1, \ldots, p\}$
p	Adaptive observer gain
p_i, p_i^e	Smooth vector field
p^{new}	New/changed vector field
p_{μ_r}	Probability density
P	Canonical projection $P : \mathcal{X} \to \mathcal{X}/\mathcal{S}^*$
P^{-r}	Right inverse of P (i.e. $PP^{-r} = I$)
$\mathcal{P}$	Residual vector space
q	Dimension of z, order of residual generator
Q	Involutive conditioned invariant unobservability distribution
Q	Torque
Q_{eng}	Engine torque
Q_{prop}	Propeller developed torque
Q_f	Friction torque
Q_0	Propeller torque coefficient
$Q_{\|n\|n}, Q_{\|n\|V_a}$	Propeller torque coefficients
r,r_y,r_Θ	Residual vector $[r_1 \ldots r_p]^T$, output vector of the cascaded system , $r \in \mathbb{R}^p$
r_i	i^{th} residual or i^{th} component of residual vector r
R_i	Fault signature
$R(U)$	Hull resistance
$R(\hat{x}, u)$	Observer gain

$\mathbb{R}$	Real space
$\mathbb{R}^n$	n-dimensional real space
$\mathbb{R}^+$	Positive real space
s	Dimension of w or number of disturbances
s, s_i	Log-likelihood ratio
$\sup$	Supremum, the least upper bound
S	Observer gain
S_k	Cumulative sum
$\mathcal{S}$	Subspace
$\mathcal{S}(\mathcal{L}_i)$	(C, A)-u.o.s. containing the range of L_i denoted by $\mathcal{L}_i$
$\mathcal{S}^e$	Subspace
$\mathcal{S}^\perp$	Annihilator for $\mathcal{S}$
$\mathcal{S}^*$	$\mathcal{S}^* = \inf\ \underline{\mathcal{S}}(\mathcal{L}_i)$ infimal element of $\underline{\mathcal{S}}(\mathcal{L}_i)$
$\underline{\mathcal{S}}(\mathcal{L})$	Set of all (C, A)-unobservability subspaces containing the subspace $\mathcal{L}$
t	Time
t_0	Initial time or starting point of time
t_T	Thrust deduction number
T	Thrust
T_{prop}	Propeller developed thrust
T_{ext}	External force (due to wind and waves) imposed on the ship speed
T_d	Detection time
T_s	Sampling time
$T_{\|n\|n}$, $T_{\|n\|V_a}$	Propeller thrust coefficients
$T(\cdot)$	Coordinate transform
u	Input vector $[u_1 u_2 \dots u_m]^T$, where $u \in \mathcal{U}$
u_{ref}	Reference signal for the input u
u^e	Input vector of cascaded system, $u^e \in \mathcal{U}^e = \mathcal{U} \oplus \mathcal{M}_2$
u_i	i^{th} input or i^{th} component of input vector u
$u_{\dot{\theta}}$	Output of pitch controller
U	Ship speed
U_m	Measured ship speed
U_{max}	Maximal ship speed

$\hat{U}$	Ship speed estimate
$\mathcal{U}$	Input vector space
$\mathcal{U}^e$	Input vector space of cascaded system $\mathcal{U}^e = \mathcal{U} \oplus \mathcal{M}_2$
V	Lyapunov function
$\dot{V}$	Time derivative of the Lyapunov function
V_a	Max. advanced speed
w	Disturbance vector $[w_1 w_2 \dots w_s]^T$, where $w \in \mathbb{R}^s$
w_i	i^{th} disturbance signal
w, $\tilde{w}$	New input vector
w^{new}	New/changed disturbance vector
w	Wake fraction
$\mathcal{W}$	(C, A)-invariant subspace
$\underline{\mathcal{W}}(\mathcal{L})$	Set of all (C, A)-invariant subspaces containing the subspace $\mathcal{L}$
W_1, W_2, W_3	Continuous positive definite functions
$x, \tilde{x}$	State vector $[x_1 x_2 \dots x_n]^T$, where $x \in \mathcal{X}$
x_0	Initial condition $x_0 = x(t = 0)$
$\hat{x}$	Estimate of the state (vector) x
$x^e, \tilde{x}^e$	State vector of cascaded system, $x^e \in \mathcal{X}^e = \mathcal{X} \oplus \mathcal{Z}$
$\dot{x}(t)$	time derivative of $x(t)$
x_i	i^{th} state or i^{th} component of state vector x
$X_{\dot{U}}$	Added mass in surge
$\mathcal{X}$	Vector space
$\mathcal{X}^e$	State vector space of cascaded system $\mathcal{X}^e = \mathcal{X} \oplus \mathcal{Z}$
$\mathcal{X}^{'}$	Dual space of $\mathcal{X}$
$\mathcal{X}/\mathcal{S}$	Factor space of $\mathcal{X}$ with respect to $\mathcal{S}$
$y, \tilde{y}$	Output vector $[y_1 y_2 \dots y_l]^T$, where $y \in \mathcal{Y}$
$\hat{y}$	Estimate of the output (vector) y
y_i	i^{th} output or i^{th} component of output vector y
Y	Fuel index
Y_m	Measured fuel index
Y_{PI}	Governor output
Y_{lb}, Y_{ub}, Y_{PIb}	Boundaries for fuel index
$\mathcal{Y}$	Output vector space
z	State vector $[z_1 z_2 \dots z_q]^T$, where $z \in \mathcal{Z}$, $d(\mathcal{Z}) = q$

z_i	i^{th} component of state vector z
$\mathcal{Z}$	State vector space
0	Zero vector, zero space, etc.
α	Index number
$\tilde{\alpha}_{ij}$	Real number, coefficient
$\tilde{\beta}_i$	Real number, coefficient
Δ	Unobservability space or distribution
$\Delta\, k_y$	Diesel engine gain fault
$\Delta\, n_{sensor}$	Shaft speed sensor fault
$\Delta\, \dot{n}_{sensor}$	Time derivative of shaft speed sensor fault
$\Delta\theta$	Fault on the propeller pitch
$\Delta\, \theta_{sensor}$	Pitch sensor fault
$\Delta\, \dot{\theta}_{sensor}$	Time derivative of pitch sensor fault
$\Delta\, \dot{\theta}_{inc}$	Pitch actuator hydraulic fault
$\overline{\Delta}$	Involutive closure of distribution Δ
ϵ	Code vector or estimation error $\epsilon = \xi^1 - \hat{\xi}^1$
κ, κ_i	Threshold
λ	Eigenvalue, $\lambda \in \Lambda$
λ^*	Complex conjugate of eigenvalue λ
Λ	Set of eigenvalues
μ_r	Mean value of the signal r
$\mu_{r_{nofault}}$	Mean value of the signal r in the faultfree case
$\mu_{r_{fault}}$	Mean value of the signal r in the faulty case
ν	Fault, complete fault vector $[\nu_1 \nu_2 \ldots \nu_k]^T$, where $\nu \in \mathcal{M}$ and $k_i = 1$
ν^{new}	New/changed fault vector
ν_i	Fault vector, $\nu_i \in \mathcal{M}_i$
$\nu_{\Delta n}, \nu_{\Delta\theta}$	New fault signal, to implement sensor faults as pseudo-actuator faults
$\overline{\nu}_i$	Fault vector, $\overline{\nu}_i \in \mathcal{M}_i$
ν_i	i^{th} component of fault vector ν
ν_n	Measurement noise concerning shaft speed measurement
ν_U	Measurement noise concerning ship speed measurement
ν_Y	Measurement noise concerning fuel index measurement

ν_θ	Measurement noise concerning pitch measurement
Ω	Subspace, range, area, coding set
Ω_u	Range of u
Ω_x	Range of x
Ω_j	j^{th} coding set, set of numbers
Ω^*	Subspace
Φ	Structure matrix
$\Phi(t, t_0)$	Transition matrix
$\Phi(\cdot)$	Change of output coordinates
$\psi(u, y)$	Smooth vector field
$\varphi(x, y)$	Smooth vector field
ρ_i^u	Characteristic number with respect to u
ρ_i^ν	Characteristic number with respect to ν
$\sigma(A)$	Spectrum (eigenvalues) of A
σ_r^2	Variance of the signal r
Σ_*^P	Involutive conditioned invariant distribution
τ_i	Time cons. in the governor
τ_c	Time cons. in the diesel engine
θ	Constant number
θ	Propeller pitch
θ_m	Measured propeller pitch
θ_{ref}	Propeller pitch reference
θ_{min}, θ_{max}	Boundaries for pitch
$\dot{\theta}_{min}$, $\dot{\theta}_{max}$	Boundaries for pitch
Θ	Parameter (vector), fixed codistribution
Θ_{nom}	Nominal value of the parameter (vector) Θ
$\hat{\Theta}$	Estimate of the parameter (vector) x
ξ	State vector $(\xi_1 \xi_2 \dots \xi_n)^T$
ξ^1	State vector $\xi^1 = (\xi_1, \dots, \xi_k)$
$\hat{\xi}^1$	Estimation of ξ^1
ξ^2	State vector $\xi^2 = (\xi_{k+1}, \dots, \xi_n)$
$\frac{\partial}{\partial x_i}$	Partial derivative
$(\cdot)^\perp$	Annihilator
$\inf(.)$, $(\cdot)^*$	Infimal element

$span\{\cdot\}$	Spanned vector space.

Abbreviations

ANN	Artificial neural network
ATOMOS	Advanced Technology to Optimize Maritime Operational Safety
BJDFP	Beard Jones detection filter problem
CAISA	(C, A)-invariant subspace algorithm
COSY	control of complex systems
CPP	Controllable pitch propeller
CUSUM	Cumulative sum
DDEP	Disturbance decoupled estimation problem
DOS	Dedicated observer scheme
FDI	Fault detection and isoltaion
FDIFP	FDI filter problem
FMEA	Failure mode and effect analysis
FPA	Fault propagation analysis
FPRG	Fundamental problem of residual generation
FTC	Fault tolerant control
FTCS	Fault-tolerant control system
$h.o.t.$	Higher order terms
l-NLFPRG	Local nonlinear fundamental problem of residual generation
LTI	linear, time-invariant
LTV	linear, time-variant
NLFPRG	Nonlinear fundamental problem of residual generation
rl-NLFPRG	Regular local nonlinear fundamental problem of residual generation
o.c.a.	Observability codistribution algorithm
SA	Structural analysis

SNF	Statens Naturvidenskabelige Forskningsråd (Danish Research Council)
STVF	Statens Teknisk Videnskabelige Forskningsråd (Danish Research Council)
u.o.s.	Unobservability subspaces

Terminology

The terminology used in FTCS has only during the recent years approached an agreement in the published material. The Safeprocess Technical Committee of IFAC has compiled a list of suggested definitions (Isermann and Ballé (1997)), which is generally in coherence with the terminology used throughout this thesis. Some of the definitions are changed according to the terminology presented in Blanke *et al.* (2000).

Active fault-tolerant system	A fault-tolerant system where faults are explicitly detected and handled. See also passive fault-tolerant system.
Analytical redundancy	Use of more than one not necessarily identical ways to determine a variable, where one way uses a mathematical process model in analytical form.
Availability	Probability that a system or equipment will operate satisfactorily and effectively at any point of time.
Constraint	A functional relation between variables and parameters of a system. Constrains may be specified in different forms, including linear and nonlinear differential equations, and tabular relations with logic conditions between variables.
Decision logic	The functionality that determines which remedial action(s) to execute in case of a reported fault and which alarm(s) shall be generated.
Detector	An algorithm that performs fault detection and isolation.
Discrepancy	An abnormal behaviour of a physical value or inconsistency between more physical values and the relationship between them.

Fail-safe	The ability to sustain a failure and retain the capability to make a safe close-down. An example could be a system where the occurrence of a single fault can be determined but not isolated and where the fault cannot be accommodated to continue operation.
Fail-operational	The ability to operate with no change in objectives or performance despite of any single failure.
Failure	Permanent interruption of a systems ability to perform a required function under specified operating conditions.
Failure effect	The consequence of a failure mode on the operation, function, or status of an item.
Failure mode	Particular way in which a failure can occur.
Fault detection	Determination of faults present in a system and time of detection.
Fault accommodation	A change in controller parameters or structure to avoid the consequences of a fault. The input-output between controller and plant is unchanged. The original control objective is achieved although performance may degrade.
Fault diagnosis	Determination of kind, size, location, and time of occurrence of a fault. Includes fault detection, isolation and identification.
Fault isolation	Determination of kind, location, and time of detection of a fault. Follows fault detection.
Fault modeling	Determination of a mathematical model to describe a specific fault effect.
Fault propagation analysis	Analysis to determine how certain fault effects propagate through the considered system.
Fault-tolerance	The ability of a controlled system to maintain control objectives, despite the occurrence of a fault. A degradation of control performance may be accepted. Fault-tolerance can be obtained through fault accommodation or through system and/or controller reconfiguration.
Hardware redundancy	Use of more than one independent instrument to accomplish a given function.

Incipient fault	A fault where the effect develops slowly e.g. clogging of a valve). In opposite to an abrupt fault.
Passive fault-tolerant system	A fault-tolerant system where faults are not explicitly detected and accommodated, but the controller is designed to be insensitive to a certain restricted set of faults. See also active fault-tolerant system.
Qualitative model	A system model describing the behavior with relations among system variables and parameters in heuristic terms such as causalities or if-then rules.
Quantitative model	A system model describing the behavior with relations among system variables and parameters in analytical terms such as differential or difference equations.
Reconfiguration	Change in input-output between the controller and plant through change of controller structure and parameters. The original control objective is achieved although performance may degrade.
Reliability	Probability of a system to perform a required function under normal conditions and during a given period of time.
Remedial action	A correcting action (reconfiguration or a change in the operation of a system) that prevents a certain fault to propagate into an undesired end-effect.
Residual	Fault information carrying signals, based on deviation between measurements and model based computations.
Safety system	Electronic system that protects local subsystems from permanent damage or damage to environment when potential dangerous events occur.
Severity	A measure on the seriousness of fault effects using verbal characterization. Severity considers the worst-case damage to equipment, damage to environment, or degradation of a system's operation.
Structural analysis	Analysis of the structural properties of the models, i.e. properties that are independent on the actual values of the parameter.
Threshold	Limit value of a residual's deviation from zero, so if exceeded, a fault is declared as detected.

Chapter 1

Introduction

Interest in fault detection and isolation (FDI) for nonlinear systems has grown significantly in recent years. Its design is one important step towards fault-tolerant control systems (FTCS). In a FTCS occurring faults are handled in such a way that it can still perform in an acceptable manner. This is preferred to shut down of (sub-)systems caused by occurring faults. Obviously, the actions for fault handling are different for each potential fault. Hence, it is required to diagnose which actual faults might be present in a system.

This thesis considers observer-based FDI for nonlinear systems. The design is based on the geometric approach. It is applied to analyze the considered system and to choose suitable subsystems for the observer design. A nonlinear ship propulsion system is used as an illustrative application example. Furthermore, stability aspects concerning the observer design are mentioned. Finally, the novel concept of fault-output decoupling is introduced to integrate FDI aspects in the control design and to improve FDI possibilities.

1.1 Background and Motivation

The level of automation has reached a high level, both, in industry and in daily-life. Still, the number of tasks taken over by computers is growing every day; in airplanes, biomedical applications like pacemakers, cars, CD-players, robots, ships, telephones, television, and numerous others. Only in few of them possible faults, in e.g. actuators and sensors, have been considered during the design. However, in most applications they are not considered. This leads to several

difficulties during the occurrence of a fault. Often a small fault can have a big impact on a control system. In one example, a simple sensor fault, caused an auto-pilot on board a ship to steer it in a wrong direction. This was not noticed on-time by the officer on watch (obviously trusting the auto-pilot) and caused heavy damage to the ship as it sailed onto ground. In another example a temperature sensor caused an emergency shut-off system to turn off the ship's diesel engine to prevent overheating. As a consequence the ship was not able to maneuver and caused a collision in the harbor while docking. Most of these kind of accidents could be prevented when the possible faults would be considered during the control design.

In airplane design the possible sensor faults are considered by implementing redundant sensors (*hardware redundancy*). This makes the design more expensive due to a higher degree of complexity of the design and the extra hardware costs. The fuel consumption is also increased due to the higher weight. As a result of the hardware redundancy the system becomes *fail-operational*, i.e. even if a sensor fault occurs, the redundant sensors will provide correct information. Therefore, the system will keep on performing as if nothing happened. Due to the high costs the fail-operational approach is seldom implemented in systems which are not considered to be high risk. However, with the growing demand in availability, efficiency, quality, reliability, and safety fault handling has become an important issue. As a result control systems with fault handling capabilities are considered. They are also known as *fault-tolerant control systems* (FTCS). The goal is to handle occurring faults in such a way that the system can still perform in an acceptable manner and that shut down of (sub-)systems is prevented.

The design of fault-tolerant control systems includes several different tasks. First, all possible faults have to be modeled (*fault modeling*) that can occur in the considered system. Then a *fault propagation analysis* (FPA) is carried out to analyze which impact the single faults have on the system. As a result the severity of the faults and possible *fault handling* strategies can be determined. However, the most essential part for a FTCS design is *fault detection and isolation* (FDI). Its design is required to judge when and which fault has occurred in order to initiate the correct fault handling at the right point of time.

1.2 Overview of previous and related work

The topic of fault detection and isolation (FDI) has been of interest since the beginning of the 1970s. In the start the research was mainly concentrated on the area of aeronautics and aviation. An essential body of literature has been produced since due to contributions from several research areas. Different research groups proposed FDI approaches based on the expertise from their own field and/or the experience with a specific class of systems. The high diversity of solutions has also been driven by the growing interest from industry in FDI. This was mainly due to the hope of improving efficiency, safety, and reliability of process automation.

Most methods are covered by the term *model-based fault detection and isolation*. The idea is to use the *analytic redundancy* given by a model of the system, i.e. cross checking between expected/predicted and measured behavior. The methods use a system model and the observables of the system (control and measurement signals) to generate *residuals*. Residuals are measures for the discrepancy between expected and measured system behavior. Their analysis leads to model-based fault detection and isolation. However, there exist also many other methods that are not considered as model-based, e.g. the fuzzy-approach (Kiupel and Frank (1997)), the artificial neural network (ANN) approach (Köppen-Seliger and Frank (1996)), or the stochastic signal analysis (Basseville and Nikiforov (1994)).

The field of model-based FDI for linear systems is well-studied. Key references can be found in Chen and Patton (1999); Gertler (1998); Isermann and Ballé (1997); Patton (1997); Frank (1996); Massoumnia *et al.* (1989); Willsky (1976). There exist several solutions for different linear FDI problems. On the opposite, the area of FDI for nonlinear systems is not covered completely yet. For some nonlinear systems it was shown to be sufficient to use linearization around operating points in order to apply linear FDI methods. However, in general this is often not possible due to hard nonlinearity (e.g. saturation effects or non-analytic behavior) or the inefficiency of linearization. Hence, several FDI approaches have been improved to also handle nonlinear systems, e.g. the observer-based approach, the parity space approach, and the parameter estimation approach. Also fuzzy observers and artificial neural networks were considered for nonlinear systems.

Recently, new approaches were proposed for the class of input-affine nonlinear systems (linear in the input). Especially the observer-based FDI approach for nonlinear systems has gained a lot of interest (García and Frank (1997); Hammouri *et al.* (1999); Nijmeijer and Fossen (1999); Åström *et al.* (2000)).

An interesting question for the observer design is to decide which (sub-)system should be observed for residual generation. In Izadi-Zamanabadi (1999) an example is given how this problem can be solved applying the structural analysis (Staroswiecki and Declerck (1989); Cassar *et al.* (1994)). Another solution is the application of the geometric approach. It was originally introduced by Massoumnia *et al.* (1989) for the linear case. In the last two years it has been extended to nonlinear systems (Hammouri *et al.* (1998, 1999); DePersis and Isidori (1999); DePersis (1999)). However, only little application experience exists from using the geometric approach for FDI in nonlinear systems.

In practice the FDI design is seldom considered during the control design, but often designed later on top of the control. Hence, it is impossible for the FDI designer to influence the controller design, e.g. to improve the FDI possibilities by adding sensors. However, as pointed out by Bøgh (1997), this is inevitable for the design of fault-tolerant control systems. This is also described in detail in Patton (1997).

In Chapter 2 a general introduction to model-based FDI is given. It describes some of the most common model-based FDI approaches and different aspects of residual generation.

1.3 Objectives and contributions

This thesis focuses on observer-based fault detection and isolation for nonlinear systems. One of the objectives is to give an overview over the geometric approach towards observer-based FDI and to apply it to a ship propulsion system. The latter is done to investigate its applicability. Furthermore, it considers stability issues for the observer design. The goal is to stress the necessity of recognizing the resulting time-variance when linearizing a nonlinear system along a trajectory. Finally, the novel idea of fault-output decoupling is proposed based on the well-studied input-output decoupling problem. It points out the importance of considering FDI properties already during the control design and shows

one way to achieve that.

In order to address these objectives the thesis contributes in the following way:

- Different important facts about residual generation and evaluation are addressed in Chapter 2. Different model-based FDI approaches are mentioned. Furthermore, coding sets for the residual evaluation are stated, as e.g. defined by Gertler (1998).
- A detailed review of the geometric approach towards fault detection and isolation is given. Starting from linear systems, covering state-affine nonlinear systems up to input-affine nonlinear systems. Furthermore, its basic concept of using unobservability subspaces/distributions is pointed out.
- As an application example the geometric approach introduced by DePersis and Isidori (1999); DePersis (1999) is applied to different FPRGs. These fundamental problems of residual generation (FPRG) are defined for a nonlinear ship propulsion benchmark (Izadi-Zamanabadi and Blanke (1997, 1999)).
- Several observers are designed to obtain successful FDI. The structure of two of them is based on the results from the geometric approach. Stability is proven based on Gauthier *et al.* (1992).
- An adaptive nonlinear observer (Blanke *et al.* (1998); Blanke and Lootsma (1999)) is designed and simulated. Its simulation results show fast detection possibilities. They are compared with the results obtained by the geometric approach.
- Several simulation results are given to illustrate the successful FDI for the ship propulsion benchmark. The designed observers are able to detect and isolate all implemented faults. The requirements for detection time are fulfilled as well.
- Based on the simulation results the advantages and disadvantages of the geometric approach are discussed.
- Stability aspects are considered. It is shown how important it is to consider the resulting time-variance when linearizing a nonlinear system along a trajectory.

- The novel idea of fault-output decoupling is proposed to show a possibility of combining FDI and control design. The concept of complete and efficient fault-output decoupling is introduced and discussed. Furthermore, an application example is given for illustration.

1.4 Thesis Outline

The thesis is organized as follows:

Chapter 2 gives a brief introduction into the field of model-based fault detection and isolation. The idea of observer-based FDI is briefly reviewed. Furthermore, aspects like residual structure, robustness, and performance criteria are addressed.

Chapter 3 reviews the existing geometric approaches, starting with the linear case and ending with the wide class of input-affine nonlinear systems. Both, problem formulations and solutions are presented. Furthermore, the similarities are pointed out.

Chapter 4 illustrates the application of the geometric approach to a ship propulsion system in order to obtain successful FDI. First the system is described. Then the geometric approach is applied. The detailed calculations are given in Appendix C. The results are used to design several observers for FDI. Simulation results of the ship propulsion system and the observers illustrate the obtained FDI performance. Finally, the results are discussed to evaluate the geometric approach.

Chapter 5 covers several stability aspects of observers used for FDI. It outlines the stability proof for the observers that were designed based on the geometric approach. Chapter 5 illustrates also the importance of the awareness that linearization along a trajectory leads to a time-variant system. The difference between the stability analysis for time-variant and time-invariant systems is described.

Chapter 6 introduces a novel idea, *fault-output decoupling*, to show how FDI and control design could be combined to improve FDI possibilities. The concepts of complete and efficient fault-output decoupling are defined and illustrated by a simple example.

Chapter 7 gives concluding remarks and recommendations for future work.

Chapter 2

Model-based fault detection and isolation

Fault-tolerant control systems have the ability to tolerate the occurrence of a fault by being able to continue operation while a degradation of performance may be accepted, see Blanke (1999). Continued operation is assured by handling occurring faults. To initiate the correct fault handling sufficient FDI information is required. As mentioned in the introduction there exist several approaches towards FDI. This thesis focuses on observer-based FDI for nonlinear systems which belongs to the group of model-based FDI methods.

The field of model-based FDI is well-studied. There exists a wide variety of model-based FDI approaches for linear systems, e.g. the observer-based approach, the parity space approach, and the parameter estimation approach. Key references can be found in Chen and Patton (1999); Gertler (1998); Isermann and Ballé (1997); Patton (1997); Frank (1996); Willsky (1976). Also for nonlinear systems there exist several model-based FDI methods (García and Frank (1997); Chen and Patton (1999); Åström *et al.* (2000)). Especially the observer-based approach has gained a lot of interest recently (García and Frank (1997); Frank *et al.* (1999); Hammouri *et al.* (1999); Nijmeijer and Fossen (1999); De-Persis (1999)). However, most methods only handle a specific class of nonlinear FDI problems. This is mainly due to the fact that there exist different classes of nonlinear systems and nonlinear systems also include phenomena like saturation effects or non-analytic behavior.

In this chapter different aspects of model-based FDI are addressed, starting with analytical redundancy and the use of structured residuals. Furthermore, robustness issues and performance criteria are mentioned.

2.1 Analytical redundancy

One possibility to achieve FDI is the use of *analytical redundancy*. Analytical redundancy is based on using the available signal information (known inputs and measurements) and a mathematical model of the system. A cross-check of the signal information is carried out to detect and isolate faults. For systems with *hardware redundancy* this cross-check can be carried out by comparing signal information with available redundant information supplied by redundant hardware. Using analytical redundancy means to calculate the required redundant information by using the model and the available signal information. Hence, this approach is also referred to as *model-based FDI*. A detailed description of the term *model-based FDI* is given in Chen and Patton (1999).

The model-based FDI methods are restricted by the fact that they require a precise model to obtain sufficient FDI. In practice this is not always available. Hence, other methods next to the model-based methods have been considered, e.g. the artificial neural network approach, the fuzzy approach, and the qualitative approach. They are referred to as knowledge-based and qualitative in the literature (Frank (1996)).

The restriction of the so-called knowledge-based methods is that they are depending on knowledge acquisition from the system in form of training data sets Frank (1996). In practice these sets are difficult to obtain. This is due to the fact that they must provide data from the system while the considered faults occur. However, in a real running system it is hardly possible to convince the owner of a plant to simulate all possible faults. When a knowledge-based systems can be trained sufficiently they can be used to estimate measurements based on the available signal information, hence, provide redundancy. The main advantage of these methods is that they do not require a precise analytical model.

2.2 Residuals

Normally, the consistency check based on analytical redundancy is achieved by comparing measured signals with their estimates. The resulting difference for one signal is referred to as *residual signal*; e.g. $r_i = y_i - \hat{y}_i$, $i \in \mathbf{k}$, where r_i denotes the i^{th} residual, y_i the i^{th} measured system output, $\hat{y}_i$ the estimated i^{th} system output, and k the number of residuals. Residuals are designed to be equal or converge to zero in the fault-free case ($r_i \approx 0$) and deviate significantly from zero under occurrence of a fault ($|r_i| > \kappa_i > 0$, where $\kappa_i \in \mathbb{R}$ denotes a *threshold*). Hence, the residuals represent the fault effects. Depending on the number of residuals and their design it is possible to detect and isolate occurring faults. Most model-based FDI methods incorporate two sequential steps in order to obtain FDI: 1. Residual generation, and 2. Residual evaluation.The two different steps are explained in the following two subsections.

There exist also model-based methods that are not based on residual generation, e.g. the statistical automata approach (Lunze (2000)). It provides direct fault information and does not generate residuals in order to evaluate them in a second step to take a FDI decision.

2.2.1 Residual generation

The residual generation for model-based FDI is based on exploiting the available analytical redundancy. In most approaches the analytical redundancy is represented by a set of differential equations. The goal is to generate *structured residuals* to obtained sufficient FDI. One common way to generate residuals is to estimate the system output vector y or the system parameter vector Θ. Then the estimates $\hat{y}$ and $\hat{\Theta}$ are subtracted from the real measurement y and the nominal value of the parameters Θ_{nom}. This leads to the following residual vectors:

$$r_y = y - \hat{y} \qquad \text{and} \qquad r_\Theta = \Theta_{nom} - \hat{\Theta}$$

The residual vector r_Θ corresponds to the parameter estimation approach. The residual vector r_y is typical for the observer-based approach, but is also used by the so-called parity relation approach. A good overview and comparison of these three model-based methods can be found in Chen and Patton (1999). In the following and in the rest of the thesis only the observer-based approach will be considered.

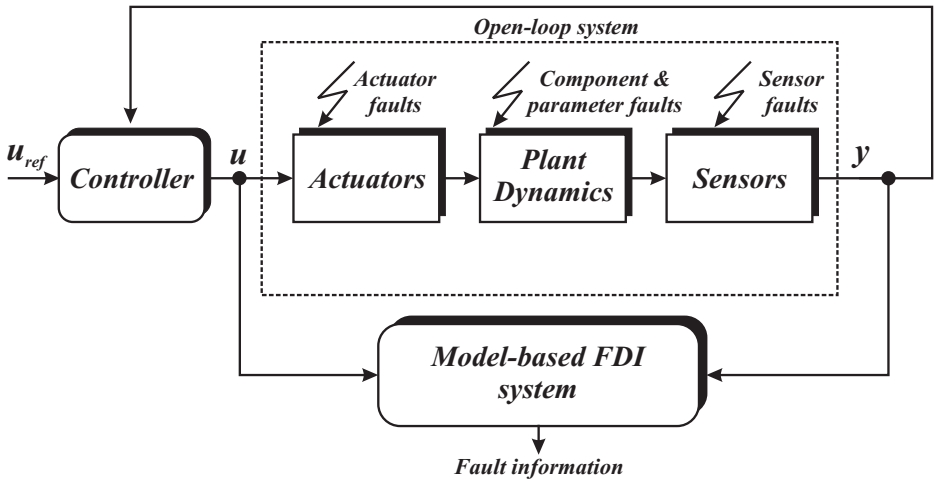

Figure 2.1: General scheme for model-based FDI.

The principle idea of model-based residual generation is illustrated in Figure 2.1. It shows the observed plant and its different parts:

- The *controller* that assures the required performance of the plant based on an external reference signal u_{ref}.
- The three given parts of the plant itself: *actuators*, *plant dynamics*, and *sensors*.
- The *model-based FDI system*.

Furthermore, it is illustrated that the possible faults can affect the actuators, the plant, and the sensors. The FDI system has two different inputs, the so-called observables: the system input u and the measured system output y. It is applied to the open-loop system.

The main task of observer-based FDI approach is to design an observer structure that generates structured residuals that enable detection and isolation of the considered faults. The existing observer-based methods generate estimates that can be subtracted from available measurements to obtain residuals (e.g. r_y). There exist many different observer-based approaches considering linear systems and different classes of nonlinear systems. Key references can be found in Chen and Patton (1999); Patton (1997); García and Frank (1997); Frank (1996); Nijmeijer

and Fossen (1999).

The next Chapter gives a detailed overview over the observer-based FDI approaches that are based on the geometric approach. It starts with one of the first observer-based FDI approaches, the Beard&Jones detection filter (BJDF) for linear systems (Beard (1971),Jones (1973)). The BJDF is based on a full-order Luenberger observer where the gain is tuned to use the prediction error (or innovation) as residual. Furthermore, the latest results for nonlinear systems based on the geometric approach Hammouri *et al.* (1998, 1999); DePersis and Isidori (1999); DePersis (1999) are described in detail.

2.2.2 Residual evaluation

Successful residual-based FDI requires appropriate residual evaluation. Residual evaluation describes the task of evaluating the residuals in order to take the following decisions: $1.$ Is there any fault present? , and $2.$ If yes, which fault(s) is/are present. Especially the second decision is depending on the fact whether only single faults (one fault at a time) or also multiple (simultaneous) faults are considered. Multiple faults are most unlikely events, unless there is a severe defect in the system which causes several faults to occur. The problem of handling multiple faults lies in the fact that resulting fault effects caused by single faults occur at the same time. Hence, they might compensate each other or they might overlap in a way that either only one of them or a complete other fault is detected and isolated.

Therefore, it is important to obtain the correct *residual structure* for correct residual evaluation. The residuals should be generated in such a way that for each fault a different set of residuals is affected (i.e. the residuals deviate significantly from zero). For multiple faults it should furthermore be guaranteed that the overlapping of the resulting fault effects does not lead to a wrong decision, e.g. missed detection of a fault or a wrong decision about which fault occurred. There exist several ways to define structured residuals that can be used for correct residual evaluation.

Structured residuals

According to Gertler (1998) a structured residual is characterized by the following property: *Any residual responds only to a specific subset of faults, and to any*

fault only a specific subset of residual responds. Following Gertler (1998) one can represent a set of p residuals in two different ways:

- in a geometric way by considering the vector $r(t) = (\, r_1(t)\ r_2(t)\ \ldots\ r_p(t)\,)^T$, where $r(t) \in \mathbb{R}^p$.
- and in a Boolean way by defining a *fault code vector* in the following way:

$$\epsilon_i(t) = \begin{cases} 1 & if \quad |r_i(t)| \geq \kappa_i \\ 0 & if \quad |r_i(t)| < \kappa_i \end{cases}$$
$$\Rightarrow \epsilon(t) = (\, \epsilon_1(t)\ \epsilon_2(t)\ \ldots\ \epsilon_p(t)\,)^T$$

  for $i \in \mathbf{p}$ and the thresholds κ_i.

Obviously, the fault code vector $\epsilon(t)$ provides the information weather the i^{th} residual $r_i(t)$ hits a defined threshold κ_i or not. When following the Boolean notation one can also define a *structure matrix* Φ in the following way, when using the fault vector $\nu(t) = (\, \nu_1(t)\ \nu_2(t)\ \ldots\ \nu_k(t)\,)^T$:

$$r \leftarrow\!\!- \ \Phi\, \nu$$

where the i^{th} column vector of Φ is defined as: $\Phi^i = \epsilon^{\nu_i}$, where ϵ^{ν_i} describes the code vector ϵ concerning the i^{th} fault. Hence, Φ is a $p \times k$ matrix that contains only ones ('1') and zeroes ('0'). The operator defined by '$\leftarrow\!\!-$' can be read as '*is affected by*'. The expression $r \leftarrow\!\!- \ 0$ is a special case and should be read like the residual r is not affected (by any fault). To illustrate this notation a simple example is given representing the structured residual where the i^{th} residual $r_i(t)$ is only affected by the i^{th} fault $\nu_i(t)$, and the number of faults k equals the number of residuals p, $k = p = 3$ (the time dependence is omitted for a better readability):

$$r = \begin{pmatrix} r_1 \\ r_2 \\ r_3 \end{pmatrix} \leftarrow\!\!- \begin{pmatrix} \nu_1 \\ \nu_2 \\ \nu_3 \end{pmatrix} = \underbrace{\begin{pmatrix} 1 & 0 & 0 \\ 0 & 1 & 0 \\ 0 & 0 & 1 \end{pmatrix}}_{\Phi} \underbrace{\begin{pmatrix} \nu_1 \\ \nu_2 \\ \nu_3 \end{pmatrix}}_{\nu}$$

which can be read as fault r_1 is affected by fault ν_1, r_2 is affected by fault ν_2, and r_3 is affected by fault ν_3. This notation offers also the possibility to consider disturbances $w_j, j \in \mathbf{s}$. They can be added to the description by treating them

like additional faults. This is done by defining also code vectors ϵ_j for them and add these to the structure matrix Φ, and adding the disturbance signals to the fault vector.

As already mentioned in Chapter 2, different kinds of structural residuals are known in the field of FDI, see e.g. Gertler (1998); Chen and Patton (1999). They can all be represented in the above given notation using corresponding structure matrices Φ. In Gertler (1998)[Chapter 7] a detailed discussion is given concerning the design of structured residuals. It provides several useful definitions like e.g.:

Undetectability in a structure A fault ν_i or disturbance w_j is *undetectable* in a residual structure if its column ϵ_i in the structure matrix Φ contains only zeroes ('0'). Note that while undetectability is undesirable for a fault, clearly this is the desirable behavior as far as disturbances are concerned.

Indistinguishability in a structure Two faults or disturbances are *indistinguishable* in a structure if their respective columns in the structure matrix are identical.

Weakly isolating structure We will refer to a structure as *weakly isolating* if all columns in the structure matrix are different and nonzero. Obviously, with such structure, all faults are detectable and all *single* faults are mutually distinguishable.

For further definitions, details, and explanations the reader is referred to Chapter 7 in Gertler (1998).

In this thesis the following general description of an efficient residual structure as introduced by Massoumnia *et al.* (1989) will be used:

In the j^{th} fault mode (i.e. when the j^{th} fault occurs; fault signal $\nu_j(t) \neq 0, j \in \mathbf{k}$), the residuals $r_i(t)$ for $i \in \Omega_j$ are nonzero, and the other residuals $r_\alpha(t)$ for $\alpha \in \mathbf{p} - \Omega_j$ decay asymptotically to zero. The specified family of coding sets $\Omega_j \subseteq \mathbf{p}, j \in \mathbf{k}$, is chosen such that, by knowing which of the residuals $r_i(t)$ are (or decay to) zero and which are not, the fault ν_j can be uniquely identified.

The different coding sets Ω_j are used to identify the occurring faults. A coding set contains a set of numbers that represents a specific subset of residuals $r_i(t), i \in \mathbf{p}$, i.e. $\Omega_j \subseteq \mathbf{p}, j \in \mathbf{k}$; where k denotes the number of faults and p the number of residuals. In case of single faults the following holds: Iff the complete set of residuals defined by the coding set Ω_j is affected by an occurring fault it can be said that the occurring fault is the j^{th} fault. For multiple faults extra conditions have to be fulfilled to avoid overlapping or cancellation of fault effects. The effects from multiple faults (e.g. ν_1 and ν_2) might add up in a way that it leads to a wrong decision (e.g. when $\Omega_1 \cup \Omega_2 = \Omega_3$ the fault ν_3 would be detected instead of ν_1 and ν_2). The simplest coding set that can handle both multiple and single faults would be $p = k$ and $\Omega_j = \{j\}$; in that case the j^{th} fault would only affect the j^{th} residual.

2.3 Robustness

Model-based FDI methods are based on a mathematical model, however, a precise and accurate model of a real system cannot be obtained. This can have different causes, e.g. an unknown structure of disturbances, different noise effects, and uncertain or time-varying (due to aging) system parameters. FDI methods that are able to handle these kind of *model uncertainty* are referred to as *robust*.

Model uncertainty can cause false and missed alarms, hence, it needs to be considered when implementing FDI. If it is not handled it can have such a strong impact that the FDI system becomes useless. There exist several approaches to handle the robustness issue. They are divided into *active* and *passive robustness* approaches. The active robustness approach deals with the model uncertainty in the residual generation phase. The goal is to avoid model uncertainty effects on the residuals. The passive robustness approach is implemented in the residual evaluation, e.g. by using time varying thresholds $\kappa(t)$, also known as *adaptive thresholds* (Clark (n.d.); Chen and Patton (1999)). One example of active robustness was already mentioned in Section 2.2.2. It handles the external disturbances by considering them as additional faults. Then the FDI system has to be designed such that these artificial faults are undetectable. This idea is also followed in the geometric approach described in the next chapter. Parameter uncertainty could be handled in the same way when it can be modeled as such a disturbance.

For further details about robust FDI the reader is referred to Chen and Patton

(1999); Patton (1997) and references therein.

2.4 Performance

Another important aspect of FDI design is the resulting performance of the obtained FDI system. It is closely related to robustness. In order to illustrate the need for good performance the following performance aspects are addressed:

False detection rate
A *false detection* (false alarm) is a fault alarm although no fault occurred. The FDI system has to be designed in such a way that the number of false alarms is acceptable low. This could mean that e.g. a high threshold is chosen to avoid false detection caused by disturbances or measurement noise. Obviously, a false detection leads to inappropriate actions in a FTCS, because initiates fault handling for a fault that is not present.

Missed detection rate
A *missed detection* (missed alarm) describes the situation that no alarm is given although a fault is present. The rate of missed alarms needs to be acceptable low. One way to achieve this is to choose a low threshold to ensure that also small faults can be detected. However, this is obviously in contrast with the solution to avoid false detection. A missed alarm has a serious effect on the FTCS as the occurring fault is not be handled.

Residual dynamics
Next to the problem of false and missed detection, the detection time, or better, the reaction time of the residuals, plays a very important role. This has mainly two reasons:

1. In order to handle faults in FTCS they need to be detected and isolated fast enough. Otherwise, the performance of the system might have reached an unacceptable level before handling is initiated.

2. When certain residuals have significantly different reaction times (detection time of a change in the residual) the result could be a false isolation. To illustrate this the following example is considered: Two faults are considered ν_1 and ν_2, with the corresponding code vectors $\epsilon_1 = (\ 1\ 0\ )^T$ and

$\epsilon_2 = (1\ 1)^T$. The second residual (r_2) reacts significantly slower than the first residual (r_1). When fault ν_2 occurs and the residual evaluation is carried out exactly at the point where the first residual has reacted, but the second not yet, this leads to a wrong residual evaluation. As a result fault ν_1 would be detected instead of ν_2.

Next to the reaction time, the response of the residual to an occurring fault is important. If the residual hits the threshold as long as the fault is present *strong detectability is obtained*. However, when it only hits the threshold during the transition of the fault ($\dot{\nu} \neq 0$) it is difficult to detect in a residual containing measurement noise effects. This might cause problems like wrong isolation or missed detection. One possibility to improve the FDI performance might be a filtering of the residual.

2.5 Summary

This section gave a brief overview over important aspects of model-based FDI. Especially the robust and performance issues are of high interest. They are a measure for the quality and applicability of a designed FDI system. The discussed issues in this chapter stressed the fact that the design of FDI is more than just generation of residuals. A complete design method is an optimization method which optimizes the above stated performance criteria. In the observer-based design this includes several aspects:

- finding an appropriate observer structure
- tuning of the observer to obtain structured residuals
- stability of the observer
- robustness issues
- optimization of the performance

These issues are addressed in the next chapter based on the geometric approach.

Chapter 3

Residual generation - geometric approach

Among the different approaches for fault detection and isolation (FDI) mentioned in Chapter 2 the geometric methods are of high interest. The geometric theory offers various advantages as it gives a general formulation of the FDI problem, and is more compact and more transparent for more general systems (like the nonlinear systems, which are considered in this thesis) than the algebraic approach. In recent years the existing geometric theory for the residual generation in linear systems based on the original work by Massoumnia (1986*a*), Massoumnia (1986*b*), and Massoumnia *et al.* (1989) has been extended. Formulations for different classes of nonlinear systems were derived in order to handle state-affine nonlinear systems (Hammouri *et al.* (1998)), and lately also the class of input-affine systems (Hammouri *et al.* (1999)). In a similar effort others recently presented more general solutions for the class of input-affine nonlinear systems (DePersis and Isidori (1999), DePersis (1999), DePersis and Isidori (2000), and references therein). The later results give a very detailed geometric description of how to tackle the residual generation problem for nonlinear systems.

This chapter gives a review of these different geometric ideas and illustrates how they are connected. They are all based on the same main idea of designing a residual generator to solve the fundamental problem of residual generation (FPRG). A formulation of the FPRG for each considered class of systems is presented in Section 3.2. The common idea is to use a residual generator based on

the mathematical model of the considered system and using the available signals - control inputs and measured outputs. This idea is also referred to as *analytical redundancy*, see chapter 2 for more details. The first geometric description of a solution for the FPRG was given by Massoumnia *et al.* (1989) for linear systems and provides necessary and sufficient conditions for a solution to exist. This original work is described in detail in the Sections 3.2.1 and 3.3.1 in order to introduce the basic idea of the geometric approach and the used geometric concepts. (The used (geometric) theory is described in Section 3.1 and Appendix A. Hence, no special background in geometric theory is required to follow the ideas presented in this chapter.) After a detailed description of the linear case it is illustrated how it has been extended to the different classes of nonlinear systems - state-affine and input-affine nonlinear systems. At the end of the chapter the results are summarized and compared to other existing approaches. Following the summary, some concluding remarks will be given. The duality of the solutions to other well-studied problems in geometric control theory is emphasized, e.g. the restricted control decoupling problem.

The application of the geometric approach is illustrated by a detailed example in Chapter 4. There the geometric approach is applied to a ship propulsion system in order to obtain successful FDI. The calculations are explained in detail (Appendix C) and simulation results are presented.

3.1 Notation and preliminaries

The notation in this chapter deviates from the notation in some of the references. This is in order to make the notation consistent throughout the chapter and the rest of the thesis. The used notation and mathematics are explained in the following. For further details the reader is referred to Appendix A, the nomenclature table at the beginning of the thesis, and the given references. The notation corresponds widely to the one used in Massoumnia (1986*b*).

In the thesis, script letters as $\mathcal{X}, \mathcal{U}$, and $\mathcal{Y}$ denote real vector spaces, with typical elements being denoted by x, u, and y. The dimension of the different vector spaces, e.g. $\mathcal{X}$, is described by $d(\mathcal{X})$. Example: $x \in \mathcal{X} \subset \mathbb{R}^n$, where $d(\mathcal{X}) = n$. The *dual space*[1] of $\mathcal{X}$ is written as $\mathcal{X}'$.

[1] For a detailed explanation of the term *dual space* the reader is referred to Appendix A.4.

The *annihilator* of $\mathcal{S}$, $\mathcal{S} \subseteq \mathcal{X}$, is denoted by $\mathcal{S}^{\perp}$; $\mathcal{S}^{\perp} = \{x^{'}\,;\, x^{'}\mathcal{S} = 0,\ x^{'} \in \mathcal{X}^{'}\}$, hence, $\mathcal{S}^{\perp} \subseteq \mathcal{X}^{'}$. The zero vector, zero space, etc. are denoted by 0.

Matrices and linear maps are both denoted by capital italic letters, e.g. A, B, and C. The maps $A : \mathcal{X} \to \mathcal{X}$, $B : \mathcal{U} \to \mathcal{X}$, and $C : \mathcal{X} \to \mathcal{Y}$ are fixed throughout and are associated with the linear system (C, A, B):
$\dot{x}(t) = Ax(t) + Bu(t);\ y(t) = Cx(t)$.
The dimensions are given by $d(\mathcal{X}) = n$, $d(\mathcal{U}) = m$, and $d(\mathcal{Y}) = l$.

$ImB = \mathcal{B}$ denotes the *image (range)* of B, $\mathcal{B} = \{y\,;\, y = Bx,\ x \in \mathcal{X}\}$. $KerC$ denotes the *kernel* of C, $KerC = \{x\,;\, Cx = 0,\ x \in \mathcal{X}\}$.

The spectrum (eigenvalues) of a matrix A is denoted by $\sigma(A)$. A bold printed integer describes a finite set of integers, e.g. $\mathbf{k} = \{1, \ldots, k\}$. A set of complex numbers $\Lambda \in \mathbb{C}$ is symmetric if $\lambda \in \Lambda$ implies $\lambda^{*} \in \Lambda$ where * denotes the complex conjugate.

If B is *injective*[2] , then B^{-l} denotes a left inverse of B (i.e. $B^{-l}B = I_m$), where I_m denotes the $m \times m$ identity matrix. If C is *surjective*[3], then C^{-r} denotes a right inverse of C (i.e. $CC^{-r} = I_l$), where I_l denotes the $l \times l$ identity matrix.

A subspace $\mathcal{S} \subseteq \mathcal{X}$ is termed *A-invariant* if $A\mathcal{S} \subseteq \mathcal{S}$; i.e. a solution $x(t)$ of the differential equation $\dot{x} = Ax$ that starts in $\mathcal{S}$ ($x(t = 0) \in \mathcal{S}$), stays in $\mathcal{S}$ ($x(t) \in \mathcal{S} \forall t \in \mathbb{R}^{+}$). Let $\mathcal{S} \subseteq \mathcal{X}$ be A-invariant; the restriction of A to $\mathcal{X}/\mathcal{S}$ is written as $A : \mathcal{X}/\mathcal{S}$. $\mathcal{X}/\mathcal{S}$ denotes the *factor space*[4] of $\mathcal{S} \subset \mathcal{X}$.

During the whole thesis $\mathcal{S}$ denotes a *(C, A)-unobservability subspace*[5] (u.o.s.).

A system is called *state-affine* when it is linear in the states. Similar, *input-affine* systems are linear in the inputs.

For a more detailed description and explanation of the used geometric concepts in this chapter the reader is referred to Wonham (1985), Nijmeijer and van der Schaft (1990), and Isidori (1995).

[2] A map $B : X \to Y$ is injective when: $Bv = Bu \Rightarrow v = u$ or equivalently $KerB = 0$.

[3] A map $C : X \to Y$ is surjective if $ImC = \mathcal{Y}$.

[4] For a detailed explanation of the term *factor space* the reader is referred to Appendix A.5.

[5] For a detailed explanation of the term *unobservability subspace* the reader is referred to Appendix A.2.

3.2 Fundamental problem of residual generation

This section describes the *fundamental problem of residual generation* (FPRG) for different classes of systems. It starts with describing the linear case for which the FPRG was originally formulated by Massoumnia *et al.* (1989) and shows how it has been extended for nonlinear systems that are either affine in the states or affine in the inputs.

3.2.1 FPRG for linear systems

The first formulation of the FPRG was stated for finite-dimensional, linear, time-invariant (LTI) systems in Massoumnia *et al.* (1989) and is based on the FDI filter problem (FDIFP) which is a generalized version of the Beard Jones detection filter problem (BJDFP). The BJDFP considers linear time-invariant systems (LTI) of the following form:

$$\dot{x}(t) = Ax(t) + Bu(t) + \sum_{i=1}^{k} L_i \nu_i(t) \tag{3.1}$$

$$y(t) = Cx(t) \tag{3.2}$$

where $x(t) \in \mathcal{X} \subset \mathbb{R}^n$ describes the states, $u(t) \in \mathcal{U} \subset \mathbb{R}^m$ the known control inputs, and $y(t) \in \mathcal{Y} \subset \mathbb{R}^l$ the measured (known) system outputs. $\nu_i(t) \in \mathcal{M}_i \subset \mathbb{R}^{k_i}$ with $i \in \mathbf{k}$ describes the behaviour (concerning time and magnitude) of the i^{th} fault and is denoted as *fault signal*. The *fault signatures* are given by the maps (matrices) $L_i : \mathcal{M}_i \to \mathcal{X}$ ($L_i \in \mathbb{R}^{n \times k_i}$). They describe in which way (direction) the fault affects the system. The size of the matrices A, B, and C is obvious from (3.1) and (3.2).

Knowledge about the fault signature L_i (*fault modeling*) is required for the considered model-based fault detection and isolation methods. The fault signal $\nu_i(t)$ is an arbitrary and unknown signal which can represent several different fault behaviours. Choosing L_i to be equal to the i^{th} column of the B matrix gives for example the possibility to model a fault in the i^{th} actuator. As $\nu_i(t)$ is arbitrary it could model a complete loss of the actuator ($\nu_i(t) = -u_i(t)$) or just an offset ($\nu_i(t) = const.$). For more details about fault modeling the reader is referred to Chapter 2 and Chen and Patton (1999). In e.g. Chen and Patton (1999) an extra term ($\sum_{i=1}^{k} R_i f_i(t)$) is added to the output equation (3.2) to model sensor faults. It is omitted here due to the fact that sensor faults can be included in a model like

(3.1) and (3.2) by adding additional dynamics (additional fault signals and states in (3.1)). A precise description of this fault modeling describing sensor faults by pseudo-actuator faults can be found in Massoumnia (1986*a*) and Hashtrudi-Zad and Massoumnia (1999).

Massoumnia (1986*b*) gives a geometric formulation of the BJDFP and necessary and sufficient conditions for its solution. It is the first geometric approach to tackle fault detection and isolation (FDI). The details of the BJDFP can be found in Beard (1971) and Jones (1973). It is based on a full-order Luenberger observer and is one of the first observer-based FDI approaches. They propose a systematic procedure to design an observer for the monitored system and tune its observer gain in such a way that the prediction error (or innovation) can be used for residual generation: In absence of faults, system disturbances, and modeling errors the residual vector is designed to tend (be equal) to zero. Under presence of a fault its length is supposed to grow significantly different from zero (*fault detection*). Furthermore, the gain is tuned in such a way that the direction of the residual vector in the residual space (output space) can be used to identify the fault (*fault isolation*). In that case the residual is also called a directional residual, see section 2.7 in Chen and Patton (1999). Obviously, when considering multiple (simultaneous) faults, the dimension of the residual space determines the maximal number of faults that can be isolated from each other. This is due to the fact that the dimension of the residual space determines the maximal number of independent directions. Otherwise the effects of two simultaneously occurring faults might add up in a way, such, that the resulting residual vector points in a direction, which is used to isolate a third fault, and vice-versa. More details about the evaluation and design of residuals is given in Chapter 2.

This first approach of a FDI filter led to the following general FDI filter problem formulation given in Massoumnia *et al.* (1989).

Definition 3.1 (Fault detection and isolation filter problem (FDIFP)): *Considering the system (3.1) and (3.2), the FDIFP is to design an LTI dynamic residual generator that takes the known signals $u(t)$ and $y(t)$ (observables of the system) as inputs and generates a set of residual vectors $r_i(t), i \in \mathbf{p}$, with the following properties:*

1. *When no fault is present, all the residuals $r_i(t)$ decay asymptotically to zero. Hence, the net transmission from $u(t)$ to the residuals is zero, and*

the modes observable from the residuals are asymptotically stable.

2. *In the j^{th} fault mode (i.e. when $\nu_j(t) \neq 0, j \in \mathbf{k}$), the residuals $r_i(t)$ for $i \in \Omega_j$ are nonzero, and the other residuals $r_\alpha(t)$ for $\alpha \in \mathbf{p} - \Omega_j$ decay asymptotically to zero. Here the pre-specified family of coding sets $\Omega_j \subseteq \mathbf{p}, j \in \mathbf{k}$, is chosen such that, by knowing which of the $r_i(t)$ are (or decay to) zero and which are not, the fault ν_j can be uniquely identified.*

Definition 3.1 uses the concept of coding sets Ω_j to identify the occurring faults. A coding set contains a set of numbers that represents a specific subset of the different residuals $r_i(t), i \in \mathbf{p}$, i.e. $\Omega_j \subseteq \mathbf{p}, j \in \mathbf{k}$; where k denotes the number of faults and p the number of residuals. If the complete set of residuals defined by the coding set Ω_j is affected by an occurring fault it can be said that the occurring fault is the j^{th} fault. The simplest coding set would be $p = k$ and $\Omega_j = \{j\}$; in that case the j^{th} fault would only affect the j^{th} residual. More details can be found in Massoumnia *et al.* (1989).

The fundamental problem of residual generation (FPRG) for LTI systems is a restricted version of the FDIFP and was for the first time stated in Massoumnia *et al.* (1989). It considers only two different faults and aims for a stable residual generator that generates a signal (*residual*) that is sensitive to one fault and insensitive to the other. Considering more than two faults leads to the extended fundamental problem of residual generation (EFPRG) which is also presented in Massoumnia *et al.* (1989). It is based on generalizing the results for the FPRG as shown later at the end of section 3.3.1.

In the following a definition of the FPRG is given for systems of the following linear form (specific version of (3.1) and (3.2) with $k = 2$):

$$\dot{x}(t) = Ax(t) + Bu(t) + L_1\nu_1(t) + L_2\nu_2(t) \tag{3.3}$$
$$y(t) = Cx(t) \tag{3.4}$$

and a residual generator of the following general form:

$$\dot{z}(t) = Fz(t) - Ey(t) + Gu(t) \tag{3.5}$$
$$r(t) = Mz(t) - Hy(t) + Ku(t) \tag{3.6}$$

where $z(t) \in \mathcal{Z} \subset \mathbb{R}^q$ and $r(t) \in \mathcal{P} \subset \mathbb{R}^p$. As shown in Massoumnia *et al.*

(1989) the system and residual equations can be combined in the following way:

$$\begin{pmatrix} \dot{x}(t) \\ \dot{z}(t) \end{pmatrix} = \begin{pmatrix} A & 0 \\ -EC & F \end{pmatrix} \begin{pmatrix} x(t) \\ z(t) \end{pmatrix} + \begin{pmatrix} B & L_2 \\ G & 0 \end{pmatrix} \begin{pmatrix} u(t) \\ \nu_2(t) \end{pmatrix} + \begin{pmatrix} L_1 \\ 0 \end{pmatrix} \nu_1(t) \tag{3.7}$$

$$r(t) = \begin{pmatrix} -HC & M \end{pmatrix} \begin{pmatrix} x(t) \\ z(t) \end{pmatrix} + \begin{pmatrix} K & 0 \end{pmatrix} \begin{pmatrix} u(t) \\ \nu_2(t) \end{pmatrix} \tag{3.8}$$

The system (3.7) and (3.8) can also be written in the following obvious way:

$$\dot{x}^e(t) = A^e x^e(t) + B^e u^e(t) + L^e \nu_1(t) \tag{3.9}$$

$$r(t) = H^e x^e(t) + K^e u^e(t) \tag{3.10}$$

where $x^e(t) \in \mathcal{X}^e = \mathcal{X} \oplus \mathcal{Z}$ and $u^e(t) \in \mathcal{U}^e = \mathcal{U} \oplus \mathcal{M}_2$.

Definition 3.2 (Massoumnia *et al.* (1989))(Fundamental problem of residual generation (FPRG)): *Considering the system (3.3) and (3.4), the linear FPRG is to design an LTI dynamic residual generator by finding the appropriate matrices in (3.5) and (3.6) such that the following constrains are satisfied for system (3.9) and (3.10):*

(i) *r is unaffected*[6] *by u^e*

(ii) *The map from ν_1 to r is input observable*[7]

and that the observable modes of the pair (H^e, A^e) be asymptotically stable, so that the contribution to $r(t)$ of initial conditions in (3.9) and (3.10) dies out asymptotically .

While Condition (i) assures that the residual will not be affected by the control input $u(t)$ and the other fault $\nu_2(t)$, Condition (ii) assures that a fault $\nu_1(t)$ can be *seen* (detected) in the residual. Without Condition (ii) it might happen that the fault might only affect states of the residual generator (3.5) that do not affect the residual (3.6). A detailed discussion about this condition is given in Massoumnia *et al.* (1989).

[6] For a definition of *unaffected* see Appendix A.1.

[7] For a definition of *input observability* see Appendix A.6.

Remark 3.3 Even if not stated explicitly, solving the FPRG handles in principal several different aspects of efficient FDI. Condition (i) assures that neither the input nor the second fault ν_2 affect the residual, hence, it prevents *false alarms* and helps to isolate fault ν_1 from fault ν_2. As the second fault ν_2 could also represent a disturbance Condition (i) also handles the problem of *robustness* against disturbances. The problem of *missed alarms* is handled by Condition (ii) which assures that the fault ν_1 will have an effect on the residual. Stability of the residual generator is considered in the additional comment in Definition 3.2. Section 3.2.3 addresses these aspects more explicit for the nonlinear systems that are affine in the inputs, faults, and disturbances.

As mentioned in Remark 3.3 the fundamental problem of residual generation (FPRG) as it is defined in Definition 3.2 incorporates the basic idea to handle all important aspects of successful FDI. Therefore, it has recently been extended in the literature to nonlinear systems. These extended versions are presented in the next two sections.

3.2.2 FPRG for state-affine nonlinear systems

The previous chapter presented a definition of the linear FPRG. In this section a generalization of the linear FPRG to the class of state-affine systems up to output injection (Hammouri *et al.* (1998)) is described. Next to Kinnaert *et al.* (1995), Yu and Shields (1994) and Kinnaert (1999) it is one of the first approaches considering an extension of the FPRG to a special class of nonlinear systems. It gives a definition of the problem and a sufficient condition for a solution to exist. The condition and a solution for the problem using a Kalman-like observer will be presented in section 3.3.2.

The approach considers systems of the following kind (the time dependence is omitted for a better readability):

$$\dot{x} = A(u)x + \psi(u,y) + L_1(x)\nu_1 + L_2(x)\nu_2 \tag{3.11}$$
$$y = Cx \tag{3.12}$$

and a smooth residual generator system of the form:

$$\dot{z} = f_r(z,u,y) \tag{3.13}$$
$$r = h_r(z,u,y) \tag{3.14}$$

where $x(t) \in \mathcal{X} \subset \mathbb{R}^n$, $u(t) = (u_1(t), \ldots, u_m(t)) \in \mathcal{U}$ an open subset of $\mathbb{R}^m$, $\nu_i \in \mathbb{R}$, $i = 1, 2$, and $y(t) \in \mathcal{Y} \subset \mathbb{R}^l$. $A(u)$ is a $n \times n$ matrix which is analytic with respect to u. $\psi(u, y)$ and $L_i(x)$, $i = 1, 2$ are analytic vector fields. $z(t) \in \mathbb{R}^q$ and $r(t) \in \mathbb{R}^p$. f_r and h_r are of class $\mathcal{C}^\infty$. Obviously, $r(t) = r(x(0), z(0), u, \nu_1, \nu_2, t)$.

In Hammouri *et al.* (1998) the following definition of the FPRG for the above presented class of systems (3.11) and (3.12) is given:

Definition 3.4 (Fundamental problem of residual generation (FPRG) for state affine systems up to output injection): *System (3.13) and (3.14) is a residual generator for the detection and isolation of the fault ν_1 in system (3.11) and (3.12) if there exists $\mathcal{U}$, a set of admissible controls defined on $\mathbb{R}^+$, such that:*

(i) *For $\nu_1 = 0$, $\forall u \in \mathcal{U}$; $\forall x(0) \in \mathbb{R}^n$, $\forall z(0) \in \mathbb{R}^q$; $\forall \nu_2 \in L^\infty_{loc}$ (the space of locally bounded measurable functions):*
$r(x(0), z(0), u, 0, \nu_2, t) \to 0$ *as* $t \to +\infty$

(ii) *For $\nu_2 = 0$, $\forall u \in \mathcal{U}$; $\forall z(0) \in \mathbb{R}^q$, $\exists x(0) \in \mathbb{R}^n$; $\exists t \geq 0$; $\exists \nu_1, \overline{\nu}_1 \in L^\infty_{loc}$ such that $r(x(0), z(0), u, \nu_1, 0, t) \neq r(x(0), z(0), u, \overline{\nu}_1, 0, t)$.*

Comparing Definition 3.2 with Definition 3.4 shows that both include the same requirements for the residual generator. The residual signal has to be insensitive to the second fault $\nu_2(t)$, sensitive to the first fault $\nu_1(t)$, and have stable dynamics for each initial condition. The different formulations result from the fact that they handle different classes of systems.

3.2.3 FPRG for input-affine nonlinear systems

In the last two years different definitions of the FPRG for nonlinear systems that are affine in the inputs, faults, and disturbances were given (see e.g. Hammouri *et al.* (1999), DePersis and Isidori (1999), or Åström *et al.* (2000)[chapter 10]). This section presents the definition given in DePersis (1999). It does not only treat the basic idea of the linear FPRG (Section 3.2.1) and expands it to nonlinear systems, but it also includes the EFPRG (Massoumnia *et al.* (1989)) and robustness against disturbance (see e.g. Chen and Patton (1999)). As stated in Remark 3.3 the classical FPRG contains the basic idea of how to handle other

faults and thereby also disturbances, but it was not stated explicitly as it is done in the following definition for the following class of systems:

$$\dot{x} = f(x) + \sum_{i=1}^{m} g_i(x)u_i + l(x)\nu + \sum_{i=1}^{s} p_i(x)w_i \tag{3.15}$$

$$y_j = h_j(x), \quad j \in \mathbf{l} \tag{3.16}$$

in which the states x are defined on a neighborhood $\mathcal{N}$ of the origin in $\mathbb{R}^n$. u_i, $i \in \mathbf{m}$, denotes the inputs and y_j, $j \in \mathbf{l}$, the outputs. $\nu \in \mathbb{R}$ is a scalar fault signal with the nonlinear fault signature $l(x)$. $f(x)$, $g_i(x), i \in \mathbf{m}$, $l(x)$, and $p_i(x), i \in \mathbf{s}$ are smooth vector fields and $h_j(x), j \in \mathbf{l}$ are smooth functions. Furthermore, let $f(0) = 0$ and $h(0) = 0$. $w = [w_1 w_2 \dots w_s]^T \in \mathbb{R}^s$ describes all the disturbances and other fault signals that should not affect the residual. Hence, the following nonlinear version of the FPRG is able to handle the problems of fault isolation, robustness against disturbances, false alarms and missed detection as mentioned in Remark 3.3.

For the given class of systems the following definition of the local nonlinear FPRG (DePersis (1999)) can be given:

Definition 3.5 (Local nonlinear fundamental problem of residual generation (l-NLFPRG)): *Considering the system of the form (3.15) and (3.16) the l-NLFPRG is to find, if possible, a filter*

$$\dot{z} = \tilde{f}(y, z) + \sum_{i=1}^{m} \tilde{g}_i(y, z)u_i \tag{3.17}$$

$$r = \tilde{h}(y, z) \tag{3.18}$$

where $z \in \mathbb{R}^q$, $r \in \mathbb{R}^p$, $1 \leq p \leq l$. $\tilde{f}(y, z)$, $\tilde{g}_i(y, z), i \in \mathbf{m}$, and $\tilde{h}(y, z)$ are smooth vector fields, with $\tilde{f}(0, 0) = 0$ and $\tilde{h}(0, 0) = 0$, such that, when considering the cascaded system (with obvious meaning of the symbols, similar to (3.9) and (3.10))

$$\dot{x}^e = f^e(x^e) + \sum_{i=1}^{m} g_i^e(x^e)u_i + l^e(x^e)\nu + \sum_{i=1}^{s} p_i^e(x^e)w_i \tag{3.19}$$

$$r = h^e(x^e) \tag{3.20}$$

defined on $\mathcal{N}^e$, a neighborhood of $x^e = (x, z) = (0, 0)$, the following properties hold:

(i) *if* $\nu = 0$*, then* r *is unaffected*[8] *by* u_i*,* w_j*,* $\forall i, j$*;*

(ii) r *is affected*[9] *by* ν*;*

(iii) $\lim_{t\to\infty} \|r(t; x^0, z^0; u_1, \ldots, u_m, \nu = 0, w_1, \ldots, w_s)\| = 0$ *for any initial condition* x^0*,* z^0 *in a suitable set containing the origin* $(x, z) = (0, 0)$*, and any set of admissible inputs (note that the convergence to zero of the residual is required in absence of the fault (*$\nu = 0$*)).*

For linear systems (3.1) and (3.2) this definition of the l-NLFPRG reduces exactly to Definition 3.2. In Definition 3.5 Condition (i) assures robustness, i.e. that the control signals u_i and the disturbances (and other faults) u_l do not affect the residual in the fault-free case ($\nu = 0$) and, therefore, cannot generate false alarms. For robustness against model uncertainty it has to be possible to model the uncertainties as additional disturbances u_l. For more details about robustness against model uncertainty see the review in Chen and Patton (1999).

In the case that $\nu \neq 0$ the inputs and disturbances may affect the residual, because Condition (ii) assures that they cannot vanish the effect of the fault ν on the residual and, hence, cannot cause missed alarms. Obviously, solving the l-NLFPRG means finding a residual generator which is robust against disturbances. Condition (iii) assures its stability.

[8] For a definition of *unaffected* see Appendix A.1.
[9] For a definition of *affected* see Appendix A.1.

3.3 Solving the FPRG

Different geometric solutions exist for the above described residual generation problems. They are all based on the geometric concept of using unobservability subspaces (originally introduced as complementary observability subspaces by Willems and Commault (1981)) that was first presented for linear systems in Massoumnia (1986*b*) and Massoumnia *et al.* (1989). Hence, this approach is described in detail in the next section and followed by its extended versions for the different classes of nonlinear systems. Each section presents conditions for a solution to exist. Additionally, different designs to solve the corresponding version of the FPRG are presented.

3.3.1 Solution for linear systems

The fundamental problem of residual generation (FPRG) as formulated in Definition 3.2 can be solved by the method presented in Massoumnia *et al.* (1989). It uses the geometric concept of an unobservability subspace to derive a solution and sufficient and necessary conditions for its existence. The idea has been derived from the results presented in Massoumnia (1986*b*) and White and Speyer (1987) which have been inspired by the work in Beard (1971) and Jones (1973); e.g. Massoumnia (1986*b*) gives an original geometric approach to handle a generalized version of the Beard Jones detection filter problem (BJDFP). It uses a full-order observer which, however, limits significantly the classes of problems that have solutions - because the set of possible failure modes (ν_i, $i \in \mathbf{k}$) must satisfy a strong mutual detectability condition (Massoumnia (1986*b*)) - but it also makes the FDI problem and the design process appear more complicated than necessary (Massoumnia *et al.* (1989)).

In the following an approach taken from Massoumnia *et al.* (1989) is presented that does not have these structural constrains. It uses a more general, finite-dimensional, causal, LTI system as residual generator (see (3.5) and (3.6)) to solve the FPRG. Hence, necessary and sufficient conditions can be obtained for a wider class of systems than in (Massoumnia (1986*b*)).

As a starting point the cascaded system (3.9) and (3.10) as given in Section 3.2.1

is considered:

$$\dot{x}^e(t) = A^e x^e(t) + B^e u^e(t) + L^e \nu_1(t) \quad (3.21)$$

$$r(t) = H^e x(t) + K^e u^e(t) \quad (3.22)$$

It can be seen directly that in order to assure that the residual $r(t)$ is not sensitive to the input signal $u(t)$ and the second fault $\nu_2(t)$ it has to be insensitive concerning the new constructed input $u^e(t)$ (see also Condition (i) in Definition 3.2). This leads to the following conditions:

$$K^e = 0 \quad (3.23)$$

$$\text{and} \quad \langle A^e | \mathcal{B}^e \rangle \subseteq \mathcal{S}^e := \langle KerH^e | A^e \rangle \quad (3.24)$$

where condition (3.23) assures that input $u^e(t)$ has no direct effect on the residual. The subspace $\mathcal{S}^e$ denotes the unobservability subspace of the cascaded system, i.e. all states $x^e \in \mathcal{S}^e$ cannot be observed from the residual. It is defined by $\mathcal{S}^e := \langle KerH^e | A^e \rangle = KerH^e \cap A^{e-1} KerH^e \cap \cdots \cap A^{e-n+1} KerH^e$ where $A^{e-k} KerH^e = \{x : A^{ek} x \in KerH^e\}$. $\langle KerH^e | A^e \rangle$ is also called the maximal A^e-invariant subspace contained in $KerH^e$, i.e. the unobservable subspace of (H^e, A^e). $\langle A^e | \mathcal{B}^e \rangle = \mathcal{B}^e + A^e \mathcal{B}^e + \cdots + A^{en-1} \mathcal{B}^e$ describes the reachable subspace that is reachable by the input $u^e(t)$ in the state equation (3.21). Hence, Condition (3.24) assures that the input $u^e(t)$ does not affect the residual indirectly via the states' dynamics. $\langle A^e | \mathcal{B}^e \rangle$ is also called the infimal A^e-invariant subspace containing $\mathcal{B}^e$, i.e. the reachable subspace of (A^e, B^e). To fulfill Condition (ii) in Definition 3.2 it is clear that the following condition has to be fulfilled to assure that all states affected by the fault ν_1 are observable from the residual:

$$L^e \text{ is injective} \quad \text{and} \quad \mathcal{L}^e \cap \mathcal{S}^e = 0, \quad \text{where} \quad \mathcal{L}^e = ImL^e \quad (3.25)$$

In Massoumnia *et al.* (1989) it is shown that the conditions (3.23)-(3.25) lead to the following conditions for the original system (3.3) and (3.4):

$$\mathcal{S} \in \mathcal{S}(\mathcal{L}_2), \quad (3.26)$$

$$L_1 \text{ is injective} \quad \text{and} \quad \mathcal{L}_1 \cap \mathcal{S} = 0 \quad (3.27)$$

where $\mathcal{S}$ is a (C, A)-unobservable subspace[10] (u.o.s.) and $\mathcal{S}(\mathcal{L}_2)$ is a family of (C, A)-u.o.s.es containing the range of L_2 denoted by $\mathcal{L}_2$. Obviously, conditions (3.26) and (3.27) hold only if the following condition is fulfilled:

[10] For its calculation see Appendix A.2.

$$\mathcal{S}^* \cap \mathcal{L}_1 = 0 \tag{3.28}$$

where $\mathcal{S}^* = \inf \underline{\mathcal{S}}(\mathcal{L}_2)$. Condition (3.28) can be proven to be also sufficient (Massoumnia *et al.* (1989)), which leads to the following theorem:

Theorem 3.6 *The linear fundamental problem of residual generation (FPRG), Definition 3.2, has a solution if and only if:*

$$\mathcal{S}^* \cap \mathcal{L}_1 = 0. \tag{3.29}$$

The proof of the sufficiency of Condition (3.29) in Massoumnia *et al.* (1989) describes a design procedure for the 6 matrices (design parameters) of the residual generator (3.5) and (3.6) and, hence, to a solution. It is based on the following steps[11] (where the dimension of the residual generator (observer) is given by $q = n - d(\mathcal{S}^*)$):

(1) Find a $n \times l$ matrix D_0 such that $D_0 \in \underline{\mathcal{D}}(\mathcal{S}^*)$, i.e. such that $(A + D_0 C)\mathcal{S}^* \subseteq \mathcal{S}^*$.

(2) Find a canonical projection $P : \mathcal{X} \to \mathcal{X}/\mathcal{S}^*$, i.e. a $q \times n$ matrix that projects the states x into a q-dimensional subspace that is not affected by the second fault ν_2.

(3) Calculate the $q \times q$ matrix $A_0 = (A + D_0 C : \mathcal{X}/\mathcal{S}^*)$, such that $A_0 : \mathcal{X}/\mathcal{S}^* \to \mathcal{X}/\mathcal{S}^*$ and $A_0\, P = P\,(A + D_0 C)$.

(4) Let the $p \times l$ matrix H be a solution of $KerHC = \mathcal{S}^* + KerC$.

(5) Let the $p \times q$ matrix M be the unique solution of: $MP = HC$.

(6) Then by construction, the pair (M, A_0) is observable, so there exists a $q \times p$ matrix D_1, such that $\sigma(F) = \Lambda$, where $F = A_0 + D_1 M$ and Λ is an arbitrary self-conjugate set. This gives the freedom to shape the behaviour of the residual and to assure the stability of the residual generator (3.5) and (3.6).

[11] The reader unfamiliar with the notation or terms is referred to Appendix A.2.

After following this procedure and denoting the right inverse of P by P^{-r}, the missing matrices, E, G, and K (for F, H, and M see above) of the residual generator (3.5) and (3.6) can be calculated as follows:

$$D = D_0 + P^{-r}D_1H \qquad E = PD \qquad G = PB \qquad K = 0.$$

When defining $e(t) = z(t) - Px(t)$ the error dynamics of the residual generator that solves the linear FPRG can be derived:

$$\dot{e}(t) = Fe(t) - PL_1\nu_1(t) \tag{3.30}$$
$$r(t) = Mz(t) - Hy(t) = Me(t). \tag{3.31}$$

The dimension of the residual generator (observer) is given by $q = n - d(\mathcal{S}^*)$, i.e. it is not a full-order observer ($q < n$) as used in the original work by Massoumnia (1986*b*).

Remark 3.7 (Massoumnia *et al.* (1989)) *Obviously, as there might be other unobservability subspaces $\mathcal{S} \supset \mathcal{S}^*$ that satisfy $\mathcal{S} \cap \mathcal{L}_1 = 0$ the dimension of the residual generator could be further reduced. But as there does not exist a systematic way to obtain such an u.o.s. as it does for the infimal u.o.s. $\mathcal{S}^*$ a residual generator having a lower dimension is difficult to design. As there exists a systematic way*[12] *to calculate the infimal u.o.s. $\mathcal{S}^*$ the Condition (3.29) can be checked straightforward. If it is fulfilled the design of the residual generation can be achieved by following the above given procedure.*

In Massoumnia *et al.* (1989) the *generic* solvability[13] of the FPRG is mentioned for the arbitrary system matrices A, C, L_1, and L_2 with the respective dimensions $n \times n$, $l \times n$, $n \times k_1$, and $n \times k_2$. It says that the FPRG generically has a solution if and only if $k_1 + k_2 \leq n$ and $k_2 < l$. For the proof the reader is referred to Massoumnia (1986*a*). Further information concerning the generic solvability of the linear FPRG is given in Hashtrudi-Zad and Massoumnia (1999), where also the concept of generic solvability is described in a clear and understandable way.

The linear FPRG is a reduced version of the FDIFP. This can be seen for $k = 2$

[12] For the algorithm see Appendix A.2.

[13] A problem whose solvability depends on a set of parameters is said to be *generically solvable* if it is solvable for almost every set of the parameter values (Hashtrudi-Zad and Massoumnia (1999)).

in Definition 3.1. An *extension* of the above solved FPRG, hence, also referred to as EFPRG, is briefly considered in the following. The EFPRG is equal to the FDIFP when for the later only the coding sets $\Omega_i = \{i\}, i \in \mathbf{k}$ are considered. Obviously, the EFPRG gives the possibility to handle several faults, and therefore, also disturbances when they are treated as additional faults. Furthermore, it can detect and isolate simultaneous faults from each other. By following the same geometric idea as for the FPRG Massoumnia *et al.* (1989) give the following result for the EFPRG:

Theorem 3.8 *The extension of the linear fundamental problem of residual generation (EFPRG) has a solution if and only if:*

$$\mathcal{S}_i^* \cap \mathcal{L}_i = 0, \quad i \in \mathbf{k} \qquad \textit{where} \quad \mathcal{S}_i^* := \inf \underline{\mathcal{S}}(\sum_{j \neq i} \mathcal{L}_i) \tag{3.32}$$

where $\mathcal{S}_i^*$ denotes the smallest unobservability subspace that includes all fault effects $\mathcal{L}_j$ from the faults $\nu_j, j \neq i$.

A family of fault signatures satisfying the condition (3.32) is called a *strongly identifiable* family. Hence, Theorem 3.8 is equivalent to the statement that the extension of the linear fundamental problem of residual generation (EFPRG) has a solution if and only if the family of handled fault events is strongly identifiable. For the generic solvability of the EFPRG the reader is referred to Hashtrudi-Zad and Massoumnia (1999).

This section presented the basic geometric concept of using unobservability subspaces to solve the linear FPRG and its extension, the EFPRG. Necessary and sufficient conditions for a solution to exist were given as well as a design procedure for a LTI residual generator. The following sections show how this result by Massoumnia *et al.* (1989) has been generalized for different classes of nonlinear systems.

3.3.2 Solution for state-affine nonlinear systems

A solution for the FPRG for state affine systems up to output injection (described by Definition 3.4 in section 3.2.2) is given in this section. It is taken from Hammouri *et al.* (1998) and provides a sufficient condition for its existence. The proposed residual generator has the structure of a Kalman-like observer which

is applicable to the class of state affine systems. The considered systems (3.11) and (3.12):

$$\dot{x} = A(u)x + \psi(u,y) + L_1(x)\nu_1 + L_2(x)\nu_2, \quad y = Cx \tag{3.33}$$

obviously, also include linear and bilinear systems.

Applying a linear output transformation (constant matrix H, $H : \mathcal{Y} \to \mathcal{Y}$) and a $n \times l$ analytical matrix $D(u)$ the system (3.33) can be rewritten as:

$$\dot{x} = (A(u) \underbrace{+D(u)C)x - D(u)y}_{=0} + \psi(u,y) + L_1(x)\nu_1 + L_2(x)\nu_2, \tag{3.34}$$

$$y = HCx \tag{3.35}$$

The idea of the solution presented in Hammouri *et al.* (1998) is to choose $D(u)$ and H such that the unobservability subspace $\Delta(H) = Ker d\mathcal{O}(\mathcal{HC})$ of the system (3.34) and (3.35) includes the range of $L_2(x)$ but not the range of $L_1(x)$. For more details about the unobservability subspace $\Delta(H)$ and the observability subspace $d\mathcal{O}(\mathcal{HC})$ the reader is referred to Appendix A.7. Obviously, the basic idea behind this approach is the same as in the previous section and, hence, as in Massoumnia *et al.* (1989). It is based on hiding the unwanted fault effects on the states of the residual generator in an unobservability space. However, as pointed out in Hammouri *et al.* (1998) there does not exist a constructive method to determine H and $D(u)$ for a given system.

As can be seen from equation (3.34) the term $D(u)$ does not influence the dynamics of the system as $D(u)C)x - D(u)y = 0$. It is used like the output mixing map H to ease the observer design as can be seen in the following.

In Hammouri *et al.* (1998) the following theorem is given for the considered class of systems.

Theorem 3.9 *The FPRG for state affine systems up to output injection described by Definition 3.4 has a solution if there exist matrices H and $D(u)$ such that:*

$$(i) \quad L_1(x) \notin \Delta(H) \qquad (ii) \quad L_2(x) \in \Delta(H)$$

Denoting $\Delta(H)(\mathcal{L}_2(x))$ as the unobservability space containing the range of $L_2(x)$ the Conditions (i) and (ii) of Theorem 3.9 can be stated as one: $\mathcal{L}_1(x) \cap \Delta(H)(\mathcal{L}_2(x)) = 0$. So, Theorem 3.9 looks similar to Theorem 3.6. The only difference lies in the fact that $\Delta(H)(\mathcal{L}_2(x))$ is not the infimal unobservability subspace containing $\mathcal{L}_2(x)$ and that the conditions in Theorem 3.9 are only sufficient.

The interesting question is if:

$$\mathcal{L}_1(x) \cap \Delta(H)^* = 0 \tag{3.36}$$

where $\Delta(H)^* = \inf \Delta(H)(\mathcal{L}_2(x))$, is a necessary and sufficient condition for a solution of the FPRG for state affine systems up to output injection. From a logical point of view it should, because if $\mathcal{L}_1(x) \cap \Delta(H)^* = 0$ is not fulfilled it means that there are effects coming from fault ν_1 that are hidden in $\Delta(H)^*$. Decreasing $\Delta(H)^*$ to make sure that all effects from ν_1 can be observed would also allow effects from fault ν_2 to enter the observable subspace.

In Kinnaert (2001) it was pointed out that the conditions of Theorem 3.9 should be written more correctly as:

(i) There exists x such that $L_1(x) \notin \Delta(H)$

(ii) $L_2(x) \in \Delta(H) \, \forall \, x$

As a consequence, the conditions cannot be stated as one using an intersection operator as done above.

If a pair $D(u)$ and H can be found such that the conditions of Theorem 3.9 are fulfilled the considered FPRG is solvable. As a consequence a linear change of coordinates exists, i.e. a constant invertible matrix P, such that $\xi = Px$, where $\xi = (\xi_1, \ldots, \xi_n)$, $\xi^1 = (\xi_1, \ldots, \xi_k)$, and $\xi^2 = (\xi_{k+1}, \ldots, \xi_n)$) such that ξ^1 spans the k-dimensional observability subspace $d\mathcal{O}(\mathcal{HC})$ and ξ^2 spans the $(n-k)$-dimensional unobservability subspace $\Delta(H)$.

Applying this coordinate change to system (3.34) and (3.35) leads to the following system as $L_2(x) \in \Delta(H)$ for the chosen $D(u)$ and H:

$$\begin{aligned} \dot{\xi}^1 &= (\overline{A(u) + D(u)C})_1 \xi^1 - \overline{D}_1(u)y + \overline{\psi^1}(u,y) + \overline{L}_{11}(\xi)\nu_1 && (3.37) \\ \dot{\xi}^2 &= (\overline{A(u) + D(u)C})_2 \xi - \overline{D}_2(u)y + \overline{\psi^2}(u,y) + \overline{L}_{12}(\xi)\nu_1 + \overline{L}_{22}(\xi)\nu_2 \\ \overline{y} &= \overline{HC}\xi^1 && (3.38) \end{aligned}$$

where the new terms are defined in the following way:

$$
\begin{aligned}
P(A(u)+D(u)C)P^{-1} &= \begin{pmatrix} [(\overline{A(u)+D(u)C})_1 & 0] \\ (\overline{A(u)+D(u)C})_2 & \end{pmatrix}, \\
PD(u) = \begin{pmatrix} \overline{D}_1(u) \\ \overline{D}_2(u) \end{pmatrix}, & \qquad P\psi(u,y) = \begin{pmatrix} \overline{\psi}_1(u,y) \\ \overline{\psi}_2(u,y) \end{pmatrix}, \\
PL_1(P^{-1}\xi) = \begin{pmatrix} \overline{L}_{11}(\xi) \\ \overline{L}_{12}(\xi) \end{pmatrix} & \qquad PL_2(P^{-1}\xi) = \begin{pmatrix} 0 \\ \overline{L}_{22}(\xi) \end{pmatrix}, \\
\text{and} \qquad HCP^{-1} &= (\overline{HC} \qquad 0).
\end{aligned}
$$

When using the following notation

$$
\overline{A}(u) = (\overline{A(u)+D(u)C})_1 \qquad \text{and} \qquad \varphi(u,y) = -\overline{D}_1(u)y + \overline{\psi_1}(u,y)
$$

for abbreviation, the system (3.37) and (3.38) can be written as:

$$
\dot{\xi}^1 = \overline{A}(u)\xi^1 - \varphi(u,y) + \overline{L}_{11}(\xi)\nu_1 \quad \text{and} \quad \overline{y} = \overline{HC}\xi^1. \tag{3.39}
$$

Designing an observer for the obtained system (3.39) considering $\nu_1 = 0$ leads to a solution for the considered FPRG. Its estimation error (innovation) can be used as residual.

In Hammouri *et al.* (1998) the following observer structure is used:

$$
\begin{aligned}
\dot{\hat{\xi}}^1 &= \overline{A}(u)\hat{\xi}^1 + \varphi(u,y) + S^{-1}\overline{HC}^T(\overline{y} - \overline{HC}\hat{\xi}^1) && (3.40)\\
\dot{S} &= -\theta S - \overline{A}(u)^T S - S\overline{A}(u) + \overline{HC}^T\overline{HC}, \qquad S(0) > 0 && (3.41)\\
r &= \overline{y} - \overline{HC}\hat{\xi}^1 = \overline{HC}\xi^1 - \overline{HC}\hat{\xi}^1 && (3.42)
\end{aligned}
$$

Hammouri *et al.* (1998) call this observer a Kalman-like observer. It does not have a constant gain, but a time varying gain described by (3.41). Some of the important requirements to apply this observer structure are that the system has to be observable (fulfilled for (3.40) by definition of ξ_1) and its inputs have to be regularly persistent exciting or equivalently be universal[14] (for more details see Hammouri *et al.* (1998)).

[14] For a definition of universal inputs see Appendix A.7

Defining $\epsilon := \xi^1 - \hat{\xi}^1$ the estimation error dynamics take the following form:

$$\dot{\epsilon} = \overline{A}(u)\epsilon - S^{-1}\overline{HC}^T\overline{HC}\epsilon + \overline{L}_{11}(\xi)\nu_1 \quad (3.43)$$

$$\dot{S} = -\theta S - \overline{A}(u)^T S - S\overline{A}(u) + \overline{HC}^T\overline{HC}, \qquad S(0) > 0 \quad (3.44)$$

$$r = \overline{HC}\epsilon \quad (3.45)$$

For details about the observer design the reader is referred to Section 3 in Hammouri *et al.* (1998). The proof that the Conditions (i) and (ii) of Theorem 3.9 are sufficient to solve the FPRG defined by Definition 3.4 can be found there as well.

However, the presented solution is not complete, as there does not exist a design procedure for the observer as given for the linear problem in the previous section. This is due to the fact that there does not exist a constructive method to determine H and $D(u)$ for a given system. Nevertheless, it demonstrates how the geometric concept of using unobservability subspaces can be applied to state affine systems up to output injection as well. In Hammouri *et al.* (1998) two different applications are described to illustrate successfully that, in specific cases, the design of the residual generator essentially boils down to the computation of a specific unobservability subspace of the considered system.

3.3.3 Solution for input-affine nonlinear systems

The local nonlinear fundamental problem of residual generation (l-NLFPRG) as stated in Definition 3.5 is of particular interest. From all versions of the FPRG it considers the largest class of systems - the input-affine nonlinear systems. Hence, a lot of research is carried out to solve it. Some results have been published recently or are submitted, see e.g. Hammouri *et al.* (1999), DePersis and Isidori (1999), DePersis (1999), Åström *et al.* (2000)[chapter 10]), DePersis and Isidori (2000), and the references therein. This section presents the ideas developed by DePersis and Isidori of how to handle the l-NLFPRG. It considers the following class of systems, (3.15) and (3.16):

$$\dot{x} = f(x) + \sum_{i=1}^{m} g_i(x)u_i + l(x)\nu + \sum_{i=1}^{s} p_i(x)w_i \quad (3.46)$$

$$y_j = h_j(x), \quad j \in \mathbf{l} \quad (3.47)$$

As the set of disturbances w_i can be extended in order to include also other faults than the considered one (ν) solving the l-NLFPRG leads also to a solution for

the local nonlinear EFPRG.

Similar to the solutions presented above DePersis and Isidori consider the geometric approach based on the observation space of the cascaded system (3.19) and (3.20), denoted by $\mathcal{O}^e$. $\mathcal{O}^e$ is defined as the linear space (over $\mathbb{R}$) of functions on $\mathcal{X}^e$ containing all repeated Lie derivatives[15] $L_{X_1}L_{X_2}\cdots L_{X_k}h_j^e$, $j \in \mathbf{l}$, $k = 1, 2, \ldots$ with X_i, $i \in \mathbf{k}$ in the set $\{f^e, g_1^e, \ldots, g_m^e, p_1^e, \ldots, p_s^e\}$ (Definition 3.29 in Nijmeijer and van der Schaft (1990)). The observation space $\mathcal{O}^e$ defines the observability codistribution $d\mathcal{O}^e$ by setting:

$$d\mathcal{O}^e(x^e) = \text{span}\{dH(x^e),\ H \in \mathcal{O}^e\},\ x^e \in \mathcal{X}^e \tag{3.48}$$

where dH is the standard differential map: $dH(x^e) = (\frac{\partial H}{\partial x_1}, \ldots, \frac{\partial H}{\partial x_{(n+q)}})$.

Similar to the unobservability subspace for linear systems (introduced in Massoumnia (1986*b*)) the annihilator of the observability codistribution $d\mathcal{O}^e$ can be seen as the unobservability distribution $(d\mathcal{O}^e)^\perp$ of the system (3.19) and (3.20). As a consequence the Conditions (i) and (ii) of Definition 3.5 can be equally stated as shown in DePersis (1999) and DePersis and Isidori (2000) as:

$$\text{span}\{g^e, p^e\} \subset (d\mathcal{O}^e)^\perp \qquad \text{and} \qquad l^e \notin (d\mathcal{O}^e)^\perp \tag{3.49}$$

If $x^e = (x, z) = (0, 0)$ is a regular[16] point of $d\mathcal{O}^e$, then $d\mathcal{O}^e$ can be described by the smallest codistribution which is invariant under $\{f^e, g^e, p^e\}$ and contains $\text{span}\{dh^e\}$. The latter is denoted by Q^e, hence, in a neighborhood of a regular point $x^e = (0, 0)$ the following holds: $d\mathcal{O}^e = Q^e$. Therefore, condition (3.49) can be stated (according to Theorem 2 in DePersis (1999)) for regular points as:

$$\text{span}\{g^e, p^e\} \subset (Q^e)^\perp \qquad \text{and} \qquad l^e \notin (Q^e)^\perp \tag{3.50}$$

According to DePersis (1999) it is more convenient to focus on the condition (3.50) when designing a residual generator. Hence the following regular version of the l-NLFPRG is stated in DePersis (1999) and Åström *et al.* (2000)[chapter 10] and will be handled in the following.

[15] See Appendix A.7 for its definition.

[16] See Appendix A.8 for its definition.

Definition 3.10 (Regular local nonlinear fundamental problem of residual generation (rl-NLFPRG): *Find, if possible, a filter*

$$\dot{z} = \tilde{f}(y,z) + \sum_{i=1}^{m} \tilde{g}_i(y,z)u_i \tag{3.51}$$

$$r = \tilde{h}(y,z) \tag{3.52}$$

such that requirement (3.50) and Condition (iii) *of Definition 3.5 are fulfilled.*

For the linear case it is straightforward to show that this formulation of the rl-NLFPRG boils down to the original linear FPRG presented in Massoumnia *et al.* (1989), see e.g. Åström *et al.* (2000)[chapter 10].

The idea behind the following solution for the rl-NLFPRG is the same as for the problems stated above. The goal is to determine an unobservability distribution and an appropriate coordinate transformation, such that an observer for a subsystem of the transformed system performs as a desired residual generator.

In the following only the main result is summarized. For more details the reader is referred to the different publications by DePersis and Isidori.

Theorem 3.11 (Åström *et al.* (2000)[chapter 10]): *Let* Q *be an involutive conditioned invariant distribution such that*

$$\textit{span}\{p\} \subset Q \subset Ker\, d(\psi \circ h) \quad \textit{and} \quad l \notin Q.$$

for some surjection $\psi : \mathbb{R}^q \to \mathbb{R}^{\tilde{q}}$*, defined locally around* $y = 0$ *and with* $\psi(0) = 0$*. Then, there exists a change of state coordinates* $\tilde{x} = \Phi(x)$ *and a change of output coordinates* $\tilde{y} = \Psi(y)$*, defined locally around* $x = 0$ *and, respectively,* $y = 0$*, such that, in the new coordinates, the system (3.46) and (3.47) admits the normal form:*

$$\dot{\tilde{x}}_1 = \tilde{f}_1(\tilde{x}_1, \tilde{y}_2) + \tilde{g}_1(\tilde{x}_1, \tilde{y}_2)u + \tilde{l}_1(\tilde{x}_1, \tilde{x}_2)\nu_1 \tag{3.53}$$

$$\dot{\tilde{x}}_2 = \tilde{f}_2(\tilde{x}_1, \tilde{x}_2) + \tilde{g}_2(\tilde{x}_1, \tilde{x}_2)u + \tilde{p}_2(\tilde{x}_1, \tilde{x}_2)w + \tilde{l}_2(\tilde{x}_1, \tilde{x}_2)\nu_2 \tag{3.54}$$

$$\tilde{y}_1 = \tilde{h}_1(\tilde{x}_1) \tag{3.55}$$

$$\tilde{y}_2 = \tilde{h}_2(\tilde{x}_1, \tilde{x}_2) \tag{3.56}$$

with $\tilde{x}_1 \in \mathbb{R}^{\upsilon}$*,* $\upsilon :=$ *codim*(Q) *and* $\tilde{l}_1(\tilde{x}_1, \tilde{x}_2) \neq 0$ *locally around* $\Phi(0)$*.*

After transforming the system (3.46) and (3.47) successfully into a normal form (3.53) - (3.56) the next task to solve the rl-NLFPRG is to analyze the observability of the subsystem:

$$\dot{\tilde{x}}_1 = \tilde{f}_1(\tilde{x}_1, \tilde{y}_2) + \tilde{g}_1(\tilde{x}_1, \tilde{y}_2)u \quad \text{and} \quad \tilde{y}_1 = \tilde{h}_1(\tilde{x}_1) \tag{3.57}$$

Depending on how the conditioned invariant distribution Q is generated the observability can be guaranteed (see Åström *et al.* (2000)[chapter 10]). The final step is then to design an observer for the subsystem (3.57) if possible that will lead to a residual generator (3.51) and (3.52). The stability requirement for this residual generator can take different forms in order to fulfill condition (iii) of Definition 3.5. Its formulation depends specifically on the chosen observer structure and, therefore, on the considered system.

Theorem 3.11 describes the conditions under which a solution for the regular local nonlinear FPRG exists. However, there does not exist a constructive method to determine how to obtain the necessary diffeomorphism (change of coordinates). A constructive methodology to calculate the involutive conditioned invariant distribution Q is given in the following.

3.3.3.1 Calculation of the involutive conditioned invariant unobservability distribution Q

The first step to check whether a specific FPRG is solvable or not it is to compute an involutive conditioned invariant distribution[17] Q (see Theorem 3.11) that contains the unwanted disturbance and fault effects. If this distribution Q does not contain the considered fault effect (the one to be detected and isolated) a geometric solution might exist. The next step is then to find an appropriate coordinate transformation and to check the observability of the obtained subsystem. The final step is to design an observer (residual generator) that solves the FPRG. In DePersis and Isidori (2000) it is shown how to calculate the involutive conditioned invariant distribution Q (unobservability distribution) for a system of the following form:

$$\dot{x} = f(x) + \sum_{i=0}^{m} g_i(x)u_i \qquad y = h(x) \tag{3.58}$$

[17] A distribution Δ is said to be *conditioned invariant* for a system (3.58) if it satisfies $[f, \Delta \cap Ker\{dh\}] \subset \Delta$ and $[g_i, \Delta \cap Ker\{dh\}] \subset \Delta$.

where $x \in \mathcal{X}$ an open subset of $\mathbb{R}^n$, $u_i \in \mathbb{R}$, $i = 1, \ldots, m$, and $y \in \mathbb{R}^p$. $f(x)$ (also denoted as $g_0(x)$) and $g_1(x), \ldots, g_m(x)$ are smooth vector fields and $h(x)$ is a smooth map. The calculation is based on the following two algorithms (introduced in DePersis and Isidori (2000)):

Computing the involutive conditioned invariant distribution Σ_*^P: This algorithm is the nonlinear version of the recursive (C, A)-invariant subspace algorithm (CAISA), see (A.1) in Appendix A.2. It starts with the distribution

$$P = span\{p_1, p_2, \ldots, p_s\}$$

where p_i, $i = 1, \ldots, s$, are additional smooth vector fields; in this thesis they represent the column vectors of the disturbance distribution matrix $p(x)$ in order to obtain FDI. Then the following non-decreasing sequence of distributions is considered:

$$S_0 = \overline{P} \tag{3.59}$$

$$S_{k+1} = \overline{S}_k + \sum_{i=0}^{m} [g_i, \overline{S}_k \cap Ker\{dh\}] \tag{3.60}$$

where $\overline{\Delta}$ denotes the involutive closure of a distribution Δ. For every constant distribution Δ it holds that $\overline{\Delta} = \Delta$. $g_0 \ldots g_m$ stand for the column vectors of $g(x)$ **and** for $f(x)$, which is written as $f(x) = g_0(x)$ to ease the notation. $Ker\{dh\}$ denotes the distribution annihilating the differentials of the rows of the mapping $h(x)$.

Finally, k^* is defined as the finite number for which:

$$S_{k^*+1} = \overline{S}_{k^*} \tag{3.61}$$

$\overline{S}_{k^*}$ is also denoted as Σ_*^P. Then Σ_*^P is involutive, contains P and is conditioned invariant. Moreover, any other distribution Δ which is involutive, contains P, and is conditioned invariant satisfies $\Delta \supset \Sigma_*^P$.

Suppose that Σ_*^P is well-defined (i.e. equation (3.61) holds for some k^*) and non-singular, so that its annihilator $(\Sigma_*^P)^\perp$ is locally spanned by exact differentials (because Σ_*^P is by construction involutive). Suppose also that $\Sigma_*^P \cap Ker\{dh\}$ is a smooth distribution. Then it can be asserted that $(\Sigma_*^P)^\perp$ is the maximal (in the

sense of codistribution inclusion) conditioned invariant codistribution[18] which is locally spanned by exact differentials and contained in $P^{\perp}$. For more details about Σ_*^P and its computation the reader is referred to DePersis and Isidori (2000).

Observability codistribution algorithm (o.c.a.): Let Θ be a fixed codistribution then the observability codistribution algorithm is defined by the following non-decreasing sequence of codistributions:

$$Q_0 = \Theta \cap span\{dh\} \tag{3.62}$$

$$Q_{k+1} = \Theta \cap \left(\sum_{i=0}^{m} L_{g_i} Q_k + span\{dh\} \right) \tag{3.63}$$

where $span\{dh\}$ is the codistribution spanned by the differentials of the rows of the mapping $h(x)$. (To make the notation more consistent with $Ker\{dh\}$ one could use the notation $Im\{dh\}$ instead of $span\{dh\}$, however, to be consistent with the used references it is not done here.) Suppose that all codistributions of this sequence are nonsingular, so that there is an integer $k^* \leq n-1$ such that $Q_k = Q_{k^*}$ for all $k > k^*$, and set $\Omega^* = Q_{k^*}$. This result can be stated by the following notation:

$$\Omega^* = \text{o.c.a.}(\Theta)$$

The algorithm has the property that $\text{o.c.a.}(\Theta) = \text{o.c.a.}(\text{o.c.a.}(\Theta))$ and if Θ is conditioned invariant, so is the codistribution Ω^*. A codistribution Ω is called an observability codistribution if:

$$L_{g_i}\Omega \subset \Omega + span\{dh\} \quad \forall i = 0, \ldots, m$$
$$\text{o.c.a.}(\Omega) = \Omega$$

Furthermore, a distribution Δ is called an *unobservability distribution* if its annihilator $\Omega = \Delta^{\perp}$ is an observability codistribution.

When the distribution Σ_*^P is well-defined and nonsingular, and $\Sigma_*^P \cap Ker\{dh\}$ is a smooth distribution, then $\text{o.c.a.}((\Sigma_*^P)^{\perp})$ is the maximal (in the sense of codistribution inclusion) observability codistribution which is locally spanned

[18] A codistribution $\Omega = \Delta^{\perp}$ is said to be *conditioned invariant* if it satisfies $L_{g_i}\Omega \subset \Omega + span\{dh\}$ for all $i = 0, \ldots, m$.

by exact differentials and contained in $P^{\perp}$. The corresponding unobservability distribution Q can be obtained by:

$$Q = (\text{o.c.a.}((\Sigma_*^P)^{\perp}))^{\perp}$$

For more details about the o.c.a. algorithm and the calculation of Q the reader is referred to DePersis and Isidori (2000).

As a result of the algorithm Q is the smallest involutive conditioned invariant unobservability distribution that contains P (the disturbance effects) due to the maximality of o.c.a.$((\Sigma_*^P)^{\perp})$. Obviously, this Q is the most likely distribution to fulfill the condition of Theorem 3.11.

In Chapter 4 the geometric approach is applied to a ship propulsion system. For that purpose several FPRGs are defined in Section 4.2. Then different unobservability distributions Q are calculated for each FPRG, see Appendix C.

3.4 Summary

In this chapter the fundamental problem of residual generation (FPRG) was described and several approaches to obtain solutions for different classes of systems were summarized.

It was illustrated that solving the FPRG means achieving successful fault detection and isolation (FDI) that is robust against disturbances. However, the robustness concerning model uncertainty can only be handled as long as the model uncertainty can be modeled as extra disturbances. A definition of the generic solvability for the linear FPRG was given as well.

The presented solutions were all based on the same basic geometric idea introduced by Massoumnia (1986*b*). The idea starts with determining an unobservability subspace/distribution which does not include the fault that has to be detected and isolated. Additionally it includes all the fault- and disturbance effects that are not allowed to affect the residual in order to achieve successful FDI. In Massoumnia (1986*b*) this was shown to be possible in a constructive way. Furthermore, the existence of such a subspace/distribution was proven to assure a solution for the corresponding FPRG. As a consequence of the existence of such

an unobservability subspace/distribution an appropriate coordinate transformation can be found, such that one subsystem of the transformed system is only influenced by the considered fault. The final step is to built an observer for this subsystem which fulfills the tasks of a residual generator. However, there does not exist a constructive way to determine this coordinate transformation which is used to ease the final step.

Several geometric solutions were presented starting with the original approach for linear systems up to the input-affine nonlinear systems. The solution for the later includes the linear case and hence can be seen as a general approach to tackle the FPRG. There exist several other approaches to solve the FPRG in the literature, but basically they boil down to one of the versions presented above. Some of these approaches are based on finding a coordinate transformation $z = T(x)$ such that a subsystem is obtained for that an observer can be designed that solves the FPRG. They are stated in an algebraic way, see e.g. Seliger and Frank (1991*a*,*b*) and recently Kinnaert and Bahir (1999).

The geometric concept leads to a more compact notation than the algebraic one. The conditions for checking the solvability of a particular FPRG can be checked straightforward, because there exist algorithms to compute the unobservability subspace/distribution. For more details about the comparison between the algebraic and geometric approach the reader is referred to Åström *et al.* (2000)[chapter 10]. It illustrates the advantages of the geometric approach for linear systems by giving a conclusive result (Theorem 10.3.1 in Åström *et al.* (2000)) incorporating both, the algebraic and the geometric approach.

However, as can be seen from the presented solutions there does not exist a fully constructive solution to design a residual generator for the nonlinear systems yet.DePersis and Isidori refer in their recent publications DePersis (1999), DePersis and Isidori (2000), and in Åström *et al.* (2000) to articles to appear that might give a more constructive approach.

3.5 Conclusions

The above presented geometric approach to solve the nonlinear FPRG does not describe a complete new idea. It is more a general notation or problem formulation. Looking for example at other approaches it can be seen that they fit in the

same approach although they are not written in a geometric way, see e.g. Seliger and Frank (1991*a*,*b*) and Ashton and Shields (1999). As mentioned in the introduction to this chapter the geometric approach is a more compact way to treat the FPRG problem.

Following the geometric approach can lead to different results. This is due to the freedom to choose the observer structure (residual generator). In Massoumnia (1986*b*) a Luenberger observer has been applied as a residual generator. Other examples are the general structure in Massoumnia *et al.* (1989), Kalman-like observer in Hammouri *et al.* (1998), high-gain observers in Hammouri *et al.* (1999) and a backstepping observer in DePersis (1999). This variety shows how general the geometric approach can be applied. However, it has problems dealing with model uncertainty that cannot be modeled as extra disturbances, hence, needs a precise model. Furthermore, there exists no constructive result to design the residual generator for the state-affine and input-affine nonlinear systems. The main problem is to find the required coordinate transformation that helps to choose the correct observer structure and to design it. Also the generic solvability for the nonlinear FPRG is still an open question.

Another possible disadvantage might be that the geometric approach considers arbitrary fault and disturbance signals. Hence, only FPRGs can be solved where the fault is 100% decoupled from the disturbances. However, there might be FDI problems where the disturbance effect on the residual is significantly different from the fault effect. When for example the disturbance effect turns out to be limited enough one solution could be to apply a higher threshold. Another solution to handle the disturbance when its effect on the residual shows a significant different dynamic behaviour than the fault effect might be to apply a filter to get the disturbance effect out.

The disturbance problem and other application aspects are considered in Chapter 4. There the above presented geometric approach is applied to a ship propulsion system. The application results are used to design residual generators. In a concluding discussion the strong and weak points of the geometric approach for FDI will be pointed out.

As mentioned in the above cited references the geometric approach for FDI has been inspired by using the dual of certain results that are known for

other control problems, like e.g. the disturbance decoupled estimation problem (DDEP) (Wonham (1985)).Unobservability subspaces introduced by Massoumnia (1986*b*) play an important role when searching for a solution for the linear FPRG. They have been originally introduced by Willems and Commault (1981) as complementary observability subspaces to approach the disturbance decoupling problem via output measurements. For the nonlinear systems the counterpart of the conditioned invariant subspaces are the conditioned invariant distributions, introduced in Isidori *et al.* (1981). Results holding for unobservability subspaces can be derived by taking the dual of the corresponding results available for controllability subspaces. In fact, a given subspace is an unobservability subspaces if and only if its complement space is a controllability subspace. However, as also mentioned in Massoumnia *et al.* (1989), the solutions are not obtained by simply taking the dual of a familiar control problem. One of the reasons is that the goal is a residual generator that helps to take a decision and not a controller to obtain a required system behaviour.

Inspired by this idea of using the dual of known geometric approaches a new idea of *fault-output decoupling* is proposed in Chapter 6. It is based on the input-output decoupling problem.

Chapter 4

FDI for a ship propulsion system

Several approaches for fault detection and isolation in nonlinear systems have been developed, but only little experience exists from applying them to real systems. The existing application results are mostly obtained by using academic examples or small laboratory setups. This accounts especially for the recently introduced nonlinear geometric approach by DePersis and Isidori described in Chapter 3. Hence, this chapter presents FDI-application results obtained by applying the geometric approach to a simulation model of a nonlinear ship propulsion system. The simulation model is part of a ship propulsion benchmark defined and developed by Izadi-Zamanabadi and Blanke at the Department of Control Engineering at the University of Aalborg. A complete description of the benchmark can be found in Izadi-Zamanabadi and Blanke (1998).

First the part of the ship propulsion benchmark is presented that has been used to apply the geometric approach. Next to the system dynamics the fault scenario is presented. Then the application of the geometric approach to the system is illustrated in detail. The next step is the observability analysis of the results followed by nonlinear observer (residual generator) design. Additionally, in order to have results for comparison a nonlinear adaptive observer design (Blanke and Lootsma (1999)) is given. Different simulation results are presented to illustrate the FDI properties of the different observers. They are discussed in a concluding discussion at the end of this chapter.

4.1 Ship propulsion system - system description

This section describes in detail the ship propulsion system and the fault scenario that was used to apply the geometric approach presented in the previous chapter. The used simulation model is part of a ship propulsion benchmark problem that was defined by Izadi-Zamanabadi and Blanke (1997, 1999). A detailed description of the complete ship propulsion benchmark can be found in Izadi-Zamanabadi and Blanke (1998). The ship propulsion benchmark is used as a platform to develop, enhance, test, and compare new and existing methods for achieving fault tolerant control systems. International groups have contributed with results at conferences (Cocquempot *et al.* (1998); Amann *et al.* (1999); Blanke and Lootsma (1999); Edwards and Spurgeon (1999); Kerrigan and Maciejowski (1999); Schreier and Frank (1999); Zhang and Wu (1999)) and an overview is given in chapter 13 of the COSY-project monograph (Åström *et al.* (2000)).

4.1.1 Motivation for fault-tolerance in the propulsion system

Achieving fault-tolerance in a ship propulsion system has several advantages compared with the existing control strategies applied on-board marine vessels. Hence, the motivation to consider fault-tolerant control theory is presented in the following and some remarks concerning fault-operational strategies are given.

Faults in ship propulsion systems, e.g. failure of sensors or actuators, are far from being unlikely events. In the past, faults have resulted in events going along with severe damage and significant loss of capital investment. In the marine area the automation systems are not designed to be fail-operational[1]; mainly due to high costs. Considering the raising demands of safety and reliability this is not desirable. Several accidents have shown in the past how high the cost of an oil-tanker accident can be for the owners and mainly for nature. However, instead of applying fail-operational strategies to the entire automation system only local shut down mechanisms are applied. Individual machinery is shut down as soon as a critical state has been observed. This local strategy can obviously have a negative effect on the overall operation of a ship. When a prime mover is shut down, e.g. due to a sensor fault in its diesel maneuvering system, a ship looses its ability to brake and maneuver. An overall strategy based on fault-tolerant

[1] For a definition of *fail-operational* see Chapter 2.

concepts could help to handle these kind of faults in local equipment and prevent them from causing unwanted effects on the overall operation. As its application is significantly cheaper than the fail-operational strategy the motivation to study the possibilities of using them on-board is high.

4.1.2 System description

The propulsion system of a ship consists of several components, with the diesel engine and the propeller as main parts. The benchmark simulation package consists of two simulation models, one representing a one propeller/one engine system, and one describing a two propeller/two engine system. Both models are based on real data from a ferry. The technical data related to the vessel can be found in Appendix B. This section focuses on the subsystem of the ship propulsion benchmark, that is based on one engine and one controllable pitch propeller, as it has been used for the simulations in this chapter. The control system of the propulsion system has a control hierarchy consisting of two control levels. One contains the shaft speed and propeller pitch controllers and is referred to as lower-level control. The other, the coordinate control level, also called the upper-level control, comprises combinator curves for the overload controller, the handle on the bridge, ship speed controller, and an efficiency optimizer.

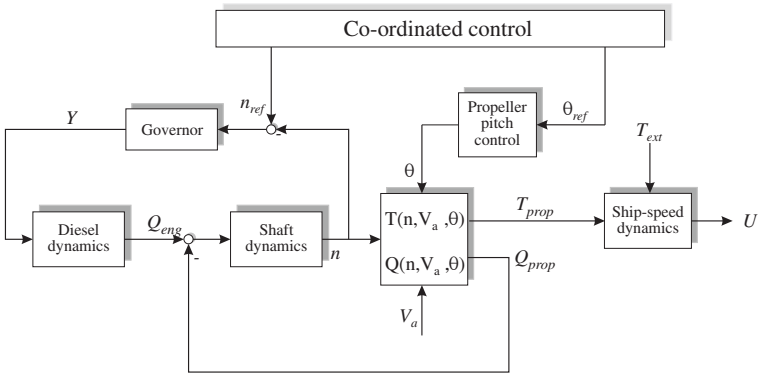

Figure 4.1: Ship propulsion system - an overview.

Fig. 4.1 gives an outline of the used propulsion system. It shows the following main components and subsystems:

- The coordinated control level: providing the set-points for the shaft speed n_{ref} and propeller pitch θ_{ref}.

- Propeller pitch controller and governor (shaft speed controller): controlling the propeller pitch θ and fuel index Y.
- Diesel dynamics (diesel engine): generating torque Q_{eng} to drive the propeller shaft depending on the fuel index.
- Shaft dynamics: describing the shaft speed n, resulting from the difference between the engine and the propeller torque.
- Propeller characteristics: describing the propeller thrust T_{prop} and torque Q_{prop}, that are determined by shaft speed, water speed V_a, and propeller pitch.
- Ship speed dynamics: describing the ship speed U resulting from the propeller thrust balanced by hull resistance and external forces T_{ext} like wind and waves.

The thrust - and as a consequence the ship speed - generated by the propulsion system is vital for the ability to maneuver and to sail a ship; without thrust the ship cannot be accelerated or stopped. In the system described in Fig. 4.1 there are two main control loops, one for the propeller pitch and one for the shaft speed. Both, the propeller pitch and the shaft speed determine the ship speed and are supervised by the co-ordinate control level. The co-ordinate control level includes strategies to optimize the fuel consumption and to avoid overload situations - details can be found in Izadi-Zamanabadi and Blanke (1998).

Obviously there are different strategies to control the ship speed. Changing from an ahead to an astern heading can be carried out in different ways, e.g. by either keeping the propeller pitch constant and reversing the diesel engine or by keeping the shaft speed constant and reversing the propeller pitch. In the simulations the shaft speed is considered to be positive.

In Fig. 4.2 a more detailed scheme of the lower control level of the propulsion system is given. It shows the two basic control loops and the different limitation and saturation effects. Details about all the values can be found in Appendix B. The system has two known inputs from the coordinated control level: the shaft-speed reference n_{ref} and the propeller-pitch reference θ_{ref}. The unknown inputs are the external forces (wind and waves) T_{ext} and the friction torque Q_f. The following measurements (system outputs) are available: diesel engine shaft speed

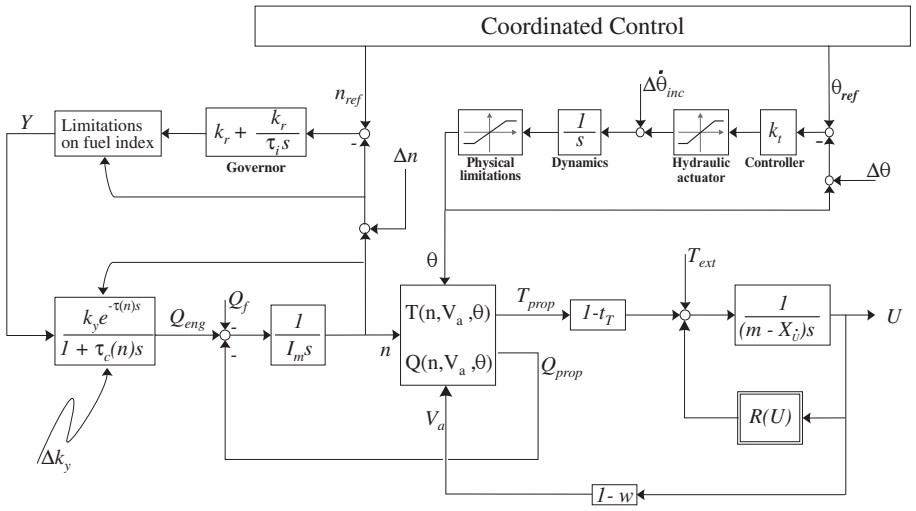

Figure 4.2: Ship propulsion system - a detailed view.

n_m, fuel index Y_m, propeller pitch position θ_m, and ship speed U_m. Furthermore, Fig. 4.2 shows the faults considered during the simulation of the system; they are described in more detail in the next section.

4.1.3 Fault scenario

Various faults can occur on-board a ship. For the ship propulsion benchmark a fixed fault scenario has been defined to have the possibility to compare the FDI results obtained by different fault-tolerant control (FTC) research groups with their methods. The considered faults of the scenario are presented in this section. They have been defined after applying a fault-propagation analysis (FPA). The FPA is a methodology to investigate how considered faults affect the operation of the system and its control under their occurrence. Furthermore, it investigates the severity of the overall effect caused by the possible faults. For a detailed description of the fault propagation analysis the reader is referred to Blanke (1996) and Bøgh (1997) as the details are not of further interest in this chapter. Results of the FPA concerning the ship propulsion benchmark are described in Izadi-Zamanabadi and Blanke (1998); Izadi-Zamanabadi (1999). They led to the fault scenario for the propulsion system given in Table 4.1.

Fault	Symbol	Sign	Type
shaft speed sensor faults	$\Delta\, n_{sensor}$	pos./neg.	additive - abrupt
pitch sensor faults	$\Delta\, \theta_{sensor}$	pos./neg.	additive - abrupt
hydraulic leak	$\Delta\, \dot{\theta}_{inc}$	neg.	additive - incipient
diesel fault	$\Delta\, k_y$	neg.	multiplicative - abrupt

Table 4.1: Faults implemented in the ship propulsion benchmark.

The four different faults listed in Table 4.1 are considered as generic faults, as they are the faults that are most likely to occur. Their detection is very important for the operation of the propulsion system when fault-tolerant strategies are applied. The severity of the faults will be discussed below, but first a description of the faults is given:

- Propeller pitch faults:
  - $\Delta\theta_{high}$: This fault can occur due to a defect in the pitch sensor or its connections. As a result the controller receives a wrong sensor measurement that is too *high* compared to the real one.
  - $\Delta\theta_{low}$: This fault can occur due to a defect in the pitch sensor or its connections. As a result the controller receives a wrong sensor measurement that is too *low* compared to the real one.
  - $\Delta\dot{\theta}_{inc}$: A leakage can occur in the (hydraulic) actuation part of the control system; in practice, often in an over-pressure valve.
- Shaft speed sensor faults:
  - Δn_{high}: This fault can occur due to a defect in the shaft speed sensor or its connections. As a result the controller receives a wrong sensor measurement that is too *high* compared to the real one.
  - Δn_{low}: This fault can occur due to a defect in the shaft speed sensor or its connections. As a result the controller receives a wrong sensor measurement that is too *low* compared to the real one.

- Gain fault in the diesel engine:
  - Δk_y: This fault describes the effect of a lower engine torque than expected for the actual fuel index. Possible causes: cylinder failure in the engine, connection problems causing reduced inlet of air, oil or fuel.

Each of the described faults has a different effect on the over-all behaviour of the ship propulsion system. Some faults are more severe than others and, therefore, need to be handled with higher priority. A list of the faults and their fault effect and its severity is given in Table 4.2.

Fault	**Fault effect**	**Severity**
$\Delta\theta_{high}$	deceleration $\longrightarrow$ maneuvering risk	high
$\Delta\theta_{low}$	acceleration $\longrightarrow$ collision risk	very high
$\Delta\dot{\theta}_{inc}$	gradual speed change $\longrightarrow$ cost increase	medium
Δn_{high}	deceleration $\longrightarrow$ maneuvering risk	high
Δn_{low}	acceleration $\longrightarrow$ collision risk	very high
Δk_y	diesel overload $\longrightarrow$ wear, slowdown	medium

Table 4.2: Fault effects and resulting severity for the propulsion system.

Fault	**Detection time**	**Fault**	**Detection time**
$\Delta\theta_{high}$	$T_d < 2T_s$	Δn_{low}	$T_d < 2T_s$
$\Delta\theta_{low}$	$T_d < 2T_s$	Δn_{high}	$T_d < 2T_s$
$\Delta\dot{\theta}_{inc}$	$T_d < 100T_s$	Δk_y	$T_d < 5T_s$

Table 4.3: Required detection time for the different faults.

The data is taken from Izadi-Zamanabadi (1999) and Izadi-Zamanabadi and Blanke (1998), where also further information concerning the faults is given, like e.g. the necessary detection time T_d for each fault (see Table 4.3). The detection time has been chosen in such a manner that the system can be reconfigured in time to prevent severe situations like the loss of the ability to maneuver the ship.

Event	Magnitude	Start time	End time
$\Delta\theta_{high}$	$-\theta - 0.7$	$180s$	$210s$
Δn_{high}	$n_{max} - n$	$680s$	$710s$
$\Delta\dot{\theta}_{inc}$	-	$800s$	$1700s$
$\Delta\theta_{low}$	$-\theta$	$1890s$	$1920s$
Δn_{low}	$-n$	$2640s$	$2670s$
Δk_y	$-0.2\,k_y$	$3000s$	$3500s$

Table 4.4: Time sequence of the simulated faults.

A predefined sequence of the above defined faults has been implemented in the simulation model. The total simulation time is $3500sec$ and the faults occur at the in Table 4.4 given points of time. This sequence has been predefined to improve the possibility to compare results obtained with different FDI approaches.

4.1.4 System dynamics

In this section a brief overview over some equations describing the ship propulsion system's dynamics, see Fig. 4.1 and Fig. 4.2, is given. Not all dynamic relations of the system are presented as not all of them are of interest in the FDI design. For a complete description of the system dynamics the reader is referred to Izadi-Zamanabadi and Blanke (1998) and Izadi-Zamanabadi (1999).

4.1.4.1 Diesel engine

Describing the dynamics of a diesel engine is often a difficult task depending on the type of engine. In the simulation of the propulsion system the diesel engine dynamics are described by the following transfer function (taken from Blanke (1981), Blanke and Andersen (1984), and Fossen (1994, pp. 246-257)):

$$Q_{eng}(s) = \frac{(k_y + \Delta k_y)}{1 + \tau_c\, s} Y(s), \tag{4.1}$$

where Q_{eng} describes the torque generated by the diesel engine, which is controlled by the fuel index Y. The parameters of the transfer function are given by k_y the gain constant of the engine, Δk_y describing the gain fault in the engine, and τ_c the time constant corresponding to torque built-up from cylinder firings.

4.1.4.2 Propeller shaft

The dynamics of the propeller shaft turning the generated engine torque into shaft speed (n) are described by the following equation based on a torque balance:

$$I_m \dot{n} = Q_{eng} - Q_{prop} - Q_f. \tag{4.2}$$

where I_m describes the resulting inertia of the shaft with all couplings. Q_{eng} denotes the torque generated by the diesel engine, Q_{prop} denotes the torque coming from the propeller (load), and Q_f describes the friction of the propeller shaft.

4.1.4.3 Ship speed

The ship is accelerated by the propeller-generated thrust (T_{prop}). The resulting ship speed (U) can be determined with the help of the following force balance describing the nonlinear dynamics:

$$(m - X_{\dot{U}})\dot{U} = R(U) + (1 - t_T)T_{prop} + T_{ext} \tag{4.3}$$

$$U_m = U + \nu_U. \tag{4.4}$$

where m denotes the mass of the ship. The $X_{\dot{U}}$ term represents an added mass in surge. $R(U)$ describes the resistance the ship experiences from the water (hull resistance). As the generated propeller thrust T_{prop} changes the flow of the water behind the ship (ship's stern) the resulting thrust accelerating the ship is reduced. This effect is described by the thrust deduction number t_T. External forces like the wind and the waves are represented by T_{ext}. The measured shaft speed signal (U_m) contains the measurement noise (ν_U) as described in Appendix B and shown in equation (4.4).

4.1.4.4 Propeller

A controllable pitch propeller (CPP) has been simulated in the ship propulsion system benchmark. The pitch (θ) describes the angle with that the propeller blades attack the water during rotation of the propeller. It can be adjusted for a CPP by turning the propeller blades via a hydraulic system over a range from -100% (full astern) over to 100% (full ahead). As a consequence there are two possibilities to control the propeller-generated thrust and torque - changing shaft speed (n) and/or propeller pitch (θ). The propeller thrust (T_{prop}) and propeller

torque (Q_{prop}) generated with a CPP can be described by the following nonlinear equations (Blanke (1981)):

$$T_{prop} = T_{|n|n}(\theta)|n|n + T_{|n|V_a}(\theta)|n|V_a \quad (4.5)$$

$$Q_{prop} = Q_0|n|n + Q_{|n|n}(\theta)|n|n + Q_{|n|V_a}(\theta)|n|V_a. \quad (4.6)$$

The propeller parameters $T_{|n|n}(\theta)$, $T_{|n|V_a}(\theta)$, Q_0, $Q_{|n|n}(\theta)$, and $Q_{|n|V_a}(\theta)$ are all, except Q_0, depending on the actual propeller pitch (θ) and difficult to obtain for a real system. The pitch-variant parameters of T_{prop} and Q_{prop} are calculated for the simulations by interpolating between tables of data measured in model propeller tests. For further details the reader is referred to Izadi-Zamanabadi and Blanke (1998) and Izadi-Zamanabadi (1999). V_a describes the velocity with which the water passes through the propeller disc. It is smaller than the ship speed U due to the hydrodynamic turbulence under the hull of the ship. It can be obtained with the help of the wake fraction (w), a hull-dependent parameter:

$$V_a = (1 - w)U. \quad (4.7)$$

For the residual generation the following special forms of (4.5) and (4.6) are implemented as stated in Fossen (1994, pp. 246-257):

$$T_{prop} = T_{|n|n}|n|n\theta + T_{|n|V_a}|n|V_a \quad (4.8)$$

$$Q_{prop} = Q_{|n|n}|n|n|\theta| + Q_{|n|V_a}|n|V_a\theta. \quad (4.9)$$

4.1.5 Controllers

In the lower-level control there are two main control loops - shaft speed control and propeller pitch control. Different controllers are applied to these loops. They are described in the following. Both loops are interconnected via the propeller dynamics. The upper-level control is not of special interest here. It generates the set-points for the shaft speed n_{ref} and the propeller pitch θ_{ref} for the lower-level control. Furthermore, the upper-level control includes an overload controller in order to avoid damage of system components, e.g. a too high demand in shaft speed would lead to a too high engine torque that could brake the shaft. For more detailed information about the upper-level control the reader is referred to Izadi-Zamanabadi and Blanke (1998) and Izadi-Zamanabadi (1999).

4.1.5.1 Shaft speed control

The shaft speed controller receives as inputs the reference signal n_{ref} from the upper-level control and the shaft speed measurement n_m. The measured shaft

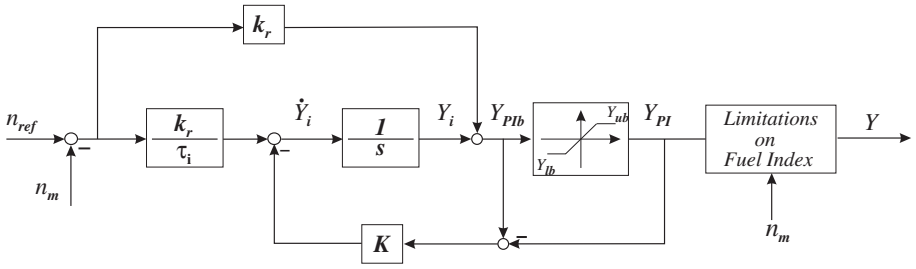

Figure 4.3: Governor - shaft speed controller.

speed can be described as follows:

$$n_m = n + \nu_n + \Delta n_{sensor} \tag{4.10}$$

where the actual shaft speed is described by n, the measurement noise by ν_n and the sensor fault is represented by Δn_{sensor}.

The shaft speed controller (governor) is a PI-controller and generates the fuel index reference signal Y. A detailed scheme of the governor is given in Fig. 4.3. The figure shows the saturation phenomena and an anti-windup as part of the integrating action, where K is the anti-windup gain. The integrating part of the governor has Y_{lb} and Y_{ub} as lower and upper bounds. Furthermore, the limitations of the fuel index, depending on the shaft speed measurement, are shown in an extra block. It limits the fuel index from above by the maximum allowed fuel inlet, which is related to constrains on the torque characteristics of the diesel engine. Obviously, the fuel index is nonnegative, which limits it from below.

The shaft speed controller can be described in detail by the following equations:

$$\dot{Y}_i = \frac{k_r}{\tau_i}\big((n_{ref} - n_m) - K(Y_{PIb} - Y_{PI})\big) \tag{4.11}$$

$$Y_{PIb} = Y_i + k_r(n_{ref} - n_m) \tag{4.12}$$

$$Y_{PI} = \min(\max(Y_{PIb}, Y_{lb}), Y_{ub}) \tag{4.13}$$

The values for the different parameters of the governor and the measurement noise can be found in Appendix B.

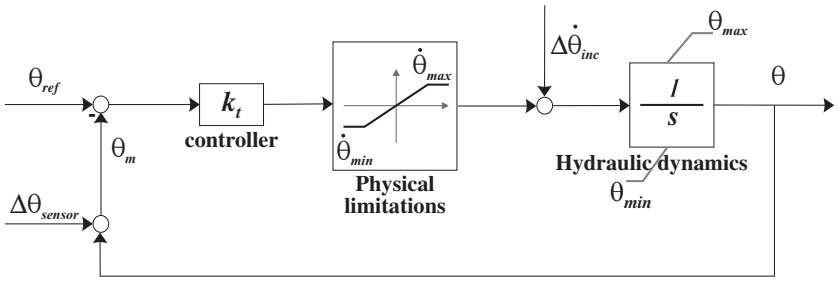

Figure 4.4: Propeller pitch control.

4.1.5.2 Propeller pitch control

The propeller pitch θ is adjusted via a hydraulic actuator turning the propeller blades. The actuator's dynamic has an integrating structure and is controlled by the pitch controller. The propeller pitch control loop can be described by the following relations:

$$\theta_m = \theta + \nu_\theta + \Delta\theta_{sensor} \tag{4.14}$$

$$u_{\dot{\theta}} = k_t \left(\theta_{ref} - \theta_m\right) \tag{4.15}$$

$$\dot{\theta} = \max(\dot{\theta}_{\min}, \min(u_{\dot{\theta}}, \dot{\theta}_{\max})) + \Delta\dot{\theta}_{inc} \tag{4.16}$$

$$\theta = \max(\theta_{\min}, \min(\theta, \theta_{\max})) \tag{4.17}$$

where θ_m describes the pitch measurement, ν_θ describes the measurement noise and $\Delta\theta_{sensor}$ stands for the pitch sensor fault. $u_{\dot{\theta}}$ denotes the controller output (not measured in the benchmark) and k_t the controller parameter (P-controller). The incipient fault in the pitch hydraulic actuator is described by $\Delta\dot{\theta}_{inc}$. As the actuator can only turn the propeller blade over a specific range it is limited by $\theta_{\min}$ and $\theta_{\max}$. Furthermore, the speed of change is limited due to the flow velocity of the hydraulic oil. That effect is described by $\dot{\theta}_{\min}$ and $\dot{\theta}_{\max}$. Fig. 4.4 shows the complete pitch control system.

4.2 Geometric FDI analysis

The in Chapter 3 presented geometric approach towards FDI for input-affine nonlinear systems has gained high interest in the last two years. However, until now, only little experience with its application has been obtained. In this section the geometric approach described in DePersis and Isidori (1999, 2000) is applied to the ship propulsion benchmark. The results are then used to design diagnostic nonlinear observers for successful FDI in the next section.

First, a nonlinear state-affine model of the propulsion system is stated as it is used in DePersis and Isidori (1999). Then different scenarios are defined in order to apply the geometric approach followed by the application results.

4.2.1 Model description

The propulsion system dynamics have to be rewritten in the following input-affine form to be able to apply the geometric approach as stated in DePersis and Isidori (2000) and Chapter 3:

$$\dot{x} = f(x) + \sum_{i=1}^{m} g_i(x)u_i + l(x)\nu + \sum_{i=1}^{s} p_i(x)w_i \tag{4.18}$$

$$y_j = h_j(x), \quad j \in \mathbf{l} \tag{4.19}$$

One way to obtain the required form (4.18) and (4.19) is to include sensor faults as pseudo-actuator faults. A procedure for that is described in Massoumnia (1986*a*) and Hashtrudi-Zad and Massoumnia (1999). For the propulsion system it can be done by adding the following additional linear dynamics to the original system for the shaft speed sensor fault:

$$\dot{x}_{\Delta n} = A_{\Delta n}x_{\Delta n} + L_{\Delta n}\nu_{\Delta n} \tag{4.20}$$

$$y_{\Delta n} = C_{\Delta n}x_{\Delta n} = \Delta n_{sensor} \tag{4.21}$$

where $\nu_{\Delta n} = \dot{\Delta n}_{sensor}$, $A_{\Delta n} = 0$, and $L_{\Delta n} = C_{\Delta n} = 1$. Obviously, the conditions as stated in Hashtrudi-Zad and Massoumnia (1999) are fulfilled, i.e. the number of columns of $L_{\Delta n}$ is equal to the number of rows in $C_{\Delta n}$, L is injective, C is surjective, and the order of the additional dynamics $(n_{\Delta n} = 1)$ is equal to (or greater than) the dimension of the sensor fault $\dim(\Delta n_{sensor}) = 1$.

The extra dynamics for the pitch sensor can be written in the same way by replacing $_{\Delta n}$ by $_{\Delta\theta}$:

$$\dot{x}_{\Delta\theta} = A_{\Delta\theta}x_{\Delta\theta} + L_{\Delta\theta}\nu_{\Delta\theta} \quad (4.22)$$

$$y_{\Delta\theta} = C_{\Delta\theta}x_{\Delta\theta} = \Delta\theta_{sensor} \quad (4.23)$$

where $\nu_{\Delta\theta} = \dot{\Delta}\theta_{sensor}$, $A_{\Delta\theta} = 0$, and $L_{\Delta\theta} = C_{\Delta\theta} = 1$.

As a result the following dynamics are obtained for the whole system when using equations (4.1) - (4.4), (4.7) - (4.11), and (4.14) - (4.17); considering positive shaft speed ($n > 0$), and neglecting the saturation phenomena, the unknown term $X_{\dot{U}}$, and the measurement noise:

$$\dot{x} = f(x) + g(x)u + l(x)\nu + p(x)w \quad (4.24)$$

$$y = h(x) \quad (4.25)$$

where

$$x = \begin{pmatrix} Q_{eng} \\ n \\ U \\ \theta \\ Y_i \\ x_{\Delta n} \\ x_{\Delta\theta} \end{pmatrix} \quad u = \begin{pmatrix} n_{ref} \\ \theta_{ref} \end{pmatrix} \quad \nu = \begin{pmatrix} \Delta k_y Y \\ \dot{\Delta} n_{sensor} \\ \dot{\Delta}\theta_{sensor} \\ \Delta\dot{\theta}_{inc} \end{pmatrix}$$

$$w = \begin{pmatrix} T_{ext} \\ Q_f \end{pmatrix} \quad y = \begin{pmatrix} n_m \\ \theta_m \\ U_m \end{pmatrix} \quad h(x) = \begin{pmatrix} n + x_{\Delta n} \\ \theta + x_{\Delta\theta} \\ U \end{pmatrix}$$

and

$$f(x) = \begin{pmatrix} -\frac{1}{\tau_c}Q_{eng} + \frac{k_y}{\tau_c}Y_i - \frac{k_y k_r}{\tau_c}(n + x_{\Delta n}) \\ \frac{1}{I_m}\left[Q_{eng} - Q_{|n|n}n^2\theta - Q_{|n|V_a}(1-w)nU\theta\right] \\ \frac{1-t_T}{m}\left[T_{|n|n}n^2\theta + T_{|n|V_a}(1-w)nU\right] + \frac{1}{m}R(U) \\ -k_t(\theta + x_{\Delta\theta}) \\ -\frac{k_r}{\tau_i}(n + x_{\Delta n}) \\ 0 \\ 0 \end{pmatrix}$$

$$g(x) = \begin{pmatrix} \frac{k_y\, k_r}{\tau_c} & 0 \\ 0 & 0 \\ 0 & 0 \\ 0 & k_t \\ \frac{k_r}{\tau_i} & 0 \\ 0 & 0 \\ 0 & 0 \end{pmatrix} \quad l(x) = \begin{pmatrix} \frac{1}{\tau_c} & 0 & 0 & 0 \\ 0 & 0 & 0 & 0 \\ 0 & 0 & 0 & 0 \\ 0 & 0 & 0 & 1 \\ 0 & 0 & 0 & 0 \\ 0 & 1 & 0 & 0 \\ 0 & 0 & 1 & 0 \end{pmatrix} \quad p(x) = \begin{pmatrix} 0 & 0 \\ 0 & -\frac{1}{I_m} \\ \frac{1}{m} & 0 \\ 0 & 0 \\ 0 & 0 \\ 0 & 0 \\ 0 & 0 \end{pmatrix}$$

Remarks: When looking at equations (4.11) and (4.13) it can be see that the fuel index Y and its measurement Y_m are functions of n_{ref} and n_m. Hence, Y_m gives no useful redundant information **when** the saturation effects are neglected no faults are considered in the governor. Governor faults have been handled in the industrial actuator benchmark introduced by Blanke and Patton (1995). The FDI-results are described in (Bøgh (1997)). Therefore, the measurement of the fuel index Y_m is omitted in the following analysis to ease the computation.

The gain fault Δk_y is modeled as an additive fault by using the notation $\nu_1 = \Delta k_y Y$.

The fault vector ν contains four different faults instead of being scalar as in Definition 3.5 for the nonlinear FPRG. This is handled in the following way: For the above system four different FPRGs are defined, one for each fault, by considering the remaining three faults as additional disturbances (i.e. including them in the disturbance vector w), more details are given in the next subsection.

During the whole analysis all initial conditions are considered to be equal zero, $x_0 = x(t = 0) = 0$. Furthermore, as the propeller has a controllable pitch (CPP) the shaft speed is considered to be positive ($n > 0$) corresponding to normal operation. Without loss of generality for the FDI problem the pitch θ is considered positive for the whole operating range.

4.2.2 Application & results

In order to apply the geometric approach, as described in the previous chapter, the FDI problem for the ship benchmark (see Section 4.1.3) has to be formulated as a combination of several different FPRGs. This is due to the fact that there are four different faults to be handled in the benchmark and that a FPRG only considers FDI for one fault at a time.

System (4.24) and (4.25) offers several possibilities to define these FPRGs, because different subsystems can be considered next to the overall system. The following scenarios are treated on the next pages:

- Complete system with controllers and disturbances Q_f and T_{ext}
- Complete system with controllers and without disturbances Q_f and T_{ext}
- Propeller pitch loop with pitch controller
- Shaft speed loop with governor and disturbances Q_f and T_{ext}
- Shaft speed loop with governor and without disturbances Q_f and T_{ext}

For each of these scenarios different FPRGs are defined and analyzed in the next subsections. The geometric approach is applied to each of them following eight steps:

Methodology for applying the geometric approach to the different FPRGs:

1. Reducing the model (4.24) and (4.25) to the subsystem of the considered FPRG.
2. Choosing the fault ν_i, $i \in \{1, \ldots, 4\}$ that is to be detected and isolated.
3. Adding the remaining 3 faults ν_j, $j \in \{1, \ldots, 4\} \wedge j \neq i$, to the disturbances $w \in \mathbb{R}^s \Rightarrow \quad \nu^{new} = \nu_i, \quad l^{new}(x) = l_i(x), \quad w^{new} = [\nu_j \quad w]^T$, and $p^{new}(x) = [l_j(x) \quad p(x)]$.
4. Determining $P = span\{p_i^{new}\}$, where p_i^{new}, $i = 1, \ldots, (s+3)$, are the column vectors of $p^{new}(x)$.
5. Using algorithm (3.59) and (3.60) to calculate Σ_*^P.
6. Using algorithm (3.62) and (3.63) to calculate $Q = (\text{o.c.a.}((\Sigma_*^P)^\perp))^\perp$.
7. If $l_i(x) \notin Q$, then designing a coordinate transformation to obtain a subsystem as described in Theorem 3.11. If $l_i(x) \in Q$, then the analyzed FPRG cannot be solved for arbitrary fault signals.
8. Observability analysis of the resulting subsystem that is only affected by the considered fault, i.e. where the corresponding components of $l_i(x) \neq 0$.

4.2.2.1 Complete system with controllers and disturbances

The complete system (4.24) and (4.25) includes four different faults; described by the four components of vector ν. Hence, four different FPRGs can be defined as stated in Table 4.5. When applying the above presented methodology in order to solve the single FPRGs the following results can be obtained (Detailed description of the calculations is given in Appendix C.1.):

Step 1 can be omitted as the complete system is considered, i.e. the model (4.24) and (4.25) is used. The next two steps (2 and 3) are covered by Table 4.5 and the reordering of the corresponding matrices. The distribution P^i,$i \in \{1,\dots,4\}$ for the ith FPRG can be determined by $P^i = span\{p_j^{new}(x)\}$, $j \in \{1,\dots,5\}$. Starting the algorithm (3.59) and (3.60) to calculate $\Sigma_*^{P^i}$ for FPRG 1 up to FPRG 4 leads in all cases to the same result: $\Sigma_*^{P^i} = P^i$.

The next step is to obtain the observability codistribution o.c.a.$((\Sigma_*^{P^i})^\perp)$. As it turns out that o.c.a.$((\Sigma_*^{P^i})^\perp) = 0$ for all i it can easily be seen that $Q^i = (\text{o.c.a.}((\Sigma_*^{P^i})^\perp))^\perp = \mathbb{R}^7$. As a consequence the condition $l^{new}(x) \notin Q^i$ is not fulfilled, hence, the FPRGs 1-4 are not solvable for arbitrary fault signals.

FPRG	**Fault** (ν^{new})	**Disturbances** (w^{new})
FPRG 1	$\Delta k_y Y$	$\dot{\Delta n}_{sensor}$, $\dot{\Delta\theta}_{sensor}$, $\Delta\dot{\theta}_{inc}$, T_{ext} , Q_f
FPRG 2	$\dot{\Delta n}_{sensor}$	$\Delta k_y Y$, $\dot{\Delta\theta}_{sensor}$, $\Delta\dot{\theta}_{inc}$, T_{ext}, Q_f
FPRG 3	$\dot{\Delta\theta}_{sensor}$	$\Delta k_y Y$, $\dot{\Delta n}_{sensor}$, $\Delta\dot{\theta}_{inc}$, T_{ext}, Q_f
FPRG 4	$\Delta\dot{\theta}_{inc}$	$\Delta k_y Y$, $\dot{\Delta n}_{sensor}$, $\dot{\Delta\theta}_{sensor}$, T_{ext}, Q_f

Table 4.5: FPRGs for the complete system with controllers and disturbances.

4.2.2.2 Complete system with controllers and without disturbances

In the previous subsection it was shown that the FPRGs 1-4 cannot be solved. Hence, there is no way to isolate one fault from the disturbances and the other faults. In order to check if one fault can be isolated from the others this section considers the complete system (4.24) and (4.25), but neglects the disturbances Q_f and T_{ext}. The resulting FPRGs are listed in Table 4.6. The motivation for trying these FPRGs comes from the fact that there might be methods to handle with the disturbance afterwards; e.g. during the residual evaluation as mentioned in the conclusions of Chapter 3.

In order to analyze the solvability of the FPRGs 5-8 the above introduced methodology is followed. For details about the calculations the reader is referred to Appendix C.2. Again the complete system is considered and the steps 2 and 3 are covered by Table 4.6 and the reordering of the corresponding matri-

ces. For each FPRG the distribution P^i, $i \in \{5, \ldots, 8\}$ can be determined by $P^i = span\{p_j^{new}(x)\}$, $j \in \{1, \ldots, 3\}$. Then the algorithm (3.59) and (3.60) is applied to calculate $\Sigma_*^{P^i}$. For FPRG 5-8 the algorithm stops at $k^* = 1$ instead of $k^* = 0$ as it did for FPRG 1-4. The next step is then to obtain the observability codistribution o.c.a.$((\Sigma_*^{P^i})^\perp)$. It turns out to be equal to zero, just like in the previous section. Hence, the unobservability distribution can be determined as: $Q^i = \mathbb{R}^7$. As a consequence the FPRGs 5-8 are not solvable, because the condition $l(x)^{new} \notin Q^i$ is not fulfilled.

FPRG	**Fault** (ν^{new})	**Disturbances** (w^{new})
FPRG 5	$\Delta k_y Y$	$\Delta\dot{n}_{sensor}$, $\Delta\dot{\theta}_{sensor}$, $\Delta\dot{\theta}_{inc}$
FPRG 6	$\Delta\dot{n}_{sensor}$	$\Delta k_y Y$, $\Delta\dot{\theta}_{sensor}$, $\Delta\dot{\theta}_{inc}$
FPRG 7	$\Delta\dot{\theta}_{sensor}$	$\Delta k_y Y$, $\Delta\dot{n}_{sensor}$, $\Delta\dot{\theta}_{inc}$
FPRG 8	$\Delta\dot{\theta}_{inc}$	$\Delta k_y Y$, $\Delta\dot{n}_{sensor}$, $\Delta\dot{\theta}_{sensor}$

Table 4.6: FPRGs for the complete system with controllers and without disturbances Q_f and T_{ext}.

4.2.2.3 Pitch loop with pitch controller

The FPRGs defined for the complete system could not be solved as shown above. Hence, this section considers only the pitch loop, which is only affected by two faults - the pitch sensor fault $\Delta\dot{\theta}_{sensor}$ and the incipient actuator fault $\Delta\dot{\theta}_{inc}$. This subsystem is linear and there are no disturbances present. Two different linear FPRGs are considered in order to investigate the possibility for detection and isolation of these two faults. They are described in Table 4.7.

To get started with the geometric analysis step 1 is to reduce the model (4.24) and (4.25) to the considered subsystem:

$$\begin{aligned} \dot{x} &= f(x) + g(x)u + l(x)\nu + p(x)w \\ y &= h(x) \end{aligned}$$

where

$$x = \begin{pmatrix} \theta \\ x_{\Delta\theta} \end{pmatrix} \quad u = \theta_{ref} \quad \nu = \begin{pmatrix} \dot{\Delta}\theta_{sensor} \\ \Delta\dot{\theta}_{inc} \end{pmatrix}$$
$$w = 0 \qquad p(x) = 0 \qquad y = \theta_m \qquad h(x) = \theta + x_{\Delta\theta}$$
$$f(x) = \begin{pmatrix} -k_t(\theta + x_{\Delta\theta}) \\ 0 \end{pmatrix} \quad g(x) = \begin{pmatrix} k_t \\ 0 \end{pmatrix} \quad l(x) = \begin{pmatrix} 0 & 1 \\ 1 & 0 \end{pmatrix}$$

FPRG	**Fault** (ν^{new})	**Disturbance** (w^{new})
FPRG 9	$\dot{\Delta}\theta_{sensor}$	$\Delta\dot{\theta}_{inc}$
FPRG 10	$\Delta\dot{\theta}_{inc}$	$\dot{\Delta}\theta_{sensor}$

Table 4.7: FPRGs for the pitch loop with controller.

When following the remaining seven steps of the introduced methodology it can be seen that the FPRG 9 and FPRG 10 are not solvable either. Reason for this is that also for FPRG 9 and FPRG 10 the condition $l(x)^{new} \notin Q^i$ is not fulfilled. To see the detailed calculations the reader is referred to Appendix C.3.

4.2.2.4 Shaft speed loop with governor and disturbances

In this section the shaft speed loop is considered. Together with the pitch loop system from the previous section it forms the complete system. Hence, the shaft speed loop is the only remaining subsystem to be analyzed. It includes the shaft speed controller (governor) and the external disturbances T_{ext} and Q_f. The pitch θ is considered as fault-free input to this subsystem, because there are other known methods to detect pitch faults and the occurence of multiple (simultaneous) faults is very unlikely. Therefore, the shaft speed loop is affected by two different faults, the diesel engine gain fault $\Delta k_y Y$ and the shaft speed sensor fault $\dot{\Delta} n_{sensor}$. Table 4.8 describes the resulting FPRGs. Model (4.24) and (4.25) can be reduced to the following model of the shaft speed loop with governor and disturbances (step 1 of the analysis methodology):

$$\begin{aligned} \dot{x} &= f(x) + g(x)u + l(x)\nu + p(x)w \\ y &= h(x) \end{aligned}$$

FPRG	**Fault** (ν^{new})	**Disturbances** (w^{new})
FPRG 11	$\Delta k_y Y$	$\dot{\Delta} n_{sensor}, T_{ext}, Q_f$
FPRG 12	$\dot{\Delta} n_{sensor}$	$\Delta k_y Y$,T_{ext}, Q_f

Table 4.8: FPRGs for the shaft speed loop with governor and disturbances.

where

$$x = \begin{pmatrix} Q_{eng} \\ n \\ U \\ Y_i \\ x_{\Delta n} \end{pmatrix} \quad u = \begin{pmatrix} n_{ref} \\ \theta \end{pmatrix} \quad \nu = \begin{pmatrix} \Delta k_y Y \\ \dot{\Delta} n_{sensor} \end{pmatrix}$$

$$w = \begin{pmatrix} T_{ext} \\ Q_f \end{pmatrix} \qquad y = \begin{pmatrix} n_m \\ U_m \end{pmatrix} \quad h(x) = \begin{pmatrix} n + x_{\Delta n} \\ U \end{pmatrix}$$

$$f(x) = \begin{pmatrix} -\frac{1}{\tau_c} Q_{eng} + \frac{k_y}{\tau_c} Y_i - \frac{k_y k_r}{\tau_c}(n + x_{\Delta n}) \\ \frac{1}{I_m} Q_{eng} \\ \frac{1}{m} R(U) + \frac{1-t_T}{m} T_{|n|V_a}(1-w)nU \\ -\frac{k_r}{\tau_i}(n + x_{\Delta n}) \\ 0 \end{pmatrix}$$

$$g(x) = \begin{pmatrix} \frac{k_y k_r}{\tau_c} & 0 \\ 0 & -\frac{1}{I_m}\left[Q_{|n|n} n^2 + Q_{|n|V_a}(1-w)nU\right] \\ 0 & \frac{1-t_T}{m} T_{|n|n} n^2 \\ \frac{k_r}{\tau_i} & 0 \\ 0 & 0 \end{pmatrix}$$

$$l(x) = \begin{pmatrix} \frac{1}{\tau_c} & 0 \\ 0 & 0 \\ 0 & 0 \\ 0 & 0 \\ 0 & 1 \end{pmatrix} \quad p(x) = \begin{pmatrix} 0 & 0 \\ 0 & -\frac{1}{I_m} \\ \frac{1}{m} & 0 \\ 0 & 0 \\ 0 & 0 \end{pmatrix}$$

The calculations for the geometric approach to solve FPRG 11 and FPRG 12 are given in Appendix C.4. They show that the FPRG 11 and FPRG 12 are not solvable either, as also here the condition $l(x)^{new} \notin Q^i$ is not fulfilled.

4.2.2.5 Shaft speed loop with governor and without disturbances

This section considers the shaft speed loop including the shaft speed controller (governor) and neglecting the external disturbances T_{ext} and Q_f. Similar to Section 4.2.2.2 this is done in order to check the possibility two isolate the two faults $\Delta k_y Y$ and $\Delta\dot{n}_{sensor}$ from each other. The disturbance might be dealt with in the residual evaluation phase. Two different FPRGs neglecting the disturbances are stated in Table 4.9.

FPRG	**Fault** (ν^{new})	**Disturbances** (w^{new})
FPRG 13	$\Delta k_y Y$	$\Delta\dot{n}_{sensor}$
FPRG 14	$\Delta\dot{n}_{sensor}$	$\Delta k_y Y$

Table 4.9: FPRGs for the shaft speed loop with governor and without disturbances.

The geometric approach is applied to analyze the solvability of FPRG 13 and 14 by following the methodology described on page 65. The detailed calculations are given in Appendix C.5. For the FPRG 13 they show that the calculation of the unobservability distribution $Q^{13} = (\text{o.c.a.}((\Sigma_*^{P^{13}})^{\perp}))^{\perp}$ leads to the following result:

$$Q^{13} = (\text{o.c.a.}(P^{13^{\perp}}))^{\perp} = P^{13} = span\left\{(0\ 0\ 0\ 0\ 1)^T\right\}$$

So it can be seen that the conditions $p(x)^{new} = (0\ 0\ 0\ 0\ 1)^T \in Q^{13}$ and $l(x)^{new} = (\frac{1}{\tau_c}\ 0\ 0\ 0\ 0)^T \notin Q^{13}$ are fulfilled, hence, a solution for FPRG 13

might exist. So, the next step in the procedure is to find a coordinate transformation as described in Theorem 3.11. This is done by applying the procedure described in DePersis and Isidori (2000) (Proposition 3). Details are given in Appendix C.5. As a result the following subsystem can be stated for the FPRG 13 that is only affected by the gain fault $\Delta k_y Y$:

$$\dot{x} = f(x) + g(x)u + l(x)\nu \tag{4.26}$$

$$y_1 = U_m = U \tag{4.27}$$

$$\tag{4.28}$$

where

$$x = \begin{pmatrix} Q_{eng} \\ n \\ U \\ Y_i \end{pmatrix} \quad u = \begin{pmatrix} n_{ref} \\ \theta \\ n_m \end{pmatrix} \quad \nu = \Delta k_y Y$$

$$f(x) = \begin{pmatrix} -\frac{1}{\tau_c} Q_{eng} + \frac{k_y}{\tau_c} Y_i \\ \frac{1}{I_m} Q_{eng} \\ \frac{1}{m} R(U) + \frac{1-t_T}{m} T_{|n|V_a} (1-w) n U \\ 0 \end{pmatrix} \quad l(x) = \begin{pmatrix} \frac{1}{\tau_c} \\ 0 \\ 0 \\ 0 \end{pmatrix}$$

$$g(x) = \begin{pmatrix} \frac{k_y k_r}{\tau_c} & 0 & -\frac{k_y k_r}{\tau_c} \\ 0 & -\frac{1}{I_m} \left[Q_{|n|n} n^2 + Q_{|n|V_a} (1-w) n U \right] & 0 \\ 0 & \frac{1-t_T}{m} T_{|n|n} n^2 & 0 \\ \frac{k_r}{\tau_i} & 0 & -\frac{k_r}{\tau_i} \end{pmatrix}$$

Hence, building an observer for the (x, y_1)-system, considering the shaft speed measurement $n_m = n + x_{\Delta n}$ as additional input, while neglecting the fault, i.e. $\nu = 0$, could solve the FPRG 13. However, this requires that the subsystem is observable and an observer can be designed.

The observability can be analyzed by taking a look at the observability codistribution (see Nijmeijer and van der Schaft (1990) or equation (3.48), on page 39):

$$d\mathcal{O}(x) = \text{span}\{dH(x),\ H \in \mathcal{O}\},\ x \in \mathcal{X}$$

For the considered subsystem it can be shown that the dimension of $d\mathcal{O}(x)$ equals the dimension of $\mathcal{X}$ ($n = 4$) as:

$$d\mathcal{O}(x) = \text{span}\{dh_2,\ dL_{g_2}h_2,\ dL_f L_{g_2}h_2,\ dL_f^2 L_{g_2}h_2\}$$

hence, the subsystem is locally observable. In Section 4.3 the possibility to design an observer for the subsystem (considering $\nu = 0$) in order to obtain a residual r that solves the FPRG 13 is investigated.

Very similar considerations are made for FPRG 14. The detailed calculations can be found in Appendix C.5. Following the procedure in order to obtain the unobservability distribution $Q^{14} = (\text{o.c.a.}((\Sigma_*^{P^{14}})^\perp))^\perp$ leads to the following result:

$$Q^{14} = (\text{o.c.a.}(S_1^{14\perp}))^\perp = span\{(1\ 0\ 0\ 0\ 0)^T, (0\ 1\ 0\ 0\ 0)^T, (0\ 0\ 0\ 1\ 0)^T\}$$

So it can be seen that the conditions $p(x)^{new} = (\frac{1}{\tau_c}\ 0\ 0\ 0\ 0)^T \in Q^{14}$ and $l(x)^{new} = (0\ 0\ 0\ 0\ 1)^T \notin Q^{14}$ are fulfilled, hence, a solution for FPRG 14 might exist. So, the next step in the procedure (described on page 65) is to find a coordinate transformation as described in Theorem 3.11. This is done by applying the procedure described in DePersis and Isidori (2000) (Proposition 3). Details are given in Appendix C.5. As a result the following subsystem can be stated for the FPRG 14 that is only affected by the sensor fault $\dot{\Delta n}_{sensor}$:

$$\begin{aligned} \dot{x} &= f(x, n_m) + g(x, n_m)u + l(x)\nu \\ y_1 &= U_m = U \\ n_m &= n + x_{\Delta n} \end{aligned}$$

where

$$x = \begin{pmatrix} U \\ x_{\Delta n} \end{pmatrix} \quad u = \theta \quad \nu = \begin{pmatrix} \dot{\Delta n}_{sensor} \end{pmatrix} \quad l(x) = \begin{pmatrix} 0 \\ 1 \end{pmatrix}$$

$$f(x, n_m) = \begin{pmatrix} \frac{1}{m}R(U) + \frac{1-t_T}{m}T_{|n|V_a}(1-w)(n_m - x_{\Delta n})U \\ 0 \end{pmatrix}$$

$$g(x, n_m) = \begin{pmatrix} \frac{1-t_T}{m}T_{|n|n}(n_m - x_{\Delta n})^2 \\ 0 \end{pmatrix}$$

When considering the fault-free subsystem, i.e. taking out the sensor fault effect, the system reduces to the subsystem:

$$\dot{x} = f(x, n_m) + g(x, n_m)u \tag{4.29}$$

$$y_1 = U_m = U \tag{4.30}$$

where

$$x = U \quad u = \theta \quad g(x, n_m) = \frac{1 - t_T}{m} T_{|n|n} n_m^2$$

$$f(x, n_m) = \frac{1}{m} R(U) + \frac{1 - t_T}{m} T_{|n|V_a} (1 - w) n_m U$$

which is obviously observable. In the Section 4.3 an observer is built for this subsystem (considering $\nu = 0$) in order to obtain a residual r that solves the FPRG 14.

4.2.3 Conclusions

From the previous section it can be seen that the FDI problem for the ship propulsion system cannot be solved in a geometric sense. Following the geometric idea, as presented by DePersis and Isidori (2000) and described in Chapter 3, does not lead to residuals that are only affected by a particular fault. This has several reasons.

One reason for this lies in the dynamics of the system. The pitch and shaft speed loop are coupled via the propeller dynamics. This makes it impossible to separate the shaft speed loop from the pitch faults. Another problem is that for the pitch sensor fault and the incipient pitch fault the points of entry into the system are only separated by an integration. That means obviously that the two faults cannot be isolated from each other, because arbitrary fault signals are considered. An abrupt hydraulic pressure loss ($\Delta\dot{\theta}_{inc}$ described by a step function) would affect the system in a similar way as a drift in the pitch measurement ($\dot{\Delta\theta}_{sensor}$ described by a ramp function). Another reason why successful FDI is not possible is that the disturbances Q_f and T_{ext} act directly on the propeller dynamics and, hence, also on the measurements. As a consequence, there exists no observable subsystem for each fault that is not effected by the disturbances as shown above.

However, these problems count also for other FDI approaches. Hence, they cannot solve the FDI problem either, unless they use additional information. For

example, some methods exploit additional information about the dynamics of the disturbances. This is not done by the geometric approach as it considers arbitrary fault and disturbance signals. So, obviously the geometric approach cannot handle FDI problems where the disturbances act in the same 'direction' as the faults.

In practice it might be possible to solve this problem by additional means, e.g. additional residual evaluation. This is due to the fact that in reality the signals are not completely arbitrary. Hence, there might exist methods to eliminate the disturbance effect on the residual, e.g. filtering the residual. When the disturbance dynamics are significantly slower than the fault dynamics a high-pass filter might help. Another situation might be that the disturbance effect is small enough, such, that the FDI problem could be solved by a higher threshold in the decision phase. These possibilities using additional methods to solve the FDI problem need specific analysis, hence, there does not exist a general approach. Therefore, FDI design cannot be fully automated.

However, the geometric approach is a powerful and systematic tool to find subsystems and structures for the observer design. This is important in order to obtain useful residuals. The advanced mathematics might be an obstacle for engineers, who are not familiar with the different geometric calculations, but once learned it is straightforward computation. Hence, it might be interesting to investigate to which degree the geometric approach could be automated (e.g. as analysis-tool) in future research.

In the next section two observers are designed based on the results from the geometric analysis given in the previous section. The goal is to generate residuals that can solve the FDI problem for the propulsion system.

4.3 Observer design for FDI

In the previous section two different locally observable subsystems, (4.26)-(4.27) and (4.29)-(4.30), were obtained by the geometric analysis of the propulsion system. Each of these subsystems is affected by only one fault when the pitch measurement is considered to be fault-free. Hence, two observers are designed in the following subsections to detect and isolate the two different shaft speed loop faults. Additionally, an observer for the pitch loop is designed to detect the pitch faults. At the end of this section an adaptive nonlinear observer is given for comparison.

4.3.1 FDI in shaft speed loop

The following two subsections describe the observer design for the obtained subsystems. The goal is to use the observers as residual generators to detect and isolate the shaft speed loop faults Δk_y and Δn_{sensor}.

4.3.1.1 FDI for the diesel engine gain fault Δk_y

Subsystem (4.26)-(4.27) is by construction only affected by the diesel engine gain fault Δk_y, when the pitch loop is considered to be fault-free. Hence, an observer is designed in the following, such, that it can be used for FDI.

To start the fault-free subsystem can be rewritten as:

$$\dot{x} = f(x) + g(x)u \tag{4.31}$$

$$y = U \tag{4.32}$$

where $x = \begin{pmatrix} n \\ U \end{pmatrix}$ $f(x) = \begin{pmatrix} 0 \\ \frac{1}{m}R(U) + \frac{1-t_T}{m}T_{|n|V_a}(1-w)nU \end{pmatrix}$

$$g(x) = \begin{pmatrix} \frac{1}{I_m}k_y & -\frac{1}{I_m}\left[Q_{|n|n}n^2 + Q_{|n|V_a}(1-w)nU\right] \\ 0 & \frac{1-t_T}{m}T_{|n|n}n^2 \end{pmatrix} \quad u = \begin{pmatrix} Y_m \\ \theta_m \end{pmatrix}$$

because the diesel engine dynamics are very fast (small τ_c) comparing to ship dynamics (4.1) can be replaced by $Q_{eng} = (k_y + \Delta k_y)Y_m$; where Y_m denotes the available fuel index measurement. To return to the original notation of the

ship dynamics the following notation is used for the subsystem:

$$\dot{n} = \frac{1}{I_m}\, k_y\, Y_m - \frac{1}{I_m}\, \left[Q_{|n|V_a}(1-w)\, n\, U + Q_{|n|n}\, n^2\right]\, \theta \tag{4.33}$$

$$\dot{U} = \frac{1}{m} R(U) + \frac{1-t_T}{m}\, T_{|n|V_a}(1-w)\, n\, U + \frac{1-t_T}{m}\, T_{|n|n}\, n^2\, \theta \tag{4.34}$$

$$y = U \tag{4.35}$$

with the fuel index measurement Y_m and the pitch measurement θ_m as external inputs. For system (4.33) and (4.35) an observer can be given of the following form:

Observer1:

$$\dot{\hat{n}} = \frac{1}{I_m}\, k_y\, Y_m - \frac{1}{I_m}\, \left[Q_{|n|V_a}(1-w)\hat{n}\hat{U} + Q_{|n|n}\hat{n}^2\right]\, \theta_m + K^{\hat{n}}_{\Delta k_y}(U_m - \hat{U}) \tag{4.36}$$

$$\dot{\hat{U}} = \frac{1}{m} R(\hat{U}) + \frac{1-t_T}{m}\, [T_{|n|V_a}(1-w)\hat{n}\hat{U} + T_{|n|n}\hat{n}^2\theta_m] + K^{\hat{U}}_{\Delta k_y}(U_m - \hat{U}) \tag{4.37}$$

$$\hat{y} = \hat{U} \tag{4.38}$$

The stability of Observer1 can be proven following Gauthier *et al.* (1992). Details of the proof are outlined in Chapter 5. For FDI a residual can be obtained using the output (ship speed estimate) of Observer1 and the ship speed measurement U_m in the following way:

$$\textbf{Residual1:} \qquad r_1 = U_m - \hat{U} \tag{4.39}$$

Residual1 is by construction only affected by the gain fault Δk_y as shown by the geometric approach (when considering the pitch signal to be fault-free). As the observer is stable the residual behaves in the fault-free case, such, that $r_1 \to 0$ for $t \to \infty$.
For the estimation errors:

$$e^1_n = n - \hat{n} \qquad\qquad e^1_U = U - \hat{U}$$

the following error dynamics can be given (as here $\theta = \theta_m$:

$$\dot{e}_n^1 = \frac{1}{I_m}\Delta k_y Y - \frac{1}{I_m}\left[Q_{|n|V_a}(1-w)(nU - \hat{n}\hat{U}) + Q_{|n|n}(n^2 - \hat{n}^2)\right]\theta_m - K_{\Delta k_y}^{\hat{n}}(U_m - \hat{U}) \tag{4.40}$$

and

$$\dot{e}_U^1 = \dot{r}_1 = \frac{1}{m}(R(U) - R(\hat{U})) + \frac{1-t_T}{m}[T_{|n|V_a}(1-w)(nU - \hat{n}\hat{U}) + T_{|n|n}(n^2 - \hat{n}^2)\theta_m] - K_{\Delta k_y}^{\hat{U}}(U_m - \hat{U}) \tag{4.41}$$

Looking at the estimation error dynamics (4.40) one could think that an occurring gain fault Δk_y would have a direct impact on $\dot{e}_n^1$ leading to a growing estimation error: $n \neq \hat{n}$. As can be seen from (4.41) this would then also affect the shaft speed estimate , i.e. $U \neq \hat{U}$. Hence, Residual1 would deviate from zero in case of a gain fault: $\underline{r_1 \neq 0}$. However, as the dynamics are nonlinear and coupled the argumentation is not that simple. Simulation results given in the next section show that the gain fault Δk_y indeed affects Residual1.

When taking a closer look it can be seen that Observer1 offers also another possibility to generate a residual when using the shaft speed measurement n_m:

$$\textbf{Residual2:} \qquad r_2 = n_m - \hat{n} \tag{4.42}$$

Obviously, this residual is also affected by the shaft speed sensor fault Δn_{sensor}. The residual dynamics can be stated as follows:

$$\dot{r}_2(n_m, \hat{n}) = \dot{e}_n^1 + \dot{\Delta n}_{sensor} \tag{4.43}$$

where $\dot{e}_n^1$ is described by (4.40). The FDI performance of Residual1 and Residual2 will be demonstrated by simulation results in the next section.

4.3.1.2 FDI for the shaft speed sensor fault Δn_{sensor}

In this subsection an observer is designed for subsystem (4.29) - (4.30) in order to detect the shaft speed sensor fault Δn_{sensor}. As shown by the geometric approach in the previous section this subsystem is only affected by one fault (Δn_{sensor}), when the pitch loop is considered to be fault-free. Hence, the observation error can be used as a residual to obtain FDI for the ship propulsion

system.

To return to the original notation the following notation is used for subsystem (4.29) - (4.30):

$$\dot{U} = \frac{1}{m} R(U) + \frac{1 - t_T}{m} \left[T_{|n|V_a} (1 - w)\, n_m\, U + T_{|n|n}\, n_m^2\, \theta \right] \tag{4.44}$$

$$y_1 = U_m = U \tag{4.45}$$

with the shaft speed measurement n_m and the pitch measurement θ as external inputs. For system (4.44) and (4.45) an observer can be given of the following form:

Observer2:

$$\dot{\hat{U}} = \frac{1}{m} R(\hat{U}) + \frac{1 - t_T}{m} \left[T_{|n|V_a} (1 - w)\, n_m\, \hat{U} + T_{|n|n}\, n_m^2\, \theta_m \right] + K_{\Delta n}^{\hat{U}} (U - \hat{U}) \tag{4.46}$$

$$\hat{y} = \hat{U} \tag{4.47}$$

The stability of Observer2 can be proven following Gauthier *et al.* (1992). Details of the proof are outlined in Chapter 5. For FDI a residual can be obtained using the output (ship speed estimate) of Observer2 and the ship speed measurement U_m in the following way:

$$\textbf{Residual3:} \qquad r_3 = U_m - \hat{U} \tag{4.48}$$

This residual is only affected by the shaft speed sensor fault Δn_{sensor} as shown by the geometric approach. The observer is stable, hence, in the fault-free case $r_3 \to 0$ for $t \to \infty$. The residual dynamics can be stated as follows:

$$\begin{aligned} \dot{e}_U^3 = \dot{r}_3 = \frac{1}{m}(R(U) - R(\hat{U})) + \frac{1 - t_T}{m} [\, & T_{|n|V_a}(1 - w)(nU - n_m \hat{U}) \\ & + T_{|n|n}(n^2 - n_m^2)\theta_m] - K_{\Delta n}^{\hat{U}} (U_m - \hat{U}) \end{aligned} \tag{4.49}$$

as $n_m = n + \Delta n_{sensor}$ equation (4.49) can rewritten as:

$$\begin{aligned} \dot{e}_U^3 = \dot{r}_3 = & \frac{1}{m}(R(U) - R(\hat{U})) + \frac{1 - t_T}{m} [\, T_{|n|V_a}(1 - w) n (U - \hat{U}) \\ & - T_{|n|V_a}(1 - w) \Delta n_{sensor} \hat{U} - T_{|n|n}(2n \Delta n_{sensor} + \Delta n_{sensor}^2)\theta_m] \\ & - K_{\Delta n}^{\hat{U}} (U_m - \hat{U}) \end{aligned} \tag{4.50}$$

Hence, Δn_{sensor} affects Residual3. The FDI performance of r_3 will be demonstrated by simulation results in the next section.

4.3.2 FDI in pitch loop

The previous section describes the design of two different residual generators (observers). The resulting residuals can be used for detection and isolation of the two shaft speed loop faults; however, only when the pitch faults are not present. This can be seen when looking at Residual1 and Residual3 and the corresponding dynamics (4.41) and (4.50), because while the system state is based on the real pitch θ the observers use the pitch measurement θ_m. Hence, this subsection describes an observer design for the pitch loop in order to detect the two pitch faults $\Delta\theta_{sensor}$ and $\Delta\dot{\theta}_{inc}$.

The pitch loop is described by the equations (4.14) - (4.17). They can be stated as follows when neglecting the measurement noise and the saturation effects:

$$u_{\dot{\theta}} = k_t\,(\theta_{ref} - \theta_m) \qquad \dot{\theta} = u_{\dot{\theta}} + \Delta\dot{\theta}_{inc} \qquad y = \theta_m = \theta + \Delta\theta_{sensor} \tag{4.51}$$

For the linear system (4.51) a linear observer can be given in the following way when neglecting the pitch faults:

Observer3:

$$\dot{\hat{\theta}} = u_{\dot{\theta}} + K^{\hat{\theta}}_{\Delta\theta}(\theta_m - \hat{\theta}) \qquad \hat{y} = \hat{\theta} \tag{4.52}$$

where $u_{\dot{\theta}} = k_t\,(\theta_{ref} - \theta_m)$ is considered as input signal. For detection of pitch faults a residual can be obtained using the output (pitch estimate) of Observer3 and the pitch measurement θ_m in the following way:

$$\textbf{Residual4:} \qquad r_4 = \theta_m - \hat{\theta} \tag{4.53}$$

The fault-free dynamics of Residual4 are given by:

$$\dot{r}_4 = \dot{\theta}_m - \dot{\hat{\theta}} = u_{\dot{\theta}} - u_{\dot{\theta}} - K^{\hat{\theta}}_{\Delta\theta}(\theta_m - \hat{\theta}) = -K^{\hat{\theta}}_{\Delta\theta}\, r_4 \tag{4.54}$$

where it can be seen that stability can be assured by choosing a positive $K^{\hat{\theta}}_{\Delta\theta}$, because the dynamics are linear.

Taking the possible pitch faults $\Delta\theta_{sensor}$ and $\Delta\dot{\theta}_{inc}$ into account, the following dynamics can be obtained for the dynamics of Residual4:

$$\begin{aligned}\dot{r}_4 &= \dot{\theta}_m - \dot{\hat{\theta}} = (\dot{\theta} + \dot{\Delta}\theta_{sensor}) - \dot{\hat{\theta}} \\ &= (u_{\dot{\theta}} + \Delta\dot{\theta}_{inc} + \dot{\Delta}\theta_{sensor}) - u_{\dot{\theta}} - K^{\hat{\theta}}_{\Delta\theta}(\theta_m - \hat{\theta}) \\ &= \Delta\dot{\theta}_{inc} + \dot{\Delta}\theta_{sensor} - K^{\hat{\theta}}_{\Delta\theta}(\theta_m - \hat{\theta}) \end{aligned} \tag{4.55}$$

From the dynamics (4.55) it can be seen that Residual4 is affected by both pitch faults, hence, the residual can be used to detect the pitch faults. The FDI performance of r_4 will be demonstrated by simulation results in the next section.

4.3.3 Adaptive nonlinear observer

Designing an observer for observable systems is not straight-forward. Depending on the system structure there are different possibilities to design an observer. Hence, the FDI performance of the different observers can be different from design to design. This subsection presents a fault detection approach (Blanke *et al.* (1998),Blanke and Lootsma (1999)) based on an adaptive nonlinear observer design given by Cho and Rajamani (1997). Its FDI performance is illustrated by simulation results in the following section for comparison with the designs given above.

The observer is designed for the following subsystem describing the torque balance (4.2):

$$I_m\dot{n} = Q_{eng} - Q_{prop} - Q_f \qquad y = n_m \tag{4.56}$$

Neglecting the disturbance Q_f (friction torque) and using the known expressions for Q_{eng} and Q_{prop} leads to the following observable subsystem (including the shaft speed loop faults and considering the pitch loop to be fault-free):

$$\dot{n} = \frac{1}{I_m}\left(k_y + \Delta k_y\right) Y - \frac{1}{I_m}\left[Q_{|n|V_a}(1-w)\,n\,U + Q_{|n|n}\,n^2\right]\,\theta \tag{4.57}$$

$$y = n + \Delta n_{sensor} \tag{4.58}$$

In order to design an adaptive observer for system (4.57) and (4.58) as described in Cho and Rajamani (1997) the system is stated for the fault-free case as follows:

$$\dot{x} = \Phi(x, u_2, u_3) + \Theta\, u_1 \tag{4.59}$$

$$y = x \tag{4.60}$$

where

$$\Phi(x, u_2, u_3) = -\frac{1}{I_m}\left[Q_{|n|V_a}(1-w)n\,U_m + Q_{|n|n}\,n^2\right]\,\theta_m$$

$$x = n, \quad u_1 = Y_m, \quad u_2 = U_m, \quad u_3 = \theta_m, \quad \Theta = \frac{1}{I_m}\,k_y$$

using the measurements Y_m, U_m, and θ_m as external inputs u_1, u_2, and u_3.

Then an observer can be designed in the following way:

Observer4:

$$\dot{\hat{n}} = -\frac{1}{I_m}\left[Q_{|n|V_a}(1-w)\,\hat{n}\,U_m + Q_{|n|n}\,\hat{n}^2\right]\,\theta_m + \hat{\Theta}\,Y_m + L\,(n_m - \hat{n}) \tag{4.61}$$

$$\hat{y} = \hat{n} \tag{4.62}$$

with the parameter update:

$$\dot{\hat{\Theta}} = p\,Y_m\,(n_m - \hat{n}) \tag{4.63}$$

and $\hat{\Theta}(t=0) = \Theta_0$. $\Theta_0 = \frac{1}{I_m}\,k_y$ describes the nominal value for parameter Θ in the fault-free case. Stability of Observer4 is proven in Blanke *et al.* (1998).

Observer4 estimates the shaft speed and adapts to the actual value of the parameter Θ. Hence, two different residuals can be generated for FDI:

Residual5: $$r_5 = n_m - \hat{n} \tag{4.64}$$

and

Residual6: $$r_6 = \Theta_{nom} - \hat{\Theta} \tag{4.65}$$

Obviously, parameter Θ changes in the propulsion system when a diesel engine gain fault occurs; $\Theta_{actual} = \frac{1}{I_m}\,(k_y + \Delta k_y)$. This will clearly affect Residual6, because $\hat{\Theta} \rightarrow \Theta_{actual}$, when no other faults occur, due to the design of Observer4. Hence, the following relations hold for Residual6:

$$r_6 = \left(\Theta_{nom} - \hat{\Theta}\right) \rightarrow \left(\frac{1}{I_m}\,k_y - \frac{1}{I_m}\,(k_y + \Delta k_y)\right) = -\frac{1}{I_m}\,\Delta k_y \tag{4.66}$$

$$\dot{r}_6 = -\dot{\hat{\Theta}} = -p\,Y_m\,(n_m - \hat{n}) = -p\,Y_m\,(n + \Delta n_{sensor} - \hat{n}) \tag{4.67}$$

The equations (4.66) and (4.67) illustrate that Residual6 is affected by both shaft speed loop faults, Δk_y and Δn_{sensor}, when $Y_m \neq 0$.

For Residual5 the following dynamics can be derived:

$$\begin{aligned}\dot{r}_5 = \dot{n_m} - \dot{\hat{n}} = &\left[\frac{1}{I_m}\left(k_y + \Delta k_y\right) - \hat{\Theta}\right]\, Y + \dot{\Delta n}_{sensor} \\ &- \frac{1}{I_m}\left[Q_{|n|V_a}(1-w)\,(n-\hat{n})U + Q_{|n|n}\left(n^2 - \hat{n}^2\right)\right]\,\theta \\ &- L\,(n-\hat{n}) - L\,\Delta n_{sensor} \end{aligned} \tag{4.68}$$

Obviously, Residual5 is also affected by both shaft speed loop faults, Δk_y and Δn_{sensor}. The FDI performance of Observer4 will be demonstrated by simulation results in the next section.

4.4 Simulation results

Section 4.3 describes the design of four different observers (residual generators). Furthermore, it shows how to generate six different residuals by using the system outputs (measurements) and the observer outputs (output estimates). This section presents simulation results obtained by applying these residual generators to the simulation model of the ship propulsion system (described in Section 4.1). For the fault simulation the fault scenario described in Section 4.1.3 is considered.

In the simulations all four faults given in Table 4.1 (page 54) are simulated to test the FDI performance of the different residuals. The total simulation time is $3500sec$ and the faults occur at the in Table 4.4 given points of time. This sequence is used to provide the possibility to compare the obtained results with those obtained by other FDI approaches.

First, simulation results are given showing the ship propulsion system's behavior in the fault-free and in the faulty case. Then simulation results illustrate the residuals's behavior and sensitivity to the different faults. Section 4.4.4 takes a closer look at the residuals's performance and how they can be used to obtain successful FDI.

4.4.1 Ship propulsion system in the fault-free case

For the simulations the fixed maneuver defined for the ship propulsion benchmark is considered. It has a duration of $3500sec$. During this maneuver the ship is accelerated three times and decelerated once.

The corresponding reference signals for the lower-level control n_{ref} and θ_{ref} are provided by the upper-level control. They are shown in Figure 4.5. The resulting measurements of shaft speed n_m, pitch θ_m, ship speed U_m, and fuel index Y_m (without measurement noise) are given in Figure 4.6 for the fault-free case.

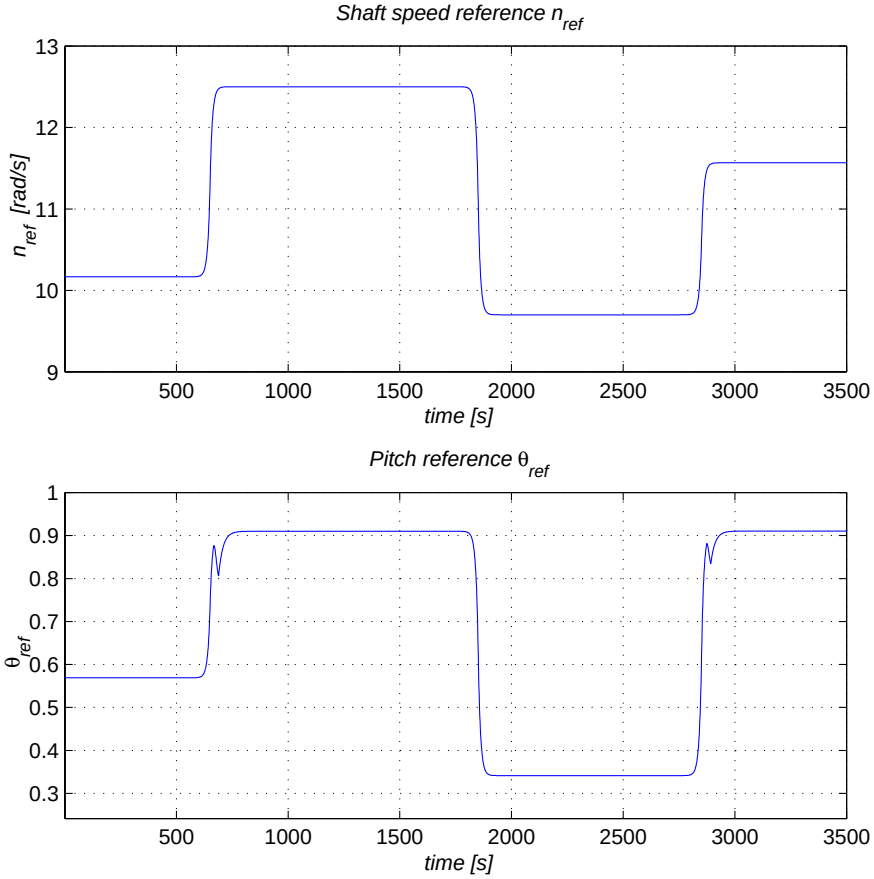

Figure 4.5: Reference signals n_{ref} and θ_{ref} provided by the upper-level control.

4.4.2 Ship propulsion system in the faulty case

For the faulty case all faults are simulated as described by Table 4.4. The resulting measurements are shown in Figure 4.7. The fault effects can be seen by comparing the measurements with those for the fault-free case given in Figure 4.6.

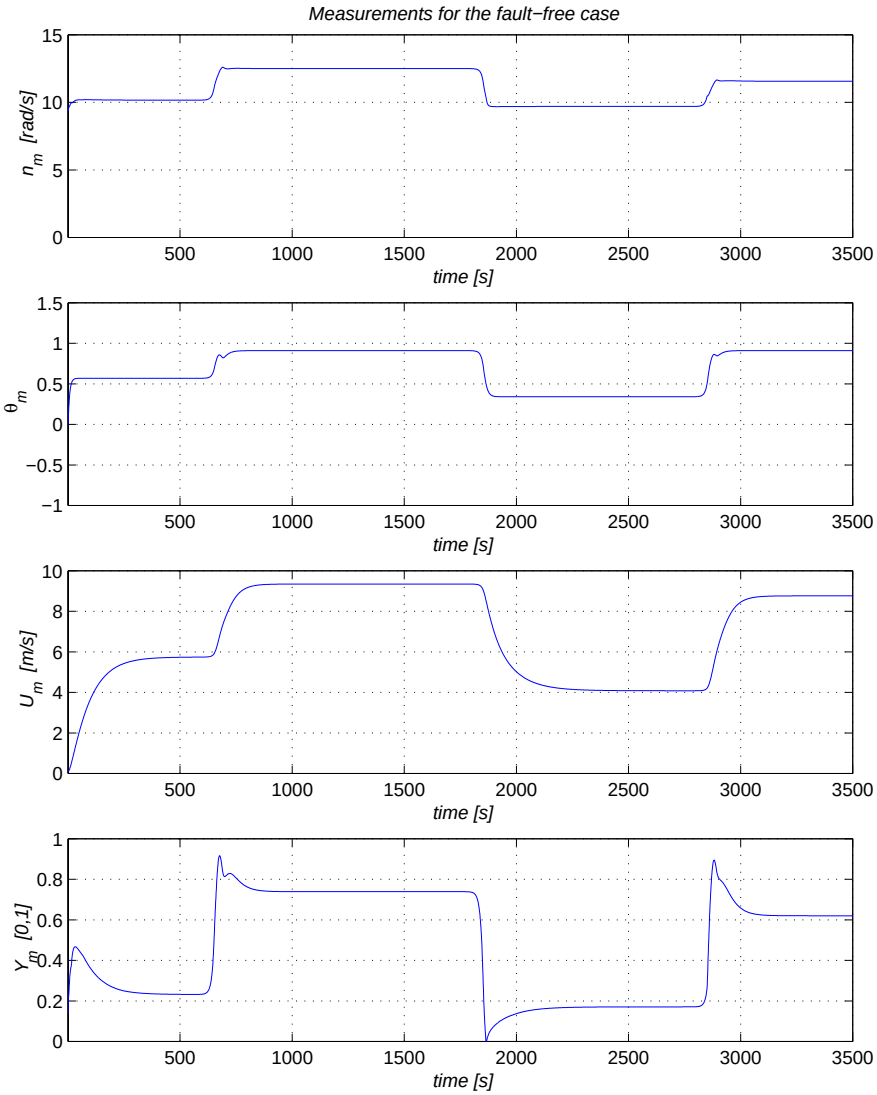

Figure 4.6: Measured shaft speed n_m, pitch θ_m, ship speed U_m, and fuel index Y_m in the fault-free case (without measurement noise).

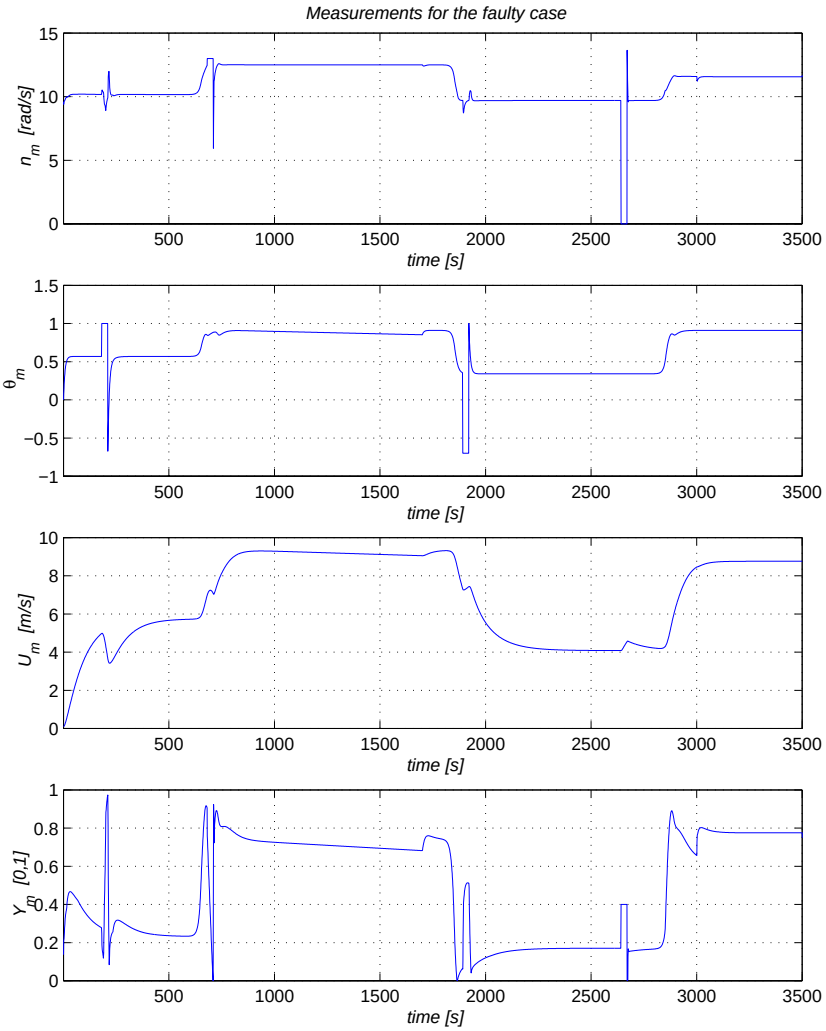

Figure 4.7: Measured shaft speed n_m, pitch θ_m, ship speed U_m, and fuel index Y_m in the faulty case (without measurement noise).

4.4.3 Residual simulation

Section 4.3 describes the generation of six different residuals. In this section the simulation results for these residuals are given for the full sequence of $3500sec.$ The simulations include all faults as described by Table 4.4. Measurement noise is not simulated to enhance visibility. Small fault effects would otherwise not be visible. However, for the residual evaluation it has been considered during the simulations. The propeller coefficients $Q_{|n|V_a}$, $Q_{|n|n}$, $T_{|n|V_a}$, and $T_{|n|n}$ are generated online by using the correct measurements and the function *TQ_const.m* for MATLAB™ . The function is part of the linear package *linear.zip* of the ship propulsion benchmark software. This is done due to the fact that the focus of this chapter lies on fault diagnosis and not on model identification.

4.4.3.1 Simulation of Residual1

Residual1 is generated in the following way:

$$r_1 = U_m - \hat{U}$$

where $\hat{U}$ is the output of Observer1 described by (4.36) - (4.38). The gains and initial conditions for the observer are chosen as follows:
$K^{\hat{n}}_{\Delta k_y} = 0.001$, $K^{\hat{U}}_{\Delta k_y} = 0.01$, $\hat{n}(t=0) = 9\,rad/s$, and $\hat{U}(t=0) = 0.1\,m/s$.
The simulation result is shown in Figure 4.8.

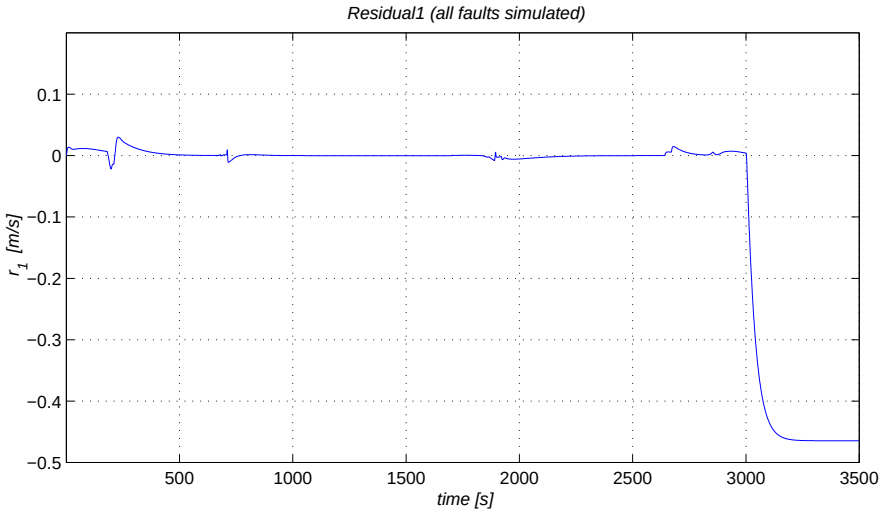

Figure 4.8: Residual1, $r_1 = U_m - \hat{U}$. Simulation including all faults and no measurement noise.

4.4.3.2 Simulation of Residual2

Residual2 is generated in the following way:

$$r_2 = n_m - \hat{n}$$

where $\hat{n}$ is the inner state of Observer1 described by (4.36) - (4.38). The gains and initial conditions for the observer are chosen as follows:
$K^{\hat{n}}_{\Delta k_y} = 0.001$, $K^{\hat{U}}_{\Delta k_y} = 0.01$, $\hat{n}(t=0) = 9\,rad/s$, and $\hat{U}(t=0) = 0.1\,m/s$.
The simulation result is shown in Figure 4.9.

4.4.3.3 Simulation of Residual3

Residual3 is generated in the following way:

$$r_3 = U_m - \hat{U}$$

where $\hat{U}$ is the output of Observer2 described by (4.46) and (4.47). The gain and initial condition for the observer are chosen as follows:
$K^{\hat{U}}_{\Delta n} = 0.05$, and $\hat{U}(t=0) = 0.1\,m/s$.
The simulation result is shown in Figure 4.10.

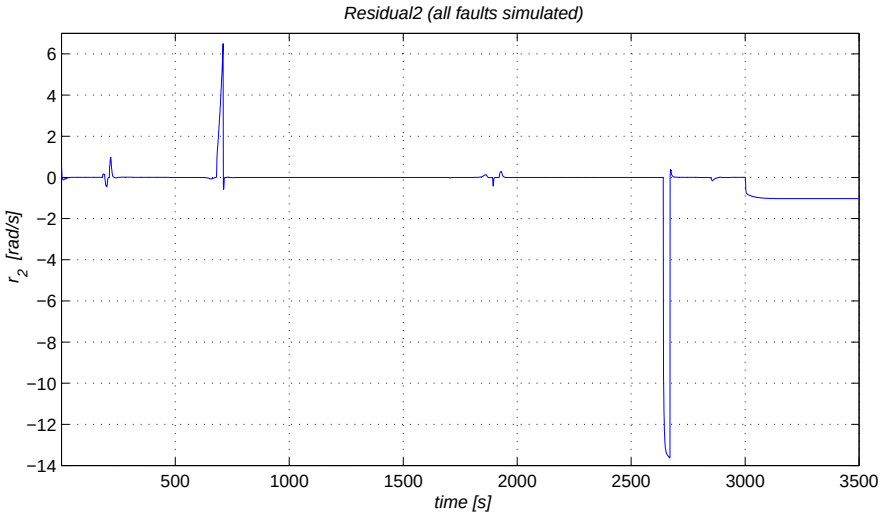

Figure 4.9: Residual2, $r_2 = n_m - \hat{n}$. Simulation including all faults and no measurement noise.

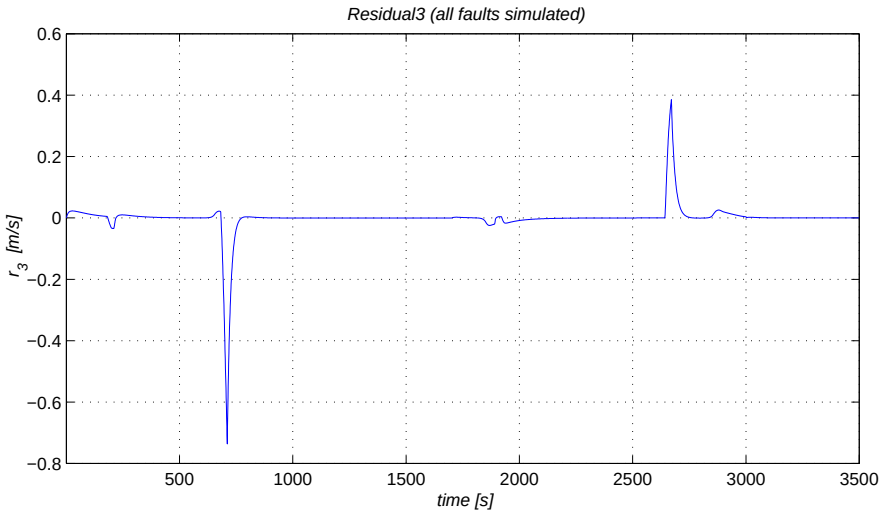

Figure 4.10: Residual3, $r_3 = U_m - \hat{U}$. Simulation including all faults and no measurement noise.

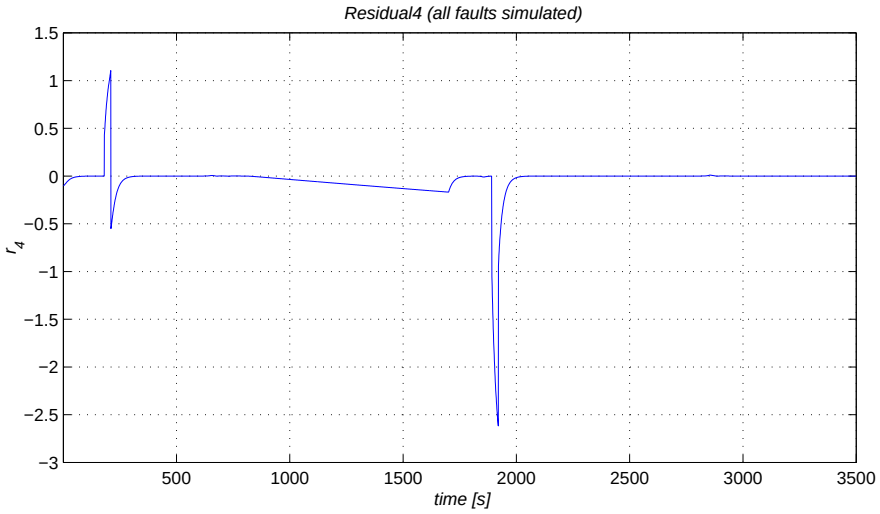

Figure 4.11: Residual4, $r_4 = \theta_m - \hat{\theta}$. Simulation including all faults and no measurement noise.

4.4.3.4 Simulation of Residual4

Residual4 is generated in the following way:

$$r_4 = \theta_m - \hat{\theta}$$

where $\hat{\theta}$ is the output of Observer3 described by (4.52). The gain and initial condition for the observer are chosen as follows:
$K^{\hat{\theta}}_{\Delta\theta} = 0.05$, and $\hat{\theta}(t = 0) = 0.1$.
The simulation result is shown in Figure 4.11.

4.4.3.5 Simulation of Residual5

Residual5 is generated in the following way:

$$r_5 = n_m - \hat{n}$$

where $\hat{n}$ is the output of Observer4 described by (4.61) - (4.63). The gains and initial conditions for the observer are chosen as follows:
$L = 0.1$, $p = 0.1$, $\hat{n}(t = 0) = 9\,rad/s$, and $\hat{\Theta}(t = 0) = \frac{1}{2}\Theta_{nom}$. The simulation result is shown in Figure 4.12.

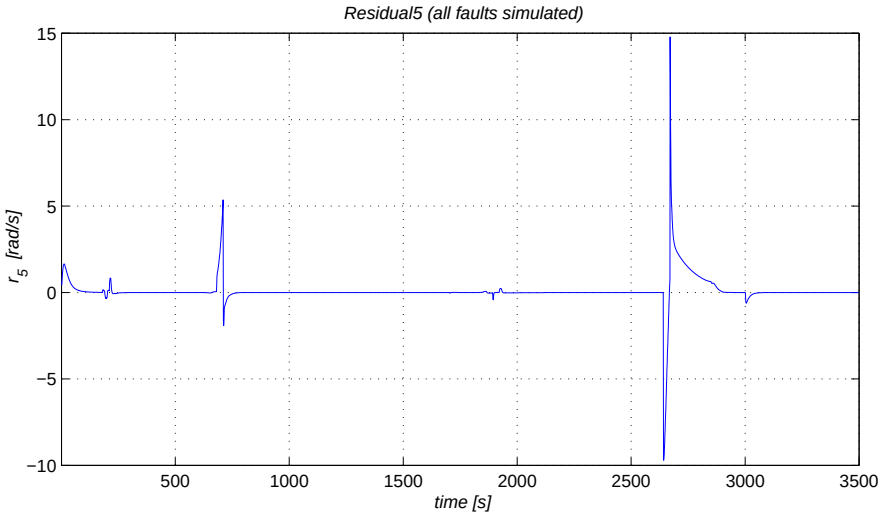

Figure 4.12: Residual5, $r_5 = n_m - \hat{n}$. Simulation including all faults and no measurement noise.

4.4.3.6 Simulation of Residual6

Residual6 is generated in the following way:

$$r_6 = \Theta_{nom} - \hat{\Theta}$$

where $\hat{\Theta}$ is the adapted parameter of Observer4 described by (4.61) - (4.63). The gains and initial conditions for the observer are chosen as follows:
$L = 0.1$, $p = 0.1$, $\hat{n}(t = 0) = 9\,rad/s$, and $\hat{\Theta}(t = 0) = \frac{1}{2}\Theta_{nom}$. The simulation result is shown in Figure 4.13.

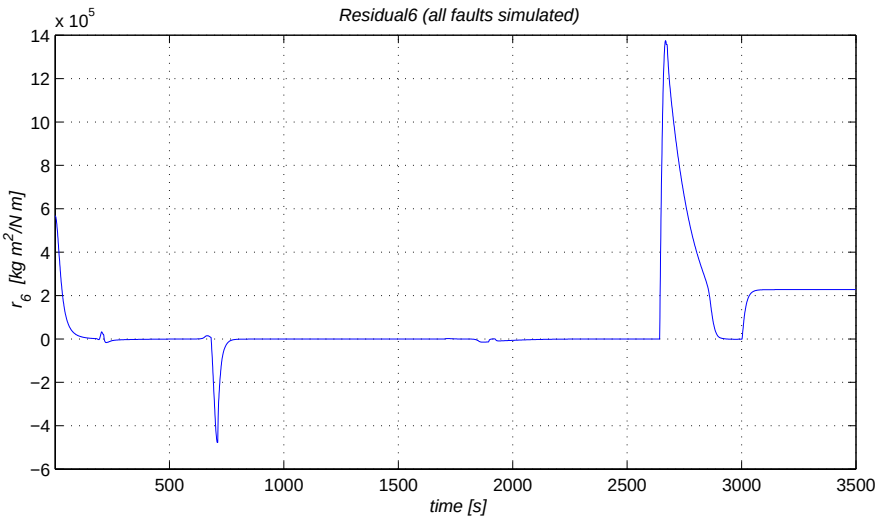

Figure 4.13: Residual6, $r_6 = \Theta_{nom} - \hat{\Theta}$. Simulation including all faults and no measurement noise.

4.4.4 FDI possibilities

As can be seen from Figures 4.8 - 4.13 the residuals react on the different faults, i.e. they deviate from zero. To investigate the resulting FDI possibilities it is necessary to take a closer look at the different residuals. In the Subsection 4.4.4.1 each fault is handled by zooming in on the six different residuals for the corresponding time of occurrence given in Table 4.4. The residuals are also plotted for the fault-free case to stress the fault effects. Robustness issues and the measurement noise are considered in Subsection 4.4.4.2 and 4.4.4.3. A final overview over the FDI possibilities is given in Subsection 4.4.4.4.

4.4.4.1 Residual overview

An overview over all six residuals is given in Figure 4.14. Figures 4.15 to 4.20 are zooming in on all residuals for each fault.

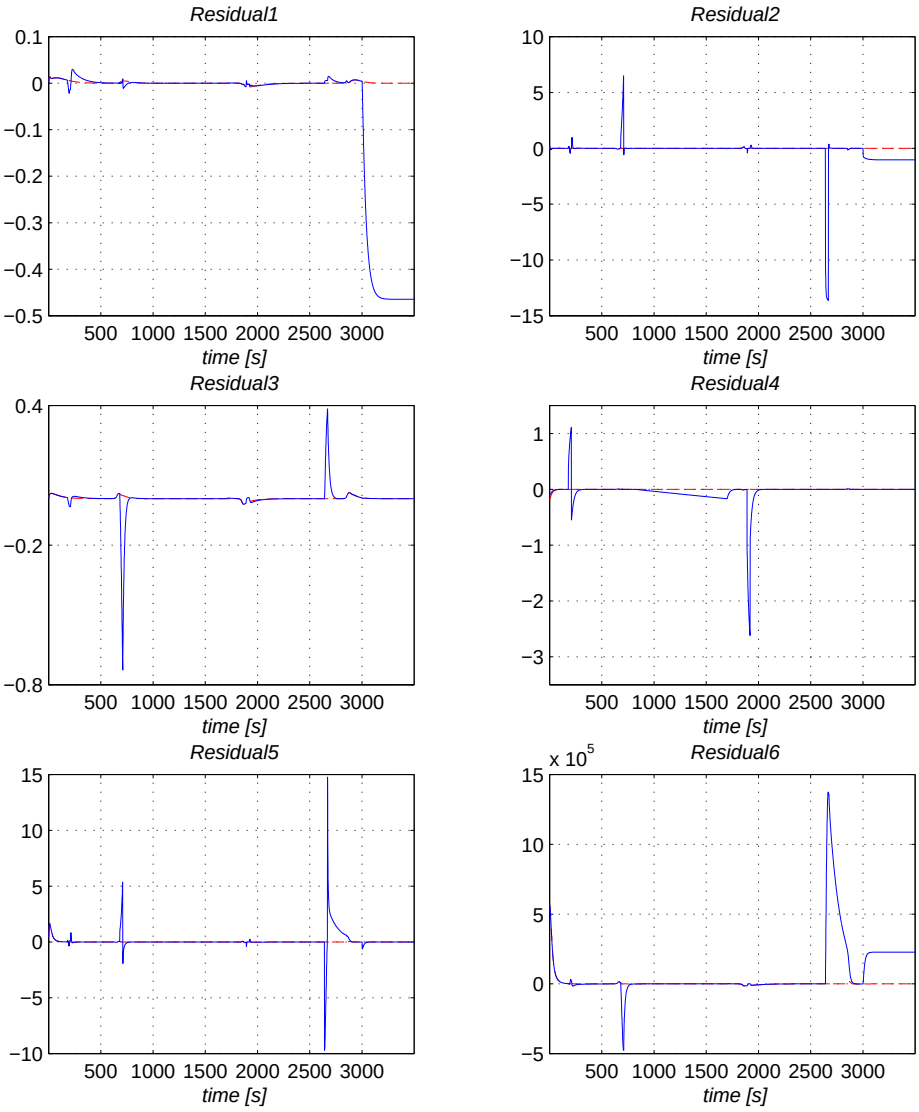

Figure 4.14: Overview over all six residuals (including all faults and no measurement noise). The solid lines show the residuals for the faulty case, while the dashed lines show the residuals for the fault-free case.

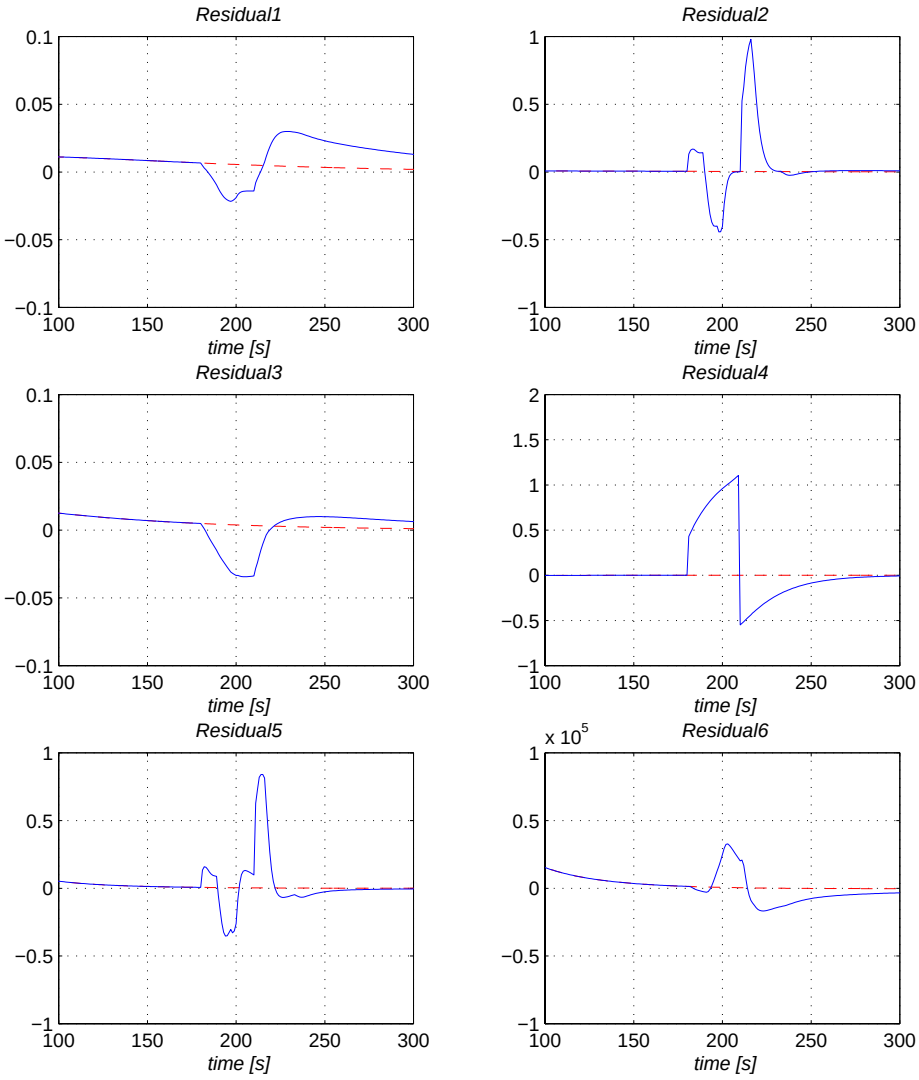

Figure 4.15: All six residuals; zoom-in for $\Delta\theta_{high}$ $(180s-210s)$. The solid lines show the residuals for the faulty case, while the dashed lines show the residuals for the fault-free case. The small deviations around $t = 100s$ are a result of the initialization phase.

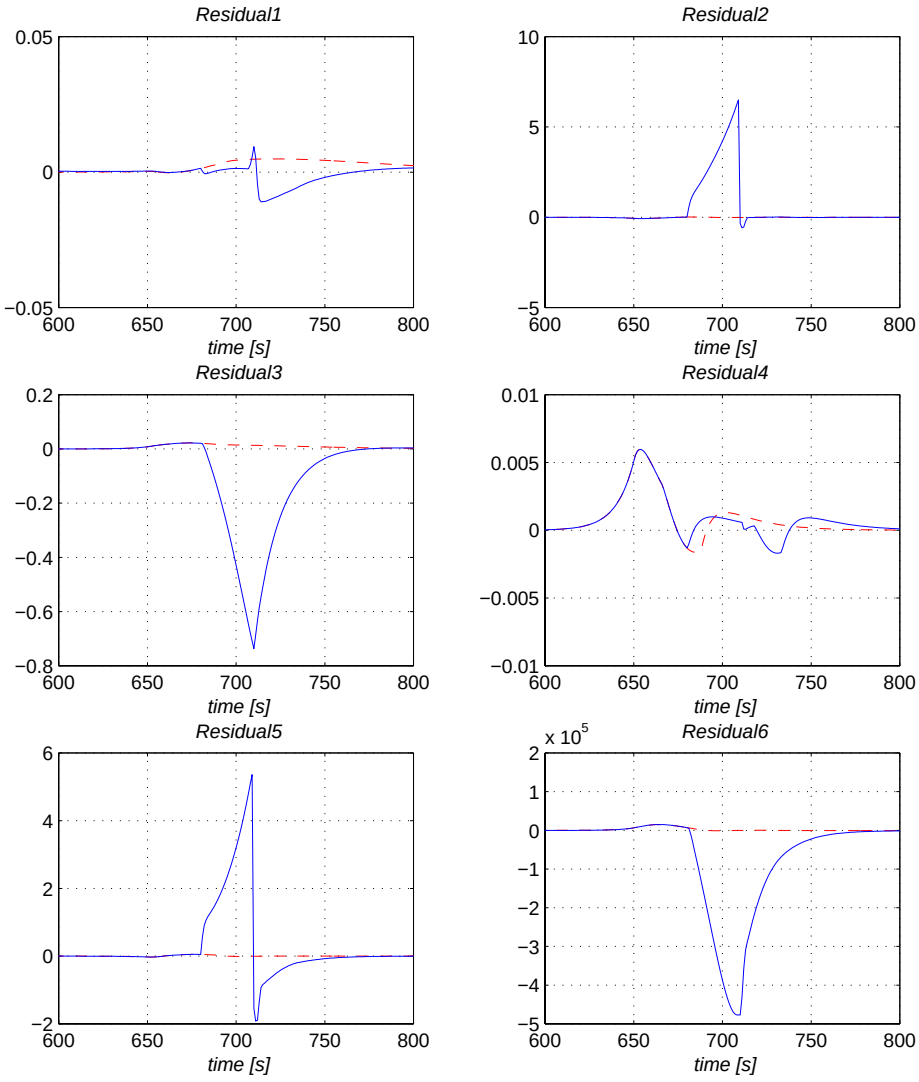

Figure 4.16: All six residuals; zoom-in for $\Delta n_{high}\,(680s-710s)$. The solid lines show the residuals for the faulty case, while the dashed lines show the residuals for the fault-free case.

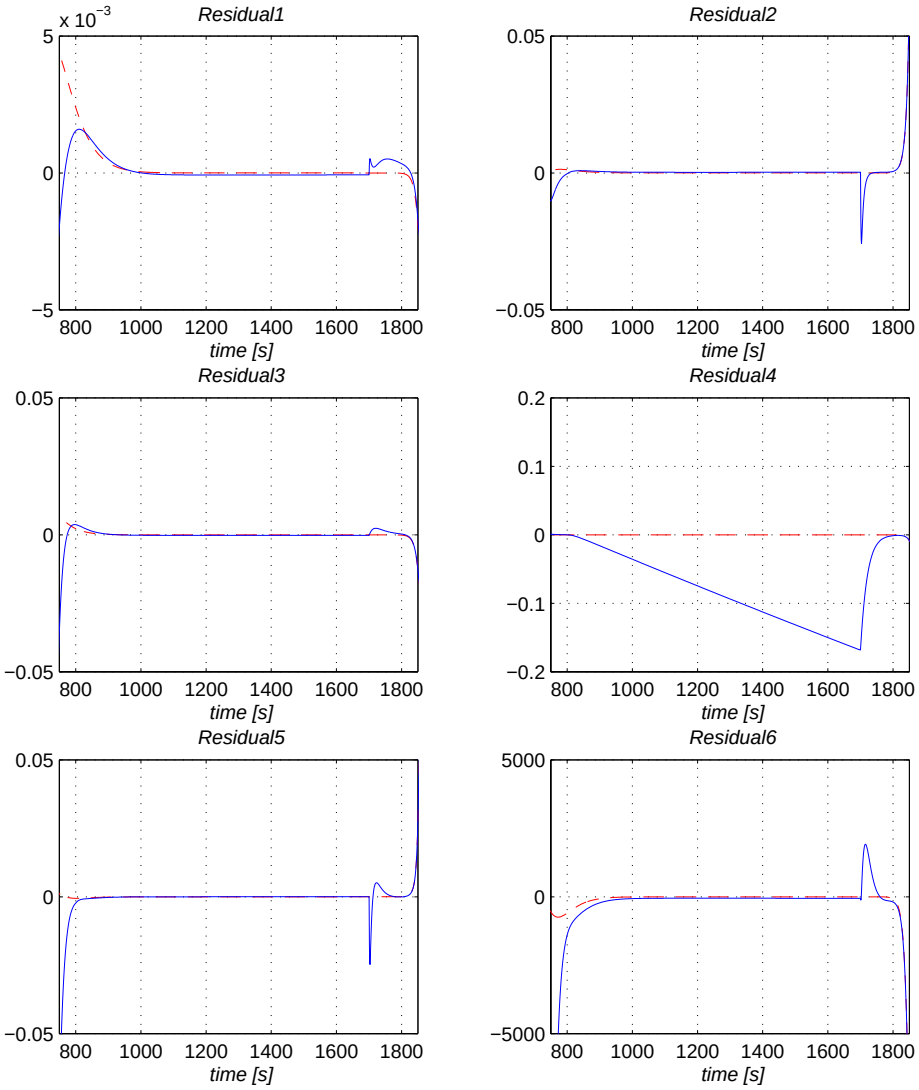

Figure 4.17: All six residuals; zoom-in for $\Delta\dot{\theta}_{inc}$ $(800s - 1700s)$. The solid lines show the residuals for the faulty case, while the dashed lines show the residuals for the fault-free case. The small deviations around $t = 800s$ are a result of the shaft speed fault Δn_{high}.

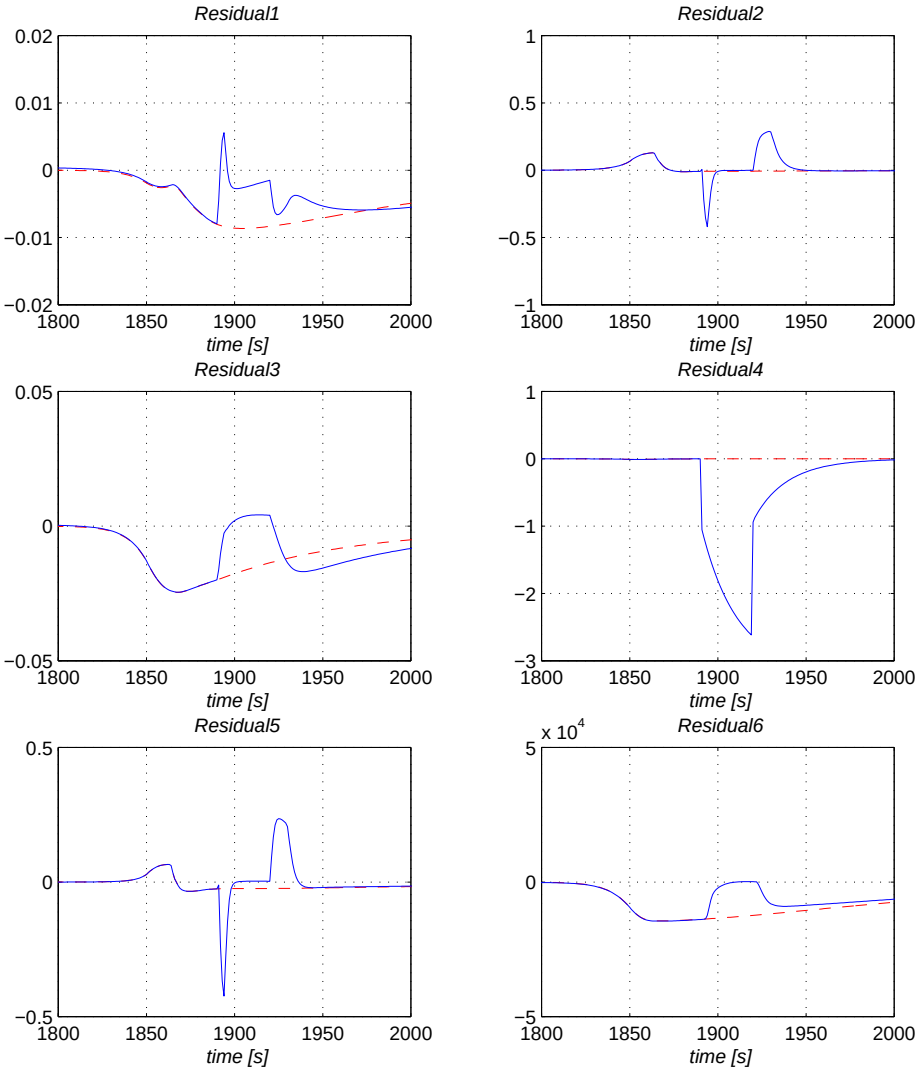

Figure 4.18: All six residuals; zoom-in for $\Delta\theta_{low}$ $(1890s - 1920s)$. The solid lines show the residuals for the faulty case, while the dashed lines show the residuals for the fault-free case.

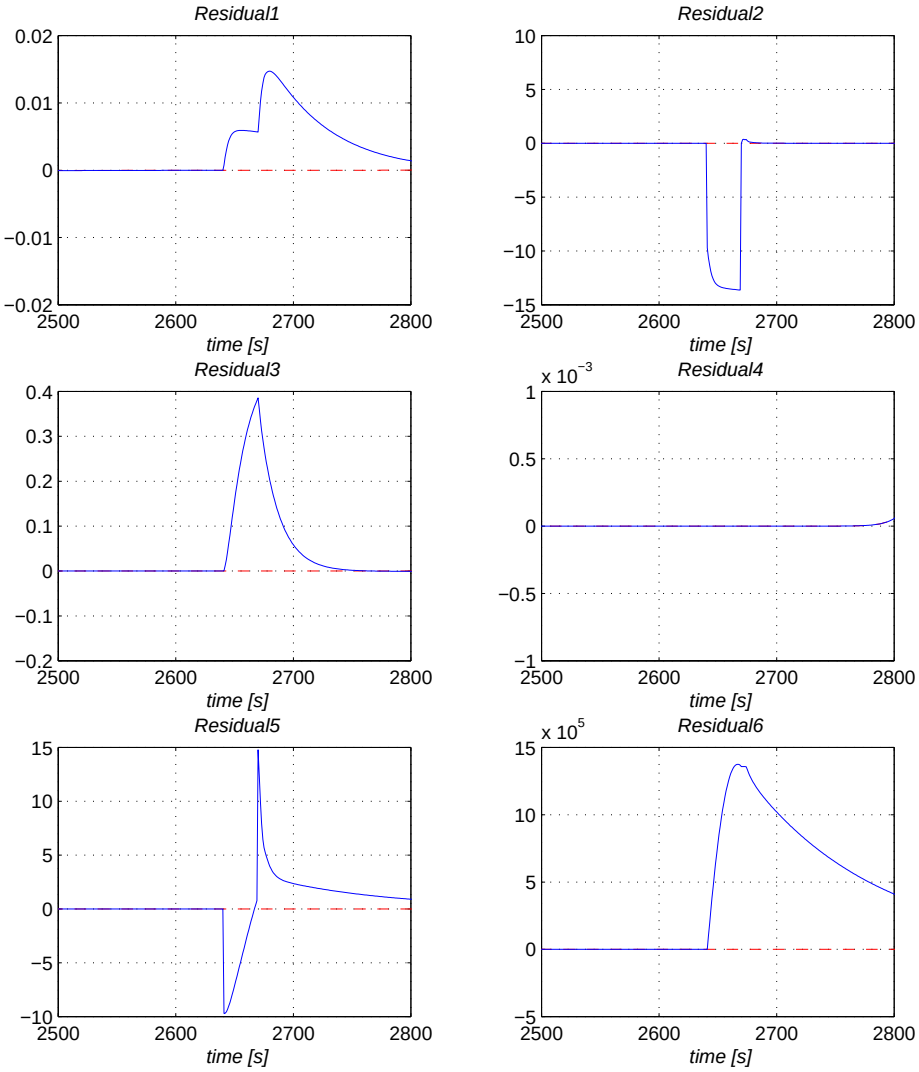

Figure 4.19: All six residuals; zoom-in for $\Delta n_{l_{ow}}$ $(2640s - 2670s)$. The solid lines show the residuals for the faulty case, while the dashed lines show the residuals for the fault-free case.

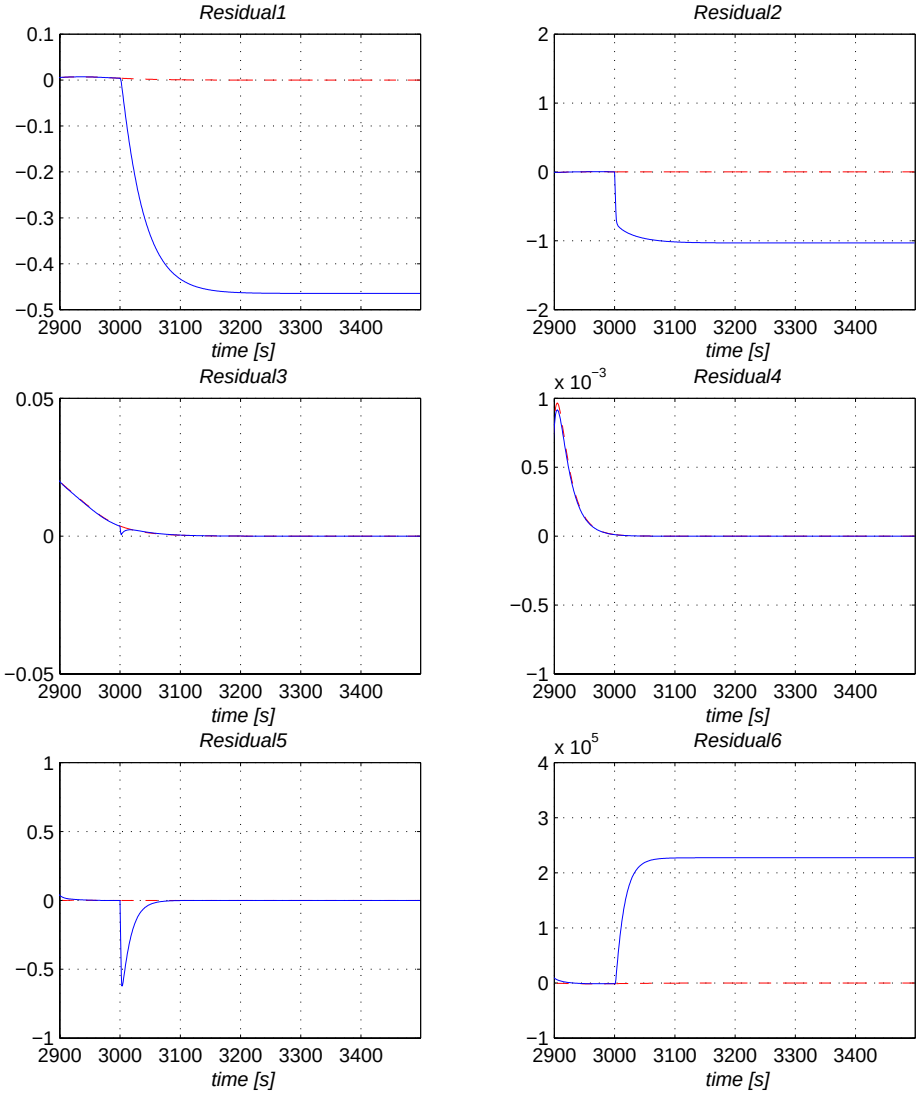

Figure 4.20: All six residuals; zoom-in for Δk_y $(3000s - 3500s)$. The solid lines show the residuals for the faulty case, while the dashed lines show the residuals for the fault-free case. The small deviations around $t = 2900s$ are a result of the shaft speed fault Δn_{low}.

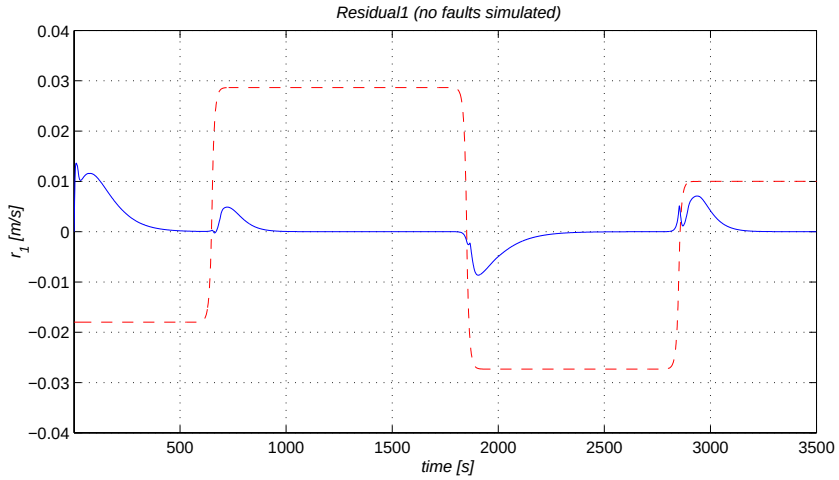

Figure 4.21: Residual1 (solid line) simulated for the fault-free case without measurement noise. Shaft speed reference n_{ref} (dashed line) is shown with different scaling and an offset for illustration.

4.4.4.2 Robustness issues

When looking at the residuals in Section 4.4.4.1 it can be seen that the fault-free residuals are not always equal zero. This can clearly be seen when looking at Residual1, Residual3, and Residual6 in Figure 4.18. In order to investigate this effect Figure 4.21 shows Residual1 for the fault-free case. It shows clearly, when comparing Residual1 with the shaft speed reference signal n_{ref} (Figure 4.5) that Residual1 deviates from zero in connection with the transitions and the startup phase. Similar effects can be shown for the other five Residuals. There are only slight differences in the dynamical behavior of the deviations. When looking at the residuals in Figures 4.8 - 4.13 it can be seen that these deviations are smaller in magnitude than the fault effects; especially than those fault effects the residuals have been designed for.

As shown in Section 4.2 the FPRGs cannot be solved when the disturbances T_{ext} and Q_f are considered. Hence, they are neglected in all the residuals simulated and shown above. Including T_{ext} in the simulations as defined by the ship propulsion benchmark (see Figure 4.22) will have a clear impact on the residuals. Figure 4.23 illustrates this for Residual1 in the fault-free case.

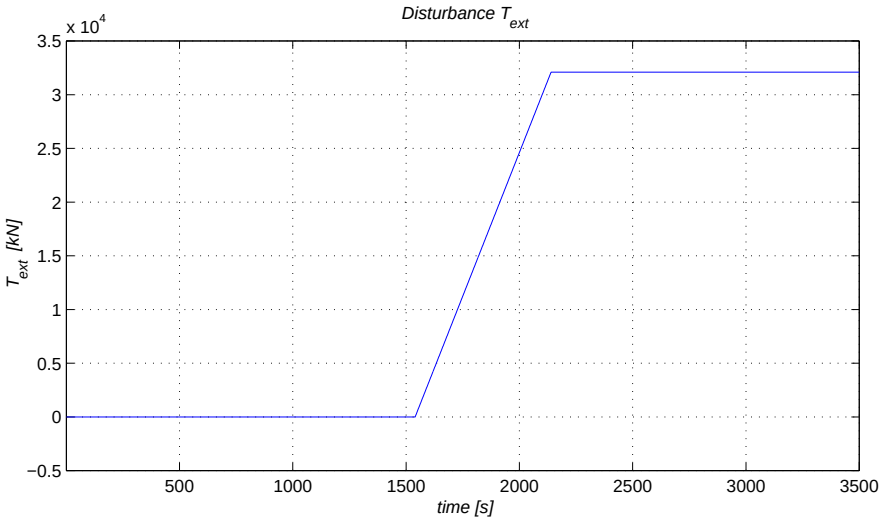

Figure 4.22: External force T_{ext} as it is implemented in the ship propulsion benchmark simulation package.

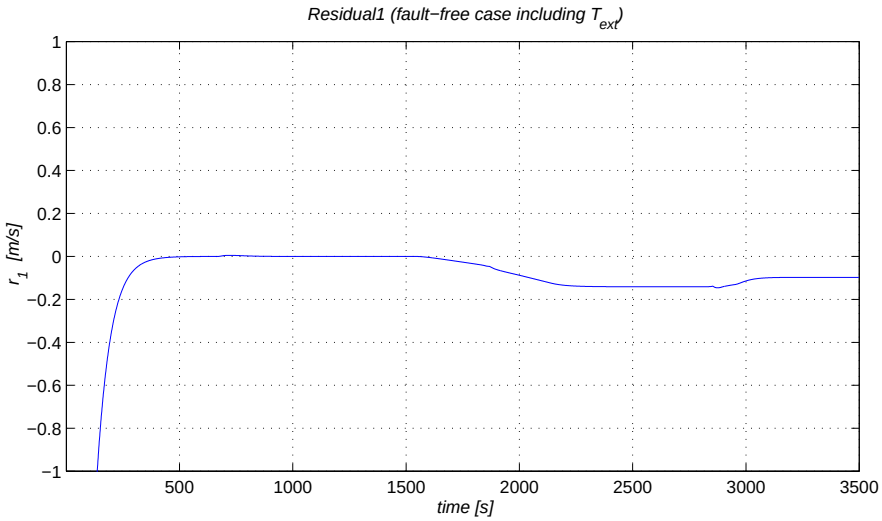

Figure 4.23: Residual1 simulated for the fault-free case without measurement noise including the disturbance T_{ext} as given in Figure 4.22. Using the initial condition $\hat{n}(t=0) = 0\,rad/s$, and $\hat{U}(t=0) = 0\,m/s$.

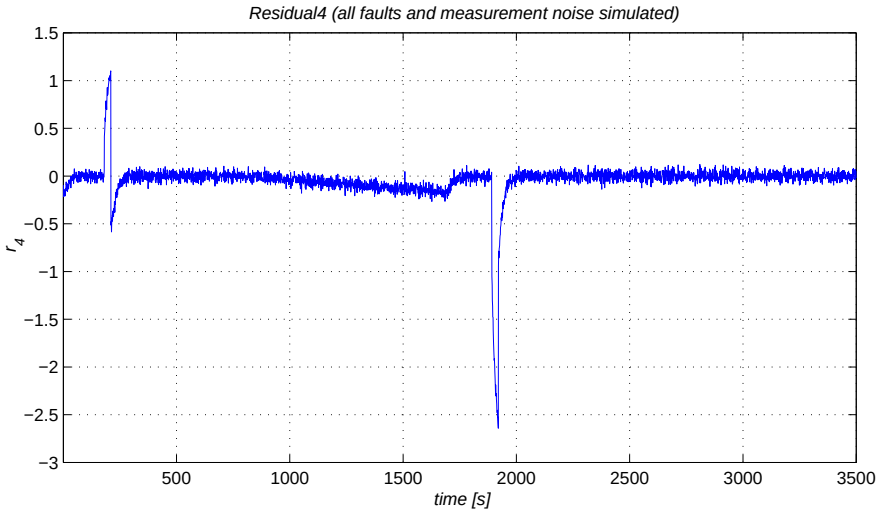

Figure 4.24: Residual4 simulated including all faults and measurement noise.

4.4.4.3 Measurement noise

Until now measurement noise has been omitted to enhance the readability of the simulation results. However, for the final residual evaluation in the next subsection to obtain fault detection and isolation for the ship propulsion system it has to be considered. In this subsection it is illustrated for Residual4 what happens when the measurement noise is considered and how it can be handled.

Figure 4.24 shows the simulation result for Residual4 when the measurement noise is considered. Obviously, the residual evaluation becomes more difficult in the presence of measurement noise than for the noise-free case given in Figure 4.11. For faults like the pitch sensor fault $\Delta\theta_{low}$ occurring at $t = 1890s$ a simple threshold testing ($threshold = \pm 0.5$) would be sufficient for detection. This is due to the abrupt occurrence and the high magnitude. However, fault effects with a lower magnitude might *hide* in the noise. Furthermore, it becomes more difficult to detect incipient faults like $\Delta\dot{\theta}_{inc}$. As can be seen from Figure 4.24 it is not possible to use a simple threshold testing due to the alternating behavior of the signal.

There exist several statistical methods to detect a change of mean value in

stochastic signals (Basseville and Nikiforov (1993, 1994)). They can be applied to solve the problem of residual evaluation for a residual containing measurement noise. A simple version of the well-known *CUSUM*-algorithm has been used for the residual evaluation in this thesis. It is described in detail in Basseville and Nikiforov (1993)[Chapter 2], hence, it will only be reviewed briefly in the following.

The cumulative sum (*CUSUM*) algorithm is used to detect a change of mean value in the residuals. For this purpose the residual signal r is considered to be Gaussian (as the measurement noise is Gaussian) having a mean value μ_r and a variance[2] σ^2, which results in the following probability density:

$$p_{\mu_r}(r) = \frac{1}{\sigma_r\sqrt{2\pi}}\, e^{-\frac{(r-\mu_r)^2}{2\sigma_r^2}} \tag{4.69}$$

The interesting question for the residual evaluation is now to decide whether the mean value is zero $\mu_r = 0$ or higher than a given threshold $\mu_r \geq threshold$. A powerful measure to test between the two hypothesis:

$$H_0: \quad \mu_r = \mu_{r_{no\,fault}} = 0 \qquad \text{and} \qquad H_1: \quad \mu_r = \mu_{r_{fault}} = threshold$$

is the log-likelihood ratio defined as:

$$s(r) = \ln \frac{p_{\mu_{r_{fault}}}(r)}{p_{\mu_{r_{no\,fault}}}(r)}. \tag{4.70}$$

The log-likelihood ratio is a positive measure when the residual r has a mean value that is closer to $\mu_{r_{fault}}$ than to $\mu_{r_{no\,fault}}$, otherwise it is negative. This can be seen easily when drawing the two corresponding Gaussian probability density functions into one diagram.

When the variance is considered to be equal for both hypothesis the log-likelihood ratio takes the following form (using (4.69) and (4.70)):

$$s_i = s(r_i) = \frac{\mu_{r_{fault}} - \mu_{r_{no\,fault}}}{\sigma_r^2}\left(r_i - \frac{\mu_{r_{no\,fault}} + \mu_{r_{fault}}}{2}\right).$$

[2] As the goal is to detect a change in mean value the variance could be calculated online. For the simulations it was estimated based on the fault-free simulations.

where r_i denotes the i^{th} sample of the residual r. The next step of the *CUSUM*-algorithm is to sum up the log-likelihood ratios s_i for the different samples. Which leads to the following *cumulative sum*:

$$S_k = \sum_{i=1}^{k} s_i$$

Obviously, the function S_k is increasing in the faulty case (when the threshold is chosen properly) and decreasing in the fault-free case. The final step of this version of the *CUSUM*-algorithm is to calculate the following decision function:

$$g_k = S_k - m_k \qquad \text{where} \qquad m_k = \min_{1 \leq j \leq k} S_j$$

As this function only becomes significantly larger than zero when the function S_k has been increasing significantly it can be used to decide whether the mean value of the residual has become significantly different from zero or not. For this purpose a second threshold h is needed:

$$g_k > h : \quad \text{the mean value of the residual is closer to } \mu_{r_{fault}}$$
$$0 \leq g_k \leq h : \quad \text{the mean value of the residual is closer to } \mu_{r_{no\,fault}}$$

For the residual evaluation it is necessary to check for a positive and a negative change in mean value ($\pm\mu_{r_{fault}}$) and to choose an appropriate value for the decision threshold h.

In the following the results from applying the *CUSUM*-algorithm to Residual4 in Figure 4.24 are given to illustrate its applicability. The simulations are based on the following values:

- $\sigma_r^2 = 0.002$, based on simulations of r_4 for the fault-free case
- $\mu_{r_{fault}}^{neg} = -0.01$, in order to detect a negative change in mean of r_4
- $\mu_{r_{fault}}^{pos} = 0.01$, in order to detect a positive change in mean of r_4

Furthermore, the decision functions g_k are reset to zero at $t = 50$, $t = 250$, $t = 350$, and $t = 1800$. This is done to enable the detection of the next fault and to compensate for the summing up from the initialization phase. The obtained decision functions are shown in Figure 4.25. Using a second threshold $h = 2.5$ leads to the decision about *fault* or *no fault* as shown in Figure 4.26. The result shows that $\Delta\theta_{high}$ can be detected at $t = 182s$, $\Delta\dot{\theta}_{inc}$ at $t = 899$, and Δn_{low} at $t = 1891$.

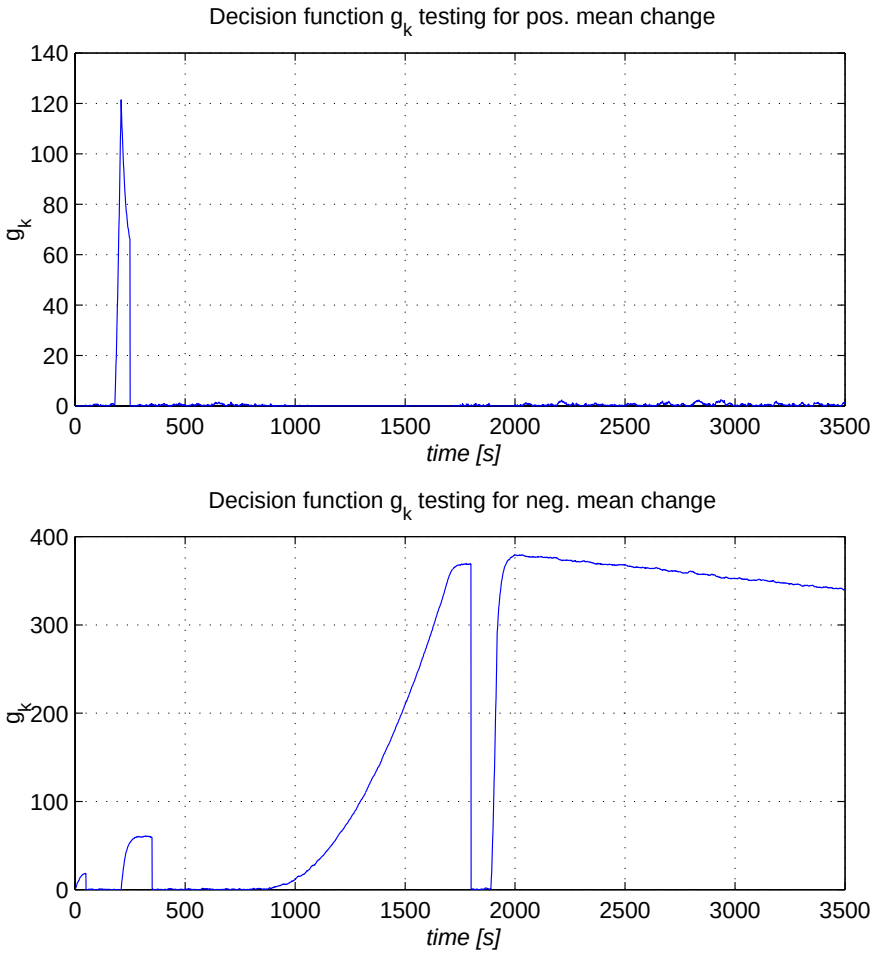

Figure 4.25: Decision functions to detect positive and negative changes in the mean value of Residual4 shown in Figure 4.24.

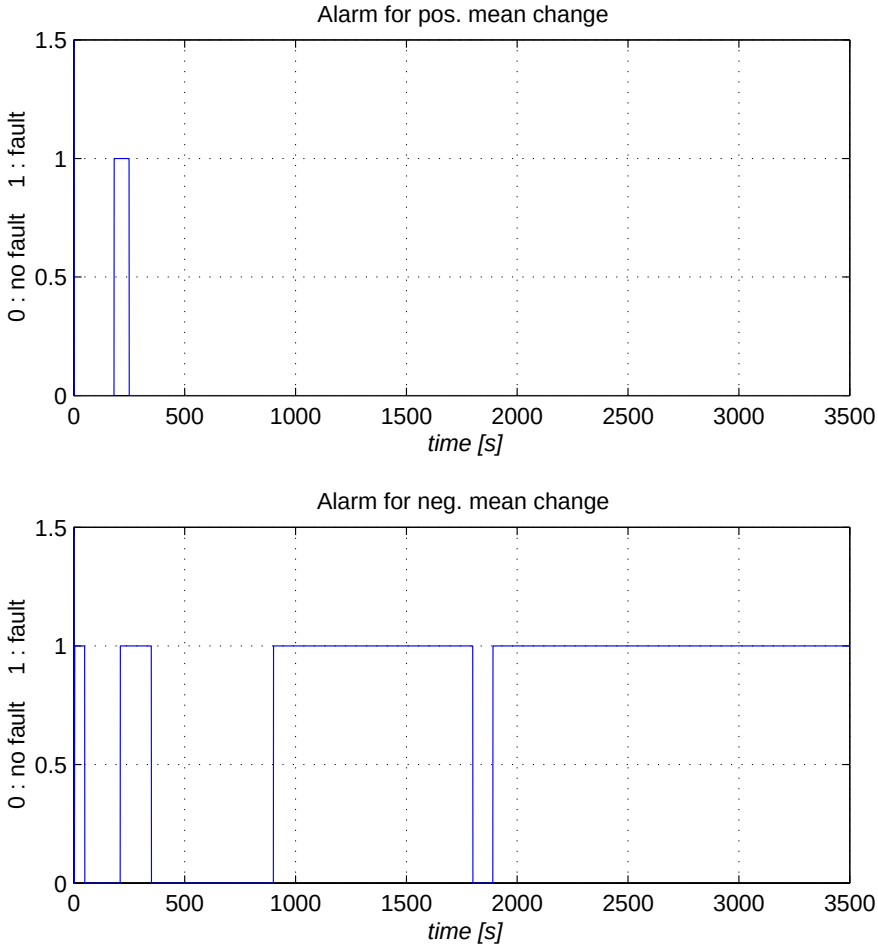

Figure 4.26: Evaluation of the decision functions given in Figure 4.25 using a threshold of $h = 2.5$.

4.4.4.4 Residual evaluation for FDI

To obtain successful fault detection and isolation (FDI) the next task after residual generation is the residual evaluation. This is done in two separate steps - fault detection and fault isolation. First, fault detection is considered.

As shown in the previous section, it is possible to detect the pitch faults $\Delta\theta_{high}$, $\Delta\dot{\theta}_{inc}$, and $\Delta\theta_{low}$ using Residual4. The detection times fulfill also the requirements given by Table 4.3.

From Figure 4.8, 4.9, and 4.10 it can be seen that also the other three faults Δn_{high}, Δn_{low}, and Δk_y can be detected. Applying a *CUSUM*-algorithm to Residual2 using $\sigma^2 = 0.005$, $\mu_{r_{fault}} = \pm 0.2$, and $h = 30$ leads to the detection times given in Table 4.10. There it can be seen that also the detection times for the shaft speed loop faults fulfill the requirements given by Table 4.3.

Fault	**Detection time**	**Fault**	**Detection time**
$\Delta\theta_{high}$	$194s$	Δn_{low}	$2641s$
$\Delta\theta_{low}$	$1895s$	Δn_{high}	$682s$
$\Delta\dot{\theta}_{inc}$	not detected	Δk_y	$3003s$

Table 4.10: Detection times for the different faults when evaluating Residual2.

The evaluation of the residuals r_1 and r_3 by using *CUSUM*-algorithms leads also to the detection of the shaft speed loop faults. However, the detection times are significantly bigger than the given requirements. They are about $10-20$ seconds slower than the values given in Table 4.3.

The next step is fault isolation. As can be seen from the simulations Residual4 only reacts on the pitch faults, which is also clear from its design, see Section 4.3. During the design it was shown that it is not possible to isolate the two pitch faults $\Delta\theta_{sensor}$ and $\Delta\dot{\theta}_{inc}$ from each other, when they are considered to be arbitrary. However, from the simulations it can be seen that they show different behavior. As a result Residual2 is only affected by $\Delta\theta_{sensor}$, hence, isolation can be obtained, when using both residuals. The shaft speed loop faults can be isolated by using the residuals r_1 and r_3 as shown in Figure 4.8 and 4.10.

4.5 Conclusions

This chapter illustrated how the geometric approach (presented in Chapter 3) was applied to a nonlinear ship propulsion system. First the propulsion system was described in detail. Then a detailed description of the geometric analysis is given. The analysis results were used to design different residual generators (observers) in order to obtain FDI. Their performance was tested by simulations based on the ship propulsion simulation package. From the application and the simulations the following conclusions can be drawn:

- As a result from the geometric analysis it can be concluded that the FDI problem as stated in Section 4.1.3 cannot be solved for arbitrary fault and disturbance signals. This can also be seen when looking at the simulation results. If the pitch faults cannot be assumed to have the behavior they show in the simulations it is clear that they cannot be isolated in the described way. Also the disturbance and transition effects could have a too big impact on the residuals.

- Obviously, it is a quite strong restriction for its applicability that the geometric approach considers arbitrary fault and disturbance signals. There might be only few systems where FDI can be achieved for that condition. In practical applications, like for the propulsion system, there is often additional information available. This is completely neglected in the geometric approach. The results above illustrate that taking them into account improves significantly the possibility to obtain sufficient FDI.

- The disturbance is a problem for successful FDI as illustrated by Figure 4.23. Only, when it can be considered to be small enough a well-chosen threshold could achieve robust FDI. Otherwise FDI is not possible.

- Also the transition effects shown in Figure 4.21 cause problems. When the threshold is chosen big enough to avoid false alarms in the worst case of transition (reversing the ship from full-ahead to full-astern) it reduces the FDI performance. Small faults might not be detected and the detection times will become longer. This problem could be handled by using time-variant thresholds, known as adaptive thresholds Clark (n.d.); Chen and Patton (1999). The deviations are caused by the fact, that the model used to calculate the propeller thrust and torque, (4.8) and (4.9), gives a fairly good approximation in the steady state cases but is less applicable during transients.

- The geometric approach is very sensitive to model uncertainties. Furthermore, the model has to be differentiable. Therefore, only the working range for $n > 0$ and $\theta > 0$ has been considered here.

- The correct tuning of the FDI system is a complex task. First the observer gains have to be chosen correctly. In the given case too high gains would reduce next to the transition and disturbance effects also the fault effects. A main problem is the residual evaluation, where several questions have to be considered: Is the threshold high enough to avoid false alarms? Is it low enough to obtain fast detection? Should it be adaptive? How to tune the *CUSUM*-algorithm? How can the fault be isolated?

- The given solution for FDI neglects the disturbances and needs further consideration concerning the questions given above for the evaluation. For the disturbance-free case complete FDI can be obtained for the propulsion system when applying a sufficient evaluation logic.

- The residuals r_1 and r_3 can by construction be used for detection and isolation of the two shaft speed fault. However, they need too much time to detect the faults. This is due to the fact that they are based on the slow ship speed dynamics. This can be seen in Figure 4.19 when comparing Residual2 (or Residual5) with Residual3. The slope of Residual3 is smaller, hence, the detection using Residual3 is slower. From this fact it can be seen that the geometric approach does not consider detection speed at all, hence, it might not be that successful in practical applications where fast detection is often required.

- Residual2, which was generated by using one of the states of Observer1, shows good FDI performance. Although it was only a '*side-effect*' of the geometric approach it detects the shaft speed loop faults as fast as required. Furthermore, it can be used to isolate the two pitch faults from each other. For this residual several thresholds could be applied. For example a threshold of $\kappa = 1.5\,rad/s$ could be applied to isolate the shaft speed sensor fault from the gain fault. This becomes clear when looking at Figure 4.9, where the gain fault effect is smaller than $1.2\,rad/s$. However, this requires additional knowledge about the possible magnitude of the faults.

- Other observer structures might be considered as e.g. shown by Observer4. However, it did not show significantly better performance than

Observer1. One important difference, however, is that Residual5 and Residual6 were designed, while Residual2 was only a kind of '*side-effect*'. Without engineering inside it would not have been considered after the geometric approach which only proposed Residual1 and Residual3. So another conclusion is that designing and tuning a sufficient FDI system cannot be completely automated.

- The subsystems obtained by the geometric approach were also obtained by using the structural analysis (Staroswiecki and Declerck (1989); Cassar *et al.* (1994)) by Izadi-Zamanabadi (1999)[Section 5.1.3].

Chapter 5

FDI Observer stability

Observers are often used in the design of fault detection and isolation (FDI). Their design for linear systems is well-studied (Chen and Patton (1999)). Observer-based FDI has been considered for different classes of nonlinear systems since the 1990s. The first designs were based on linearization around the system's operating point. This was done in order to apply the existing linear observer-based FDI methods. However, for nonlinear systems with hard or higher-order nonlinearity this turned out to be inefficient. Hence, nonlinear observer-based FDI approaches were developed (García and Frank (1997); Frank *et al.* (1999); Chen and Patton (1999)). Especially, the design based on the geometric approach gained a lot of interest in the recent years (Hammouri *et al.* (1998, 1999); DePersis and Isidori (1999); DePersis (1999)).

One important design aspect of the observer-based approach is the stability of the FDI observer. This chapter addresses two different stability aspects of the nonlinear observer-based FDI approach. First, the stability of an approach based on linearization along a trajectory is addressed. Obviously, it results in a time-varying linear system, which requires a more involved analysis when for instance stability is to be investigated. The objective is to point out in detail where and why it is incorrect to neglect the time-variance in the stability analysis when using the linearization along a trajectory. Finally, the stability proof is outlined for the nonlinear observers used in Chapter 4 for FDI in the ship propulsion system.

5.1 FDI based on linearization along a trajectory

In the past decade the idea of how to obtain successful FDI for systems with nonlinear dynamics has changed from using linearization to applying nonlinear methods (Frank *et al.* (1999)). The first methods to achieve FDI for nonlinear systems are based on linearization. The idea is to linearize the nonlinear dynamics around a working point and then apply the well-studied FDI methods designed for linear systems on the resulting linear time-invariant (LTI) system dynamics:

$$\sum_{LTI}: \begin{cases} \dot{x} = A\,x + B\,u + F_x\,\nu \\ y = C\,x + D\,u + F_y\,\nu \end{cases} \tag{5.1}$$

where $x \in \mathbb{R}^n$ denotes the states, $y \in \mathbb{R}^l$ the outputs, $\nu \in \mathbb{R}^k$ the faults, and A, B, C, D, F_x, and F_y are constant matrices of corresponding size. The limitation of this approach becomes obvious when considering systems that are highly nonlinear and systems that have different operating points. Deviations or estimation errors around an operating point (caused by the inaccuracy of the linearized model) have a negative effect on the residual generation - e.g. they could result in unwanted false alarms. To avoid this obstacle several FDI systems could be designed for all possible operating points. However, this is not very practical for real-time applications due to the resulting high number of FDI systems and the connected high computational load (Chen and Patton (1999)). Furthermore, the stability proof becomes more complex due to the switching between the different systems.

In the last decade nonlinear FDI methods have been developed in order to overcome the inaccuracy problem originating from linearized system dynamics. The first approaches are summarized in García and Frank (1997), Chen and Patton (1999), and Frank *et al.* (1999). Recently, other nonlinear methods have been developed that for example are based on geometric descriptions as presented in Chapter 3.

One of the first approaches to solve the nonlinear FDI problem with a nonlinear design, is based on a first order Taylor approximation along a trajectory depending on the system input. As a consequence it can handle different operating points. However, it leads in contrast to the linearization around a fixed operating

point to a linear time-variant (LTV) system.

$$\sum_{LTV} : \begin{cases} \dot{x} = A(t)\, x + B(t)\, u + F_x(t)\, \nu \\ y = C(t)\, x + D(t)\, u + F_y(t)\, \nu \end{cases} \tag{5.2}$$

where $x \in \mathbb{R}^n$ denotes the states, $y \in \mathbb{R}^l$ the outputs, $\nu \in \mathbb{R}^k$ the faults, and $A(t)$, $B(t)$, $C(t)$, $D(t)$, $F_x(t)$, and $F_y(t)$ are time-varying matrices of corresponding size. As shown later in Section 5.1.2 by equation (5.25) the dynamics sometimes even take a more general form $\dot{x}(t) = A(x(t), u(t))$, where $u(t)$ is an arbitrary control signal (which is exogenous). As $u(t)$ is considered to be *arbitrary* it could take many different forms next to $u(t) = t$, hence, the dynamics have to be considered as time-variant.

Even if the time-variance looks like a small change compared to the time-invariant dynamics it is known to have an important impact on the system. Time-variant systems can for example not be solved as easy as time-invariant systems. Furthermore, it is known that the stability analysis for time-variant systems is significantly different from the one for time-invariant systems. In order to ensure correctness of the stability proof one has to be aware of the difference when considering the control signal to be an arbitrary time-varying signal.

This section points out and illustrates why it is important to distinguish clearly between time-variant and time-invariant systems when analyzing stability. The stability analysis for time-variant systems is compared with the one for time-invariant systems and important differences are emphasized. At the end of the section an illustrative example is given.

5.1.1 Stability analysis for time-variant & time-invariant systems

Stability theory is based on the basic definitions that an equilibrium point is *stable* if all solutions starting from points that lie nearby the equilibrium point stay nearby; otherwise the considered equilibrium is *unstable*. It is *asymptotically stable* if all solutions starting at nearby points not only stay nearby, but also tend to the equilibrium point as time approaches infinity (Khalil (1996)).

In the following some methods are described that can be applied to prove stability of certain dynamic systems. The emphasis lies on the fact that the stability

analysis for time-variant systems is significantly different from the analysis for time-invariant systems.

5.1.1.1 Time-invariant systems

For linear time-invariant (LTI) systems, e.g. $\dot{x} = Ax$, the stability can be investigated by looking at the eigenvalues of the system matrix A. Asymptotic stability of the equilibrium point $x = 0$ is for example guaranteed for LTI-systems if the eigenvalues all lie in the open left-half plane (see e.g. theorem 3.5 and 3.6 in Khalil (1996)). For nonlinear systems of the form $\dot{x} = f(x)$ a more general formulation, also known as *Lyapunov's*[1] *indirect method*, can be stated (Theorem 3.7 in Khalil (1996)):

Theorem 5.1 *Let $x = 0$ be an equilibrium point for the nonlinear system $\dot{x} = f(x)$, where $f : D \to \mathbb{R}^n$ is continuously differentiable and $D \subset \mathbb{R}^n$ is a neighborhood of the origin. Let*

$$A = \frac{\partial f}{\partial x}(x)\bigg|_{x=0}$$

Then,

1. *The origin is asymptotically stable if $\mathcal{R}e\,\lambda_i < 0$ for all eigenvalues of A.*
2. *The origin is unstable if $\mathcal{R}e\,\lambda_i > 0$ for one or more of the eigenvalues of A.*

For time-variant systems it is not sufficient to look at the eigenvalues. There might be some exceptions, as periodic systems or slowly-varying systems. However, in general it is not possible to analyze stability of time-variant systems by looking at the eigenvalues as done in Theorem 5.1.

This is illustrated by the following example (Example 3.22 in Khalil (1996)) that considers the following time-variant system:

$$\dot{x} = A(t)\,x \tag{5.3}$$

[1] Russian engineer and mathematician

where

$$A(t) = \begin{pmatrix} -1 + \frac{3}{2}\cos^2(t) & 1 - \frac{3}{2}\sin(t)\cos(t) \\ -1 - \frac{3}{2}\sin(t)\cos(t) & -1 + \frac{3}{2}\sin^2(t) \end{pmatrix} \tag{5.4}$$

Although for each time t, the eigenvalues of $A(t)$ are given by $\lambda_{1,2} = -\frac{1}{4} \pm \frac{1}{4}\sqrt{7}j$, thus are time independent(!) and lie in the open left-half plane, the origin is not asymptotically stable. It is even unstable. This can be shown easily by looking at the solution of (5.3):

$$x(t) = \Phi(t, t_0)\, x(t_0) \tag{5.5}$$

where

$$\Phi(t, 0) = \begin{pmatrix} e^{0.5t}\cos(t) & e^{-t}\sin(t) \\ -e^{0.5t}\sin(t) & e^{-t}\cos(t) \end{pmatrix} \tag{5.6}$$

denotes the state transition matrix and $x(t_0) = x(t = 0)$ describes the initial condition. When choosing a starting point close to the origin, e.g. $x(t_0) = (0.01 \quad 0)^T$, it becomes obvious that the solution is unbounded and escapes to infinity, hence the origin is not asymptotically stable. This example illustrates clearly that the eigenvalue condition, which is often used for LTI systems, cannot be applied to time-variant systems.

5.1.1.2 Time-variant systems

An alternative method to investigate stability of a system, which is not limited to linear time-invariant systems, is Lyapunov's direct method. It is also referred to as Lyapunov's stability theorem, or just *Lyapunov stability*.

The conditions of Lyapunov's stability theorem are sufficient, but not necessary. This is due to the fact that they are based on finding and using a so-called Lyapunov function, often assigned as V. Finding an appropriate Lyapunov function is not straight forward. It can be chosen arbitrary; one of the conditions it has to obey is that it has to be a function of the systems's states $V(x)$ (other conditions are given in the following theorems). For physical reasons often the energy function is used. If the conditions of Lyapunov's stability theorem are not fulfilled it could be due to a wrongly chosen Lyapunov function candidate as well as to the fact that the system is unstable.

In the following, theorems of the Lyapunov stability theory for both time-variant and time-invariant systems are cited. For a more detailed description of the Lyapunov theory the reader is referred to the system and control literature, e.g. in Khalil (1996) a detailed description is given.

For time-invariant systems of the form $\dot{x} = f(x)$ the following theorem, known as Lyapunov's stability theorem, can be stated (Theorem 3.1 in Khalil (1996)):

Theorem 5.2 *Let $x = 0$ be an equilibrium point for $\dot{x} = f(x)$, where $f : D \to \mathbb{R}^n$, and $D \subset \mathbb{R}^n$ be a domain containing $x = 0$. Let $V : D \to \mathbb{R}$ be a continuously differentiable function, such that*

$$V(0) = 0 \quad \textit{and} \quad V(x) > 0 \textit{ in } D - \{0\} \tag{5.7}$$

$$\textit{and} \quad \dot{V}(x) \leq 0 \textit{ in } D \tag{5.8}$$

then, $x = 0$ is stable. Moreover, if

$$\dot{V}(x) < 0 \textit{ in } D - \{0\} \tag{5.9}$$

then $x = 0$ is asymptotically stable.

A function $V(x)$ fulfilling the prerequisites of Theorem 5.2 and the Conditions (5.7) and (5.8) is called a *Lyapunov function*. A function $V(x)$ satisfying condition (5.7), that is $V(0) = 0$ and $V(x) > 0$ for $x \neq 0$, is said to be *positive definite*. If it satisfies the weaker condition $V(0) = 0$ and $V(x) \geq 0$ for $x \neq 0$, it is said to be *positive semidefinite*. A function $V(x)$ is said to be *negative definite* or *negative semidefinite* if $-V(x)$ is positive definite or positive semidefinite, respectively. If $V(x)$ does not have a sign as per one of these four cases, it is said to be *indefinite*.

Theorem 5.2 treats local stability; for global stability the following theorem is given (Theorem 3.2 in Khalil (1996)):

Theorem 5.3 *Let $x = 0$ be an equilibrium point for $\dot{x} = f(x)$. Let $V : \mathbb{R}^n \to \mathbb{R}$ be a continuously differentiable function, such that*

$$V(0) = 0 \quad \textit{and} \quad V(x) > 0, \ \forall x \neq 0 \tag{5.10}$$

$$\| x \| \to \infty \Rightarrow \quad V(x) \to \infty \tag{5.11}$$

$$\dot{V}(x) < 0, \ \forall x \neq 0 \tag{5.12}$$

then $x = 0$ is globally asymptotically stable.

Theorem 5.3 is also known as Barbashin-Krasovskii theorem.

The above given theorems give sufficient conditions to check the stability of the time-invariant system $\dot{x} = f(x)$. They are not necessary as finding the Lyapunov function is not trivial, hence, often no easy task. Nevertheless, the theorems are widely used to investigate stability.

When considering time-variant systems Theorem 5.2 changes to a slightly but significant different form. For time-variant systems the following theorem can be given (Theorem 3.8 in Khalil (1996)):

Theorem 5.4 *Let $x = 0$ be an equilibrium point for $\dot{x} = f(t, x)$ and $D \subset \mathbb{R}^n$ be a domain containing $x = 0$. Let $V : [0, \infty) \times D \to \mathbb{R}$ be a continuously differentiable function, such that*

$$W_1(x) \leq V(t, x) \leq W_2(x) \tag{5.13}$$

$$\frac{\partial V}{\partial t} + \frac{\partial V}{\partial x} f(t, x) \leq -W_3(x) \tag{5.14}$$

$\forall t \geq 0, \forall x \in D$ where $W_1(x)$, $W_2(x)$, and $W_3(x)$ are continuous positive definite functions of D. Then, $x = 0$ is uniformly[2] asymptotically stable.

The difference between Theorem 5.2 and Theorem 5.4 is easy to see. In the latter the Lyapunov function depends next to the state x also explicitly on the time t, which is due to the time-dependency of the system $\dot{x} = f(t, x)$. Furthermore, the $W_i(x)$ functions are used to bound the Lyapunov function and its time derivative uniformly away from zero and to bound it from above.

[2]Uniformly means that it is independent of the initial point or starting point of time, denoted by t_0.

5.1.2 FDI stability analysis for time-varying systems

This section addresses stability aspects for diagnostic observers used for FDI in nonlinear systems. The observer design is based on a linearization along a trajectory, hence, considering a time-varying system.

In the following systems of the following form are considered:

$$\dot{x}(t) = f\left(x(t), u(t)\right), \quad x(t=0) = x_0 \tag{5.15}$$

$$y(t) = h\left(x(t)\right) \tag{5.16}$$

where $x \in \mathbb{R}^n$ describes the states of the system, $u \in \mathbb{R}^m$ the inputs, $y \in \mathbb{R}^l$ the outputs of the system, and x_0 stands for the initial system state. Furthermore, it is assumed that for any input $u(t)$ and initial state x_0 the corresponding state trajectory $x(t)$ is defined for all t and that f and h are continuously differentiable functions. In order to make the notation more readable the time dependence (t) is omitted in the following, but must be kept in mind (especially for $u(t)$).

Often the approach to design a diagnostic observer for a system as described by (5.15) and (5.16) is based on the classical Luenberger design in the following way:

$$\dot{\hat{x}} = f\left(\hat{x}, u\right) + R\left(\hat{x}, u\right)\left(y - \hat{y}\right), \quad \hat{x}(t=0) = \hat{x}_0 \tag{5.17}$$

$$\hat{y} = h\left(\hat{x}\right) \tag{5.18}$$

where $\hat{x} \in \mathbb{R}^n$ describes the states of the observer, $\hat{y} \in \mathbb{R}^l$ the outputs of the observer, $\hat{x}_0$ stands for the initial observer state, and $R\left(\hat{x}, u\right)$ denotes the observer gain matrix. In order to investigate the stability and convergence of the observer the state estimation error dynamics are analyzed:

$$e = x - \hat{x} \tag{5.19}$$

$$\dot{e} = f\left(x, u\right) - f\left(\hat{x}, u\right) - R\left(\hat{x}, u\right)\left(y - \hat{y}\right) \tag{5.20}$$

Some of the proofs for stability of existing methods are based on a first order Taylor expansion (linearization along a trajectory determined by the system input u) in the following way:

$$f\left(x, u\right) = f\left(\hat{x} + e, u\right) = f\left(\hat{x}, u\right) + D_x f\left(\hat{x}, u\right) e + h.o.t. \tag{5.21}$$

$$h(x) = h(\hat{x} + e) = h(\hat{x}) + D_x h(\hat{x}) e + h.o.t. \tag{5.22}$$

where $h.o.t.$ denotes higher order terms and D_x is a differential operator defined in the following way:

$$D_x f\left(\hat{x}, u\right) = \left.\frac{\partial f(x,u)}{\partial x^T}\right|_{x=\hat{x}} \tag{5.23}$$

This Taylor expansion approach leads to the following error dynamics:

$$\dot{e} \approx \left[D_x f\left(\hat{x}, u\right) - R\left(\hat{x}, u\right) D_x h(\hat{x})\right] e \tag{5.24}$$

Obviously, proving stability using this kind of Taylor expansion works only if the nonlinearity is not too significant and the higher order terms can be neglected. The stability can be achieved by finding a suitable observer gain matrix $R\left(\hat{x}, u\right)$.

When solving this stability problem the designer has to be very careful and aware of the time-variance of the system coming from the influence of $u(t)$ (and thus of also of $\hat{x}(t)$). For a correct stability analysis the following steps should be considered.

Time-variant dynamics First of all it is important to realize that the error dynamics are time-variant even if the time dependence is not stated explicitly. To illustrate this the error dynamics given in equation (5.24) can be considered in the following abbreviated form:

$$\dot{e} \approx A_e(\hat{x}, u)\, e \tag{5.25}$$

where $A_e(\hat{x}, u) = \left[D_x f - R\left(\hat{x}, u\right) D_x h\right]$ is a $n \times n$-matrix.
Due to the fact that the matrix A_e depends on the independent (exogenous), arbitrary input signal u (as well as $\hat{x}(t)\,(= \hat{x}(t, u))$) it has to be considered as time-variant during the stability analysis.

Stability proofs As a consequence of the time-variance of the dynamics the stability proofs for some existing diagnostic observer designs should be reconsidered. Statements saying that the error dynamics (5.25) are stable if the poles of A_e lie in the open left-half plane are obviously incorrect as shown in section 5.1.1.1 if arbitrary input signals u are allowed. Instead the stability could be proven using Lyapunov's stability theorem as stated in Theorem 5.4. Hence, the following result can be stated:

Theorem 5.5 *A FDI observer (5.17) and (5.18) for a system (5.15) and (5.16) is locally asymptotically stable if the following conditions are satisfied:*

(i) *The error dynamics can be approximated in the following way:*

$$\dot{e} \approx A_e(\hat{x}, u)\, e$$

(ii) *There exists a Lyapunov function $V(e, \hat{x}, u)$, such that*

$$W_1(e) \leq V(e, \hat{x}, u) \leq W_2(e)$$
$$\frac{\partial V}{\partial t} + \frac{\partial V}{\partial e} A_e(\hat{x}, u)e \leq -W_3(e)$$

where $W_1(e)$, $W_2(e)$, and $W_3(e)$ are continuous positive definite functions of $\mathbb{R}^n$.

5.1.3 Example

In the following an example is given to illustrate the problem of neglecting the time-variance when designing a stable observer. The example is based on linearization along a trajectory as shown in the previous section. The goal is to design a stable observer for the following system:

$$\dot{x} = \begin{pmatrix} x_1 + x_2 \\ -0.5x_1 u - 0.2x_2 \end{pmatrix} = f(x, u) \tag{5.26}$$

$$y = h(x) = x_1, \quad x(t = 0) = x_0 \tag{5.27}$$

where the input signal is bounded: $-1 \leq u \leq 1$. Considering system (5.26) and (5.27) an open-loop observer is designed having the following form (corresponding to (5.17) and (5.18)):

$$\dot{\hat{x}} = f(\hat{x}, u) + R(\hat{x}, u)(y - \hat{y}), \quad \hat{y} = h(\hat{x}) = \hat{x}_1, \quad \hat{x}(t = 0) = \hat{x}_0 \tag{5.28}$$

Its stability is achieved by choosing an appropriate gain matrix $R(\hat{x}, u)$. As derived above in Section 5.1.2 this is done by using a Taylor expansion that leads for the given example to the following error dynamics (see (5.24) and (5.25)):

$$\dot{e} = \left[D_x f\,(\hat{x}, u) - R\,(\hat{x}, u)\, D_x h(\hat{x})\right] e = A_e(\hat{x}, u)\, e \tag{5.29}$$

with

$$D_x f\left(\hat{x},u\right) = \left.\frac{\partial f(x,u)}{\partial x^T}\right|_{x=\hat{x}} = \begin{pmatrix} 1 & 1 \\ -0.5u & -0.2 \end{pmatrix}, \tag{5.30}$$

$$D_x h(\hat{x}) = \left.\frac{\partial h(x)}{\partial x^T}\right|_{x=\hat{x}} = \begin{pmatrix} 1 & 0 \end{pmatrix} \tag{5.31}$$

Choosing the gain matrix

$$R\left(\hat{x},u\right) = \begin{pmatrix} 1 & 1 \end{pmatrix}^T \tag{5.32}$$

leads to the following error dynamics:

$$\dot{e} = A_e(\hat{x},u)e \tag{5.33}$$

where

$$A_e(\hat{x},u) = \begin{pmatrix} 0 & 1 \\ -(1+0.5u) & -0.2 \end{pmatrix} \tag{5.34}$$

The eigenvalues of matrix $A_e(\hat{x},u)$ are given by $\lambda_{1,2} = -0.1 \pm j\sqrt{0.99+0.5u}$. Obviously, they lie in the left-half plane for the bounded inputs $-1 \leq u \leq 1$. However, as mentioned above it is not possible to analyze the stability of a time-variant system by checking the eigenvalues. In fact, the considered system is unstable for the input $u(t) = \cos(2t)$. This is shown in Example 13 in Rugh and Shamma (2000) (which corresponds to (5.33) and (5.34)).

5.1.4 Summary

This section pointed out that a designer using FDI methods based on a linearization along a trajectory has to be careful concerning the stability analysis. This is due to the fact that the linearization leads to a time-variant system. The main differences between the stability analysis for time-invariant and for time-variant systems were emphasized and a stability theorem (Theorem 5.5) was stated. At the end an example was given to illustrate the problematic.

5.2 Stability of the ship propulsion FDI observers

For successful observer-based FDI the stability of the observer plays an essential role. This section addresses the stability of two nonlinear observers designed for FDI in the ship propulsion system. Their design is based on results from the geometric approach and described in Section 4.3. During the simulations the observers showed stable behavior for different initial conditions. In the following the formal proof of their stability is outlined.

5.2.1 FDI for the diesel engine gain fault

An observer to detect and isolate the diesel engine gain fault Δk_y was designed in Section 4.3 for the following fault-free subsystem ((4.31)-(4.32)):

$$\dot{x} = f_{sub1}(x,u) = f(x) + g(x)u \tag{5.35}$$

$$y = U \tag{5.36}$$

where $x = \begin{pmatrix} n \\ U \end{pmatrix}$ $f(x) = \begin{pmatrix} 0 \\ \frac{1}{m}R(U) + \frac{1-t_T}{m}T_{|n|V_a}(1-w)nU \end{pmatrix}$

$$g(x) = \begin{pmatrix} \frac{1}{I_m}k_y & -\frac{1}{I_m}\left[Q_{|n|n}n^2 + Q_{|n|V_a}(1-w)nU\right] \\ 0 & \frac{1-t_T}{m}T_{|n|n}n^2 \end{pmatrix} \quad u = \begin{pmatrix} Y \\ \theta \end{pmatrix}$$

with the fuel index measurement Y and the pitch measurement θ as external inputs. Subsystem (4.33)-(4.35) is by construction only affected by the diesel engine gain fault Δk_y, when the pitch loop is considered to be fault-free. Hence, Observer1 ((4.36)-(4.38)) is designed in Section 4.3 to detect and isolate the gain fault. It has the following form:

Observer1:

$$\dot{\hat{n}} = \frac{1}{I_m}k_y Y - \frac{1}{I_m}\left[Q_{|n|V_a}(1-w)\hat{n}\hat{U} + Q_{|n|n}\hat{n}^2\right]\theta + K^{\hat{n}}_{\Delta k_y}(U-\hat{U}) \tag{5.37}$$

$$\dot{\hat{U}} = \frac{1}{m}R(\hat{U}) + \frac{1-t_T}{m}\left[T_{|n|V_a}(1-w)\hat{n}\hat{U} + T_{|n|n}\hat{n}^2\theta\right] + K^{\hat{U}}_{\Delta k_y}(U-\hat{U}) \tag{5.38}$$

$$\hat{y} = \hat{U} \tag{5.39}$$

which corresponds to a form like:

$$\dot{\hat{x}} = f_{sub1}(\hat{x}, u) + K(y - \hat{y}) \tag{5.40}$$

$$\hat{y} = h(\hat{x}) = \hat{x}_2 = \hat{U} \tag{5.41}$$

The function $f_{sub1}(x, u)$ in (5.35) is globally Lipschitz for the complete operating range $\Omega_x = \{x \,|\, 0 < n < n_{max};\ 0 < U < U_{max}\}$ and $\Omega_u = \{u \,|\, -1 < \theta < 1;\ 0 < Y < 1\}$; i.e. $\|f_{sub1}(x, u) - f_{sub1}(\hat{x}, u)\| \leq \Lambda \|x - \hat{x}\|$, with Lipschitz constant $\Lambda \in \mathbb{R}$ and $x, \hat{x} \in \Omega_x$. This is due to the physical limitations and the upper-level control of the system. The upper-level control is designed to keep the signals (n, θ) inside certain boundaries (corresponding to Ω_x) to achieve desired operation and to avoid overload situations for the shaft and the pitch. Furthermore, there are the following physical limitations: The pitch signal is physically limited by construction $-1 < \theta < 1$ like the fuel index $0 < Y < 1$. The ship speed U is limited by the top speed of the ship. The shaft speed n is limited by an emergency shut-off.

The considered subsystem is observable over the complete operating range Ω_x. This can be seen when looking at the system and its corresponding observability codistribution (Nijmeijer and van der Schaft, 1990, Theorem 3.32). The observability codistribution can be obtained as follows (see Nijmeijer and van der Schaft (1990) or equation (3.48), on page 39):

$$d\mathcal{O}(x) = \text{span}\{dH(x) | H \in \mathcal{O}\}, \quad x \in \Omega_x$$

where the *observation space* $\mathcal{O}(x)$ denotes the linear space (over $\mathbb{R}$) of functions on Ω_x containing $h(x)$, and all the repeated Lie derivatives

$$L_{X_1} L_{X_2} \cdots L_{X_k} h_j(x), \quad j \in \mathbf{l},\ k = 1, 2, \ldots$$

with X_i, $i \in \mathbf{k}$, in the set of $\{f, g_1 \ldots g_m\}$. For the considered subsystem it can be seen that

$$\begin{aligned} dh(x) &= \begin{pmatrix} 0 & 1 \end{pmatrix} \\ dL_f h(x) &= \begin{pmatrix} \dfrac{1 - t_T}{m} T_{|n|V_a}(1 - w)U & \dfrac{1}{m}\dfrac{\partial R(U)}{\partial U} + \dfrac{1 - t_T}{m} T_{|n|V_a}(1 - w)n \end{pmatrix} \\ &\Rightarrow \qquad \dim d\mathcal{O}(x) = 2 = n = \dim \Omega_x \qquad \text{for} \quad u \in \Omega_u \end{aligned}$$

Hence, the system is observable over the complete operating range Ω_x. Using the fact that $f_{sub1}(x, u)$ is globally Lipschitz and that the subsystem (5.35)-(5.36) is

observable over the complete operating range Ω_x the stability of Observer1 can be proven by using the result of Gauthier *et al.* (1992). In Gauthier *et al.* (1992) it is also shown how the observer gain K has to be chosen. For the simulations in Chapter 4 it was chosen *ad hoc*.

5.2.2 FDI observer to detect and isolate shaft speed sensor fault

In Section 4.3 an observer to detect and isolate the shaft speed sensor fault Δn_{sensor} was designed for subsystem (4.44) and (4.45). The stability of the observer (Observer2) can be proven in the same way as the stability for Observer1. However, the proof for Observer2 is shorter due to the fact that subsystem (4.44) and (4.45) is globally observable, because the only state (U) is measured.

Remark: The observer design is only meaningful due to the possible faults, because in the fault-free case all variables (n, U, θ) are either measured or known inputs.

Chapter 6

Fault-output decoupling

Fault detection and isolation (FDI) plays an important role in the design of fault-tolerant control systems (FTCS). Fault-tolerant control systems have the ability to tolerate the occurrence of a fault by being able to continue operation while a degradation of performance may be accepted, see Blanke (1999). The main task for an active approach towards fault-tolerant control (see chapter 2) is to detect and isolate the faults occurring in the system. As stated in Patton (1997) successful fault detection and isolation (FDI) should be achieved by rather simple than complex methods. The reason for this lies in the fact that the later are seldom applied in real applications due to their complexity.

One well studied and applied approach for model-based fault detection and isolation uses diagnostic observers, see e.g. Chapter 2; Frank (1996); García and Frank (1997); Frank and Ding (1997); Patton (1995); Patton and Chen (1997). The text-book Chen and Patton (1999) gives a good introduction into the field. Nevertheless, the observer-based FDI design is not always easy to apply, especially in nonlinear systems it turns out to be a difficult task.

The observer-based FDI design would be easier if each considered fault would affect one and only one specific output. In that situation a dedicated observer scheme (DOS), e.g. a bank of observers, where each observes one output, would be able to detect and isolate the faults. The later can be achieved by checking for which outputs the generated residuals are affected. Analyzing this pattern leads to FDI. In that case also multiple faults (faults being active at the same time) could be detected and isolated from each other. The isolation of multiple faults

is otherwise often a problem due to possible cancellation of the faults against each other. Thus many of the existing observer-based methods are limited to single faults (faults happening one at a time).

In this chapter the idea is proposed to use the well studied concept of input-output decoupling (Falb and Wolovich (1967); Wonham and Morse (1970); Isidori (1985); Nijmeijer and van der Schaft (1990)) for a new concept *fault-output decoupling* and combine it with the controller design in such a way that the controlled system has the property that each fault affects one and only one output. Combining the fault-output decoupling idea with the overall control objective (e.g. stabilizing the plant or solving a tracking problem) would, as mentioned above, enhance the possibilities for the fault diagnosis design. Other ideas for an integrated approach have been made before, e.g. based on a four parameter controller scheme (Nett *et al.* (1988); Jacobson and Nett (1991)) or on a robust control approach (Stoustrup *et al.* (1997)).

This chapter is not meant to give a review of the wide field of input-output decoupling, but as an introduction of the new idea of fault-output decoupling. As the theory for input-output decoupling is available for both linear and nonlinear systems it is possible to formulate the fault-output decoupling idea for both linear and nonlinear systems systems. For simplicity and a better understanding it will only be handled for linear systems in this chapter. However, the procedure of how to obtain fault-output decoupling, given at the end of this chapter, is valid for both linear and nonlinear systems.

The proposed method is introduced and demonstrated for linear systems of the following structure:

$$\dot{x} = A\,x + B\,u + L_x\,\nu_x \tag{6.1}$$

$$y = C\,x + D\,u + L_y\,\nu_y \tag{6.2}$$

where $x \in \mathbb{R}^n$ describes the states, $u \in \mathbb{R}^m$ the inputs, $y \in \mathbb{R}^l$ the outputs, $\nu_x \in \mathbb{R}^{k_x}$ and $\nu_y \in \mathbb{R}^{k_y}$ the modeled faults, and A, B, C, D, L_x and L_y are matrices of appropriate size. The overall fault vector is defined as $\nu^T = \left[\nu_x^T\ \nu_y^T\right]$ of dimension $k = k_x + k_y$. This description has been widely used in the FDI literature, see e.g. the survey papers (Gertler (1991); Frank (1991); Gertler and Kunwer (1993); Frank (1993); Patton (1994)).

Remark 1: One important aspect of the above mentioned model is that a complete loss of the i^{th} actuator is modeled by setting the i^{th} column of the matrix L_x equal to the i^{th} column of the matrix B and the i^{th} component of ν_x equal to $-u_i$, as also described in chapter 2. This could cause problems as it means that the fault signal is not just an additional independent input, but depends of the input signal. This problem will be addressed later in Remark 2 after the fault-output decoupling is introduced.

The next section introduces the concept of *complete fault-output decoupling* followed by a section describing the more practical concept of *efficient fault-output decoupling* and a section looking at how to meet the control objectives. Finally a general design procedure will be given and applied to an illustrative example.

6.1 Complete fault-output decoupling

The proposed concept of fault-output decoupling corresponds to the input-output decoupling problem which is well described for linear systems (Falb and Wolovich (1967); Wonham and Morse (1970); Wonham (1985)) and nonlinear systems (Isidori (1985); Nijmeijer and van der Schaft (1990)); yet, there is a major difference which makes the fault-output decoupling harder to obtain and, hence, needs extra consideration:*Faults are unknown and cannot be used in feedback design, i.e. they cannot be used as normal inputs when applying input-output decoupling*. As a consequence, the normal control inputs have to be used to achieve fault-output decoupling, as they are the only access to the system. One possibility to achieve it is to apply a regular static state feedback (6.3) and will be explained in the next section.

To introduce the idea of fault-output decoupling, we start with the following definition:

Definition 6.1: *A system, described by equations (6.1) and (6.2), is called* **completely fault-output decoupled** *iff after a possible relabeling of the faults, the following three properties hold:*

(i) *For each* $i \in \mathbf{l}$ *the output* y_i*, is unaffected*[1] *by the faults* $\nu_j,\ j \neq i$ *.*

(ii) *For each* $i \in \mathbf{l} \wedge i \leq k$ *the output* y_i *is affected*[2] *by the fault* ν_i *.*

(iii) $k \leq l$.

where $\mathbf{l} = \{1, \ldots, l\}$ *and* ν_j *describes the* j^{th}*-component of the fault vector* ν*,* $j \in \mathbf{k}$.

Condition (ii) assures the possibility to detect the fault ν_i by checking the output y_i. Isolation of the fault is then guaranteed by Condition (i) as it assures that no other fault affects the output y_i. Hence, *complete fault-output decoupling* means that each fault affects only one output, which is not affected by others. As stated in Condition (iii), this can only be achieved if the number of faults k is smaller than the number of outputs l. This is due to the fact, that if Condition (iii) would not be fulfilled and the first two conditions would, there would be $k-l$ faults that do not affect any output. Hence, they cannot be detected and isolated by using the outputs. However, in systems where $k > l$ some faults might be considered as a group and then be treated as one fault component in ν_i to fulfill the Condition (iii) of Definition 6.1. Obviously, this grouping makes only sense for faults that do not need to be isolated from each other. Only if they act significantly different on the outputs, due to different fault signatures, it might be possible to isolate them. This would require an additional step of residual evaluation.

The proposed method uses a regular static[3] state feedback for the system (6.1) and (6.2) of the form

$$u \;=\; M\,x \;+\; N\,w \tag{6.3}$$

where $M \in \mathbb{R}^{(m,n)}$, $N \in \mathbb{R}^{(m,m)}$ is a nonsingular matrix, and $w \in \mathbb{R}^m$ denotes the new input. The later implies that application of the feedback (6.3) will not

[1] For a definition of *unaffected* see Appendix A.1.

[2] For a definition of *affected* see Appendix A.1.

[3] A static state feedback $u = Mx + Nw$ is a state feedback with a constant gain matrix M. There are no extra dynamics involved in the feedback. The latter is referred to as dynamic state feedback (see equation (6.14) and (6.15)).

affect the controller access to the system. Goal of the method is to decouple the faults from the outputs by finding an efficient feedback during the controller design in order to ease the fault detection and isolation. This leads to the following problem formulation:

Problem 6.2: (Complete fault-output decoupling by using regular static state feedback on the inputs) *Find a regular static state feedback (6.3) (without using the fault signals, as they are unknown) for the system (6.1) and (6.2) that achieves complete fault-output decoupling when applied to the input u of the system.*

6.2 Solution for complete fault-output decoupling

As an approach to solve Problem 6.2 we use the decoupling idea also presented in Gras and Nijmeijer (1989) for time-invariant linear systems. Due to the fact, that now next to the normal inputs also faults are acting on the system, additional steps have to be introduced. To start with, we take a look at the characteristic numbers of the considered system (6.1) and (6.2). Next to the characteristic numbers, ρ_i^u, of the system with respect to the inputs a definition for the characteristic numbers, ρ_i^ν, with respect to the faults is required. In the following the definitions for the different characteristic numbers are presented.

6.2.1 Characteristic numbers

The characteristic numbers, ρ_i^u, of the system (6.1) and (6.2) with respect to the inputs, with $i \in \mathbf{l}$, describe the number of time derivatives of the i^{th} output needed such that at least one of the inputs u_j, with $j \in \mathbf{m}$, appears explicitly (see e.g. Falb and Wolovich (1967)). To illustrate this, we start with equation (6.2) and calculate the time derivatives for the i^{th} output:
(The faults are omitted in order to ease the calculations.)

$$y_i = C_i\, x + D_i\, u \qquad i \in \mathbf{l}$$

where C_i and D_i describe the i^{th} row of the matrices C and D. If the the i^{th} row of the feed-through Matrix D is nonzero at least one of the inputs will appear explicit in the output y_i. As no derivative has been calculated yet, this would mean that the characteristic number ρ_i^u of the i^{th} output is equal to zero:

$$\rho_i^u = 0$$

If the i^{th} row of the feed-through Matrix D is zero the first derivative is calculated:

$$\dot{y}_i = C_i\,\dot{x} = C_i\,A\,x\;+\;C_i\,B\,u$$

If then $C_i\,B$ is nonzero at least one of the inputs will appear explicit in $\dot{y}_i$ and the characteristic number ρ_i^u of the i^{th} output is equal to one:

$$\rho_i^u = 1$$

When $C_i\,B$ is equal to zero the calculation procedure continues:

$$\ddot{y}_i = C_i\,A\,\dot{x}\;=\;C_i\,A^2\,x\;+\;C_i\,A\,B\,u$$

If now $C_i\,A\,B$ is nonzero at least one of the inputs will appear explicit in $\ddot{y}_i$ and the characteristic number ρ_i^u of the i^{th} output is equal to two:

$$\rho_i^u = 2$$

Otherwise the calculation of the time derivatives of the outputs has to be continued until at least one output appears explicitly, which leads to the following definition:

Definition 6.3: *The characteristic numbers $\rho_1^u \ldots \rho_l^u$ of the linear system (6.1) and (6.2) with respect to the inputs $u = (\,u_1\,u_2 \ldots u_m\,)^T$ are defined in the following way:*

$$\begin{aligned} \rho_i^u &= 0 \qquad \textit{if} \qquad D_i \neq 0 \\ \rho_i^u &= \infty \qquad \textit{if} \qquad C_i\,A^k\,B = 0\,\forall\,k \geq 0 \end{aligned}$$

otherwise ρ_i^u, $i \in$ l, equals the smallest nonnegative number such that:

$$\begin{aligned} C_i\,A^k\,B \;&=\; 0 \quad \textit{for} \quad k = 0 \ldots (\rho_i^u - 2) \\ \textit{and} \quad C_i\,A^{\rho_i^u - 1}\,B \;&\neq\; 0. \end{aligned}$$

In the same way we can now introduce a definition for the characteristic numbers of the system (6.1) and (6.2) with respect to the faults. The definition looks slightly different due to the fact that the faults enter in the state equation via $L_x\,\nu_x$ and in the output equation via $L_y\,\nu_y$:

Definition 6.4: *The characteristic numbers $\rho_1^\nu \dots \rho_l^\nu$ of the linear system (6.1) and (6.2) with respect to the faults $\nu = (\nu_1\, \nu_2 \dots \nu_k)^T$ are defined in the following way:*

$$\begin{aligned} \rho_i^\nu &= 0 \qquad \text{if} \qquad L_{y_i} \neq 0 \\ \rho_i^\nu &= \infty \qquad \text{if} \qquad C_i\, A^k\, L_x = 0 \,\forall\, k \geq 0 \end{aligned}$$

otherwise ρ_i^ν, $i \in \mathbf{l}$, equals the smallest nonnegative number such that:

$$\begin{aligned} C_i\, A^k\, L_x &= 0 \quad \text{for} \quad k = 0 \dots (\rho_i^\nu - 2) \\ \text{and} \quad C_i\, A^{\rho_i^\nu - 1}\, L_x &\neq 0. \end{aligned}$$

Next to the characteristic numbers the decoupling matrix place an important role when solving the input-output decoupling problem. In the next section definitions with respect to the inputs and with respect to the faults are given.

6.2.2 Decoupling matrices

In the input-output decoupling theory the decoupling matrix plays a fundamental role, see e.g. Falb and Wolovich (1967). In the following we will give a notation of the decoupling matrix with respect to the inputs and, furthermore, introduce the decoupling matrix with respect to the faults.

Definition 6.5: *The $l \times m$ decoupling matrix for the linear system (6.1) and (6.2) with respect to the inputs u_j, with $j \in \mathbf{m}$, is for finite characteristic numbers $\rho_1^u \dots \rho_l^u$ defined as:*

$$M_{dec}^u = \begin{pmatrix} M_{dec_1}^u \\ \vdots \\ M_{dec_l}^u \end{pmatrix}$$

where for $i \in \mathbf{l}$

$$M_{dec_i}^u = \begin{cases} D_i & \text{if } D_i \neq 0 \\ C_i\, A^{\rho_i^u - 1} B & \text{if } D_i = 0 \,\wedge\, C_i\, A^k\, B = 0 \,\forall\, k = 0 \dots (\rho_i^u - 2). \end{cases}$$

Corresponding to the decoupling matrix with respect to the inputs we introduce the following definition of the decoupling matrix with respect to the faults:

Definition 6.6: *The $l \times k$ decoupling matrix for the linear system (6.1) and (6.2) with respect to the faults ν_j, with $j \in \mathbf{k}$, is for finite characteristic numbers $\rho_1^\nu \ldots \rho_l^\nu$ defined as:*

$$M_{dec}^{\nu} = \begin{pmatrix} M_{dec_1}^{\nu} \\ \vdots \\ M_{dec_l}^{\nu} \end{pmatrix}$$

where for $i \in \mathbf{l}$

$$M_{dec_i}^{\nu} = \begin{cases} L_{y\,i} & \text{if } L_{y\,i} \neq 0 \\ C_i\, A^{\rho_i^\nu - 1} L_x & \text{if } L_{y\,i} = 0 \;\wedge\; C_i\, A^k\, L_x = 0 \,\forall\, k = 0 \ldots (\rho_i^\nu - 2). \end{cases}$$

A solution for Problem 6.2 is derived and discussed in the next section.

6.2.3 Solving the complete fault-output decoupling problem

This section proposes a solution for the complete fault-output decoupling problem (Problem 6.2). The solution is closely related to the solution for the input-output decoupling problem using a regular static state feedback (6.3) for a square analytic system (6.4) and (6.5), see e.g. Falb and Wolovich (1967); Gras and Nijmeijer (1989). Therefore, the solution for the input-output decoupling will be briefly introduced first and then a solution for the fault-output decoupling with its conditions is presented.

Input-output decoupling

One solution for input-output decoupling by a regular static state feedback for the system (6.1) and (6.2) can be obtained by following the solution given in Gras and Nijmeijer (1989). Taking the system (6.1) and (6.2), omitting the faults ν, and considering it to be square, i.e. it has the same number of inputs as outputs $m = l$, the following system remains:

$$\dot{x} = A\,x + B\,u \tag{6.4}$$

$$y = C\,x + D\,u \tag{6.5}$$

where $x \in \mathbb{R}^n$ describes the states, $u \in \mathbb{R}^m$ the inputs, $y \in \mathbb{R}^l$ the outputs, A, B, C and D are matrices of appropriate size, and $m = l$. For this system the

following derivatives can be calculated:

$$\begin{pmatrix} y_1^{(\rho_1^u)} \\ \vdots \\ y_l^{(\rho_l^u)} \end{pmatrix} = \begin{pmatrix} C_1\, A^{\rho_1^u} \\ \vdots \\ C_p\, A^{\rho_l^u} \end{pmatrix} x + M_{dec}^u\, u \tag{6.6}$$

Looking at the derivatives (6.6) it can be seen that it is possible to establish input-output decoupling from the new inputs w_j to the outputs y_i by the following regular static state feedback which has the same form as (6.3):

$$u = \begin{pmatrix} u_1 \\ \vdots \\ u_m \end{pmatrix} = -\,(M_{dec}^u)^{-1} \begin{pmatrix} C_1\, A^{\rho_1^u} \\ \vdots \\ C_p\, A^{\rho_l^u} \end{pmatrix} x + (M_{dec}^u)^{-1} \begin{pmatrix} w_1 \\ \vdots \\ w_m \end{pmatrix} \tag{6.7}$$

as it leads to:

$$\begin{pmatrix} y_1^{(\rho_1^u)} \\ \vdots \\ y_l^{(\rho_l^u)} \end{pmatrix} = \begin{pmatrix} w_1 \\ \vdots \\ w_m \end{pmatrix} = w \tag{6.8}$$

The solution given by equation (6.7) obviously only holds if M_{dec}^u is invertible and that means it is nonsingular or equivalently has full rank:

$$rank\, M_{dec}^u \;=\; m \tag{6.9}$$

In Falb and Wolovich (1967); Gras and Nijmeijer (1989) the proof is given that the regular static state feedback input-output problem (as considered here) is solvable if and only if equation (6.9) holds true.

Complete fault-output decoupling

A solution for the complete fault-output decoupling problem (Problem 6.2), is derived corresponding to the solution for the input-output decoupling problem presented above. Also here the system (6.1) and (6.2) is considered to be square, i.e. $l = m$. First the case is considered that the characteristic numbers fulfill the following condition:

$$\rho_i^u \;=\; \rho_i^\nu \quad \forall i \in \mathbb{1} \tag{6.10}$$

Later the other cases where condition (6.10) does not hold will be discussed in detail. Using the condition (6.10) the following derivatives similar to equation (6.6) can be obtained:

$$\begin{pmatrix} y_1^{(\rho_1^\nu)} \\ \vdots \\ y_l^{(\rho_l^\nu)} \end{pmatrix} = \begin{pmatrix} C_1\, A^{\rho_1^\nu} \\ \vdots \\ C_p\, A^{\rho_l^\nu} \end{pmatrix} x + M_{dec}^u\, u + M_{dec}^\nu\, \nu \qquad (6.11)$$

When looking at the derivatives (6.11) it can be seen that to achieve fault-output decoupling for the considered system two different aspects have to be considered: *Is there any cross-coupling of states in the $C_i\, A^{\rho_i^\nu}\, x$ terms that causes different faults to affect the same output?* and *Which structure does the decoupling matrix M_{dec}^ν have?* If the later has more than one nonzero element in one row there is no possibility to obtain complete fault-output decoupling, as it is not possible to prevent certain faults from effecting the output signals y by direct compensation. This is due to the important difference that fault signals are unknown, hence, they cannot be compensated by using them in a feedback.

To avoid the mentioned cross-coupling of states in the $C_i\, A^{\rho_i^\nu}\, x$ terms the inputs u_i can be used for a regular static state feedback in the same way as in the input-output decoupling problem (see (6.7) and (6.8)):

$$u = \begin{pmatrix} u_1 \\ \vdots \\ u_m \end{pmatrix} = -\,(M_{dec}^u)^{-1} \begin{pmatrix} C_1\, A^{\rho_1^\nu} \\ \vdots \\ C_m\, A^{\rho_l^\nu} \end{pmatrix} x + (M_{dec}^u)^{-1} \begin{pmatrix} w_1 \\ \vdots \\ w_m \end{pmatrix} \qquad (6.12)$$

By applying the feedback (6.12) the equation (6.11) turns into

$$\begin{pmatrix} y_1^{(\rho_1^\nu)} \\ \vdots \\ y_l^{(\rho_l^\nu)} \end{pmatrix} = \begin{pmatrix} w_1 \\ \vdots \\ w_m \end{pmatrix} + M_{dec}^\nu\, \nu \qquad (6.13)$$

Looking at equation (6.13) and keeping the result for the input-output decoupling problem in mind the following theorem can be given :

Theorem 6.7 *Complete fault-output decoupling can be achieved for a square analytic system of the form (6.1) and (6.2), which fulfills condition (6.10) by the regular static state feedback (6.12) if the following two conditions are fulfilled:*

(i) *The decoupling matrix M^u_{dec} is invertible.*

(ii) *The decoupling matrix M^ν_{dec} can be written in a diagonal form after possible relabeling of the faults.*

Remark 2: When looking at the feedback (6.12) it can be seen that the inputs are used to cancel out the cross-couplings $C_i\, A^{\rho^\nu_i}\, x$, with $i \in \mathbf{l}$. This is done to achieve the wanted fault-output decoupling as described by (6.13). As already mentioned in Remark 1 a complete loss of the i^{th} actuator can be modeled by setting the i^{th} column of the matrix L_x equal to the i^{th} column of the matrix B and the i^{th} component of ν_x equal to $-u_i$. This would mean that the control action of the i^{th} input (u_i) is destroyed (compensated) by the fault. Hence, the compensation of the cross-coupling terms achieved by this input is lost. This will, however, only effect one predefined output. This is due to the fault-output decoupling. The actuator fault was modeled and taken care of during the fault-output decoupling design. Hence, the decoupling effect is only lost for exactly that output that by design is only affected by the actuator fault. So when this lost compensation affects the predefined input it has exactly the desired affect. If it would also affect other outputs it would proof that the fault-output decoupling was not designed correctly.

In the following the case will be considered that condition (6.10) is not fulfilled. This is done by discussing the possibilities to achieve fault-output decoupling for the situations $\rho^u_i < \rho^\nu_i$ and $\rho^u_i > \rho^\nu_i$.

$\rho^u_i < \rho^\nu_i$: If the characteristic number with respect to the inputs is smaller than the characteristic number with respect to the faults it means that there exists at least one derivative of the output $y_i^{(\rho^u_i)}$ where the inputs enter explicitly before the faults do. This gives an additional freedom, because the inputs u_i, $i \in \mathbf{m}$ could then be used for an additional state feedback to influence the output y in such a way, by compensating certain states, that some faults or even all faults do not enter/affect the output y_i. The additional state feedback could be of the following structure

$$u \;=\; M^*\, x \;+\; N^*\, v$$

where $M^* \in \mathbb{R}^{(m,n)}$ and $N^* \in \mathbb{R}^{(m,m)}$ is a nonsingular matrix. That would give the possibility to influence the decoupling matrix M^{ν}_{dec}. The exact possibilities of the freedom available have been well studied in connection with the disturbance-decoupling problem (DDP), see e.g. Wonham and Morse (1970); Wonham (1985); Isidori (1985); Nijmeijer and van der Schaft (1990). Another useful option might be in this case to apply a dynamic state feedback:

$$\dot{z} = A_z\, z + B_{zx}\, x + B_{zv}\, v \tag{6.14}$$

$$u = C_z\, z + D_{zx}\, x + D_{zv}\, v \tag{6.15}$$

where $z \in \mathbb{R}^s$ describes the states of the dynamic feedback, $x \in \mathbb{R}^n$ the system states, $u \in \mathbb{R}^m$ the inputs to the system, $v \in \mathbb{R}^m$ the new inputs to the overall system, $y \in \mathbb{R}^l$ the system outputs, and A_z, B_{zx}, B_{zv}, C_z, D_{zx}, and D_{zv} are matrices of appropriate size. Applying a specific number of integrations on the input could for example lead to the situation that condition (6.10) is fulfilled for the new input signals v_i, $i \in \mathbf{m}$. However, this idea requires further study, which is not in the scope of this thesis.

$\rho^u_i > \rho^\nu_i$: If the characteristic number with respect to the inputs is bigger than the characteristic number with respect to the faults it means that there exists at least one derivative of the output $y_i^{(\rho^u_i)}$ where the faults enter explicitly before the inputs do. Hence, the fault-output decoupling problem cannot be solved in this case as there is no possibility to compensate possible cross-coupling of states in the $C_i\, A^{\rho^\nu_i}\, x$ terms or to influence the decoupling matrix M^{ν}_{dec}.

6.3 Efficient fault-output decoupling

In the previous sections the concept of complete fault-output decoupling, see Definition 6.1 and Problem 6.2, has been introduced. A solution and the condition when it can be obtained was derived and stated in Theorem 6.7. In this section we take a look at what to do when complete fault-output decoupling cannot be obtained due to the structure of the considered system. Would that mean that fault-output decoupling is not applicable at all? The answer is 'no'. By discussing problems with a non-diagonal decoupling matrix M^{ν}_{dec} and with sensor faults it will be illustrated why. As a result an additional definition of fault-output decoupling, next to the *complete* fault-output decoupling, will be given. It is called *efficient* fault-output decoupling for FDI.

6.3.1 Problems with complete fault-output decoupling

Complete fault-output decoupling (introduced in the previous section) experiences two main problems. First the decoupling matrix M^{ν}_{dec} will not always have the desired structure as described by Condition (ii) in Theorem 6.7 and second complete fault-output decoupling does not always make sense.

The problem of a non-diagonal structure (after possible relabeling of the faults) of the decoupling matrix with respect to the faults might be solvable for the case that $\rho^{u}_{i} < \rho^{\nu}_{i}$. As mentioned in the previous section the theory known from the disturbance decoupling problem (DDP) or an additional feedback might lead to a solution in this situation. However, if the structure of M^{ν}_{dec} cannot be changed to be diagonal due to the fact that the fault signals are unknown, complete fault-output decoupling cannot be achieved. This strongly limits the systems it can be applied to.

However, even if *complete* fault-output decoupling cannot be obtained, *partial* fault-output decoupling might be possible. For FDI purposes a partial decoupling might already be efficient enough. This can be explained by a simple example. Consider a system with two outputs y_1 and y_2, which is affected by two faults ν_1 and ν_2. If the decoupling matrix M^{ν}_{dec} has the following triangular structure

$$M^{\nu}_{dec} \;=\; \begin{pmatrix} 1 & 0 \\ 1 & 1 \end{pmatrix} \tag{6.16}$$

it is obvious that we cannot achieve complete fault-output decoupling. Nevertheless, a decoupling matrix as given in (6.16) is still good enough for partial fault-output decoupling. If the conditions (6.10) and (i) of Theorem 6.7 are fulfilled the possible cross-coupling of states in the $C_i\, A^{\rho^{\nu}_{i}}\, x$ terms can be canceled, which leads to a structure as given in equation (6.13). This would assure that the output y_1 is only affected by fault ν_1 and the output y_2 can be affected by both faults ν_1 and ν_2. This is efficient enough to detect and isolate the faults when the rule of exclusion is applied. So in case of single faults it becomes obvious that complete fault-output decoupling is not required to assure efficient FDI.

Next to the rule of exclusion a sufficient decision logic could be based on a kind of binary coding using the outputs (y_i: faulty or non-faulty) like presented in Massoumnia *et al.* (1989) with its practical risks, e.g. if one output reacts faster

than the others and the fault decision is taken too early a false alarm is the result. As already mentioned in Chapter 2, different kinds of structural residuals are known in the field of FDI, see e.g. Gertler (1991); Chen and Patton (1999). They can be described by the coding sets used in Definition 6.8 and in Definition 3.1.

Next to the problem with the structure of the decoupling matrix another important problem has to be considered. There are situations where complete fault-output decoupling is not desirable. To illustrate this another simple example is used. If a system with two inputs and three outputs is considered to be affected by three different faults, the following problem might occur. Consider one sensor fault and two actuator faults, each of them affecting one of the two inputs. If this system fulfills the conditions of Theorem 6.7 complete fault output-decoupling can be obtained. However, this would lead to a loss of controllability in the system. *Explanation:* Complete fault output decoupling would lead to the situation that each output is affected by one and only one of the three faults. So, two outputs are affected by actuator faults and one is affected by the sensor fault. Actuator faults enter the system in the same way as the control inputs, as a result decoupling an output from them means automatically decoupling it from the corresponding inputs. Hence, the output, which is only affected by the sensor fault, is no longer affected by the inputs. If it would be affected by one of the inputs, clearly, one of the actuator faults would affect it as well, which contradicts the definition of complete fault-output decoupling. So in this case complete fault-output decoupling would destroy the ability to steer or control the considered output by the input signals. This explains why not every system is suitable for complete fault-output decoupling. In the next section a concept to overcome this difficulty is introduced.

6.3.2 Efficient fault-output decoupling

As a consequence of the mentioned disadvantages of *complete* fault-output decoupling a new definition introducing *efficient* fault-output decoupling is given:

Definition 6.8: *A system, described by equations (6.1) and (6.2), is called efficiently fault-output decoupled if it has the following property:*
In the j^{th} fault mode (i.e. when $\nu_j(t) \neq 0, j \in \mathbf{k}$), only the outputs $y_i(t)$ for $i \in \Omega_j$ are affected. The pre-specified family of coding sets $\Omega_j \subseteq \mathbf{l}, j \in \mathbf{k}$, is chosen such that, by knowing which of the outputs $y_i(t)$ are affected and which are not, the fault ν_j can be uniquely identified.

For a more detailed description of the coding sets Ω_j the reader is referred to page 24. Obviously, the question if a system is *efficiently fault-output decoupled* or not and which coding sets to chose depends also on the fact if single or multiple faults are considered.

The mentioned difference between considering single faults (faults happening one at a time) and multiple faults (faults being active at the same time) becomes clear when looking again at the example given above with the decoupling matrix (6.16). The mentioned example is only able to handle single faults when using the mentioned efficient fault-output decoupling. Explanation: It can easily be seen that if fault ν_1 occurs it is not possible to detect and isolate a simultaneous occurrence of fault ν_2 by only looking at the outputs as ν_1 already affects all. Additional FDI steps are required to handle multiple faults in this case. Obviously, complete fault-output decoupling is able to handle both single and multiple faults.

The given Definition 6.8 leads to the following problem statement corresponding to Problem 6.2:

Problem 6.9:(Efficient fault-output decoupling by using regular static state feedback on the inputs and decision logic) *Find a regular state feedback (6.3) (without using the fault signals, as they are unknown) for the system (6.1) and (6.2) and a decision logic that achieves efficient fault-output decoupling when applied to the inputs of the system.*

6.4 Controller design to meet the control objectives

After using successfully one of the two concepts that are described in the previous sections a fault-output decoupled system can be obtained. However, the resulting system does not yet meet the control objectives, hence, does not yet perform as necessary for normal operation. As stated in Gras and Nijmeijer (1989) the proposed feedback (6.12) is not the only solution to achieve the decoupling. Due to the fact that the resulting system is not asymptotically stable it is even a bad solution. In the input-output decoupling theory the complete set of linear state feedbacks that could be used to decouple the system (6.1) and (6.2) are given, see e.g. Gilbert (1969); Wonham and Morse (1970). In this section a description of a subset of these possible control laws will be introduced. It can then

be applied additional to the control law (6.12) without affecting the decoupling. For a more detailed study the reader is referred to Gilbert (1969); Wonham and Morse (1970).

So, to be able to use the fault-output decoupling in practice the following problem has to be solved.

Problem 6.10: (Meeting the control objectives without affecting the fault-output decoupling) *Design a controller for the overall fault-decoupled system that meets the control objectives and does not affect the fault-output decoupling.*

In this section a subset of possible controls is introduced. To start with, it is shown that the input-output decoupled system (see equations (6.4)-(6.8)) can be written in a *normal form*. Namely, by defining for $i \in \mathbf{m}$:

$$z^i \;=\; \left(z_{i1}, \ldots, z_{i\rho_i^u}\right) = \left(y_i, \dot{y}_i, \ldots, y_i^{(\rho_i^u-1)}\right) \tag{6.17}$$

and letting $\overline{z}$ be $(n-\rho)$, where $\rho = \sum_{i=1}^{m} \rho_i^u$, supplementary linear coordinate functions such that $z = (\overline{z}, z^1, \ldots, z^m) = Sx$ form new coordinates, for some nonsingular matrix $S \in \mathbb{R}^{(n,n)}$. With respect to these new coordinates the state equations for the decoupled system (6.1,6.2,6.4-6.8) can be written as:

$$\dot{z^i} \;=\; A_i\, z^i + b_i\, w_i, \qquad i \in \mathbf{m}, \tag{6.18}$$

$$\dot{\overline{z}} \;=\; \overline{f}\, z \,+\, \overline{g}\, w \tag{6.19}$$

where $\overline{f} \in \mathbb{R}^{(n-\rho,n)}$, $\overline{g} \in \mathbb{R}^{(n-\rho,m)}$, and the pairs (A_i, b_i), $i \in \mathbf{m}$, are in Brunovsky canonical form:

$$A_i = \begin{pmatrix} 0 & 1 & 0 & \cdots & 0 \\ \vdots & & \ddots & & \\ 0 & & \cdots & 1 & 0 \\ 0 & & \cdots & 0 & 1 \\ 0 & & \cdots & & 0 \end{pmatrix}_{\rho_i^u \times \rho_i^u} \quad \text{and} \quad b_i = \begin{pmatrix} 0 \\ \vdots \\ \vdots \\ 0 \\ 1 \end{pmatrix}_{\rho_i^u \times 1} \tag{6.20}$$

The outputs are described by:

$$y_i \;=\; C_i\, z_i, \qquad \text{where} \quad C_i = (1, 0, \ldots, 0)_{1\times\rho_i^u} \quad \text{and} \quad i \in \mathbf{l} \tag{6.21}$$

When looking at the normal form, it can be seen that the regular static state feedback in equation (6.7) can be modified for the linear case as follows:

$$w_i = \tilde{\alpha}_{i1}\, y_i + \tilde{\alpha}_{i2}\, \dot{y}_i + \ldots + \tilde{\alpha}_{i\rho_i^u}\, y_i^{(\rho_i^u - 1)} + \tilde{\beta}_i\, \tilde{w}_i \tag{6.22}$$

where $\tilde{\alpha}_{ij},\ \tilde{\beta}_i \in \mathbb{R}$.

As known from the input-output decoupling theory combining (6.22) with (6.7) can be used to decouple and control a system (6.1) and (6.2). In a similar way Problem 6.10 can be solved by combining (6.22) with the feedback (6.12). Note that (6.22) describes output feedback and not state feedback. The state knowledge is only required for the decoupling (6.12) and in some cases not all states are required for the decoupling.

However, the decoupled system cannot be controlled arbitrarily. When looking at the normal form of the decoupled system it can be seen that there are some states $\overline{z}$ that cannot be influenced. So if for example that part of the dynamics is unstable the system cannot be stabilized, at least not if we want to preserve the decoupling. In the theory for input-output decoupling it has been shown that these states are connected to the zero dynamics (or system zeros) of the original system. As a consequence the system (6.1) and (6.2) has to be minimumphase in order to use the fault-output decoupling idea, otherwise the decoupled system cannot be stabilized.

If for the system the condition $\rho = \sum_{i=1}^{m} \rho_i^u = n$ is fulfilled the control law (6.22) gives full freedom to place the n poles of the fault-decoupled system; note that this corresponds to the case that the zero dynamics is trivial, or equivalently the system has no zeros. If $\rho = \sum_{i=1}^{m} \rho_i^u < n$ then $n - \rho$ poles are fixed and cannot be moved. Further research of how the known theory for the controller design for input-output decoupled systems can be used for fault-output decoupled systems is required.

6.5 Design procedure to obtain a fault-output decoupled system

This section presents a scheme of how to apply the proposed idea of fault-output decoupling. By following the different steps and using the in the previous chapters mentioned theory the control designer will find out if the system can be fault-output decoupled or not.

To achieve fault-output decoupling for a system (6.1) and (6.2) the following procedure should be followed:

- step 1: Separate the faults in maximal l different groups as l output signals are available. Only faults should be grouped together that can be isolated by their different effect on the output or do not have to be isolated from each other.
- step 2: Decouple the l fault groups from the output by considering the above introduced concepts of complete and efficient fault-output decoupling. Keep in mind that the faults are not measurable.
- step 3: Design a controller that meets the controller task and preserves the fault-output decoupled structure.

If these three steps are performed successfully fault-output decoupling and satisfying controller performance can be achieved. This leads to a system where the fault diagnosis task could be performed by a dedicated observer scheme (DOS), e.g. by a bank of diagnostic observers monitoring each one system output.

The application of the design method will be illustrated in the next section. During the application it can be seen that step 2 of the procedure is not trivial. It needs special consideration as there might be different solutions of how to decouple and different decision logics that could be used. In certain systems additional FDI techniques might be required.

As also mentioned in the previous chapter it is important that the fault-output decoupled system can be controlled in a way to meet the control objectives. One condition for this is that the considered system is minimumphase or in other words has stable zero dynamics.

The design procedure can also be applied to nonlinear systems if the concepts given in the previous chapters are also formulated for the nonlinear case.

6.6 Application example

In this section the proposed design procedure from the previous section will be applied to a modified linearized aircraft model for lateral motion. The original model is presented in Mudge and Patton (1988). During the application comments are given to explain and discuss each step of the in the previous chapter given design procedure.

6.6.1 Model description

First, the modified system model based on a linearized aircraft model for lateral motion presented in Mudge and Patton (1988) is introduced. Then the model will be changed corresponding to equations (6.1) and (6.2) in order to include faults and to obtain stable zero dynamics.

6.6.1.1 Original model

As stated in Mudge and Patton (1988) a stick fixed linearization established by considering small changes about a chosen state trajectory of the nonlinear system gives the following linear lateral motion model:

$$\dot{x} = A\,x + B\,u \tag{6.23}$$

$$y = C\,x \tag{6.24}$$

where:

$$x = \begin{pmatrix} x_1 \\ x_2 \\ x_3 \\ x_4 \\ x_5 \\ x_6 \\ x_7 \end{pmatrix} \begin{matrix} \text{: sideslip velocity} \\ \text{: roll rate} \\ \text{: yaw rate} \\ \text{: roll angle} \\ \text{: yaw angle} \\ \text{: rudder angle} \\ \text{: aileron angle} \end{matrix} \tag{6.25}$$

$$A = \begin{pmatrix} a_{11} & 0 & a_{13} & a_{14} & 0 & a_{16} & 0 \\ a_{21} & a_{22} & a_{23} & 0 & 0 & 0 & a_{27} \\ a_{31} & 0 & a_{33} & 0 & 0 & a_{36} & 0 \\ 0 & 1 & 0 & 0 & 0 & 0 & 0 \\ 0 & 0 & 1 & 0 & a_{55} & 0 & 0 \\ 0 & 0 & 0 & 0 & 0 & a_{66} & 0 \\ 0 & 0 & 0 & 0 & 0 & 0 & a_{77} \end{pmatrix} \tag{6.26}$$

$$B^T = \begin{pmatrix} 0 & 0 & 0 & 0 & 0 & b_{61} & 0 \\ 0 & 0 & 0 & 0 & 0 & 0 & b_{72} \end{pmatrix} \quad \text{and} \quad u = \begin{pmatrix} u_1 \\ u_2 \end{pmatrix} \tag{6.27}$$

$$C = \begin{pmatrix} 1 & 0 & 0 & 0 & 0 & 0 & 0 \\ 0 & 0 & 0 & 1 & 0 & 0 & 0 \\ 0 & 0 & 0 & 0 & 1 & 0 & 0 \end{pmatrix} \tag{6.28}$$

In the following we will use the system with a modified A matrix, i.e. compared to the original A matrix in Mudge and Patton (1988) two values are changed. The original values for $a_{55}^{old} = 0$ and a_{36}^{old} are changed to $a_{55}^{new} = -0.1$ and $a_{36}^{new} = -a_{36}^{old}$ in order to get stable zero dynamics. The values used for the simulations are given in Appendix D.

6.6.1.2 Model including faults

To consider fault isolation and detection aspects the equations (6.23) and (6.24) have to be modified in the following way:

$$\dot{x} = A\,x + B\,u + L_x\,\nu_x \tag{6.29}$$

$$y = C\,x + L_y\,\nu_y \tag{6.30}$$

The vectors ν_x and ν_y stand for the modeled and considered faults. Depending on their effect matrices L_x and L_y they can describe different faults. Some examples:

- if $L_x = B$ then $\nu_x^T = \begin{pmatrix} \nu_{x1} & \nu_{x2} \end{pmatrix}$ describes actuator faults.

- if $L_y = I_3$ then $\nu_y^T = \begin{pmatrix} \nu_{y1} & \nu_{y2} & \nu_{y3} \end{pmatrix}$ describes sensor faults.

I_3 stands for the 3x3 identity matrix. Of course other faults are possible, like component faults (modeled by parameter changes), but they are not considered here.

6.6.2 Demonstration of the method

In this section we will introduce a specific fault scenario for the presented model and then apply the design method given in section 6.5 in order to obtain fault-output decoupling.

6.6.2.1 Fault scenario

The considered faults are faults on both actuators (ν_{a1} and ν_{a2}) and a fault on the third output sensor ν_{s3}, which leads to the system description:

$$\dot{x} = A\,x + B\,u + L_x\,\nu_x \tag{6.31}$$

$$y = C\,x + L_y\,\nu_y \tag{6.32}$$

with

$$L_x = B \quad , \qquad \nu_x^T = \begin{pmatrix} \nu_{a1} & \nu_{a2} \end{pmatrix} \tag{6.33}$$

$$\text{and} \quad L_y = \begin{pmatrix} 0 & 0 & 0 \\ 0 & 0 & 0 \\ 0 & 0 & 1 \end{pmatrix} \quad , \qquad \nu_y^T = \begin{pmatrix} 0 & 0 & \nu_{s3} \end{pmatrix} \tag{6.34}$$

6.6.2.2 Applying the design procedure

Having defined the fault scenario, equations (6.31) - (6.34), and knowing the system model, equations (6.25) - (6.28), we can start applying the proposed method by following the procedure given in section 6.5:

Step 1 (fault grouping): In the lateral motion example we have three outputs, the sideslip velocity, $y_1 = x_1$, the roll angle, $y_2 = x_4$, and the yaw angle, $y_3 = x_5$. As only three faults are considered, $\nu^T = \begin{pmatrix} \nu_{a1} & \nu_{a2} & \nu_{s3} \end{pmatrix}$, every fault can be considered for itself, i.e. it is not necessary to group some faults together. Therefore, step 1 is in this case easily handled and we proceed with step 2.

Step 2 (fault-output decoupling): As the system has two inputs and three outputs complete fault-output decoupling for the given fault scenario is not feasible. This is due to the in Section 6.3.1 discussed problem. If complete fault-output decoupling was achievable the third output y_3 would only be affected by the sensor fault ν_{s3} and be decoupled from the actuator faults ν_{a1} and ν_{a2}. As a consequence the third output would also be decoupled from the two inputs and hence uncontrollable. As this is not desirable efficient fault-output decoupling will be considered. Efficient fault-output decoupling can be achieved, because it is possible to decouple the first two outputs of the system from the actuator faults such that for this subsystem complete fault-output decoupling is obtained. Then the third output does not have to be decoupled form the actuator faults. This is due to the fact that by the rule of exclusion the following logic makes it possible to detect and isolate the faults (FDI) anyway:

- if output y_1 is faulty ν_{a1} has occurred
- if output y_2 is faulty ν_{a2} has occurred
- if **only** output y_3 is faulty ν_{s3} has occurred

To continue the decoupling matrix, M^{ν}_{dec}, with respect to the faults will be derived, hence, first the characteristic numbers, ρ^{ν}_i, with respect to the faults are calculated.
Starting with the output y_1:

$$y_1^{(0)} = x_1 \tag{6.35}$$

$$y_1^{(1)} = \dot{x_1} = a_{11}x_1 + a_{13}x_3 + a_{14}x_4 + a_{16}x_6 \tag{6.36}$$

$$\begin{aligned} y_1^{(2)} &= a_{11}[a_{11}x_1 + a_{13}x_3 + a_{14}x_4 + a_{16}x_6] + \\ &\quad + a_{13}[a_{31}x_1 + a_{33}x_3 + a_{36}x_6] + \\ &\quad + a_{14}[x_2] + a_{16}[a_{66}x_6 + b_{61}u_1 + \underline{b_{61}\nu_{a1}}] \end{aligned} \tag{6.37}$$

$$\Rightarrow \text{ characteristic number for } y_1 : \ \rho_1^{\nu} = 2 \tag{6.38}$$

continuing with with the output y_2:

$$
\begin{aligned}
y_2^{(0)} &= x_4 && (6.39)\\
y_2^{(1)} &= \dot{x_4} = x_2 && (6.40)\\
y_2^{(2)} &= \dot{x_2} = a_{21}x_1 + a_{22}x_2 + a_{23}x_3 + a_{27}x_7 && (6.41)\\
y_2^{(3)} &= a_{21}[a_{11}x_1 + a_{13}x_3 + a_{14}x_4 + a_{16}x_6] + \\
&\quad +a_{22}[a_{21}x_1 + a_{22}x_2 + a_{23}x_3 + a_{27}x_7] + \\
&\quad +a_{23}[a_{31}x_1 + a_{33}x_3 + a_{36}x_6] + \\
&\quad +a_{27}[a_{77}x_7 + b_{72}u_2 + \underline{b_{72}\nu_{a2}}] && (6.42)\\
&\Rightarrow \text{ characteristic number for } y_2 : \rho_2^{\nu} = 3 && (6.43)
\end{aligned}
$$

and finally for the output y_3:

$$
\begin{aligned}
y_3^{(0)} &= x_5 + \underline{\nu_{s3}} && (6.44)\\
&\Rightarrow \text{ characteristic number for } y_3 : \rho_3^{\nu} = 0 && (6.45)
\end{aligned}
$$

As a result, the fault-output decoupling matrix M_{dec}^{ν} can be derived as follows:

$$
\begin{aligned}
\frac{\partial y_1^{(\rho_1^{\nu})}}{\partial \nu} &= \begin{pmatrix} a_{16}b_{61} & 0 & 0 \end{pmatrix} && (6.46)\\
\frac{\partial y_2^{(\rho_2^{\nu})}}{\partial \nu} &= \begin{pmatrix} 0 & a_{27}b_{72} & 0 \end{pmatrix} && (6.47)
\end{aligned}
$$

$$
\begin{aligned}
\frac{\partial y_3^{(\rho_3^{\nu})}}{\partial \nu} &= \begin{pmatrix} 0 & 0 & 1 \end{pmatrix} && (6.48)\\
\Rightarrow \quad M_{dec}^{\nu} &= \begin{pmatrix} a_{16}b_{61} & 0 & 0 \\ 0 & a_{27}b_{72} & 0 \\ 0 & 0 & 1 \end{pmatrix} && (6.49)
\end{aligned}
$$

As can be seen from Mudge and Patton (1988) the coefficients $a_{16}b_{61}$ and $a_{27}b_{72}$ are not equal to zero and therefore the decoupling matrix has full rank. It is even diagonal. Keeping in mind why we changed from complete to efficient fault-output decoupling only the following subsystem of derivatives is considered:

$$
\begin{pmatrix} y_1^{(\rho_1^{\nu})} \\ y_2^{(\rho_2^{\nu})} \end{pmatrix} = \begin{pmatrix} C_1\, A^{\rho_1^{\nu}} \\ C_2\, A^{\rho_2^{\nu}} \end{pmatrix} x \; + \; M_{dec}^{u*}\, u \; + M_{dec}^{\nu*} \begin{pmatrix} \nu_{a1} \\ \nu_{a2} \end{pmatrix} \qquad (6.50)
$$

$$\text{with} \quad M_{dec}^{u*} = \begin{pmatrix} C_1\, A^{\rho_1^\nu - 1}\, B \\ C_2\, A^{\rho_2^\nu - 1}\, B \end{pmatrix} = \begin{pmatrix} a_{16}b_{61} & 0 \\ 0 & a_{27}b_{72} \end{pmatrix} \tag{6.51}$$

$$\text{and} \quad M_{dec}^{\nu*} = \begin{pmatrix} a_{16}b_{61} & 0 \\ 0 & a_{27}b_{72} \end{pmatrix} = M_{dec}^{u*}. \tag{6.52}$$

The fact that M_{dec}^{u*} equals $M_{dec}^{\nu*}$ is due to the fact that actuator faults are considered, $L_x = B$. As mentioned before the elements from matrix M_{dec}^{u*} are nonzero, which implies that the matrix is invertible. In order to obtain complete fault-output decoupling for the first two outputs with respect to the actuator faults the following regular static state feedback can be derived from the equations (6.50) to (6.52):

$$u = \begin{pmatrix} u_1 \\ u_2 \end{pmatrix} = -\,(M_{dec}^{u*})^{-1} \begin{pmatrix} C_1\, A^{\rho_1^\nu} \\ C_2\, A^{\rho_2^\nu} \end{pmatrix} x + (M_{dec}^{u*})^{-1} \begin{pmatrix} w_1 \\ w_2 \end{pmatrix} \tag{6.53}$$

which leads to the following completely fault-decoupled subsystem:

$$\begin{pmatrix} y_1^{(\rho_1^\nu)} \\ y_2^{(\rho_2^\nu)} \end{pmatrix} = \begin{pmatrix} w_1 \\ w_2 \end{pmatrix} + \begin{pmatrix} a_{16}b_{61} & 0 \\ 0 & a_{27}b_{72} \end{pmatrix} \begin{pmatrix} \nu_{a1} \\ \nu_{a2} \end{pmatrix}. \tag{6.54}$$

When looking at the equations (6.37) and (6.42) the feedback can be written in the following form which corresponds with (6.3):

$$u = M\, x + (M_{dec}^{u*})^{-1} \begin{pmatrix} w_1 \\ w_2 \end{pmatrix} \tag{6.55}$$

where

$$M = -\,(M_{dec}^{u*})^{-1} \begin{pmatrix} C_1\, A^{\rho_1^\nu} \\ C_2\, A^{\rho_2^\nu} \end{pmatrix} \tag{6.56}$$

$$\Rightarrow \quad M \;=\; -\begin{pmatrix} \frac{a_{11}^2+a_{13}a_{31}}{a_{16}b_{61}} & \frac{a_{21}a_{11}+a_{22}a_{21}+a_{23}a_{31}}{a_{27}b_{72}} \\ \frac{a_{14}}{a_{16}b_{61}} & \frac{a_{22}^2}{a_{27}b_{72}} \\ \frac{a_{11}a_{13}+a_{13}a_{33}}{a_{16}b_{61}} & \frac{a_{21}a_{13}+a_{22}a_{23}+a_{23}a_{33}}{a_{27}b_{72}} \\ \frac{a_{11}a_{14}}{a_{16}b_{61}} & \frac{a_{21}a_{14}}{a_{27}b_{72}} \\ 0 & 0 \\ \frac{a_{11}a_{16}+a_{13}a_{36}+a_{16}a_{66}}{a_{16}b_{61}} & \frac{a_{21}a_{16}+a_{23}a_{36}}{a_{27}b_{72}} \\ 0 & \frac{a_{22}a_{27}+a_{27}a_{77}}{a_{27}b_{72}} \end{pmatrix}^T \tag{6.57}$$

Applying the feedback given by equation (6.55) the system (6.31) and (6.32) is completely fault-output decoupled regarding the two actuator faults and the first two outputs. Hence, efficient fault-output decoupling has been achieved when considering the above introduced decision logic and single faults. For multiple faults it is necessary to be able to isolate the sensor fault with additional FDI means. This can according to Chen and Patton (1999) be achieved straightforward, e.g. by diagnostic observers, hence, it is possible. So, performing step 2 successfully has shown the capability of the new introduced idea of fault-output decoupling to improve the fault isolation possibilities.

Step 3 (Controller design to meet control objectives): After establishing efficient fault-output decoupling the last step to design a controller to meet the control objectives and which preserves the decoupling has to be carried out.

In this example the control objective is chosen to be that the system is asymptotically stable. In order to achieve this the control possibilities as described in section 6.4 are considered in the following:

$$w_i \;=\; \tilde{\alpha}_{i1}\, y_i \;+\; \tilde{\alpha}_{i2}\, \dot{y}_i \;+\; \ldots \;+\; \tilde{\alpha}_{i\rho_i^u}\, y_i^{(\rho_i^u-1)} \;+\; \tilde{\beta}_i\, \tilde{w}_i \tag{6.58}$$

where $\tilde{\alpha}_{ij}$, $\tilde{\beta}_i \in \mathbb{R}$. For the considered control objective the external access $\tilde{w}_i$ can be omitted which leads to the following control law:

$$w_1 = \tilde{\alpha}_{11}\, y_1 + \tilde{\alpha}_{12}\, \dot{y}_1 \tag{6.59}$$

$$w_2 = \tilde{\alpha}_{21}\, y_2 + \tilde{\alpha}_{22}\, \dot{y}_2 + \tilde{\alpha}_{23}\, \ddot{y}_2 \tag{6.60}$$

Choosing the controller parameters $\tilde{\alpha}_{ij}$ e.g. to be -10 gives a stable performance of the system, which has the following eigenvalues:

$$\begin{aligned} \lambda_1 &= -0.1\,, \quad \lambda_2 = -58.12\,, \quad \lambda_{3,4} = -0.49 \pm 0.93\, i, \\ \lambda_5 &= -9\,, \quad \lambda_6 = -8.87 \quad \lambda_7 = -1.13 \end{aligned}$$

where $\lambda_1 = -0.1$ and $\lambda_2 = -58.12$ are the poles given by the zero dynamics.

Remark 3: It is straightforward to show that the decoupled system (6.31) and (6.32) with (6.55) is controllable, hence, a general state feedback could be used to place all the poles of the system arbitrarily, but as mentioned earlier in section 6.4 this would destroy the decoupling. The restriction given by the objective to preserve the decoupling can be clearly seen in the example. Two poles ($n - \rho$), λ_1 and λ_2, are fixed and the others can be assigned arbitrarily.

Simulations In a simulation of the modified aircraft example the above designed feedbacks (6.55) and (6.59) are applied. The first one to achieve fault-output decoupling and the second one to stabilize the system. The used parameters can be found in Appendix D. During the simulation applied fault signals are given in the first sub-figure of Fig. 6.1.

Three different faults were simulated in the following order, first actuator fault 1, ν_{a1} starting at 10 seconds, then actuator fault 2, ν_{a2}, starting at 30 seconds, and at the end sensor fault 3, ν_{s3}, starting at 50 seconds. The simulated outputs are shown in the last three sub-figures of Fig. 6.1. It can be clearly seen that the outputs react in such a way, that the decision logic, as designed in step 2, is efficient enough to detect and isolate the faults with a bank of observers that monitor the single outputs. Hence, the proposed method has been applied successfully.

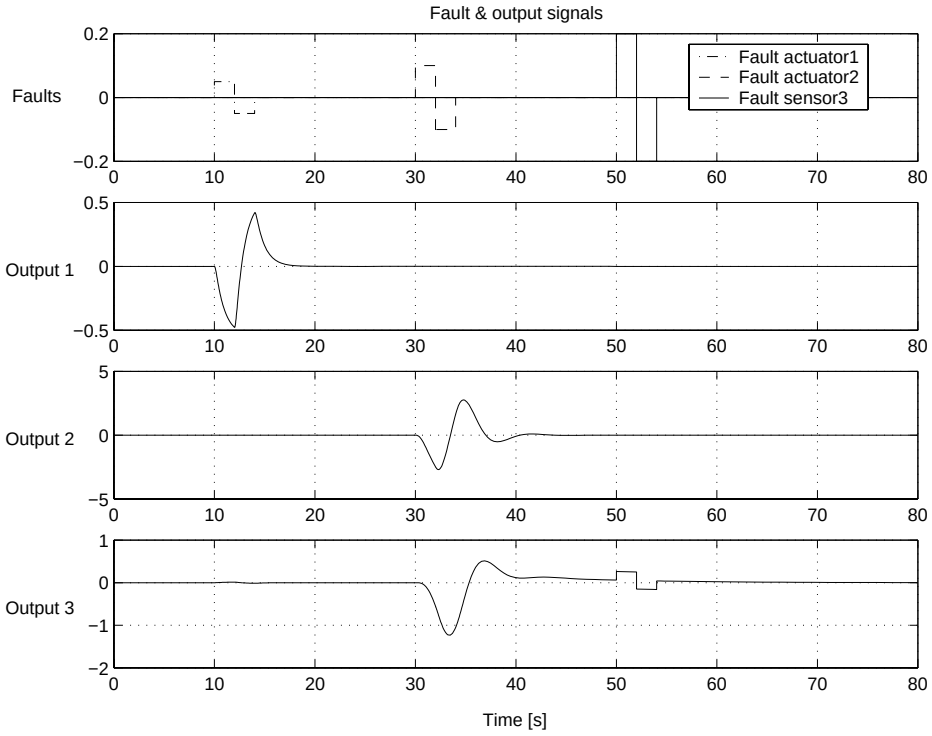

Figure 6.1: Output and fault signals from the simulation of the fault-output decoupled modified aircraft example.

6.7 Conclusions

In this chapter the novel idea of fault-output decoupling to improve the fault detection and isolation possibilities has been presented. It is based on integrating fault-output decoupling in the controller design such that the design of fault detection and isolation can be performed easier, e.g. by applying dedicated observer scheme (DOS).

The idea is strongly connected to the well studied problems of input-output and disturbance decoupling. Hence, not all details of the theory were investigated and stated in this chapter. The interested reader is referred to the given references in the chapter as this chapter is meant to present a new idea and not to give a review of existing theory.

It was shown how state feedback is used to obtain fault-output decoupling. Hence, state knowledge is required. This is from a FDI-point-of-view very restrictive, because full-state knowledge opens the possibility to use other FDI methods. However, in control theory many different control strategies exist that are based on state feedback. In those cases the state knowledge is available anyway, hence, it could be used to improve the FDI possibilities. At present, however, the FDI design is not considered during the controller design for most systems.

A design procedure to obtain successful fault-output decoupling, to ease the fault isolation task, and to meet the controller objectives has been introduced. Its application has been illustrated on a modified linearized aircraft model for lateral motion. The simulations show that the fault-output decoupling has successfully been achieved.

In this chapter only linear systems were considered to make it more understandable. However, as the input-output decoupling theory is also well studied for nonlinear systems fault-output decoupling should apply to them as well. The design procedure presented in Section 6.5 is applicable to both linear and nonlinear systems.

There are still a lot of open questions concerning the new idea of fault-output decoupling. They require further research to decide whether it is applicable or not. Hence, some recommendations for further research are given in Chapter 7 at the end of this thesis.

Chapter 7

Conclusions and Recommendations

This thesis considered different aspects of fault detection and isolation (FDI). The design of nonlinear observers for FDI in nonlinear systems was studied in detail using the so-called geometric approach. This chapter summarizes the work presented in this thesis. The main results and conclusions are reviewed. Directions and recommendations for further investigations are identified.

7.1 Conclusions

Theory and application were combined in this thesis. The thesis first described the geometric approach and discussed how to use this mathematical theory on the fault diagnosis problem. Then application of the theory was illustrated on a nonlinear ship propulsion system. Furthermore, the thesis considered some stability aspects of observer design. Finally, it introduced the novel idea of fault-output decoupling.

A number of conclusions can be drawn based on the accomplishments of this thesis:

- The idea of model-based fault detection was explained briefly. This was done by addressing the following aspects: analytical redundancy, residual generation, residual evaluation, robustness concerning model uncertainty, and performance issues.

- A detailed review was given on fault-diagnostic observers using the geometric approach. The review started with a description of the original idea introduced by Massoumnia (1986*b*) to solve the fundamental problem of residual generation (FPRG) for linear systems. It ended with the latest results for input-affine nonlinear systems by DePersis (1999); DePersis and Isidori (1999, 2000). Both problem formulations and solutions were presented. Furthermore, the similarities and the common idea of the geometric approaches were pointed out.

- A nonlinear ship propulsion system was used as application example. The geometric approach was applied by considering several FPRGs for different subsystems and fault scenarios. Detailed calculations were given to illustrate the application of the geometric approach and its different geometric algorithms. Only two FPRGs could be solved when neglecting the disturbances.

- As a result it can be concluded that the FDI problem as stated in Section 4.1.3 cannot be solved for arbitrary fault and disturbance signals.

- The results for the two solvable FPRGs were used to design two nonlinear observers for FDI. They were designed to detect and isolate the two possible shaft speed loop faults in the propulsion system. Furthermore, a linear observer was designed to detect the pitch loop faults in the system. For comparison an adaptive nonlinear observer was designed as well. Six residuals were obtained based on these observers.

- Different simulations (neglecting the disturbances) were carried out to test the FDI performance of the different observers. From the simulation results it could be seen that all faults could be handled according to the requirements as long as multiple faults could be neglected and additional considerations were made.

- It was illustrated how the measurement noise and possible disturbances affect the residuals. A *CUSUM*-algorithm was used to illustrate that the measurement noise could be handled. However, it was also shown that the disturbances could not be handled. Their occurrence would lead to false alarms. This was also shown by the geometric approach, because the corresponding FPRGs were not solvable.

- The correct tuning of the FDI system is a complex task. It is a optimization problem considering several problems, as finding an appropriate observer structure, tuning of the observer to obtain structured residuals, stability of the observer, robustness issues, and the performance. The geometric approach handles most of these aspects, however, it does not consider the residual dynamics, which might cause problems as shown for the ship propulsion system where some residuals react too slow.

- The geometric approach proved to be a powerful tool for FDI design, but additional work is needed to obtain a complete solution for successful FDI.

- The subsystems obtained by the geometric approach were also obtained by using the structural analysis (Staroswiecki and Declerck (1989); Cassar *et al.* (1994)) by Izadi-Zamanabadi (1999)[Section 5.1.3].

- Different aspects of the stability of observer-based FDI were addressed. The stability for the nonlinear observers designed for the ship propulsion system was outlined. Furthermore, the importance of the awareness that linearization along a trajectory leads to a time-variant system was emphasized.

- The novel idea of *fault-output decoupling* was presented to show how FDI and control design could be combined to improve FDI possibilities. The concepts of complete and efficient fault-output decoupling was defined and illustrated by a simple example.

7.2 Recommendations

Some aspects and topics are not covered in this thesis. They are listed in the following, as it is believed that future investigation is needed or could be beneficial:

- The solutions presented for the ship propulsion's FDI problem neglects the disturbances. For real application a way to handle the disturbances need to be found. This might be possible by disturbance estimation (e.g. for T_{ext} based on weather data) or additional sensors, e.g. measuring the torque or the thrust.

- The correct tuning of the FDI algorithm for the ship propulsion system needs further investigation, like e.g. which thresholds to chose and how to tune the observers in an optimal way.

- The residuals r_1 and r_3 can by construction be used for detection and isolation of the two shaft speed fault. However, they need too much time to detect the faults. This is due to the fact that they are based on the slow ship speed dynamics. This kind of problem due to the residual's dynamics is believed to be an important aspect for real applications. However, so far it has not been considered often in model based approaches. A unified FDI design methodology considering all important aspects for successful FDI is still missing and therefore still a topic for further research.

- Furthermore, it is believed to be an interesting topic to attempt to combine the geometric approach with the structural analysis. Both methods provide information to determine subsystems for the observer design in order to obtain observer-based FDI.

- The new idea of fault-output decoupling needs further research. The topics to be addressed are e.g. its robustness, ability to handle nonlinear systems, required knowledge of the states, and what kind of faults can be handle. When looking at the equations (6.13) and (6.54) it can be seen that it is also an interesting question if the fault-output decoupling idea could be used for fault estimation.

Appendix A

Geometric theory and other mathematical concepts

This appendix presents and explains the different geometric and system theory concepts used in this thesis. Throughout the thesis footnotes are used to refer to the different sections below. Each gives an explanation of the corresponding concept and refers to further literature.

A.1 Affected/unaffected

Section 3.3 in Isidori (1995) gives a detailed description of the definitions for output invariance and the concept of affected/unaffected. In the following the definition as stated in DePersis (1999) is repeated.

The j^{th} output $y_j(t; x^0; u_1, \ldots, u_m)$ corresponding to an initial condition x^0 and to the set of input functions $u_1, \ldots, u_m$ is *unaffected* by (or *invariant* under) the i^{th} input u_i if, for any initial condition x^0 in $\mathbb{U}$ ($\mathbb{U}$ being an open set of $\mathbb{R}^n$ - or, more abstract, the state space manifold, - on which the system is defined) and any collection of *admissible* input functions $u_1, \ldots, u_{i-1}, u_{i+1}, \ldots, u_m$, there holds:

$$\begin{aligned} & y_i(t; x^0; u_1, \ldots, u_{i-1}, u_a, u_{i+1}, \ldots, u_m) \\ = & \, y_i(t; x^0; u_1, \ldots, u_{i-1}, u_b, u_{i+1}, \ldots, u_m) \end{aligned}$$

for all $t \geq 0$ and any pair u_a, u_b. The j^{th} output $y_i(t; x^0; u_1, \ldots, u_m)$ is said to be *affected* by u_i if it is *not unaffected* by u_i.

A.2 Algorithm to obtain the u.o.s. $\mathcal{S}^*$

In this section a detailed description is given of how to obtain the infimal unobservability subspace $\mathcal{S}^*$ as it is used in section 3.3.1 to solve the linear FPRG in geometric way. The given description can also be found in Massoumnia *et al.* (1989).

A subspace $\mathcal{W} \subseteq \mathcal{X}$ is called (C, A)-invariant if there exists a map $D : \mathcal{Y} \to \mathcal{X}$ such that $(A + DC)\mathcal{W} \subseteq \mathcal{W}$ (see e.g. Wonham (1985)). Let $\mathcal{W}$ be (C, A)-invariant then $\underline{D}(\mathcal{W})$ denotes the class of all maps D such that $(A + DC)\mathcal{W} \subseteq \mathcal{W}$. Let $\mathcal{L} \subseteq \mathcal{X}$; the family of (C, A)-invariant subspaces containing $\mathcal{L}$ is denoted by $\underline{\mathcal{W}}(\mathcal{L})$. The family $\underline{\mathcal{W}}(\mathcal{L})$ is closed under intersection (i.e., if $\mathcal{W}_1 \in \underline{\mathcal{W}}(\mathcal{L})$ and $\mathcal{W}_2 \in \underline{\mathcal{W}}(\mathcal{L})$, then $\mathcal{W}_1 \cap \mathcal{W}_2 \in \underline{\mathcal{W}}(\mathcal{L})$); hence $\underline{\mathcal{W}}(\mathcal{L})$ contains an infimal element $\mathcal{W}^* := \inf \underline{\mathcal{W}}(\mathcal{L})$. Also $\mathcal{W}^* = \lim \mathcal{W}^k$ (limit attained for finite k) where $\mathcal{W}^k$ is given in the following recursive algorithm (CAISA : (C, A)-invariant subspace algorithm, see Wonham (1985)):

$$\mathcal{W}^{k+1} = \mathcal{L} + A(\mathcal{W}^k \cap KerC), \qquad \mathcal{W}^0 = 0. \tag{A.1}$$

A subspace $\mathcal{S} \subseteq \mathcal{X}$ is a (C, A)-unobservability subspace (u.o.s.) if $\mathcal{S} = \langle KerHC|A + DC\rangle$ for some output injection map $D : \mathcal{Y} \to \mathcal{X}$ and measurement transformation $H : \mathcal{Y} \to \mathcal{Y}$; where $\langle KerC|A\rangle = KerC \cap A^{-1}KerC \cap \cdots \cap A^{-n+1}KerC$, and $A^{-k}KerC = \{x : A^k x \in KerC\}$. $\mathcal{S}$ is the unobservable subspace of the pair $(HC, A + DC)$, and the spectrum of $A + DC : \mathcal{X}/\mathcal{S}$ can be assigned to an arbitrary symmetric set Λ by appropriate choice of D if the pair $\{C, A\}$ is observable. $\underline{\mathcal{S}}(\mathcal{L})$ denotes the class of u.o.s. containing $\mathcal{L}$. The class of u.o.s. $\underline{\mathcal{S}}(\mathcal{L})$ is closed under intersection; therefore, it contains an infimal element $\mathcal{S}^* := \inf \underline{\mathcal{S}}(\mathcal{L})$, (see e.g. Wonham (1985)). Also $\mathcal{S}^* = \lim \mathcal{S}^k$ is given by a recursive algorithm (UOSA : unobservability subspace algorithm, see Wonham (1985)) using the result from (A.1):

$$\mathcal{S}^{k+1} = \mathcal{W}^* + (A^{-1}\mathcal{S}^k) \cap KerC, \qquad \mathcal{S}^0 = \mathcal{X}. \tag{A.2}$$

Moreover, $\mathcal{S}^* = \langle KerC + \mathcal{W}^*|A + DC\rangle$ for $\mathcal{W}^* := \inf \underline{\mathcal{W}}(\mathcal{L})$ and $D \in \underline{D}(\mathcal{W}^*)$, see Wonham (1985).

A.3 Conditioned invariant distribution

Conditioned invariant distributions the nonlinear counterpart of the conditioned invariant subspaces were introduced in Isidori *et al.* (1981).

A distribution $\mathcal{S}$ is a conditioned invariant distribution for the system:

$$\begin{aligned} \dot{x} &= f(x) + \sum_{i=1}^{m} g_i(x)u_i + l(x)\nu + \sum_{i=1}^{s} p_i(x)w_i \\ y_j &= h_j(x), \quad j \in \mathbf{l} \end{aligned}$$

if it fulfills the following conditions:

$$[X, \mathcal{S} \cap Ker(dh)] \subset \mathcal{S}$$

for each $X \in \{f, g_1, \ldots, g_m\}$. Where the Lie bracket $[X, Y]$ for two vector fields $X(x)$ and $Y(x)$ is defined as follows:

$$[X, Y](x) = [X(x), Y(x)] = [\frac{\partial Y}{\partial x}(x)\, X(x) - \frac{\partial X}{\partial x}(x)\, Y(x)]$$

$\frac{\partial f}{\partial x}$ denotes the Jacobian matrix of $f = (f_1, f_2, \ldots, f_m)^T$:

$$\frac{\partial f}{\partial x} = \begin{pmatrix} \frac{\partial f_1}{\partial x_1} & \cdots & \frac{\partial f_1}{\partial x_n} \\ \vdots & & \vdots \\ \frac{\partial f_m}{\partial x_1} & \cdots & \frac{\partial f_m}{\partial x_n} \end{pmatrix} \tag{A.3}$$

A.4 Dual spaces

For a vector space or distribution $\mathcal{X} \subset \mathbb{R}^n$ there exists a group of linear functions f such that $f : \mathcal{X} \to \mathbb{R}$. This group of functions defines the *dual space* $\mathcal{X}^{'} \subset \mathbb{R}^n$ or also denoted as $\mathcal{X}^T$. So obviously, for $x \in \mathcal{X}$ and $x^{'} \in \mathcal{X}^{'}$ the following holds: $x^{'}\, x \in \mathbb{R}$. One known simple example: The dual space of the column vectors is the space of row vectors.

A.5 Factor spaces

In Wonham (1985) the following definition of a factor space is given:

Let $\mathcal{S} \subset \mathcal{X}$. Call vectors $x, y \in \mathcal{X}$ equivalent mod $\mathcal{S}$ if $x - y \in \mathcal{S}$. We define the factor space (or quotient space) $\mathcal{X}/\mathcal{S}$ as the set of all equivalence classes:

$$\bar{x} \triangleq \{y : \, y \in \mathcal{X}, \, y - x \in \mathcal{S}\}, \quad x \in \mathcal{X} \tag{A.4}$$

For linear spaces it can be shown that:

$$\dim \mathcal{X}/\mathcal{S} = \dim \mathcal{X} - \dim \mathcal{S} \triangleq \operatorname{codim} \mathcal{S}$$

To explain and illustrate the definition given by Wonham (1985) the following example is given:

Let $\mathcal{X} = \mathbb{R}^2$, where $x = \begin{pmatrix} x_1 & x_2 \end{pmatrix}^T \in \mathcal{X}$. Furthermore, define a subspace $\mathcal{S}_1 = \begin{pmatrix} s_1 & 0 \end{pmatrix}^T$ where $s_1 \in \mathbb{R}$. Hence, the dimension of $\mathcal{S}_1$ is one, $\dim \mathcal{S}_1 = 1$. To understand the definition (A.4) one can start by choosing one arbitrary point $\hat{x} = \begin{pmatrix} \hat{x}_1 & \hat{x}_2 \end{pmatrix}^T \in \mathcal{X}$ and look at (A.4):

$$\bar{\hat{x}} = \{y : \, y \in \mathcal{X}, \, y - \hat{x} \in \mathcal{S}_1\} \tag{A.5}$$

Then it can be seen that $\bar{\hat{x}}$ describes the following line:

$$y = \hat{x} + \begin{pmatrix} s_1 & 0 \end{pmatrix}^T \tag{A.6}$$

hence, one can see that the set of all equivalence classes $\bar{x}$ describes the set of all parallel lines to the line defined by $\mathcal{S}_1$. This is the *factor space* (or *quotient space*) $\mathcal{X}/\mathcal{S}_1$. Together with $\mathcal{S}_1$ it spans $\mathcal{X}$. $\mathcal{X}/\mathcal{S}_1$ is isomorph to the subspace $\mathcal{S}_2 = \begin{pmatrix} 0 & s_2 \end{pmatrix}^T$ where $s_2 \in \mathbb{R}$.

Hence, it can somehow be seen as: $\mathcal{X}$ *'minus/modulo'* $\mathcal{S}_1$.

A.6 Input observability

In Definition 3.2 the map condition '*The map from ν_1 to r is input observable*' is given. As discussed in Massoumnia *et al.* (1989) it is one of the possible criteria to decide whether a nonzero fault signal ($\nu_1(t) \neq 0$) will affect the residual $r(t)$ or not. The most natural approach would be to require that the transfer matrix $G_{r\nu_1}(s)$ from $\nu_1(s)$ to $r(s)$ is *left invertible*, so that *any* nonzero $\nu_1(t)$ results in a nonzero $r(t)$. Another approach would be to use the weaker requirement that the system relating $\nu_1(t)$ to $r(t)$ should be *input observable*. A system (C, A, B) is input observable if B is monic and the image of B (ImB) does not intersect the unobservable subspace of (C, A). In terms of transfer matrices, left invertibility is equivalent to the columns of $C(sI - A)^{-1}B$ being linearly independent over the field of rational s, while input observability is equivalent to independence over the field of real numbers. When the fault signal ν_1 is scalar ($k_1 = 1$) input observability is equivalent to the left invertibility of the system relating $\nu_1(t)$ to $r(t)$, and hence if $\nu_1(t) \neq 0$ then $r(t) \neq 0$ (see also *Remark1* in Hammouri *et al.* (1998)).

Even if the system relating $\nu_1(t)$ to $r(t)$ is only input observable and not left invertible, *almost any* nonzero $\nu_1(t)$ will produce a nonzero residual $r(t)$. This is because it is extremely unlikely that an arbitrary nonzero $\nu_1(t)$ will hide itself for all t in the nullspace of the mapping from $\nu_1(t)$ to $r(t)$. It may therefore be argued that the requirement of left invertibility is too stringent for FDI purposes (Massoumnia *et al.* (1989)).

A.7 Observability and unobservability spaces for state-affine systems

The solution of the FPRG presented in Section 3.3.2 for state-affine systems uses observability and unobservability spaces. In the following these terms are explained according to the definition given in Hammouri *et al.* (1998) for the following class of system:

$$\dot{x} = A(u)x, \qquad y = [c_1 x, \ldots, c_l x]^T = Cx \tag{A.7}$$

where $x(t) \in \mathcal{X} \subset \mathbb{R}^n$, $u(t) = (u_1(t), \ldots, u_m(t)) \in \mathcal{U}$ and open subset of $\mathbb{R}^m$, and $y(t) \in \mathcal{Y} \subset \mathbb{R}^l$. $A(u)$ is a $n \times n$ matrix which is considered to be analytic with respect to u.

System (A.7) is observable if and only if for every pair of initial states, (x_1^0,x_2^0), $x_1^0 \neq x_2^0$, there exists an admissible control $u : [0, T] \to \mathcal{U}$ and a time instant $t \in [0, T]$ such that $y(x_1^0, u, t) \neq y(x_2^0, u, t)$, where $y(x_1^0, u, t) = Cx_1(t)$, and $x_1(t)$ is the unique trajectory of (A.7) such that $x_1(0) = x_1^0$. If such an input u exists, it is called to distinguish (x_1^0,x_2^0). An input $u : [0, T] \to \mathcal{U}$, which distinguishes every (x_1^0,x_2^0), $x_1^0 \neq x_2^0$ is said to be universal on $[0, T]$.

The observation space, $\mathcal{O}(\mathcal{C})$, of a system described by (A.7) is defined as the smallest vector space containing each output function $c_1 x, \ldots, c_l x$ and being closed under the Lie derivative L_X, where X stands for the vector fields $A(u)x$, with $u \in \mathcal{U}$. The Lie derivative is in this case defined as $L_X f(x) = \sum_{i=1}^{n} \frac{\partial f}{\partial x_i}(x_1, \ldots x_n) X(x_1, \ldots x_n)$, where $f(x)$ is a function, $x = (x_1, \ldots x_n) \in \mathbb{R}^n$, and $X(x)$ is a vector field. A simple calculation shows that $\mathcal{O}(\mathcal{C})$ is the linear vector space (over $\mathbb{R}$) spanned by the family of linear functions $\{c_1 x, \ldots, c_l x\} \cup \{c_i A(u_1) \ldots A(u_r)x;\ i = 1, r \geq 1, \text{ and } u_1, \ldots, u_r \in \mathcal{U}\}$. Hence $\dim \mathcal{O}(\mathcal{C}) \leq n$. Set $d\mathcal{O}(\mathcal{C}) = \{d\tau;\ \tau \in \mathcal{O}(\mathcal{C})\}$, where $d\tau$ is the standard differential map: $d\tau(x) = (\frac{\partial \tau}{\partial x_1}, \ldots, \frac{\partial \tau}{\partial x_n})$. Clearly, $d\mathcal{O}(\mathcal{C})$ is the real vector space spanned by $\{c_1, \ldots, c_l\} \cup \{c_i A(u_1) \ldots A(u_r);\ i = 1, r \geq 1, \text{ and } u_1, \ldots, u_r \in \mathcal{U}\}$. It is also called the *observability* subspace. Notice that $\dim \mathcal{O}(\mathcal{C}) = \dim d\mathcal{O}(\mathcal{C}) = k_o$. This space allows one to define a geometric notion of observability, namely the rank observability condition. System (A.7) is observable in the sense of rank if $\dim d\mathcal{O}(\mathcal{C}) = n$ holds globally. For linear systems this is equivalent to the Kalman observability rank condition. Similarly, the observability rank condition is satisfied for a state-affine system if and only if it

is observable (Hammouri *et al.* (1998)). In the case that $\dim d\mathcal{O}(\mathcal{C}) = k_o < n$, i.e. $d\mathcal{O}(\mathcal{C})$ describes a k_o-dimensional subspace of $\mathbb{R}^n$, set $\Delta = Ker d\mathcal{O}(\mathcal{C})$. Then Δ describes a $(n - k_o)$-dimensional subspace of $\mathbb{R}^n$, also referred to as *unobservability* subspace. This subspace can also be considered as the orthogonal space (annihilator) of $d\mathcal{O}(\mathcal{C})$ in $\mathbb{R}^n$ ($\Delta = (d\mathcal{O}(\mathcal{C}))^{\perp}$).

A.8 Regular point of a distribution

In Isidori (1995) the following explanation for a regular point of a distribution is given in section 1.3:

A distribution Δ, defined on an open set $\mathcal{X}$, is *nonsingular* if there exists an integer d such that for the dimension of the distribution the condition

$$dim\,(\Delta(x)) = d$$

holds for all x in $\mathcal{U}$. Hence, a distribution is regular if and only if it has constant dimension.

A point x_0 of $\mathcal{X}$ is said to be a *regular* point of a distribution Δ, if there exists a neighborhood $\mathcal{N}_0$ of x_0, where $\mathcal{N}_0 \subset \mathcal{X}$, with the property that Δ is nonsingular on $\mathcal{N}_0$. Each point of $\mathcal{X}$ which is not a regular point is said to be a *point of singularity*.

Appendix B

Technical data of ship propulsion system

The ship propulsion benchmark provides two different simulation models. In this thesis the simulation model of the propulsion system with one engine and one propeller has been used. It has been designed with the help of real data from a ferry with a length of $147.2\ m$ and a displacement of $12.840\ m^3$ (fully loaded). In this appendix the parameters used in the simulation model are presented as they are given in Izadi-Zamanabadi and Blanke (1998); Izadi-Zamanabadi (1999).

B.1 Disturbances

Two disturbance sources are considered to simulate the friction torque of the shaft and the external forces (hull friction, waves, and wind):

Source	**Name**	**Value**
Q_f	friction torque	$0.05 * Q_{eng,max}$
T_{ext}	external force	$0.1 * T_{max}$

Table B.1: Disturbances.

B.2 Ship parameters

This section describes the ship parameters as they are used in the simulation model:

Parameter	Value	Description	Unit
I_m	$0.25 \cdot 10^6$	inertia	kg m^2
m	13.282	weight (fully loaded)	tons
m	10.359	weight (unloaded)	tons
D	6.123	propeller diameter	m
ρ	1025	water density	kg/ m^3
N	6	number of cylinders	-
k_t	0.15	pitch angle control gain	-
k_y	$1.137 \cdot 10^6$	engine gain	Nm
k_r	0.2211	governor gain	$rad^{-1}s$
K	226	anti-windup gain	-
τ_i	5	time cons. in the PI	s
U_{max}	9.7	max. ship speed	m/s
n_{max}	120	max. shaft speed	RPM
$V_{a,max}$	8.54	max. advanced speed	m/s
$Q_{eng,max}$	1137	max. torque (motor)	kNm
$T_{prop,max}$	889.8	max. developed thrust	kN
$Q_{prop,max}$	1063	max. developed torque	kNm
$X_{\dot{U}}$	0	added mass in surge	kg

Table B.2: Ship parameters.

B.3 Saturation & limitations

In the simulation model the following limitations and saturations have been considered:

Paramater	Value	Description	Unit
$\dot{\theta}_{max}$	0.2	max limit on pitch rate	-
$\dot{\theta}_{min}$	-0.2	min limit on pitch angle	-
θ_{max}	1	max limit on pitch angle	-
θ_{min}	-0.7	min limit on pitch angle	-
$n_{max,a}$	120	max allowed shaft speed.	RPM
Y_{lb}	0	lower bound for fuel index	-
Y_{ub}	1	upper bound for fuel index	-
k_f	0.05	gain in overload controller	-
k_b	1	gain in overload controller	-
ϵ	0.05	threshold in overload contr.	-
θ_{min}	-0.7	min limit on pitch angle	-
$n_{max,a}$	120	max allowed shaft speed.	RPM
Y_{lb}	0	lower bound for fuel index	-

Table B.3: Saturation & limitations.

B.4 Measurement noise

Measurement noise has been added to make the simulation model realistic. The noise on the measurements is considered to be white and Gaussian having a zero mean and has been generated and added as follows:

Signal	**Name**	**Standard deviation**
ν_U	ship speed	$0.01 * U_{max}(9.7m/s)$
ν_n	shaft speed	$0.005 * n_{max}(124RPM)$
ν_θ	propeller pitch	$0.0425 * \theta_{max}(1)$
ν_Y	fuel index	$0.005 * Y_{max}(1)$

Table B.4: Measurement noise.

Appendix C

Application of the geometric approach to the ship benchmark

The detailed calculations for the application of the geometric approach to the ship propulsion benchmark are described in this chapter. Each section handles one group of FPRGs as defined in Section 4.2.2.

C.1 Complete system with controllers and disturbances

Calculations for FPRG 1:

$$\nu^{new} = \Delta k_y Y \quad \text{and} \quad w^{new} = (\dot{\Delta n}_{sensor}\ \dot{\Delta\theta}_{sensor}\ \dot{\Delta\theta}_{inc}\ T_{ext}\ Q_f)^T$$

$$P^1 = span\left\{ \begin{pmatrix} 0\\0\\0\\0\\0\\1\\0 \end{pmatrix}, \begin{pmatrix} 0\\0\\0\\0\\0\\0\\1 \end{pmatrix}, \begin{pmatrix} 0\\0\\0\\1\\0\\0\\0 \end{pmatrix}, \begin{pmatrix} 0\\0\\\frac{1}{m}\\0\\0\\0\\0 \end{pmatrix}, \begin{pmatrix} 0\\-\frac{1}{I_m}\\0\\0\\0\\0\\0 \end{pmatrix} \right\}$$

Following the algorithm (3.59) and (3.60) to calculate $\Sigma_*^{P^1}$ starts with:

$$S_0^1 = \overline{P^1} = P^1 \qquad \text{(as } P^1 \text{ is constant)}$$

Furthermore:

$$h(x) = \begin{pmatrix} h_1(x) & h_2(x) & h_3(x) \end{pmatrix}^T = \begin{pmatrix} n + x_{\Delta n} & \theta + x_{\Delta\theta} & U \end{pmatrix}^T$$

$$\Rightarrow \begin{cases} dh_1 = (0\ 1\ 0\ 0\ 0\ 1\ 0) \\ dh_2 = (0\ 0\ 0\ 1\ 0\ 0\ 1) \\ dh_3 = (0\ 0\ 1\ 0\ 0\ 0\ 0) \end{cases} \quad \text{as} \quad x = (Q_{eng}\ n\ U\ \theta\ Y_i\ x_{\Delta n}\ x_{\Delta\theta})^T$$

$$\Rightarrow Ker\{dh\} = span\left\{ \begin{pmatrix} 1 \\ 0 \\ 0 \\ 0 \\ 0 \\ 0 \\ 0 \end{pmatrix}, \begin{pmatrix} 0 \\ -1 \\ 0 \\ 0 \\ 0 \\ 1 \\ 0 \end{pmatrix}, \begin{pmatrix} 0 \\ 0 \\ 0 \\ -1 \\ 0 \\ 0 \\ 1 \end{pmatrix}, \begin{pmatrix} 0 \\ 0 \\ 0 \\ 0 \\ 1 \\ 0 \\ 0 \end{pmatrix} \right\}.$$

$$\Rightarrow S_0^1 \cap Ker\{dh\} = span\left\{(0\ -1\ 0\ 0\ 0\ 1\ 0)^T, (0\ 0\ 0\ -1\ 0\ 0\ 1)^T\right\}.$$

The next step of the algorithm (3.60) leads to:

$$S_{k+1}^1 = \overline{S}_k^1 + \sum_{i=0}^{m}[g_i, \overline{S}_k^1 \cap Ker\{dh\}] \Rightarrow S_1^1 = \overline{S}_0^1 + \sum_{i=0}^{2}[g_i, \overline{S}_0^1 \cap Ker\{dh\}]$$

$$\Rightarrow S_1^1 = S_0^1 + \sum_{i=0}^{2}[g_i, S_0^1 \cap Ker\{dh\}] \Rightarrow S_1^1 = S_0^1 + [f, S_0^1 \cap Ker\{dh\}]$$

as $g_1(x)$, $g_2(x)$, and $S_0^1 \cap Ker\{dh\}$ are constant.

$$[f, S_0^1 \cap Ker\{dh\}] = -\frac{\partial f}{\partial x}\left(S_0^1 \cap Ker\{dh\}\right), \text{ as } S_0^1 \cap Ker\{dh\} \text{ is constant.}$$

$$[f, (0\ -1\ 0\ 0\ 0\ 1\ 0)^T] = (0\ -\frac{1}{I_m}[2Q_{|n|n}n\theta + Q_{|n|V_a}(1-w)U\theta]$$
$$\frac{1-t_T}{m}[2T_{|n|n}n\theta + T_{|n|V_a}(1-w)U]\ 0\ 0\ 0\ 0)^T$$

and

$$[f,(0\ 0\ 0\ -1\ 0\ 0\ 1)^T] = (0\ -\frac{1}{I_m}[Q_{|n|n}n^2 + Q_{|n|V_a}(1-w)nU] \quad \frac{1-t_T}{m}T_{|n|n}n^2\ 0\ 0\ 0\ 0)^T$$

as

$$\frac{\partial f}{\partial x} = \begin{pmatrix} -\frac{1}{\tau_c} & -\frac{k_y k_r}{\tau_c} & 0 \\ \frac{1}{I_m} & -\frac{1}{I_m}[2Q_{|n|n}n\theta + Q_{|n|V_a}V_a\theta] & -\frac{1}{I_m}Q_{|n|V_a}(1-w)n\theta \\ 0 & \frac{1-t_T}{m}[2T_{|n|n}n\theta + T_{|n|V_a}V_a] & \frac{1}{m}\frac{\partial R(U)}{\partial U} + \frac{1-t_T}{m}T_{|n|V_a}(1-w)n \\ 0 & 0 & 0 \\ 0 & -\frac{k_r}{\tau_i} & 0 \\ 0 & 0 & 0 \\ 0 & 0 & 0 \end{pmatrix}$$

$$\begin{pmatrix} 0 & \frac{k_y}{\tau_c} & -\frac{k_y k_r}{\tau_i} & 0 \\ -\frac{1}{I_m}[Q_{|n|n}n^2 + Q_{|n|V_a}nV_a] & 0 & 0 & 0 \\ \frac{1-t_T}{m}T_{|n|n}n^2 & 0 & 0 & 0 \\ -k_t & 0 & 0 & -k_t \\ 0 & 0 & -\frac{k_r}{\tau_i} & 0 \\ 0 & 0 & 0 & 0 \\ 0 & 0 & 0 & 0 \end{pmatrix}$$

where $V_a = (1-w)U$.

$$\begin{aligned} \Rightarrow \quad & [f, S_0^1 \cap Ker\{dh\}] \subset S_0^1 \\ \Rightarrow \quad & S_1^1 = S_0^1 + [f, S_0^1 \cap Ker\{dh\}] = S_0^1 \\ \Rightarrow \quad & k^* = 0 \qquad \Rightarrow \qquad \underline{\Sigma_*^{P^1} = P^1} \end{aligned}$$

$\Sigma_*^{P^1}$ is well-defined (as equation (3.61) holds for $k^* = 0$) and nonsingular (as it is constant). Hence, its annihilator $(\Sigma_*^{P^1})^\perp$ is locally spanned by exact differentials (because $\Sigma_*^{P^1}$ is by construction involutive). It can also be seen above that $\Sigma_*^{P^1} \cap Ker\{dh\}$ is a smooth distribution. Hence, $(\Sigma_*^{P^1})^\perp$ is the maximal (in the sense of codistribution inclusion) conditioned invariant codistribution which is locally spanned by exact differentials and contained in $P^{1\perp}$ (according to DePersis and Isidori (2000)).

Next step in the procedure (described on page 65) is to calculate the involutive conditioned invariant distribution Q^1 (unobservability distribution):

$$Q^1 = (\text{o.c.a.}((\Sigma_*^{P^1})^\perp))^\perp = (\text{o.c.a.}(P^{1\perp}))^\perp$$

Applying the observability codistribution algorithm (o.c.a.) (see page 43), in order to calculate o.c.a.$(P^{1\perp})$, starts with:

$$Q_0 = P^{1\perp} \cap span\{dh\}$$

where

$$\begin{aligned} P^{1\perp} &= span\left\{(1\ 0\ 0\ 0\ 0\ 0\ 0), (0\ 0\ 0\ 0\ 1\ 0\ 0)\right\} \\ span\{dh\} &= span\left\{(0\ 1\ 0\ 0\ 0\ 1\ 0), (0\ 0\ 0\ 1\ 0\ 0\ 1), (0\ 0\ 1\ 0\ 0\ 0\ 0)\right\}. \end{aligned}$$

Hence, it is easy to see that $Q_0 = 0$. The next step of the algorithm:

$$Q_{k+1} = P^{1\perp} \cap \left(\sum_{i=0}^{3} L_{g_i} Q_k + span\{dh\} \right)$$

leads to:

$$\begin{aligned} Q_1 = P^{1\perp} \cap \left(\sum_{i=0}^{3} L_{g_i} Q_0 + span\{dh\} \right) &= P^{1\perp} \cap span\{dh\} = Q_0 = 0 \\ \Rightarrow \quad & \text{o.c.a.}(P^{1\perp}) = 0 \\ \Rightarrow \quad & \underline{Q^1 = (\text{o.c.a.}(P^{1\perp}))^\perp = \mathbb{R}^7} \\ \Rightarrow \quad & \underline{l(x)^{new} = \left(\tfrac{1}{\tau_c}\ 0\ 0\ 0\ 0\ 0\ 0 \right)^T \in Q^1} \end{aligned}$$

As a result it can be seen that the FPRG 1 is not solvable in the geometric sense described in Chapter 3 . The calculations for the FPRG 2 - FPRG 4 are similar and therefore omitted here.

C.2 Complete system with controllers and without disturbances

Calculations for FPRG 5:

$$\nu^{new} = \Delta k_y Y \quad \text{and} \quad w^{new} = (\dot{\Delta n}_{sensor}\ \dot{\Delta\theta}_{sensor}\ \dot{\Delta\theta}_{inc})^T$$

$$P^5 = span\left\{(0\ 0\ 0\ 0\ 0\ 0\ 1)^T, (0\ 0\ 0\ 0\ 0\ 1\ 0)^T, (0\ 0\ 0\ 1\ 0\ 0\ 0)^T\right\}$$

Now the algorithm (3.59) and (3.60) is used to calculate $\Sigma_*^{P^5}$:

$$S_0^5 = \overline{P^5} = P^5 \qquad \text{(as } P^5 \text{ is constant)}$$
$$\Rightarrow S_0^5 \cap Ker\{dh\} = span\left\{(0\ 0\ 0\ -1\ 0\ 0\ 1)^T\right\}.$$

$$S_{k+1}^5 = \overline{S}_k^5 + \sum_{i=0}^{m}[g_i, \overline{S}_k^5 \cap Ker\{dh\}] \ \Rightarrow\ S_1^5 = \overline{S}_0^5 + \sum_{i=0}^{2}[g_i, \overline{S}_0^5 \cap Ker\{dh\}]$$
$$\Rightarrow\ S_1^5 = S_0^5 + \sum_{i=0}^{2}[g_i, S_0^5 \cap Ker\{dh\}] \ \Rightarrow\ S_1^5 = S_0^5 + [f, S_0^5 \cap Ker\{dh\}]$$

as $g_1(x)$, $g_2(x)$, and $S_0^5 \cap Ker\{dh\}$ are constant.

$[f, S_0^5 \cap Ker\{dh\}] = -\dfrac{\partial f}{\partial x}\left(S_0^5 \cap Ker\{dh\}\right)$, as $S_0^5 \cap Ker\{dh\}$ is constant.

$$[f, (0\ 0\ 0\ -1\ 0\ 0\ 1)^T] = (0\ -\frac{1}{I_m}[Q_{|n|n}n^2 + Q_{|n|V_a}(1-w)nU]\ \ \frac{1-t_T}{m}T_{|n|n}n^2\ 0\ 0\ 0\ 0)^T$$

$$\Rightarrow S_1^5 = span\left\{\begin{pmatrix}0\\0\\0\\0\\0\\1\\0\end{pmatrix}, \begin{pmatrix}0\\0\\0\\0\\0\\0\\1\end{pmatrix}, \begin{pmatrix}0\\0\\0\\1\\0\\0\\0\end{pmatrix}, \begin{pmatrix}0\\-\frac{1}{I_m}[Q_{|n|n}n^2 + Q_{|n|V_a}nV_a]\\\frac{1-t_T}{m}T_{|n|n}n^2\\0\\0\\0\\0\end{pmatrix}\right\}$$

where $V_a = (1-w)U$.

$$\Rightarrow \qquad S_0^5 \neq S_1^5 \quad \Rightarrow \qquad k^* \neq 0$$

$$S_2^5 = \overline{S}_1^5 + \sum_{i=0}^{2}[g_i, \overline{S}_1^5 \cap Ker\{dh\}] = S_1^5 + [f, S_1^5 \cap Ker\{dh\}]$$

as $g_1(x)$, $g_2(x)$, and $S_0^1 \cap Ker\{dh\}$ are constant. It can easily be checked that:

$$S_1^5 \cap Ker\{dh\} = S_0^5 \cap Ker\{dh\} = span\left\{(0\ 0\ 0\ -1\ 0\ 0\ 1)^T\right\}.$$

$$\Rightarrow \qquad S_2^5 = S_1^5 + [f, S_0^5 \cap Ker\{dh\}] \qquad \Rightarrow \qquad S_2^5 = S_1^5$$
$$\Rightarrow \qquad k^* = 1 \qquad \Rightarrow \qquad \underline{\Sigma_*^{P^5} = S_1^5}$$

$\Sigma_*^{P^5}$ is well-defined (as equation (3.61) holds for $k^* = 1$) and nonsingular as long as the shaft speed is not zero ($\mathbf{n \neq 0}$). It can be seen above that $\Sigma_*^{P^5} \cap Ker\{dh\}$ is a smooth distribution. Hence, $(\Sigma_*^{P^5})^\perp$ is the maximal (in the sense of codistribution inclusion) conditioned invariant codistribution which is locally spanned by exact differentials and contained in $P^{5\perp}$ when $n \neq 0$ (according to DePersis and Isidori (2000)).

Next step in the procedure (described on page 65) is to calculate the involutive conditioned invariant distribution Q^5 (unobservability distribution):

$$Q^5 = (\text{o.c.a.}((\Sigma_*^{P^5})^\perp))^\perp = (\text{o.c.a.}(S_1^{5\perp}))^\perp$$

Applying the observability codistribution algorithm (o.c.a.) (see page 43), in order to calculate o.c.a.$(S_1^{5\perp})$, starts with:

$$Q_0 = S_1^{5\perp} \cap span\{dh\}$$

$$S_1^{5\perp} = span\{(1\ 0\ 0\ 0\ 0\ 0\ 0), (0\ \frac{1-t_T}{m}\, T_{|n|n} n^2 \quad \frac{1}{I_m}[Q_{|n|n} n^2 + Q_{|n|V_a}(1-w)nU]\ 0\ 0\ 0\ 0)^T, (0\ 0\ 0\ 0\ 1\ 0\ 0)\}$$

$$span\{dh\} = span\left\{(0\ 1\ 0\ 0\ 0\ 1\ 0), (0\ 0\ 0\ 1\ 0\ 0\ 1), (0\ 0\ 1\ 0\ 0\ 0\ 0)\right\}.$$

Hence, it is easy to see that $Q_0 = 0$ (as $n > 0$). The next step in the algorithm:

$$Q_{k+1} = S_1^{5\perp} \cap \left(\sum_{i=0}^{3} L_{g_i} Q_k + span\{dh\} \right)$$

leads to:

$$\begin{aligned} Q_1 = S_1^{5\perp} \cap \left(\sum_{i=0}^{3} L_{g_i} Q_0 + span\{dh\} \right) &= S_1^{5\perp} \cap span\{dh\} = Q_0 = 0 \\ \Rightarrow \quad & \text{o.c.a.}(S_1^{5\perp}) = 0 \\ \Rightarrow \quad & \underline{Q^5 = (\text{o.c.a.}(S_1^{5\perp}))^{\perp} = \mathbb{R}^7} \\ \Rightarrow \quad & \underline{l(x)^{new} = \left(\tfrac{1}{\tau_c}\ 0\ 0\ 0\ 0\ 0\ 0 \right)^T \in Q^5} \end{aligned}$$

As a result it can be seen that the FPRG 5 is not solvable. The calculations for the FPRG 6 - FPRG 8 are very similar and therefore omitted here.

C.3 Pitch loop with pitch controller

Calculations for FPRG 9:

$$\nu^{new} = \dot{\Delta\theta}_{sensor} \quad \text{and} \quad w^{new} = \Delta\dot{\theta}_{inc}$$

$$P^9 = span\left\{(1\ 0)^T\right\}$$

Now the algorithm (3.59) and (3.60) is used to calculate $\Sigma_*^{P^9}$:

$$S_0^9 = \overline{P^9} = P^9 \qquad (\text{as } P^9 \text{ is constant})$$

$$\begin{aligned} h(x) = (\theta + x_{\Delta\theta}) \quad &\Rightarrow\ dh = (1\ 1) \quad \Rightarrow\ Ker\{dh\} = span\left\{(-1\ 1)^T\right\} \\ &\Rightarrow\ S_0^9 \cap Ker\{dh\} = 0 \end{aligned}$$

$$
\begin{aligned}
S^9_{k+1} &= \overline{S}^9_k + \sum_{i=0}^{m}[g_i, \overline{S}^9_k \cap Ker\{dh\}] \\
&\Rightarrow\ S^9_1 = S^9_0 + \sum_{i=0}^{2}[g_i, S^9_0 \cap Ker\{dh\}] \\
&\Rightarrow\ S^9_0 = S^9_1 \quad \Rightarrow\ k^* = 0 \quad \text{as} \quad S^9_0 \cap Ker\{dh\} = 0. \\
&\Rightarrow\ \underline{\Sigma^{P^9}_* = S^9_0 = P^9 = span\left\{(\,1\ 0\,)^T\right\}}
\end{aligned}
$$

$\Sigma^{P^9}_*$ is well-defined (as equation (3.61) holds for $k^* = 0$) and nonsingular. Hence,its annihilator $(\Sigma^{P^9}_*)^\perp$ is locally spanned by exact differentials (because $\Sigma^{P^9}_*$ is by construction involutive). It can be seen above that $\Sigma^{P^9}_* \cap Ker\{dh\} = 0$ is a smooth distribution. Hence, $(\Sigma^{P^9}_*)^\perp$ is the maximal (in the sense of codistribution inclusion) conditioned invariant codistribution which is locally spanned by exact differentials and contained in ${P^9}^\perp$ (according to DePersis and Isidori (2000)).

Next step in the procedure (described on page 65) is to calculate the involutive conditioned invariant distribution Q^9 (unobservability distribution):

$$Q^9 = (\text{o.c.a.}((\Sigma^{P^9}_*)^\perp))^\perp = (\text{o.c.a.}({P^9}^\perp))^\perp$$

Applying the observability codistribution algorithm (o.c.a.) (see page 43), in order to calculate o.c.a.$({P^9}^\perp)$, starts with:

$$Q_0 = {P^9}^\perp \cap span\{dh\}$$

$${P^9}^\perp = span\,\{(\,0\ 1\,)\} \quad \text{and} \quad span\{dh\} = span\{(\,1\ 1\,)\}$$

hence, it is easy to see that $Q_0 = 0$.

$$
\begin{aligned}
&\Rightarrow \quad \text{o.c.a.}({P^9}^\perp) = 0 \\
&\Rightarrow \quad \underline{Q^9 = (\text{o.c.a.}({P^9}^\perp))^\perp = \mathbb{R}^2} \\
&\Rightarrow \quad \underline{l(x)^{new} = (\,0\ 1\,)^T \in Q^9}
\end{aligned}
$$

As a result it can be seen that the FPRG 9 is not solvable. The calculations for the FPRG 10 are very similar and therefore omitted here.

C.4 Shaft speed loop with governor and disturbances

Calculations for FPRG 11:

$$\nu^{new} = \Delta k_y Y \quad \text{and} \quad w^{new} = (\dot{\Delta n}_{sensor}\ T_{ext}\ Q_f)^T$$

$$P^{11} = span\left\{(0\ 0\ 0\ 0\ 1), (0\ 0\ \frac{1}{m}\ 0\ 0), (0\ -\frac{1}{I_m}\ 0\ 0\ 0)\right\}$$

Now the algorithm (3.59) and (3.60) is used to calculate $\Sigma_*^{P^{11}}$:

$$S_0^{11} = \overline{P^{11}} = P^{11} \qquad \text{(as } P^{11} \text{ is constant)}$$

$$h(x) = \begin{pmatrix} n + x_{\Delta n} & U \end{pmatrix}^T \Rightarrow \begin{cases} dh_1 = (0\ 1\ 0\ 0\ 1) \\ dh_2 = (0\ 0\ 1\ 0\ 0) \end{cases}$$

$$\Rightarrow Ker\{dh\} = span\left\{(1\ 0\ 0\ 0\ 0)^T, (0\ -1\ 0\ 0\ 1)^T, (0\ 0\ 0\ 1\ 0)^T\right\}$$

$$\Rightarrow S_0^{11} \cap Ker\{dh\} = span\left\{(0\ -1\ 0\ 0\ 1)^T\right\}$$

$$S_{k+1}^{11} = \overline{S}_k^{11} + \sum_{i=0}^{m}[g_i, \overline{S}_k^{11} \cap Ker\{dh\}]$$

$$\Rightarrow S_1^{11} = \overline{S}_0^{11} + \sum_{i=0}^{2}[g_i, \overline{S}_0^{11} \cap Ker\{dh\}]$$

$$\Rightarrow S_1^{11} = S_0^{11} + [f, S_0^{11} \cap Ker\{dh\}] + [g_2, S_0^{11} \cap Ker\{dh\}]$$

as $g_1(x)$, S_0^{11}, and $S_0^{11} \cap Ker\{dh\}$ are constant.

$$[f, S_0^{11} \cap Ker\{dh\}] = -\frac{\partial f}{\partial x}\left(S_0^{11} \cap Ker\{dh\}\right)$$

, as $S_0^{11} \cap Ker\{dh\}$ is constant.

$$[f, (0\ -1\ 0\ 0\ 1)^T] = (0\ 0\ -\frac{1 - t_T}{m} T_{|n|V_a}(1 - w)U\ 0\ 0)^T$$

,as

$$\frac{\partial f}{\partial x} = \begin{pmatrix} -\frac{1}{\tau_c} & -\frac{k_y\, k_r}{\tau_c} & 0 & \frac{k_y}{\tau_c} & -\frac{k_y\, k_r}{\tau_c} \\ \frac{1}{I_m} & 0 & 0 & 0 & 0 \\ 0 & \frac{1-t_T}{m}\, T_{|n|V_a} V_a & \frac{1}{m}\frac{\partial R(U)}{\partial U} + \frac{1-t_T}{m}\, T_{|n|V_a} n(1-w) & 0 & 0 \\ 0 & -\frac{k_r}{\tau_i} & 0 & 0 & -\frac{k_r}{\tau_i} \\ 0 & 0 & 0 & 0 & 0 \end{pmatrix}.$$

$$[g_2, (0\ -1\ 0\ 0\ 1)^T] = (0\ \frac{1}{I_m}[2Q_{|n|n} n + Q_{|n|V_a}(1-w)U] - \frac{1-t_T}{m}\, 2T_{|n|n} n\ 0\ 0)^T$$

,as

$$\frac{\partial g_2}{\partial x} = \begin{pmatrix} 0 & 0 & 0 & 0 & 0 \\ 0 & -\frac{1}{I_m}[2Q_{|n|n} n + Q_{|n|V_a}(1-w)U] & -\frac{1}{I_m} Q_{|n|V_a}(1-w) n & 0 & 0 \\ 0 & \frac{1-t_T}{m}\, 2T_{|n|n} n & 0 & 0 & 0 \\ 0 & 0 & 0 & 0 & 0 \\ 0 & 0 & 0 & 0 & 0 \end{pmatrix}.$$

$$\begin{aligned} &\Rightarrow \quad [g_i, (0\ -1\ 0\ 0\ 1)^T] \subset S_0^{11} \\ &\Rightarrow \quad S_1^{11} = S_0^{11} \\ &\Rightarrow \quad k^* = 0 \quad \Rightarrow \quad \underline{\Sigma_*^{P^{11}} = P^{11}} \end{aligned}$$

$\Sigma_*^{P^{11}}$ is well-defined (as equation (3.61) holds for $k^* = 0$) and nonsingular (as it is constant). Hence, its annihilator $(\Sigma_*^{P^{11}})^\perp$ is locally spanned by exact differentials (because $\Sigma_*^{P^{11}}$ is by construction involutive). It can also be seen above that $\Sigma_*^{P^{11}} \cap Ker\{dh\}$ is a smooth distribution. Hence, $(\Sigma_*^{P^{11}})^\perp$ is the maximal (in the sense of codistribution inclusion) conditioned invariant codistribution which is locally spanned by exact differentials and contained in $P^{11\perp}$ (according to DePersis and Isidori (2000)).

Next step in the procedure (described on page 65) is to calculate the involutive conditioned invariant distribution Q^{11} (unobservability distribution):

$$Q^{11} = (\text{o.c.a.}((\Sigma_*^{P^{11}})^\perp))^\perp = (\text{o.c.a.}(P^{11\perp}))^\perp$$

Applying the observability codistribution algorithm (o.c.a.) (see page 43), in order to calculate o.c.a.$(P^{11\perp})$, starts with:

$$Q_0 = P^{11\perp} \cap span\{dh\}$$

$$P^{11\perp} = span\left\{(1\ 0\ 0\ 0\ 0), (0\ 0\ 0\ 1\ 0)\right\}$$
$$span\{dh\} = span\left\{(0\ 1\ 0\ 0\ 1), (0\ 0\ 1\ 0\ 0)\right\}$$

hence, it is easy to see that $Q_0 = 0$. The next step in the algorithm:

$$Q_{k+1} = P^{11\perp} \cap \left(\sum_{i=0}^{3} L_{g_i} Q_k + span\{dh\}\right)$$

leads to:

$$Q_1 = P^{11\perp} \cap \left(\sum_{i=0}^{3} L_{g_i} Q_0 + span\{dh\}\right) = P^{11\perp} \cap span\{dh\} = Q_0 = 0$$

$$\Rightarrow \quad \text{o.c.a.}(P^{11\perp}) = 0$$

$$\Rightarrow \quad \underline{Q^{11} = (\text{o.c.a.}(P^{11\perp}))^{\perp} = \mathbb{R}^5}$$

$$\Rightarrow \quad \underline{l(x)^{new} = \left(\ \tfrac{1}{\tau_c}\ 0\ 0\ 0\ 0\right)^T \in Q^{11}}$$

As a result it can be seen that the FPRG 11 is not solvable. The calculations for the FPRG 12 are very similar and therefore omitted here.

C.5 Shaft speed loop with governor and without disturbances

Calculations for FPRG 13:

$$\nu^{new} = \Delta k_y Y \quad \text{and} \quad w^{new} = \dot{\Delta} n_{sensor}^T$$

$$P^{13} = span\left\{(0\ 0\ 0\ 0\ 1)^T\right\}$$

Now the algorithm (3.59) and (3.60) is used to calculate $\Sigma_*^{P^{13}}$:

$$\begin{aligned} S_0^{13} &= \overline{P^{13}} = P^{13} \qquad \text{(as } P^{13} \text{ is constant)} \\ &\Rightarrow\ S_0^{13} \cap Ker\{dh\} = 0 \end{aligned}$$

$$\begin{aligned} S_{k+1}^{13} &= \overline{S}_k^{13} + \sum_{i=0}^{m} [g_i, \overline{S}_k^{13} \cap Ker\{dh\}] \\ &\Rightarrow\ S_1^{13} = S_0^{13} + \sum_{i=0}^{2} [g_i, S_0^{13} \cap Ker\{dh\}] \\ &\Rightarrow\ S_1^{13} = S_0^{13} \\ &\Rightarrow\ k^* = 0 \qquad \Rightarrow\ \underline{\Sigma_*^{P^{13}} = P^{13}} \end{aligned}$$

$\Sigma_*^{P^{13}}$ is well-defined (as equation (3.61) holds for $k^* = 0$) and nonsingular (as it is constant). Hence, its annihilator $(\Sigma_*^{P^{13}})^\perp$ is locally spanned by exact differentials (because $\Sigma_*^{P^{13}}$ is by construction involutive). It can also be seen above that $\Sigma_*^{P^{13}} \cap Ker\{dh\}$ is a smooth distribution. Hence, $(\Sigma_*^{P^{13}})^\perp$ is the maximal (in the sense of codistribution inclusion) conditioned invariant codistribution which is locally spanned by exact differentials and contained in $P^{13\perp}$ (according to DePersis and Isidori (2000)).

Next step in the procedure (described on page 65) is to calculate the involutive conditioned invariant distribution Q^{13} (unobservability distribution):

$$Q^{13} = (\text{o.c.a.}((\Sigma_*^{P^{13}})^\perp))^\perp = (\text{o.c.a.}(P^{13\perp}))^\perp$$

Applying the observability codistribution algorithm (o.c.a.) (see page 43), in order to calculate o.c.a.$(P^{13\perp})$, starts with:

$$Q_0 = P^{13\perp} \cap span\{dh\}$$

$$\begin{aligned} P^{13\perp} &= span\,\{(1\ 0\ 0\ 0\ 0), (0\ 1\ 0\ 0\ 0), (0\ 0\ 1\ 0\ 0), (0\ 0\ 0\ 1\ 0)\} \\ span\{dh\} &= span\,\{(0\ 1\ 0\ 0\ 1), (0\ 0\ 1\ 0\ 0)\} \\ \Rightarrow \qquad Q_0 &= span\,\{(0\ 0\ 1\ 0\ 0)\} \end{aligned}$$

The next step in the algorithm:

$$Q_{k+1} = P^{13^{\perp}} \cap \left(\sum_{i=0}^{3} L_{g_i} Q_k + span\{dh\} \right)$$

leads to:

$$Q_1 = P^{13^{\perp}} \cap \left(\sum_{i=0}^{3} L_{g_i}(0\ 0\ 1\ 0\ 0) + span\{dh\} \right)$$

Calculating $L_{g_i}(0\ 0\ 1\ 0\ 0)$:

$$\begin{aligned}
&L_{g_0}(0\ 0\ 1\ 0\ 0) = L_f(0\ 0\ 1\ 0\ 0) = dL_f U \\
&\quad = \left(0\ \frac{1-t_T}{m} T_{|n|V_a}(1-w)U \quad \frac{1}{m}\frac{\partial R(U)}{\partial U} + \frac{1-t_T}{m} T_{|n|V_a} n(1-w)\ 0\ 0 \right) \\
&L_{g_1}(0\ 0\ 1\ 0\ 0) = dL_{g_1} U = 0 \\
&L_{g_2}(0\ 0\ 1\ 0\ 0) = dL_{g_2} U = (0\ \frac{1-t_T}{m}\ 2T_{|n|n} n\ 0\ 0\ 0)
\end{aligned}$$

$$\begin{aligned}
&\Rightarrow \left(\sum_{i=0}^{3} L_{g_i}(0\ 0\ 1\ 0\ 0) + span\{dh\} \right) \\
&\qquad\qquad = span\left\{(0\ 1\ 0\ 0\ 0), (0\ 0\ 1\ 0\ 0), (0\ 0\ 0\ 0\ 1)\right\} \\
&\Rightarrow Q_1 = P^{13^{\perp}} \cap \left(\sum_{i=0}^{3} L_{g_i}(0\ 0\ 1\ 0\ 0) + span\{dh\} \right) \\
&\qquad\qquad = span\left\{(0\ 1\ 0\ 0\ 0), (0\ 0\ 1\ 0\ 0)\right\} \\
&\Rightarrow Q_1 \neq Q_0
\end{aligned}$$

So the next step is:

$$Q_2 = P^{13^{\perp}} \cap \left(\sum_{i=0}^{3} L_{g_i} Q_1 + span\{dh\} \right)$$

Calculating $L_{g_i}(0\ 1\ 0\ 0\ 0)$:

$$L_{g_0}(0\ 1\ 0\ 0\ 0) = L_f(0\ 1\ 0\ 0\ 0) = dL_f n = \left(\frac{1}{I_m}\ 0\ 0\ 0\ 0\right)$$
$$L_{g_1}(0\ 1\ 0\ 0\ 0) = dL_{g_1} n = 0$$
$$L_{g_2}(0\ 1\ 0\ 0\ 0) = dL_{g_2} n = (0\ -\frac{1}{I_m}[2Q_{|n|n}n + Q_{|n|V_a}(1-w)U] - \frac{1}{I_m}Q_{|n|V_a}(1-w)n\ 0\ 0)$$

$$\Rightarrow \left(\sum_{i=0}^{3} L_{g_i} Q_1 + span\{dh\}\right) = span\{(1\ 0\ 0\ 0\ 0), (0\ 1\ 0\ 0\ 0), (0\ 0\ 1\ 0\ 0), (0\ 0\ 0\ 0\ 1)\}$$
$$\Rightarrow Q_2 = P^{13^\perp} \cap \left(\sum_{i=0}^{3} L_{g_i} Q_1 + span\{dh\}\right) = span\{(1\ 0\ 0\ 0\ 0), (0\ 1\ 0\ 0\ 0), (0\ 0\ 1\ 0\ 0)\}$$
$$\Rightarrow Q_2 \neq Q_1$$

Hence, the next step is:

$$Q_3 = P^{13^\perp} \cap \left(\sum_{i=0}^{3} L_{g_i} Q_2 + span\{dh\}\right)$$

Calculating $L_{g_i}(1\ 0\ 0\ 0\ 0)$:

$$L_{g_0}(1\ 0\ 0\ 0\ 0) = L_f(1\ 0\ 0\ 0\ 0) = dL_f Q_{eng} = \left(\left(-\frac{1}{\tau_c}\right)\ \left(-\frac{k_y k_r}{\tau_c}\right)\ 0\ \frac{k_y}{\tau_c}\ \left(-\frac{k_y k_r}{\tau_c}\right)\right)$$
$$L_{g_1}(1\ 0\ 0\ 0\ 0) = dL_{g_1} n = 0$$
$$L_{g_2}(1\ 0\ 0\ 0\ 0) = dL_{g_2} n = 0$$

$$\Rightarrow \left(\sum_{i=0}^{3} L_{g_i} Q_2 + span\{dh\}\right) = \mathbb{R}^5$$

$$\Rightarrow Q_3 = P^{13^\perp} \cap \left(\sum_{i=0}^{3} L_{g_i} Q_1 + span\{dh\}\right) = P^{13^\perp}$$

$$\Rightarrow Q_3 \neq Q_2$$

So the final step is:

$$Q_4 = P^{13^\perp} \cap \left(\sum_{i=0}^{3} L_{g_i} Q_3 + span\{dh\}\right)$$

As $Q_2 \subset Q_3$ and $\left(\sum_{i=0}^{3} L_{g_i} Q_2 + span\{dh\}\right) = \mathbb{R}^5$
it is easy to see that also $\left(\sum_{i=0}^{3} L_{g_i} Q_3 + span\{dh\}\right) = \mathbb{R}^5$.
Hence, $Q_4 = P^{13^\perp} = Q_3$

$$\Rightarrow \quad \text{o.c.a.}(P^{13^\perp}) = P^{13^\perp}$$

$$\Rightarrow \quad \underline{Q^{13} = (\text{o.c.a.}(P^{13^\perp}))^\perp = P^{13} = span\left\{(0\ 0\ 0\ 0\ 1)^T\right\}}$$

$$\Rightarrow \quad \underline{p(x)^{new} \in Q^{13}} \quad \text{and} \quad \underline{l(x)^{new} = \left(\tfrac{1}{\tau_c}\ 0\ 0\ 0\ 0\right)^T \notin Q^{13}}$$

As a result it can be seen that the FPRG 13 might be solvable. The next step is now to obtain a coordinate transformation as described in Theorem 3.11. In the following the procedure described in DePersis and Isidori (2000) (Proposition 3) is applied in order to find such a coordinate transformation.

Checking conditions: As shown above $P^{13^\perp}$ is an observability codistribution. Let n_1 denote the dimension of $P^{13^\perp}$, hence, $n_1 = 4$. $P^{13^\perp}$ is spanned by exact differentials as $P^{13^\perp} = (\Sigma_*^{P^{13}})^\perp$ (see above). $span\{dh\} = span\{(0\ 1\ 0\ 0\ 1), (0\ 0\ 1\ 0\ 0)\}$ is nonsingular as it is constant. Let $l - n_2$ ($l = 2$, number of outputs) denote the dimension of $P^{13^\perp} \cap span\{dh\} = span\{(0\ 0\ 1\ 0\ 0)\}$, hence $n_2 = l - 1 = 2 - 1 = 1$.

Coordinate transformation: After checking the conditions the first step towards the coordinate transformation is to choose a $\Psi_1 : \mathbb{R}^l \rightarrow \mathbb{R}^{l-n_2} = \mathbb{R}^1$ such, that:

$$P^{13^\perp} \cap span\{dh\} = span\{d(\Psi_1 \circ h)\}$$

One possibility to do so is $\Psi_1(y) = h_2(x) = U$:

$$span\{d(\Psi_1 \circ h)\} = span\{d(U)\} = span\{(0\ 0\ 1\ 0\ 0)\} = P^{13^\perp} \cap span\{dh\}$$

Choosing a selection matrix $H_2 = (1\ 0)$ and combining it with Ψ_1 in the following way:

$$y^{new} = \begin{pmatrix} y_1^{new} \\ y_2^{new} \end{pmatrix} = \Psi(y) = \begin{pmatrix} \Psi_1(y) \\ H_2 y \end{pmatrix}, \quad \text{with } \frac{\partial \Psi(y)}{\partial y} = \begin{pmatrix} 0 & 1 \\ 1 & 0 \end{pmatrix} \tag{C.1}$$

gives a local diffeomorphism at y° in $\mathbb{R}^l$, where $y^\circ = h(x^\circ)$ and $x^\circ \in \mathcal{X}$.

The second step is to choose a neighborhood $\mathcal{U}^\circ$ of x° and a function $\Phi_1 : \mathcal{U}^\circ \rightarrow \mathbb{R}^{n_1} = \mathbb{R}^4$ such that $P^{13^\perp} = span\{d\Phi_1\}$ at any point of $\mathcal{U}^\circ$. Here the following Φ_1 is chosen: $\Phi_1(x) = (Q_{eng}\ n\ U\ Y_i)^T$, hence, the following transformation is a local diffeomorphism at x° in $\mathcal{X}$:

$$\Phi(x) = \begin{pmatrix} \Phi_1(x) \\ H_2 h(x) \end{pmatrix} = \begin{pmatrix} x_1^{new} \\ x_2^{new} \end{pmatrix} = \begin{pmatrix} x_{11}^{new} \\ x_{12}^{new} \\ x_{13}^{new} \\ x_{14}^{new} \\ x_2^{new} \end{pmatrix} = \begin{pmatrix} Q_{eng} \\ n \\ U \\ Y_i \\ n + x_{\Delta n} \end{pmatrix} \tag{C.2}$$

where it is easy to see that the matrix $\frac{\partial \Phi(x)}{\partial x}$ has full rank.

The shaft speed loop system including the controller can be stated in the following form when applying the coordinate transformation (C.1) and (C.2) and neglecting the disturbances Q_f and T_{ext}:

$$\begin{aligned}
\dot{x_1}^{new} &= \tilde{f}_1(x_1^{new}, x_2^{new}) + \tilde{g}_1(x_1^{new}, x_2^{new})u + \tilde{l}_1(x^{new})\nu^{new} \\
\dot{x_2}^{new} &= \tilde{f}_2(x_1^{new}, x_2^{new}) + \tilde{g}_2(x_1^{new}, x_2^{new})u + \tilde{l}_2(x^{new})\nu^{new} + \tilde{p}_2(x^{new})w^{new} \\
y_1^{new} &= \tilde{h}_1(x_1^{new}) \\
y_2^{new} &= x_2^{new}
\end{aligned}$$

which corresponds to the transformed form stated in Theorem 3.11.

For solving the FPRG 13 the ${x_1}^{new}$-subsystem can be extracted:

$$\dot{{x_1}}^{new} = \tilde{f}_1(x_1^{new}, y_2^{new}) + \tilde{g}_1(x_1^{new}, y_2^{new})u + \tilde{l}_1(x^{new})\nu^{new} \tag{C.3}$$

$$y_1^{new} = \tilde{h}_1(x_1^{new}) \tag{C.4}$$

(C.3) and (C.4) can be stated in the original coordinates as follows:

$$\begin{aligned} \dot{x} &= f(x, y_2) + g(x)u + l(x)\nu \\ y_1 &= U_m = U \\ y_2 &= n_m = n + x_{\Delta n} \end{aligned}$$

where

$$x = \begin{pmatrix} Q_{eng} \\ n \\ U \\ Y_i \end{pmatrix} \quad u = \begin{pmatrix} n_{ref} \\ \theta \end{pmatrix} \quad \nu = \begin{pmatrix} \Delta k_y Y \end{pmatrix}$$

$$f(x, y_1) = \begin{pmatrix} -\frac{1}{\tau_c} Q_{eng} + \frac{k_y}{\tau_c} Y_i - \frac{k_y k_r}{\tau_c} y_1 \\ \frac{1}{I_m} Q_{eng} \\ \frac{1}{m} R(U) + \frac{1-t_T}{m} T_{|n|V_a}(1-w)nU \\ -\frac{k_r}{\tau_i} y_2 \end{pmatrix} \quad l(x) = \begin{pmatrix} \frac{1}{\tau_c} \\ 0 \\ 0 \\ 0 \end{pmatrix}$$

$$g(x) = \begin{pmatrix} \frac{k_y k_r}{\tau_c} & 0 \\ 0 & -\frac{1}{I_m} \left[Q_{|n|n} n^2 + Q_{|n|V_a}(1-w)nU \right] \\ 0 & \frac{1-t_T}{m} T_{|n|n} n^2 \\ \frac{k_r}{\tau_i} & 0 \end{pmatrix}$$

Hence, building an observer for the (x, y_1)-system, while neglecting the fault, i.e. $\nu = 0$, and considering y_2 as an additional input, could solve the FPRG 13. However, this requires that the subsystem is locally observable and an observer can be designed.

Calculations for FPRG 14:

$$\nu^{new} = \dot{\Delta} n_{sensor} \quad \text{and} \quad w^{new} = \Delta k_y Y$$

$$P^{14} = span\left\{(1\ 0\ 0\ 0\ 0)^T\right\}$$

Now the algorithm (3.59) and (3.60) is used to calculate $\Sigma_*^{P^{14}}$:

$$S_0^{14} = \overline{P^{14}} = P^{14} \qquad \text{(as } P^{14} \text{ is constant)}$$

$$\Rightarrow S_0^{14} \cap Ker\{dh\} = span\left\{(1\ 0\ 0\ 0\ 0)^T\right\}$$

$$S_{k+1}^{14} = \overline{S}_k^{14} + \sum_{i=0}^{m} [g_i, \overline{S}_k^{14} \cap Ker\{dh\}]$$
$$\Rightarrow\ S_1^{14} = S_0^{14} + [f, S_0^{14} \cap Ker\{dh\}] + [g_2, S_0^{14} \cap Ker\{dh\}]$$

as $g_1(x)$ and $S_0^{14} \cap Ker\{dh\}$ are constant.

$$[f, S_0^{14} \cap Ker\{dh\}] = -\frac{\partial f}{\partial x}\left(S_0^{14} \cap Ker\{dh\}\right)$$
as $S_0^{14} \cap Ker\{dh\}$ is constant.

$$[f, (1\ 0\ 0\ 0\ 0)^T] = (-\frac{1}{\tau_c}\ \frac{1}{I_m}\ 0\ 0\ 0)^T \qquad [g_2, (1\ 0\ 0\ 0\ 0)^T] = 0$$

$$\Rightarrow \quad S_1^{14} = span\left\{(1\ 0\ 0\ 0\ 0)^T, (0\ 1\ 0\ 0\ 0)^T\right\} \quad \Rightarrow \quad S_1^{14} \neq S_0^{14}$$

so the next step is: $S_2^{14} = S_1^{14} + \sum_{i=0}^{2} [g_i, S_1^{14} \cap Ker\{dh\}]$.
As $S_1^{14} \cap Ker\{dh\} = S_0^{14} \cap Ker\{dh\} = span\left\{(1\ 0\ 0\ 0\ 0)^T\right\}$

it is easy to see that $S_2^{14} = S_1^{14}$.

$$\Rightarrow \quad k^* = 1 \qquad \Rightarrow \quad \underline{\Sigma_*^{P^{14}} = S_1^{14} = span\left\{(1\ 0\ 0\ 0\ 0)^T, (0\ 1\ 0\ 0\ 0)^T\right\}}$$

$\Sigma_*^{P^{14}}$ is well-defined (as equation (3.61) holds for $k^* = 1$) and nonsingular (as it is constant). Hence, its annihilator $(\Sigma_*^{P^{14}})^\perp$ is locally spanned by exact differentials (because $\Sigma_*^{P^{14}}$ is by construction involutive). It can also be seen above that $\Sigma_*^{P^{14}} \cap Ker\{dh\}$ is a smooth distribution. Hence, $(\Sigma_*^{P^{14}})^\perp$ is the maximal (in the sense of codistribution inclusion) conditioned invariant codistribution which is locally spanned by exact differentials and contained in $P^{14^\perp}$ (according to DePersis and Isidori (2000)).

The next step in the procedure (described on page 65) is to calculate the involutive conditioned invariant distribution Q^{14} (unobservability distribution):

$$Q^{14} = (\text{o.c.a.}((\Sigma_*^{P^{14}})^\perp))^\perp = (\text{o.c.a.}(S_1^{14^\perp}))^\perp$$

Applying the observability codistribution algorithm (o.c.a.) (see page 43), in order to calculate o.c.a.$(S_1^{14^\perp})$, starts with:

$$Q_0 = S_1^{14^\perp} \cap span\{dh\}$$

$$\begin{aligned} S_1^{14^\perp} &= span\{(0\ 0\ 1\ 0\ 0), (0\ 0\ 0\ 1\ 0), (0\ 0\ 0\ 0\ 1)\} \\ span\{dh\} &= span\{(0\ 1\ 0\ 0\ 1), (0\ 0\ 1\ 0\ 0)\} \\ \Rightarrow \qquad Q_0 &= span\{(0\ 0\ 1\ 0\ 0)\} \end{aligned}$$

The next step in the algorithm:

$$Q_{k+1} = S_1^{14^\perp} \cap \left(\sum_{i=0}^{3} L_{g_i} Q_k + span\{dh\} \right)$$

leads to:

$$Q_1 = S_1^{14^\perp} \cap \left(\sum_{i=0}^{3} L_{g_i}(0\ 0\ 1\ 0\ 0) + span\{dh\} \right)$$

Taking the following result from above it can be seen that:

$$\left(\sum_{i=0}^{3} L_{g_i}(0\ 0\ 1\ 0\ 0) + span\{dh\} \right) = span\{(0\ 1\ 0\ 0\ 0), (0\ 0\ 1\ 0\ 0), (0\ 0\ 0\ 0\ 1)\}$$

$$\Rightarrow Q_1 = S_1^{14^\perp} \cap \left(\sum_{i=0}^{3} L_{g_i}(0\ 0\ 1\ 0\ 0) + span\{dh\} \right)$$
$$= span\{(0\ 0\ 1\ 0\ 0), (0\ 0\ 0\ 0\ 1)\}$$
$$\Rightarrow Q_1 \neq Q_0$$

So the next step is:

$$Q_2 = S_1^{14^\perp} \cap \left(\sum_{i=0}^{3} L_{g_i} Q_1 + span\{dh\} \right)$$

Calculating $L_{g_i}(0\ 0\ 0\ 0\ 1)$: $\quad L_{g_i}(0\ 0\ 0\ 0\ 1) = L_{g_i} x_{\Delta n} = 0$

$$\Rightarrow \left(\sum_{i=0}^{3} L_{g_i} Q_0 + span\{dh\} \right) = \left(\sum_{i=0}^{3} L_{g_i} Q_1 + span\{dh\} \right)$$
$$\Rightarrow \quad Q_2 = Q_1 = span\{(0\ 0\ 1\ 0\ 0), (0\ 0\ 0\ 0\ 1)\}$$
$$\Rightarrow \quad \text{o.c.a.}(S_1^{14^\perp}) = span\{(0\ 0\ 1\ 0\ 0), (0\ 0\ 0\ 0\ 1)\}$$
$$\Rightarrow \quad \underline{Q^{14} = (\text{o.c.a.}(S_1^{14^\perp}))^\perp = span\{(1\ 0\ 0\ 0\ 0)^T}$$
$$\underline{(0\ 1\ 0\ 0\ 0)^T, (0\ 0\ 0\ 1\ 0)^T\}}$$
$$\Rightarrow \quad \underline{p(x)^{new} \in Q^{14}} \quad \text{and} \quad \underline{l(x)^{new} = (0\ 0\ 0\ 0\ 1)^T \notin Q^{14}}$$

As a result it can be seen that the FPRG 14 might be solvable. The next step is now to obtain a coordinate transformation as described in Theorem 3.11. In the following the procedure described in DePersis and Isidori (2000) (Proposition 3) is applied in order to find such a coordinate transformation.

Checking conditions: o.c.a.$(S_1^{14^\perp})$ is by definition an observability codistribution. Let n_1 denote the dimension of o.c.a.$(S_1^{14^\perp})$, hence, $n_1 = 2$. It is easy to see o.c.a.$(S_1^{14^\perp})$ is spanned by exact differentials (e.g. $d(U)$ and $d(x_{\Delta n})$). $span\{dh\} = span\{(0\ 1\ 0\ 0\ 1), (0\ 0\ 1\ 0\ 0)\}$ is nonsingular as it is constant. Let $l - n_2$ ($l = 2$, number of outputs) denote the dimension of o.c.a.$(S_1^{14^\perp}) \cap span\{dh\} = span\{(0\ 0\ 1\ 0\ 0)\}$, hence $n_2 = l - 1 = 2 - 1 = 1$.

Coordinate transformation: After checking the conditions the first step towards the coordinate transformation is to choose a $\Psi_1 : \mathbb{R}^l \rightarrow \mathbb{R}^{l-n_2} = \mathbb{R}^1$

such, that:

$$\text{o.c.a.}(S_1^{14\perp}) \cap span\{dh\} = span\{d(\Psi_1 \circ h)\}$$

One possibility to do so is $\Psi_1 = h_2(x) = U$:

$$\begin{aligned} span\{d(\Psi_1 \circ h)\} = span\{d(U)\} &= span\,\{(0\ 0\ 1\ 0\ 0)\} \\ &= \text{o.c.a.}(S_1^{14\perp}) \cap span\{dh\} \end{aligned}$$

Choosing a selection matrix $H_2 = (1\ 0)$ and combining it with Ψ_1 in the following way:

$$y^{new} = \begin{pmatrix} y_1^{new} \\ y_2^{new} \end{pmatrix} = \Psi(y) = \begin{pmatrix} \Psi_1(y) \\ H_2 y \end{pmatrix}, \quad \text{with} \quad \frac{\partial \Psi(y)}{\partial y} = \begin{pmatrix} 0 & 1 \\ 1 & 0 \end{pmatrix} \tag{C.5}$$

gives a local diffeomorphism at y° in $\mathbb{R}^l$, where $y^\circ = h(x^\circ)$ and $x^\circ \in \mathcal{X}$.

The second step is to choose a neighborhood $\mathcal{U}^\circ$ of x° and a function $\Phi_1 : \mathcal{U}^\circ \to \mathbb{R}^{n_1} = \mathbb{R}^2$ such that $\text{o.c.a.}(S_1^{14\perp}) = span\{d\Phi_1\}$ at any point of $\mathcal{U}^\circ$. Here the following Φ_1 is chosen: $\Phi_1(x) = (U\ x_{\Delta n})^T \in \mathbb{R}^2$. Choosing additionally a $\Phi_3(x) = (Q_{eng}\ Y_i)^T \in \mathbb{R}^2$ leads to the following local diffeomorphism at x° in $\mathcal{X}$:

$$\Phi(x) = \begin{pmatrix} \Phi_1(x) \\ H_2 h(x) \\ \Phi_3(x) \end{pmatrix} = \begin{pmatrix} x_1^{new} \\ x_2^{new} \\ x_3^{new} \end{pmatrix} = \begin{pmatrix} x_{11}^{new} \\ x_{12}^{new} \\ x_2^{new} \\ x_{31}^{new} \\ x_{32}^{new} \end{pmatrix} = \begin{pmatrix} U \\ x_{\Delta n} \\ n + x_{\Delta n} \\ Q_{eng} \\ Y_i \end{pmatrix} \tag{C.6}$$

The shaft speed loop system including the controller can be stated in the following form when neglecting the disturbances Q_f and T_{ext} after applying the coordinate transformation (C.5) and (C.6):

$$\begin{aligned} \dot{x_1}^{new} &= \tilde{f}_1(x_1^{new}, x_2^{new}) + \tilde{g}_1(x_1^{new}, x_2^{new})u + \tilde{l}_1(x^{new})\nu^{new} \\ \dot{x_2}^{new} &= \tilde{f}_2(x^{new}) + \tilde{g}_2(x^{new})u + \tilde{l}_2(x^{new})\nu^{new} + \tilde{p}_2(x^{new})w^{new} \\ \dot{x_3}^{new} &= \tilde{f}_3(x^{new}) + \tilde{g}_3(x^{new})u + \tilde{l}_3(x^{new})\nu^{new} + \tilde{p}_3(x^{new})w^{new} \\ y_1^{new} &= \tilde{h}_1(x_1^{new}) \\ y_2^{new} &= x_2^{new} \end{aligned}$$

This description can be interpreted as a special version of the form stated in Theorem 3.11. For solving the FPRG 14 the ${x_1}^{new}$-subsystem can be extracted:

$$\dot{{x_1}}^{new} = \tilde{f}_1(x_1^{new}, y_2^{new}) + \tilde{g}_1(x_1^{new}, y_2^{new})u + \tilde{l}_1(x^{new})\nu^{new} \tag{C.7}$$

$$y_1^{new} = \tilde{h}_1(x_1^{new}) \tag{C.8}$$

The equations (C.7) and (C.8) can be given as follows by using the original coordinates:

$$\begin{aligned} \dot{x} &= f(x, y_2) + g(x, y_2)u + l(x)\nu \\ y_1 &= U_m = U \\ y_2 &= n_m = n + x_{\Delta n} \end{aligned}$$

where

$$x = \begin{pmatrix} U \\ x_{\Delta n} \end{pmatrix} \quad u = \theta \quad \nu = \dot{\Delta} n_{sensor} \quad l(x) = \begin{pmatrix} 0 \\ 1 \end{pmatrix}$$

$$f(x) = \begin{pmatrix} \frac{1}{m}R(U) + \frac{1-t_T}{m}T_{|n|V_a}(1-w)(y_2 - x_{\Delta n})U \\ 0 \end{pmatrix}$$

$$g(x, y_1) = \begin{pmatrix} \frac{1-t_T}{m}T_{|n|n}(y_2 - x_{\Delta n})^2 \\ 0 \end{pmatrix}$$

Hence, building an observer for the (x, y_1)-system, considering y_2 as additional input, and neglecting the fault, i.e. $\nu = 0$, could solve the FPRG 14. However, this requires that the subsystem is locally observable and an observer can be designed.

Appendix D

Simulation parameters for modified linearized aircraft model

In this section the values for the parameters used in the simulation of the modified linearized aircraft model for lateral motion as described in chapter 6 are given.

In the A-matrix only two values are changed compared to the original system in Mudge and Patton (1988). The original values for $a_{55}^{old} = 0$ and a_{36}^{old} are changed to $a_{55}^{new} = -0.1$ and $a_{36}^{new} = -a_{36}^{old}$ in order to get stable zero dynamics. Which leads to the following system:

$$\begin{aligned} \dot{x} &= A\,x + B\,u \\ y &= C\,x \end{aligned}$$

where:

$$x = \begin{pmatrix} x_1 \\ x_2 \\ x_3 \\ x_4 \\ x_5 \\ x_6 \\ x_7 \end{pmatrix} \begin{array}{l} : \text{sideslip velocity} \\ : \text{roll rate} \\ : \text{yaw rate} \\ : \text{roll angle} \\ : \text{yaw angle} \\ : \text{rudder angle} \\ : \text{aileron angle} \end{array}$$

$$A = \begin{pmatrix} -0.277 & 0 & -32.9 & 9.81 & 0 & -5.432 & 0 \\ -0.103 & -8.325 & 3.75 & 0 & 0 & 0 & -28.64 \\ 0.365 & 0 & -0.639 & 0 & 0 & 9.49 & 0 \\ 0 & 1 & 0 & 0 & 0 & 0 & 0 \\ 0 & 0 & 1 & 0 & -0.1 & 0 & 0 \\ 0 & 0 & 0 & 0 & 0 & -10 & 0 \\ 0 & 0 & 0 & 0 & 0 & 0 & -5 \end{pmatrix}$$

$$B^T = \begin{pmatrix} 0 & 0 & 0 & 0 & 0 & 20 & 0 \\ 0 & 0 & 0 & 0 & 0 & 0 & 10 \end{pmatrix}$$

$$C = \begin{pmatrix} 1 & 0 & 0 & 0 & 0 & 0 & 0 \\ 0 & 0 & 0 & 1 & 0 & 0 & 0 \\ 0 & 0 & 0 & 0 & 1 & 0 & 0 \end{pmatrix}$$

Bibliography

Amann, P., J. M. Peronne, G. L. Gissinger and P. M. Frank (1999). Benchmark Application of Fuzzy Observers to fault Detection on a Ship Propulsion System. In proc.: *Proc. European Control Conference 1999, ECC'99*. Karlsruhe, Germany.

Ashton, S.A. and D.N. Shields (1999). *New Directions in Nonlinear Observer Design*. Chap. Fault detection observer for a class of nonlinear systems, pp. 353–373. Springer-Verlag, London.

Åström, K.J., Albertos, P., Blanke, M., Isidori, A., Santz, R. and Schaufelberger, W., Eds.) (2000). *Control of Complex Systems*. Springer Verlag.

Basseville, M. and I. Nikiforov (1994). *Statistical Change Detection*. Prentice Hall.

Basseville, M. and I. V. Nikiforov (1993). *Detection of Abrupt Changes: Theory and Application*. Information and System Science. Prentice Hall. New York.

Beard, R. V. (1971). Failure Accommodation in Linear Systems Through Self-Reorganization. PhD thesis. Man Vehicle Laboratory. Cambridge, Massachusetts. Rept. MVT-71-1.

Blanke, M. (1981). Ship Propulsion Losses Related to Automatic Steering And Prime Mover Control. PhD thesis. Technical University of Denmark (DTU).

Blanke, M. (1996). A component based approach to industrial fault detection and isolation. In proc.: *Fault Detection, Pulp and Paper, Biotechnology*. Vol. N. 13th IFAC World Congress. pp. 97–102.

Blanke, M. (1999). Fault-tolerant control systems. In: *Advances in Control* (P. M. Frank, Ed.). Chap. 6, pp. 171–196. Springer Verlag. London.

Blanke, M. and J. S. Andersen (1984). On Dynamics of Large Two Stroke Diesel Engines: New Results from Identification.. In proc.: *Proceedings 9th IFAC World Conference*. Budapest.

Blanke, M. and R. J. Patton (1995). Industrial Actuator Benchmark for Fault Detection and Isolation. *Control Engineering Practice* **3**(12), 1727–1730.

Blanke, M. and T. F. Lootsma (1999). Adaptive Observer for Diesel Fault Detection in Ship Propulsion Benchmark. In proc.: *Proc. European Control Conference 1999, ECC'99*. Karlsruhe, Germany.

Blanke, M., C. W. Frei, F. Kraus, R. J. Patton and M. Staroswiecki (2000). *Fault-Tolerant Control Systems*. Chap. 8, pp. 165–189. in Åström *et al.* (2000).

Blanke, M., R. Izadi-Zamanabadi and T. F. Lootsma (1998). Fault Monitoring and Reconfigurable Control for a Ship Propulsion Plant. *Journal of Adaptive Control and Signal Processing* pp. 671–688.

Bøgh, S. A. (1997). Fault Tolerant Control Systems - a Development Method and Real-Life Case Study. PhD thesis. Dept. of Control Eng., Aalborg University, Denmark.

Cassar, J. Ph., M. Staroswiecki and P. Declerck (1994). Structural Decomposition of Large Scale Systems for the Design of Failure Detection and Isolation Procedures. *Systems Science* **20**(1), 31–42.

Chen, J. and R. J. Patton (1999). *Robust Model-based Fault Diagnosis for Dynamic Systems*. Kluwer Academic Publishers.

Cho, Y.M. and R. Rajamani (1997). A Systematic approach to adaptive observer synthesis for nonlinear systems. *IEEE Transactions of Automatic Control* **42**(4), 534–537.

Clark, R. N. (n.d.). State estimation schemes for instrument fault detection. In: *Fault Diagnosis in Dynamic Systems: Theory and Application* (R. J. Patton, P. M. Frank and R. N. Clark, Eds.). Chap. 2, pp. 21–45. Prentice Hall.

Cocquempot, V., R. Izadi-Zamanabadi, M. Staroswiecki and M. Blanke (1998). Residual Generation for the Ship Benchmark Using Structural Approach. In proc.: *IEE Control'98*. Swansea, UK.

DePersis, C. (1999). A necessary condition and a backstepping observer for nonlinear fault detection. In proc.: *Proc. of the 38th Conf. on Decision & Control*. Phoenix, Arizona USA.

DePersis, C. and A. Isidori (1999). On the Problem of Residual Generation for Fault Detection in Nonlinear Systems and some Related Facts. In proc.: *Proc. European Control Conference 1999, ECC'99*. Karlsruhe, Germany.

DePersis, C. and A. Isidori (2000). A Geometric Approach to Nonlinear Fault Detection and Isolation. In proc.: *IFAC Safeprocess2000*. pp. 209–214.

Edwards, C. and S. K. Spurgeon (1999). A Sliding Mode Observer Based FDI Scheme for the Ship Benchmark. In proc.: *Proc. European Control Conference 1999, ECC'99*. Karlsruhe, Germany.

Falb, P.L. and W.A. Wolovich (1967). Decoupling in the design and synthesis of multivariable control systems. *IEEE Trans. Automat. Contr.* **12**, 651–659.

Fossen, Thor I. (1994, pp. 246-257). *Guidance and Control of Ocean Vehicles*. John Wiley & Sons.

Frank, P. M. (1991). Enhancement of robustness in observer-based fault detection. In proc.: *Preprints of IFAC/IMACS Symposium SAFEPROCESS'91*. Vol. 1. Baden-Baden. pp. 275–287. "A modified version also published in *Int. J. Control*, Vol.59, No.4, 955-981, 1994".

Frank, P. M. (1993). Advances in observer-based fault diagnosis. In proc.: *Proc. of Int. Conf. on Fault Diagnosis: TOOLDIAG'93*. Toulouse. pp. 817–836.

Frank, P. M. (1996). Analytical and Qualitative Model-based Fault Diagnosis - A Survey and Some New Results. *European Journal of Control* **2**(1), 6–28.

Frank, P. M. and X. Ding (1997). Survey of robust residual generation and evaluation methods in observer-based fault detection systems. *J. of Process Control* **7**(6), 403–424.

Frank, P. M., G. Schreier and E. A. García (1999). *New Directions in Nonlinear Observer Design*. Chap. Nonlinear Observers for Fault Detection and Isolation, pp. 399–422. Springer-Verlag, London.

García, E. A. and P. M. Frank (1997). Deterministic Nonlinear Observer-Based Approaches to Fault Diagnosis: A Survey. *Control Engineering Practice* **5**(5), 663–760.

Gauthier, J.P., H. Hammouri and S. Othman (1992). A Simple Observer for Nonlinear Systems Applications to Bioreactors. *IEEE Transactions of Automatic Control* **37**(6), 875–880.

Gertler, J. J. (1991). Analytical redundancy methods in Failure detection and isolation. In proc.: *Preprints of IFAC/IMACS Symposium SAFEPROCESS'91*. Vol. 1. Baden-Baden. pp. 9–21. also published in a revised version in "*Control Theory and Advanced Technology*, Vol. 9, No.1, 259-285, 1993".

Gertler, J. J. (1998). *Fault Detection and Diagnosis in Engineering Systems*. 1 ed. Marcel Dekker Inc.

Gertler, J. J. and M. K. Kunwer (1993). Optimal residual decoupling for robust fault diagnosis. In proc.: *Proc. of Int. Conf. on Fault Diagnosis: TOOLDIAG'93*. Toulouse. pp. 436–452.

Gilbert, E.G. (1969). The decoupling of multivariable systems by state feedback. *SIAM J. Contr. & Optimiz.* **7**, 50–63.

Gras, L.C.J.M. and H. Nijmeijer (1989). Decoupling in nonlinear systems:from linearity to nonlinearity. *IEE Proc.-D: Control Theory & Appl.* **136**(2), 53–62.

Hammouri, H., M. Kinnaert and E. H. Yaagoubi (1998). Fault Detection and Isolation for State Affine Systems. *European Journal of Control* (4), 2–16.

Hammouri, H., M. Kinnaert and E. H. Yaagoubi (1999). Observer-Based Approach to Fault Detection and Isolation for Nonlinear Systems. *IEEE Trans. Automat. Contr.* **44**(10), 1879–1884.

Hashtrudi-Zad, S. and M. A. Massoumnia (1999). Generic solvability of the failure detection and identification problem. *Automatica* **35**, 887–893.

Isermann, R. and P. Ballé (1997). Trends in the Application of Model-Based Fault Detection and Diagnosis of Technical Processes. *Control Engineering Practice* **5**(5), 709–719.

Isidori, A. (1985). *Nonlinear control systems: an introduction*. Vol. 72 of *Lecture Notes Contr. Inf. Sci.*. Springer-Verlag.

Isidori, A. (1995). *Nonlinear control systems*. 3 ed. Springer-Verlag.

Isidori, A., A.J. Krener, C. Gori-Giorgi and S.Monaco (1981). Nonlinear decoupling via feedback: A differential geometric approach. *IEEE Trans. Automat. Contr.* **26**(2), 331–345.

Izadi-Zamanabadi, R. (1999). Fault-tolerant Supervisory Control - System Analysis and Logic Design. PhD thesis. Dept. of Control Eng., Aalborg University, Denmark.

Izadi-Zamanabadi, R. and M. Blanke (1997). A Ship Propulsion System as a Benchmark for Fault-tolerant Control. *IFAC Safeprocess 97, Hull, England*. pp 1074-1082.

Izadi-Zamanabadi, R. and M. Blanke (1998). Ship Propulsion System as a Benchmark for Fault-tolerant Control. Technical report. Control Engineering Dept., Aalborg University. Fredik Bajers Vej 7C, DK-9220 Aalborg, Denmark.

Izadi-Zamanabadi, R. and M. Blanke (1999). A Ship Propulsion System as a Benchmark for Fault-tolerant Control. *Control Engineering Practice* **7**(2), 227–239.

Jacobson, C. A. and C. N. Nett (1991). An integrated approach to controls and diagnostics using the four parameter control. *IEEE Control Syst. Mag.* **11**(6), 22–29.

Jones, H. L. (1973). Failure Detection in Linear Systems. PhD thesis. Dept. of Aeronautics and Astronautics, Massachusetts Institute of Technology. Mass.,USA.

Kerrigan, E.C. and J.M. Maciejowski (1999). Fault tolerant control of a ship propulsion system using model predictive control. In proc.: *Proc. European Control Conference*. Karlsruhe.

Khalil, H.K. (1996). *Nonlinear Systems*. Prentice Hall, New Jersey.

Kinnaert, M. (1999). Robust fault detection based on observers for bilinear systems. *Automatica* **35**, 1829–1842.

Kinnaert, M. (2001). Private communication.

Kinnaert, M. and L. E. Bahir (1999). *New Directions in Nonlinear Observer Design*. Chap. Innovation Generation for Bilinear Systems with Unknown Inputs, pp. 445–465. Springer-Verlag, London.

Kinnaert, M., Y. Peng and H. Hammouri (1995). The Fundamental Problem of Residual Generation for Bilinear Systems up to Output Injection. In proc.: *3rd European Control Conference*. pp. 3777–3782.

Kiupel, N. and P. M. Frank (1997). A Fuzzy FDI Decision Making System for the Support of the Human Operator. In proc.: *IFAC Safeprocess'97*. pp. 731–736.

Köppen-Seliger, B. and P. M. Frank (1996). Neural Network in Model-Based Fault Diagnosis. In proc.: *13th IFAC World Congress*. 7f-02 5. pp. 67–72.

Lootsma, T.F. and R. Izadi-Zamanabadi (2001). Observer-based FDI for gain fault detection in ship propulsion benchmark - geometric approach. In proc.: *submitted*.

Lunze, J. (2000). Diagnosis of Quantised Systems. In proc.: *IFAC Safeprocess2000*. pp. 28–39.

Massoumnia, M. A. (1986*a*). A Geometric Approach to Failure Detection and Identification in Linear Systems. PhD thesis. Massachusetts Institute of Technology. Mass., USA.

Massoumnia, M. A. (1986*b*). A geometric approach to the synthesis of failure detection filters. *IEEE Trans. Automat. Contr.* **AC-31**(9), 839–846.

Massoumnia, M. A., G. C. Verghese and A. S. Willsky (1989). Failure detection and identification. *IEEE Trans. Automat. Contr.* **34**(3), 316–321.

Mudge, S. K. and R. J. Patton (1988). Analysis of the techniques of robust eigenstructure assignment with application to aircraft control. *IEE Proc.-D: Control Theory & Appl.* **135**(7), 275–281.

Nett, C. N., C. A. Jacobson and A. T. Miller (1988). An integrated approach to controls and diagnostics: The 4-parameter controller. In proc.: *Proc. 1988 Amer. Contr. Conf.*. pp. 824–835.

Nijmeijer, H. and A.J. van der Schaft (1990). *Nonlinear Dynamical Control Systems*. Springer-Verlag, New York.

Nijmeijer, H. and Fossen, T. I., Eds.) (1999). *New Directions in Nonlinear Observer Design*. Springer-Verlag, London.

Patton, R. J. (1994). Robust model-base fault diagnosis: The state of the art. In proc.: *Preprints of the IFAC Sympo. on Fault Detection, Supervision and Safety for Technical Processes: SAFEPROCESS'94*. Vol. 1. Espoo, Finland. pp. 1–27.

Patton, R. J. (1995). Robust model-based fault diagnosis: The 1995 situation. In proc.: *Proc. IFAC Workshop on Supervision and Fault Diagnosis in the Chemical Process Industries, Newcastle, UK.*. pp. 55–78.

Patton, R. J. (1997). Fault Tolerant Control: The 1997 Situation. In proc.: *IFAC Safeprocess'97*. Hull, United Kingdom. pp. 1033–1055.

Patton, R.J. and J. Chen (1997). Observer-based fault detection and isolation: robustness and applications. *Control Engineering Practice* **5**(5), 671–682.

Rugh, W.J. and J.S. Shamma (2000). Research on gain scheduling - Survey paper. *Automatica* **36**, 1401–1425.

Schreier, G. and P. M. Frank (1999). Fault Tolerant Ship Propulsion Control: Sensor Fault Detection Using a Nonlinear Observer. In proc.: *Proc. European Control Conference 1999, ECC'99*. Karlsruhe, Germany.

Seliger, R. and P. M. Frank (1991*a*). Fault-Diagnosis by Disturbance decoupled Nonlinear Observers. In proc.: *30th Conference on Decision and Control, CDC'91*. pp. 2248–2253.

Seliger, R. and P. M. Frank (1991*b*). Robust component fault detection and isolation in nonlinear dynamic systems using nonlinear unknown input observers. In proc.: *Preprints of IFAC/IMACS Symp. SAFEPROCESS'91*. Vol. 1. Baden-Baden. pp. 313–318.

Staroswiecki, M. and P. Declerck (1989). Analytical redundancy in non-linear interconnected systems by means of structural analysis. Vol. II. IFAC-AIPAC'89. Nancy. pp. 23–27.

Stoustrup, Jakob, M. J. Grimble and H. H. Niemann (1997). Design of Integrated Systems for the Control and Detection of Actuator/Sensor Faults. *Sensor Review* **17**(2), 138–149.

White, J. E. and J. L. Speyer (1987). Detection filter design: spectral theory and algorithm. *IEEE Trans. Automat. Contr.* **AC-32**(7), 593–603.

Willems, J.C. and C. Commault (1981). Disturbance decoupling by measurement feedback with stability or pole placement. *SIAM J. Contr. & Optimiz.* **19**(4), 490–504.

Willsky, A. S. (1976). A Survey of Design Methods for Failure Detection in Dynamic Systems. *Automatica* **12**(6), 601–611.

Wonham, W.M. (1985). *Linear Multivariable Control: a geometric approach*. Springer-Verlag, Berlin.

Wonham, W.M. and A. S. Morse (1970). Decoupling and pole assignment in linear multivariable systems: a geometric approach. *SIAM J. Contr. & Optimiz.* **8**(1), 1–18.

Yu, D.L. and D. N. Shields (1994). A fault detection methods for a nonlinear system and its application to a hydraulic test rig. In proc.: *Preprints of the IFAC Sympo. on Fault Detection, Supervision and Safety for Technical Processes: SAFEPROCESS'94*. Vol. 1. Espoo, Finland. pp. 305–310.

Zhang, Y. and N. E. Wu (1999). Fault Diagnosis for A Ship Propulsion Benchmark: Part I. In proc.: *Proc. 14th IFAC World Congress*. Beijing, P.R. China. pp. 569–574.